The influence of post-translational modifications on biology of the linker histone HIS-24 in *Caenorhabditis elegans*

PhD Thesis

Dissertation
for the award of the degree
'Doctor of Philosophy' (Ph.D.)
Division of Mathematics and Natural Sciences
of the Georg-August-University Göttingen

submitted by
Maja Studencka
born in Żywiec, Poland

2012

Thesis Supervisor:

Dr. Monika Jedrusik-Bode

Dissertation Examining Committee:

Prof. Dr. Sigrid Hoyer-Fender (1_{st} Referee)
Department of Zoology–Developmental Biology, University of Göttingen

Prof. Dr. Michael Kessel (2_{nd} Referee)
Department Developmental Biology, Max Planck Institute for Biophysical Chemistry

Prof. Dr. Detlef Doenecke
Department of Molecular Biology, University of Göttingen

Prof. Dr. André Fiala
Department of Molecular Neurobiology of Behavior, University of Göttingen

Prof. Dr. Reinhard Schuh
Department of Molecular Developmental Biology, Max Planck Institute for Biophysical Chemistry

Dr. Dieter Klopfenstein
Department of Biophysics, University of Göttingen

Date of oral exam: 11.06.2012

Affidavit

I hereby declare that the presented thesis "The influence of post-translational modifications on biology of the linker histone HIS-24 in *Caenorhabditis elegans*" has been written independently and with no other sources and aids than quoted.

Göttingen, May 7th, 2012

List of publications

Studencka M., Wesołowski R., Opitz L., Salinas-Riester G., Wisniewski J.R., Jedrusik-Bode M. Transcriptional repression of Hox genes by *C. elegans* HP1/HPL and H1/HIS-24. In revision.

Studencka M., Konzer A., Moneron G., Wenzel D., Opitz L., Salinas-Riester G., Bedet C., Krüger M., Hell S.W., Wisniewski J.R., Schmidt H., Palladino F., Schulze E., Jedrusik-Bode M. (2012). Novel roles of Caenorhabditis elegans heterochromatin protein HP1 and linker histone in the regulation of innate immune gene expression. Mol Cell Biol. 32(2), 251-65.

Kaczmarek K., Studencka M., Meinhardt A., Wieczerzak K., Thoms S., Engel W., Grzmil P. (2011). Overexpression of peroxisomal testis-specific 1 protein induces germ cell apoptosis and leads to infertility in male mice. Mol Biol Cell. 22(10), 1766-79.

Kaczmarek K., Niedzialkowska E., Studencka M., Schulz Y., Grzmil P.. (2009). Ccdc33, a predominantly testis-expressed gene, encodes a putative peroxisomal protein. Cytogenet Genome Res. 126(3), 243-52.

Table of Contents

Acknowledgements

I would like to gratefully and sincerely thank Dr. Monika Jedrusik-Bode for her guidance, understanding, and most importantly for her patience. Her wide knowledge and her logical way of thinking have been of great value for me. Her encouraging and personal guidance have provided a good basis for the present thesis.

I am also very grateful to my PhD Thesis committee Prof. Sigrid Hoyer-Fender and Prof. Michael Kessel for their input, detailed and constructive comments, valuable discussions and accessibility throughout this work.

I am grateful to Prof. Gregor Eichele for giving me the opportunity to work in his department and for his helpful discussions.

I am grateful to all collaborators: Dr. Francesca Palladino for plasmids, antibodies and *C. elegans* strains; Dr. Gael Moneron for his amazing STED microscopy analyses as well as for his enthusiasm and patience; Dr. Dirk Wenzel for the excellent electron microscopy pictures and Rania Nakad for the *Bacillus thuringiensis* bacterial strain and for her help in the establishing the *C. elegans* infection procedure.

I want to thank the Caenorhabditis Genetics Center (CGC) for *C. elegans* strains.

Many thanks to all members of the *Genes and Behaviour* department for the pleasant time throughout my thesis, for the constant help, and advices. Especially I want to thank Ana Martinez Hernandez and Inga Urban for their great help in several steps of my thesis.

I would like to thank Nikolai Petkau for helping me with reagents, protocols and for many advices he gave me during my work in the lab.

Many, many thanks to Dr. Aleksandra Kata for help and support, for giving me such a pleasant time when living in dormitory, for dry humor about scientist's life and exciting time we spent together.

I thank my parents for their faith in me and allowing me to be as ambitious as I wanted. It was under their watchful eye that I gained so much drive and an ability to tackle problems head on.

Finally, and most importantly, I would like to thank Grzegorz. His great support, encouragement, patience and unwavering love were undeniably the bedrock upon which the past few years of my life have been built.

Summary

In the eukaryotic nucleus the genome is packaged into a nucleoprotein complex known as chromatin. The chromatin is composed of DNA, core histones (H2A, H2B, H3, H4), linker histones (H1) as well as non-histone proteins. Such a specific compaction of DNA is necessary for the packaging of a very large genome of eukaryotic cells into the nucleus and it plays an essential role in the maintenance of the chromosomal integrity.

On the other hand, the proper chromatin organization has a crucial function in DNA repair and in regulation of gene expression. During the transcription process the chromatin structure changes from highly condensed, ordered and inaccessible to an unfolded and genetically active form. Transition between the active and repressive chromatin states can be established, among others, by post-translational modifications (PTMs) of histones. These covalent changes are found to be important for regulation of DNA accessibility for recruitment of further chromatin effector proteins. Apart from well-known modification of the H3 and H4 core histone tails, post-translational changes of the H1 linker histone are also critical for the modulation of particular chromatin states.

Linker histones (H1) are highly abundant eukaryotic chromatin proteins, which associate with linker DNA fragments, completing the chromatin fibre formation. Recent studies have reported that the post-translational methylation of the mammalian histone H1 is specifically recognised by the chromodomain of heterochromatin protein 1 (HP1). However, the exact biological role of linker histone association with HP1 has not yet been elucidated.

In the present study, the physiological function of post-translational modification of the *C. elegans* linker histone variant HIS-24 was determined. *C. elegans* H1 variant HIS-24 was found to be recognised by the HP1-like proteins HPL through the mono-methylated lysine 14 of the linker histone. While mammalian HP1 protein was found to specifically interact with the di-methylated form of H1, the one of two *C. elegans* heterochromatin protein homologues HPL-1 was identified to bind selectively the mono-methylated form of nematode histone variant HIS-24.

The transcriptional profiles analysis of *his-24* and *hpl* deficient *C. elegans* animals revealed that HIS-24 and HPL-2 proteins play gene-specific roles, rather than a general repressive function. Phenotypic investigation of the *C. elegans* HIS-24 and HPL-2 proteins functions showed that both chromatin associated factors allow normal reproduction, somatic gonad development and vulva cell fate decision. Interestingly, the study showed that HIS-24 and HPL-2 also play a role in regulation of male tail development, and *his-24* and *hpl-2* loss of function mutation causes posterior transformations of mating structures in *C. elegans.* The genetic study of *his-24* and *hpl-2* mutants using a GFP-tagged reporter of two *Hox* genes showed ectopic expression of MAB-5 and EGL-5 homeodomain transcription factors. They are expressed in the posterior region of *C. elegans* and are required for development of sensory rays in male. The biochemical analyses using chromatin immunoprecipitation (ChIP) approach confirmed that expression of *mab-5* and *egl-5* Hox genes is negatively regulated by HIS-24. Moreover, the immunoprecipitation experiments showed that mono-methylated HIS-24K14me1 specifically binds to the H3K27me3 chromatin mark, which is associated with the *Hox* genes silencing. Additionally, expression of wild type form of the HIS-24::GFP but not HIS-24A14K::GFP resulted in complete restoration of male ray development, suggesting that the observed changes in male tail development depend on HIS-24 methylation. These results

indicate that HIS-24K14me1 and HPL-2 may serve as essential protein components in the establishment and/or maintenance of the repressive chromatin structure at the *Hox* genes.

In addition, the investigation of the biological function of the HIS-24 and the HP1-like proteins HPL-1 and HPL-2 revealed the cooperative transcriptional regulation of immune response-related genes. By using the genome profiling and quantitative proteome analysis approaches, the present study provides first insight into the HIS-24K14me1 and HPL-1-dependant negative regulation of genes encoding antimicrobial factors. The analysis of sensitivity to infection with gram-positive bacteria of *C. elegans his-24* and *hpl* mutant strains showed that the absence of HIS-24 histone variant results in increased sensitivity to infection. Further, investigation of *C. elegans* transgenic lines revealed that especially the presence of the mono-methylated form of HIS-24 is crucial for proper innate immune response process.
In addition, microscopic analysis *C. elegans* intestinal cells revealed that bacterial infection is also associated with changes in the localisation of HIS-24 variant. In particular, post-translationally modified form of HIS-24 alters its localisation from mostly nuclear, in uninfected nematodes, to both nuclear and cytoplasmic in the intestinal cells of infected animals.
The study points to a specific immune response-related role of the *C. elegans* linker histone HIS-24. Furthermore, they imply a relationship between the post-translational modification of HIS-24 and the protection against penetration by microorganisms in the *C. elegans* organism.

Taken together, the study demonstrates that the H1 linker histone is not only important for chromatin structure changes, and it should not be considered as a general repressor of transcription. Obtained results show that HIS-24 can regulate expression of specific genes and its post-translationally modified form is essential for the *C. elegans* male tail development as well as for the immune response modulation.

Zusammenfassung

Im eukaryontischen Zellkern ist das Erbgut in einen Nukleoprotein-Komplex, das sogenannte Chromatin verpackt. Chromatin setzt sich aus DNA, den Core-Histonen (H2A, H2B, H3, H4), Linker-Histonen (H1) und Nicht-Histon-Proteinen zusammen. Eine solche spezifische Kompaktierung von DNA ist notwendig, um das große eukaryontische Genom im Zellkern zu verpacken und spielt eine essentielle Rolle bei der Aufrechterhaltung chromosomaler Integrität.
Andererseits hat die korrekte Organisation des Chromatins eine essentielle Rolle bei DNA-Reparatur und bei der Regulation der Genexpression. Während des Transkriptionsvorgangs verändert sich die Chromatinstruktur von hochkondensiert, geordnet und unzugänglich hin zu einer entfalteten und genetisch aktiven Form. Der Übergang von aktiven hin zu repressiven Chromatinzuständen kann u.a. durch posttranslationale Modifikationenen (PTMs) von Histonen ermöglicht werden. Diese kovalenten Änderungen sind wichtig für die Regulation der Zugänglichkeit der DNA, um weitere chromatinverändernde Proteine zu rekrutieren. Neben den bekannten Modifikationen der H3 und H4 Core-Histonschwänze sind auch posttranslationale Modifikationen der H1 Linker-Histone wichtig für die Modulation bestimmter Chromatin-Zustände.
Linker-Histone (H1) sind häufig vorkommende eukaryontische Chromatin-Proteine, die mit Linker-DNA-Fragmenten assoziieren und so die Chromatinfaserkonformation vervollständigen. Aktuelle Studien zeigten, dass die posttranslationale Methylierung des Säugetier-Histon H1 spezifisch von der Chromodomäne des Heterochromatin Protein 1 (HP1) erkannt wird. Die exakte biologische Rolle der Assoziation zwischen Linker-Histon und HP1 konnte jedoch noch nicht geklärt werden. In der vorliegenden Studie wurde die physiologische Funktion der posttranslationalen Modifikation der *C. elegans* Linker-Histon Variante HIS-24 untersucht. Die *C. elegans* H1Variante HIS-24 wird von dem HP1-ähnlichen Proteinen HPL anhand des monomethylierten Lysin 14 des Linker-Histons erkannt. Während das Säugetier-HP1-Protein spezifisch mit der dimethylierten Form von H1 interagiert, stellte sich heraus, dass eines der beiden *C. elegans* Heterochromatin-Protein-Homologe HPL-1 selektiv die monomethylierte Form des Nematoden-Histonvariante HIS-24 bindet. Die Analyse der Transkriptionsprofile von *his-24*- und *hpl*-defizienten *C. elegans* Tieren deckten auf, dass HIS-24- und HPL-2-Proteine eine genspezifische Rolle spielen und keine generelle repressive Funktion haben. Phänotypische Untersuchungen der *C. elegans* HIS-24- und HPL-2-Proteinfunktionen haben gezeigt dass beide chromatin-assoziierten Faktoren normale Reproduktion, Entwicklung der somatischen Gonaden und Vulva-Schicksalsbestimmung erlauben.
Interessanterweise konnte die Studie zeigen, dass HIS-24 und HPL auch eine Rolle bei der Regulation der männlichen Schwanzentwicklung spielen und eine *loss-of-function* Mutation von *his-24* und *hpl-2* eine posteriore Transformationen der Kopulationsstrukturen bei *C. elegans* verursacht. Die genetische Untersuchung von *his-24*- und *hpl*-2-Mutanten unter Verwendung von GFP-getaggten Reportern zweier *Hox*-Gene, zeigte ektopische Expression der Homöodomänen-Transkriptionsfaktoren MAB-5 und EGL-5. Sie werden in der posterioren Region von *C. elegans* exprimiert und für die Entwicklung der *sensory rays* der Männchen benötigt. Die biochemischen Analysen mit Chromatin-Immunopräzipitation

(ChIP) bestätigten, dass die Expression der *Hox*-Gene *mab-5* und *egl-5* negativ von HIS-24 reguliert wird.

Desweiteren zeigten die Immunopräzipitations-Experimente, dass monomethyliertes HIS-24K14me1 spezifisch an den Chromatinmarker H3K27me3 bindet, welches mit der Stummschaltung von *Hox*-Genen assoziiert ist.
Zusätzlich konnte durch die Expression der Wildtypform des HIS-24::GFP, jedoch nicht des HIS-24A14K::GFP, die Entwicklung der männlichen *rays* komplett wiederhergestellt werden, was nahelegt dass die beobachteten Veränderungen in der Entwicklung des männlichen Schwanzes von der Methylierung von HIS-24 abhängig sind. Diese Ergebnisse lassen vermuten, dass HIS-24K14me1 und HPL-2 als essentielle Proteinkomponenten bei der Etablierung und/oder Aufrechterhaltung der repressiven Chromatinstruktur bei den *Hox*-Genen dienen.
Darüberhinaus ergab die Untersuchung der biologischen Funktion des HIS-24- und der HP1-ähnlichen Proteine HPL-1 und HPL-2 die kooperative transkriptionelle Regulation von für die Immunantwort verantwortlichen Genen. Durch die Anwendung von Genom-Profiling und quantitativer Proteomanalyse verschafft die vorliegende Studie einen ersten Einblick in die HIS-24K14me1- und HPL-1-abhängige negative Regulation von Genen, die antimikrobielle Faktoren enkodieren. Die Analyse der Empfindlichkeit gegenüber Infektionen mit Gram-positiven Bakterien der *C. elegans his-24*- und *hpl*-mutanten Stämme zeigte, dass das Fehlen der HIS-24 Histon-Variante die Anfälligkeit gegenüber Infektionen erhöht. Außerdem ergab die Untersuchung der transgenen *C. elegans* Linien, wie wichtig insbesondere die Anwesenheit der monomethylierten Form der HIS-24 für die angeborene Immunantwort ist.

Zusätzlich offenbarte die mikroskopische Analyse von *C. elegans* Darmzellen, dass die bakterielle Infektion auch mit Änderungen in der Lokalisation der HIS-24 Variante assoziiert ist. Insbesondere die posttranslational modifizierte Form von HIS-24 ändert ihre Lokalisation von meist nuklear, in nicht infizierten Nematoden, hin zu sowohl nuklearer als auch zytoplasmatischer Lokalisation in den Darmzellen infizierter Tiere.
Die Studie weist auf eine spezifische, auf die Immunantwort bezogene Rolle des *C. Elegans* Linker-Histon HIS-24 hin. Darüberhinaus ist eine Beziehung zwischen der posttranslationalen Modifikation von HIS-24 und den Schutz gegen das Eindringen von Mikroorganismen in den Organismus von *C. Elegans* naheliegend.

Zusammenfassend verdeutlicht die Studie, dass Histon H1 nicht nur wichtig für Veränderungen der Chromatinstruktur ist, und nicht als allgemeine Repressor der Transkription betrachtet werden sollte. Die erbrachten Ergebnisse zeigen, dass HIS-24 die Expression spezifischer Gene regulieren kann und seine posttranslational modifizierte Form essentiell für die Schwanzentwicklung der *C. elegans* Männchen sowie auch für die Modulation der Immunantwort ist.

List of figures

List of tables

Abbreviations

α	anti- (antibody)
A	ampere
ADP	adenosine diphosphate
Arg	arginine
bp	base pair(s)
C	Celsius
ChIP	chromatin immunoprecipitation
CpG	cytosine and guanine separated by one phosphate
cDNA	complementary DNA
ddH_2O	double distilled water
dH_2O	distilled water
DNA	deoxyribonucleic acid
dNTP	deoxyribonucleoside triphosphate
dsRNA	double-stranded ribonucleic acid
EM	electron microscopy
FDR	false discovery rate
g	gram
GFP	green fluorescent protein
Gly	glycine
IF	immunofluorescence
IgG	immunoglobulin G
IP	immunoprecipitation
K	lysine
L/l	liter
log	logarithm
logFC	log-transformed fold change
Lys	lysine
m	milli
M	molar
Mb	megabase(s)
me	methyl group
mRNA	messenger ribonucleic acid
n	nano
N	normality
PD	peptide pull-down
pH	potential of hydrogen
RNA	ribonucleic acid
RNAi	RNA interference
rpm	rotations per minute
RT	room temperature
SD	standard deviation
sec	second(s)
SEM	standard error of mean
Ser	serine
Thr	threonine
U	unit(s)
UV	ultraviolet
V	voltage
v/v	volume per volume
vol.	volume
vs.	versus
w/v	weight per volume
WB	western blot
wt	wild type
µ	micro

1 Introduction

1.1 Structural features of the histone H1 family and their role in chromatin fiber condensation

In the eukaryotic nucleus, chromosomal DNA is compacted into a nucleoprotein complex known as chromatin. It is a dynamic structure formed of DNA, histones and many chromatin-associated factors. The most fundamental level of chromatin organization is a particulate unit, the nucleosomal core particle. In the nucleosome, approximately 1.65 left-handed superhelical turns of DNA are wrapped twice around an octamer of the four core histones H2A, H2B, H3 and H4 [1, 2]. The nucleosome core particle forms the first level of chromatin condensation, the 10 nm fiber also known as a "beads on a string". In most organisms, nucleosomes are separated by a linker DNA that is associated with a single molecule of a fifth histone, the linker histone H1. The H1 molecule binds to DNA entering and exiting the nucleosomal core particle, completing the nucleosome [3-6]. H1 binding facilitates the shift of the chromatin structure towards the more condensed form by the folding of the nucleosomal array into the fiber with a diameter of a ~ 30 nm what coordinates the positioning of nucleosomes [7].

The linker histones H1 are a family of lysine-rich proteins. The metazoan H1 histone exhibits a tripartite structural organization [8]. It consists of a globular domain containing a winged-helix fold, which is flanked by a short N-terminal tail and a long, extremely lysine rich C-terminal tail (CTD) that comprises almost half of the protein (Figure 1.1 A, B) [9]. The highly conserved globular domain with a diameter of 2.9 nm is the only one that displays three α-helices structures in solution. It contains at least two DNA-binding motifs situated on opposite sides of the molecule. The first is formed by the mentioned winged-helix domain, and the second is a cluster formed by conserved basic residues [10]. These two domains enable the binding of different DNA molecules that results in a presence of tram-track structure [11].

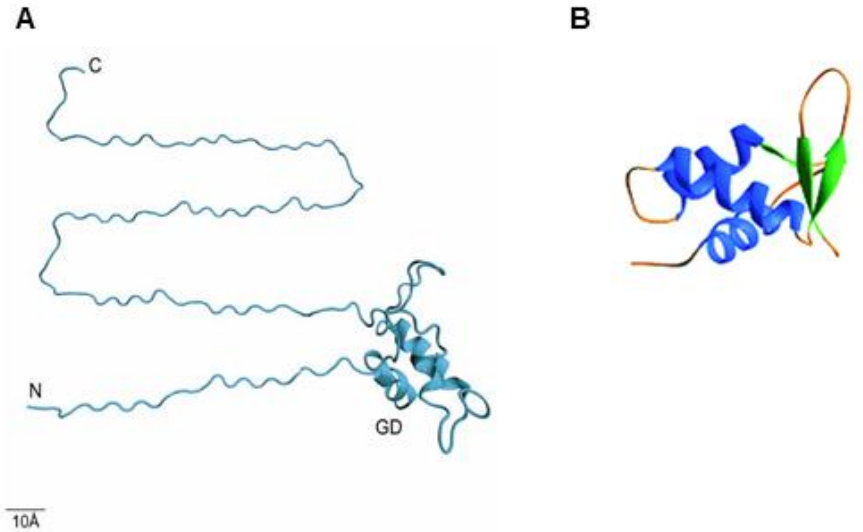

Figure 1.1 Model of the H1 linker histone structure. Ribbon diagram of the 3D structure of *Gallus gallus* linker histone H1 **(A)**. The winked helix motif structure of the mammalian linker histone H5 **(B).** Figures taken from [12].

Despite the positioning of the globular domain along the nucleosome, the globular domain is not the one which binds to the linker DNA. The highly positive charged C-terminal domain is rather the one responsible for association with DNA through nonspecific electrostatic interactions [13]. The specific, amino acid composition of the CTD (~ 40% Lys and Arg, < 10% hydrophobic residues) allows ionic interactions of this domain with the linker DNA [13]. The long CTD domain has the potential to mediate multiple, simultaneous interactions when bound to the nucleosome. Recent studies revealed that the C-terminal tail consists of two sub-domains [14, 15, 16]. These two motifs give the CTD domain its unique amino acids composition and specific localisation in relation to the globular domain what enables correct chromatin folding. As mentioned earlier, only globular domain forms a higher order α-helices structure in solution. However, careful analysis of C-terminus showed that this domain is an intrinsically disordered one and can adopt a specific structure when bound to a nucleosome [16]. Interestingly, the structure of the C-terminal tail bound to DNA is distinct from that formed upon nucleosome interaction indicating that C-terminal domain can adopt many different structural conformations [16]. While the globular domain directs binding to the nucleosome, the lysine-rich C-terminal is responsible for stabilization of nucleosome arrays folding into chromatin fibers, but is also required for high affinity binding to chromatin *in vivo* [4, 14, 17].

In contrast to the C-terminal tail, the N-terminal domain of the linker histone H1 is short and flexible [6]. A detailed study of the rat H1.0 N-terminal motif revealed that the first half of this domain does not contain basic residues and is not expected to interact strongly with DNA [18]. The second half of the N-terminus is highly basic with 1 Arg and 5 Lys residues. Importantly, this region is localised closely to the globular domain what suggests its involvement in the binding stabilization of the central domain to chromatin [18]. Interestingly, the positively-charged second half of the N-terminus can form the α-helix structure where the basic residues are distributed in two clusters with opposite orientation [18]. This type of arrangement may have a role in the organization of the nucleosomal or the linker DNA in chromatin. Remarkably, analysis of the mammalian H1e peptide revealed that it exhibits the presence of two helical elements, which are separated by Gly-Gly motif that forms a flexible linker between two helical regions [18]. This motif enables orientation of helical elements in many axes what may allow simultaneous binding of two separate DNA fragments [18]. Importantly, the Gly-Gly motif is found in many H1 subtypes of vertebrates. As it has been postulated, the N-terminal domain does not seem to be critical for chromatin folding [19] but it may play an important role in modulating the binding affinity of the histone H1 to chromatin [20].

1.2 Evolution and dispensability of H1 linker histone variants

1.2.1 Origin and evolution of H1 linker histone variants

While the core histones' origin can be traced to archaebacteria [21, 22], there is no evidence for the presence of H1 genes in any of the archae genome [23]. Therefore, the evolution of the linker histones appears to have occurred in another way [22]. Interestingly, genes that encode basic proteins in several eubacteria show substantial similarity to the C-terminus of a

metazoan histone H1 [22]. Hence it has been suggested that the lysine-rich DNA binding proteins found in eubacteria are evolutionary related to the H1 linker histones [22].
It is thought that initially linker histones were composed only of a C-terminal tail and the globular domain containing winged helix motif appeared later in the evolution (Figure 1.2) [22]. For example, euglenozoan protists like the kinetoplastids *Trypanosoma cruzi* and *Trypanosoma brucei* possess linker histones without the winged helix motif, but their amino acid composition and structure is similar to the C-terminal tail of H1 in mycetozoans, chlorophytes, plants and animals (Figure 1.2) [22]. H1 related proteins with high structural and compositional similarity to C-terminus are also found in the protist phylum Alveolata, such as the histones of the hypotrich ciliate *Oxytricha sp.* and in Entamoebida like *Entamoeba hystolytica* (Figure 1.2) [22]. On the other hand, the comparison of the H1 variants of mycetozoans and chlorophytes containing winged helix motif revealed that despite high conservation of the globular domain, these two groups display significant variability of C-terminal. This suggested that the H1 linker histone with the winged helix region probably appeared independently in at least two lines of eukaryotes [22].

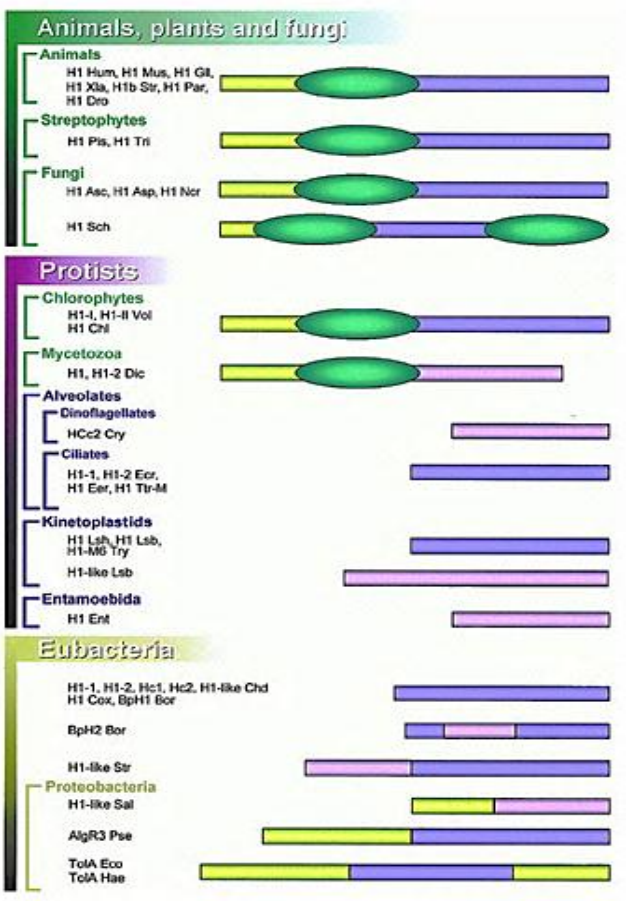

Figure 1.2 Schematic diagram of the H1 linker histones evolution. The purple rods indicate the lysine rich C-terminal tail similar to H1b histone in the sea urchin *Strongylocentrotus purpuratus*. The pink rods stand for regions that display decreased similarity to the C-terminus of *S. purpuratus* histone. The green oval represents the winged helix motif. Yellow indicates the amino termini that are not similar to either the globular domain or C-terminal tail of *S. purpuratus*. Illustration taken from [22].

Interestingly, apart from the well-documented H1 association with chromosomes, also other function, which seemed to appear early in the evolution, has been suggested for the H1 linker histones. The observation of Multinger *et al.* revealed that cytoplasmic fraction of H1 displays association with flagellar microtubules [24]. Importantly this phenomenon was not restricted to a single group of organisms, but instead it was observed in sea urchin, green algae *Chramydomonas*, and in some Protista [24]. The presence of H1 additional function in distinct groups of organisms implicated that these specific properties of the linker histone started to occur relatively early in the evolution [24]. Consistently, *in vitro* studies performed by Jerzmanowski and Cole showed that the H1 linker histone is displaced from the chromosomes during mitosis which leaded to the presence of a free H1 fraction in the nucleus [25]. As it was suggested, this free H1 may then influence the structure of microtubules and in turn the plane of cell division [26]. Although there is not enough data supporting the hypothesis about dual behaviour of H1, the described studies indicated that an extrachromosomal function of H1 in establishment of the microtubular structure may be an evolutionary conserved phenomenon.

Unlike core histones, linker histones display a significantly higher extent of variability and showed lesser conservation among the eukaryotes. Although the sequence of the winged helix domain is conserved through evolution in animals, plants, and fungi, the N- and C-terminal domains are very heterogeneous in amino acid composition but also in length. The lack of a tertiary structure in the terminal domains seems to be the reason of the generally higher tolerance of amino acid exchange in the N- and C-terminus [18].

The wide range of substitutions observed in the H1 gene promotes the functional differentiation of the particular subtypes. In addition to nucleotide replacement, insertions, deletions and duplication events, other mechanisms appear to be important in the H1 linker histone evolution [6, 18]. It is thought that the H1 variants evolved from one gene by its duplications. Among these linker histone variants, called paralogs, the core domain is highly conserved, but the N- and C-terminal tails show strong variability [6]. However, when similar H1 variants are compared between species, there is remarkable similarity in both globular and terminal domains. In particular, comparison of the H1 variants among mammals reveals very high sequence similarity in the globular domain and the both tails [27]. For example, the human H1.4 variant shares 93.6% sequence identities with the mouse H1e linker histone [6]. The nearer the species, the less is the divergence, like in *Pan troglodytes* where H1.2 variant has just one amino acid difference from its human counterpart [27]. This can be explained by the fact that the same H1 genes between species are orthologues, which means that they have originated from a common ancestor gene and then were separated by speciation [6].

1.2.2 Dispensability of H1 linker histone variants

Despite the significant role of the linker histones in the chromatin fiber condensation [3-7], its dispensability for cell viability has been the subject of several analyses in recent years [28-32]. The early insight into the role of linker histones came from the study of H1 depletion effects in the ciliated protozoan *Tetrahymena thermofila* [28]. These single celled organisms

possess two types of nuclei: diploid micronucleus, essential for conjugation, and polyploidy macronucleus. Both nuclei types carry a single copy of H1 gene, deletion of which enables study of the linker histone dispensability. *Tetrahymena* strains lacking either the micronuclear, macronuclear or both histones H1 are viable and exhibit growth similar to that observed in the wild type organisms [28, 29]. However, depletion of the linker histone results in substantial decondensation of chromatin [28, 29]. Similar results were observed in the multicelled filamentous ascomycete *Ascolobus immersus*, whose chromatin displayed aberration of folding. Moreover, the H1 silencing did not appear to decrease the immediate viability of the fungus, but it caused significant decrease in its overall life span [28]. In both described examples, the chromatin exhibited less dense packaging what resulted in accessibility of DNA to a wide variety of regulatory factors. As it was suggested, this could affect the expression of several control genes, which might be incorrectly repressed or activated [28, 29]. Aberrant expression patterns could then cumulate and lead to decrease long term survival. Although H1 linker histone seems not to be essential for viability of single cellular organisms, the loss of its functions results in defects in chromatin folding, and it may influence the long term life span.

In contrast to unicellular organisms, H1 deletion studies turned out to be more difficult in higher eukaryotes by reason of the presence of many H1 variants encoded by separated genes. Unfortunately, the compensation mechanism between particular subtypes additionally complicates the analysis of H1 deletion effects [29]. Most of the studies on the H1 linker histone importance in animals have been done in mice. Initially, the effects of H1 depletion were analysed in mice mutants carrying single gene knockout of certain variant [30]. Remarkably, many of these knockout studies revealed the dispensability of somatic H1 [30] but also of sperm H1t [31], where the depletion of mentioned variants seemed to be compensated by the increased expression of the other linker histones [30, 31]. Interestingly, sequential inactivation of genes for three mouse H1 variants H1c, H1d and H1e, performed by the Skoultchi group, resulted in embryonic lethality due to several developmental defects [32]. In depth analysis of this depletion in mouse embryonic stem cells (ES cells) revealed dramatic changes in chromatin structure, such as decreased global nucleosome spacing, reduced local chromatin compaction, and decreases in certain core histone modifications [32].

As mentioned above, however, the presence of the H1 linker histone is dispensable in simple, multicelled organisms, most likely the growth dependence on H1 by the higher eukaryotes represents an evidence for the indispensability of linker histones for survival.

1.3 Classification of H1 variants

The linker histone families in metazoans and in other multicelled eukaryotes are extremely heterogeneous (Figure 1.3). They contain tissue-specific protein such as H5 linker histone, present only in the nucleated erythrocytes of birds [33], and also protamine-like (PL-1) proteins presented only in sperm [34]. The presence of multiple linker histone family members produces an additional level of complexity during analysis of H1 function.

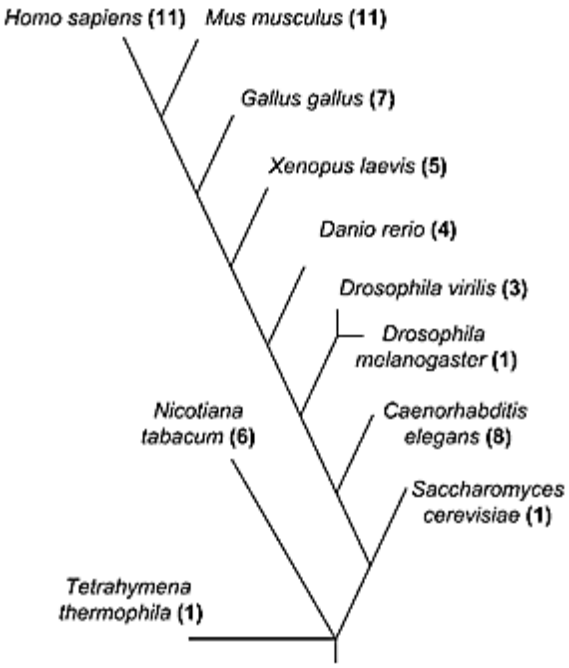

Figure 1.3 Number of the linker histone H1 variants in several species. The species are shown on an evolutionary tree and the number of H1 variants is indicated in parentheses. Figure taken from [6].

H1 family members can be classified in several subgroups according to different criteria. On one hand, particular variants can be subdivided according to their expression. In this way, human linker histones form three groups of variants: these which are expressed in almost every somatic cell during S-phase of the cell cycle and are located within large histone gene cluster (H1.1-H1-5 linker histone variants), two histones with a variant expression in somatic cells (H1.0 and H1X), and those expressed only in germ cells, like oocyte-specific H1oo variant or testis-specific H1t, H1T2 and HILS1 [6, 35]. The somatic expressed *H1* genes are located together with core histone genes within two extensive clusters on the short arm of chromosome 6 in human or on chromosome 13 in mouse [35]. A smaller histone gene cluster, without *H1* genes is localised on human chromosome 1 and murine chromosome 3, whereas all non-clustered *H1* genes are localised on other chromosomes [35]. On the other hand, human H1 family members can be subgrouped in replication-dependent variants (H1.1-H1.5, and H1t), expressed mainly in S-phase, replication-independent variants (replacement histone variants like H1.0 and H1X), and those expressed for all cell cycle [6].

1.3.1 Characterisation of the human H1 variants

The mammalian H1 family is the most divergent class of histone proteins with genes encoding for eleven different H1 subtypes identified to date (Table 1.1). Unfortunately, the identification of the function of particular H1 variants is still in its beginning.

Table1.1 Summary of the human H1 linker histone variants. Data taken from [35].

H1 protein	Gene name	Gene locus	Expression
H1.1	*HIST1H1A*	6p21.3-22	Ubiquitous
H1.2	*HIST1H1C*	6p21.3-22	Ubiquitous
H1.3	*HIST1H1D*	6p21.3-22	Ubiquitous
H1.4	*HIST1H1E*	6p21.3-22	Ubiquitous
H1.5	*HIST1H1B*	6p21.3-22	Ubiquitous
H1t	*HIST1H1T*	6p21.3-22	Spermatocytes
H1T2	*H1FNT*	12q13.11	Spermatids
H1oo	*H1FOO*	3q21.3	Oocytes
HILS1	*HILS1*	17q21.33	Spermatids
H1X	*H1FX*	3q21.3	Ubiquitous
H1.0	*H1FV*	22q13.1	Differentiated cells

As previously mentioned, genes coding for the H1.1–H1.5 somatic histone variants are clustered on chromosome 6 and they are ubiquitously expressed in all body tissues throughout development [35]. Interestingly, these genes are intronless with relatively short 5' and 3' non-coding sequences. Their mRNAs form a hairpin-loop structure, which plays role in the transcriptional regulation during the S-phase [35]. The H1.1 linker histone variant is encoded by the *HIST1HA* gene which is expressed in every somatic cell (Table 1.1). As it has been shown by the Hendzel group, H1.1-GFP protein expressed in human neuroblastoma cells, displayed chromatin binding throughout all cell cycle [36]. Importantly, chromatin association of fusion protein was observed both in interphase and mitotic cells [36]. Detailed studies of H1.1 histone binding to chromatin revealed that deletion of the N-terminal domain very slightly reduces the binding affinity, whereas deletion of C-terminus almost completely disturbs association with chromatin [37]. Moreover, specific mutations of the C-terminal domain identified two novel residues, Thr-152 and Ser-183 that control the binding of histone H1.1 *in vivo* [37]. H1.2, the second H1 linker histone variant, is also ubiquitously expressed and it is thought to play a role in DNA repair mechanism in response to X-ray irradiation [38]. Although all the H1 linker histones are similar to each other, only histone H1.2 has a high metabolic stability [38]. The main difference that distinguishes between histone H1.2 and other variants is the sequence localised at the C-terminal region. All H1 variants, except H1.2, possess the KXXKP motif, which is thought to abolish the proapoptotic activity of the H1 linker histones other than H1.2 [38]. The H1.3 histone variant is localised to the same gene cluster as H1.1 and H1.2, close to genes encoding all four core histones [39]. Although, the H1.3 exact functions are still unknown, studies performed by Jordan and colleagues revealed that this linker histone variant is incorporated into chromatin during cell reprogramming to pluripotency [40]. The H1.4 linker histone variant is encoded by *HIST1HE* gene that is

localised next to the H2B gene on the short arm of chromosome 6. This linker histone variant is known to be involved in heterochromatinisation process in somatic cells. Its post-translational modification, in particular methylation, directly contributes to the transcriptional repression of genes by recruitment of the chromatin folding factors to DNA (see section 1.4) [41, 42]. The H1.5 linker histone is the last somatic variant clustered on chromosome 6 and it is encoded by ubiquitously expressed *HIST1H1B* gene. Similarly to H1.4, the H1.5 linker histone variant is important for the establishing of facultative heterochromatin structure [43]. As reported by the Herrera group, the H1.5 variant, like H1.4, influences the chromatin folding by its interaction with heterochromatin protein 1α (HP1α) [43].

Moreover, the somatic H1 linker histone variants can differ in their localisation. Importantly, the differences occur even in the subnuclear localisation of particular variants. The human H1.5 variant is mainly localised to the nuclear periphery [44], whereas the H1.2 distribution is highly associated with DNA [45]. The diverse *in vivo* distribution of specific histone variants was also observed between different chromatin states. H1.1-H1.3 variants of human H1 linker histone are mainly associated with euchromatin, while H1.4 and H1.5 variants are enriched in heterochromatin regions [46].

The above-mentioned classification of the H1 histone variants distinguish a well described group of variants exclusively expressed in the germ cells, such as testis-specific H1t, H1T2 and HILS1 or oocyte-specific H1oo variant [6, 35].

The H1t histone variant was initially isolated from the rat testis [47] and later the *HIST1H1T* gene was also identified in monkeys [48], mice [49] and humans [50]. This histone is present only in male germ cells where its expression is limited to spermatocytes [51]. The *HIST1H1T* gene is transcribed in mid- and late-pachytene spermatocytes, whereas the translated H1t variant can be found exclusively in pachytene spermatocytes and early haploid spermatids [51]. The presence of the H1t variant is required for the chromatin condensation and it is thought to contribute to the exchange of histone to protamine during spermiogenesis [51]. The H1T2 is second H1 linker histone variant, exclusively expressed in male germline. The *H1FNT* gene encodes the histone variant with an arginine-serine-rich domain and an ATP/GTP binding site [52]. This variant is essential during the elongation phase of spermiogenesis where it, apart from the transition proteins and protamines, facilitates the proper DNA condensation during the elongation phase. As it has been observed, the H1T2 histone specifically localised at the apical pole of the spermatid what resulted in polarity within the spermatid nucleus [53]. Similarly to H1t, H1T2 is specifically involved in the replacement of histones with protamines during spermiogenesis [52]. Additionally, this group of the H1 variants includes also a spermatid-specific linker histone H1-like protein (HILS1), which is specifically expressed in elongating and elongated spermatids [54]. Interestingly, human and also murine *HILS1* gene is located in intron 8 of the α-sarcoglycan genes and it is actively transcribed in nuclei of spermatids [54]. HILS1 displays biochemical properties that are similar to those of linker histones, such as chromatin aggregation [54]. Moreover, the HILS1 variant is a member of the winged helix/forkhead protein superfamily, and may regulate gene transcription, DNA repair, and other chromosome processes [54]. It is thought that HILS1 is unlikely to function as a typical linker histone as it differs significantly from other linker histone family members and is expressed in elongating and elongated spermatids

where core histones are absent [54].
The subgroup of germline-specific H1 linker histones is also represented by the oocyte specific linker (H1) histone, termed H1oo in mammals. The H1oo is present in the secondary follicle oocyte and in one-cell embryos, but is not detected anymore in the blastomeres at the two-cell stage [55]. Unlike in most of histone variant genes, *H1oo* gene consists of introns and its mRNA is polyadenylated [56]. The analysis performed by the Adashi laboratory revealed that H1oo is a mammalian homolog of the oocyte-specific histone B4 (frog) and of the cs-H1 histone (sea urchin), therefore it is believed to play the same conserved role during mammalian oogenesis and early embryogenesis [56]. The same group suggested that mammalian H1oo may control transcription by changing the structure of chromatin during oocyte development and it may also function as a specific gene repressor since the oocytes devoid of functional somatic linker histones [56].

The last subgroup of human linker histone is formed by two histones H1.0 and H1X with a variant expression in somatic cells. Both variants, similarly to H1oo linker histone, have polyadenylated mRNAs [35]. The *H1.0* gene is only expressed in some cell types and encodes for the histone protein, which is the smallest and most lysine-rich member of the H1 family. The gene's association with chromatin has been linked to transcriptional changes occurring during differentiation. H1.0 was first detected in tissues exhibiting a low rate of cell division [57]. As reported, the H1.0 recruitment can be induced in cultured cells upon growth inhibition. On the other hand, the amount of H1.0 in the chromatin decreases when cells start to proliferate [57]. H1.0 was also found to accumulate in various cells that are induced to differentiate by sodium butyrate, a histone deacetylase inhibitor. Therefore, expression of the *H1.0* gene, which occurs when cells start a differentiation program, has also been associated with core histone acetylation [58]. In contrast to H1.0, the H1X variant is ubiquitously expressed [35]. During the interphase, it accumulates in the nucleolus and is distributed at the chromosome periphery during mitosis [35]. Interestingly, expression analysis of the H1X variant revealed that it exhibits a cell-cycle-dependent change of the nuclear distribution [59]. The H1X variant exhibits a nucleolar accumulation during the G_1 phase where it is associated with the chromatin, while during S phase and G_2 it shows regular distribution in the nucleus [59].

1.4 Post-translational modifications of the H1 linker histone variants

Similar to core histones, the linker histone H1 can also be post-translationally modified. The best-analysed modification, that attracted the most attention, is phosphorylation. However, recent studies have shown that also other post-translational modifications, such as acetylation, methylation, ubiquitination, N-formylation and poly(ADP)-ribosylation are important modifications of the linker histones.
The H1 variants can be phosphorylated at numerous serine and threonine residues in the N- and C-terminal tails as a response to many cellular stimuli. The level of phosphorylation usually changes within the cell cycle. It is lower in G1 phase and increases constantly during S and G2 with the highest level observed at the end of G2 phase [60]. The consequence of phosphorylation is the destabilization of the H1 binding to chromatin what causes an increase

accessibility to transcription factors. The H1 phosphorylation can positively or negatively influence expression of specific genes [61]. For example, phosphorylation of H1.2 linker histone variant at T146 enhances p53 transcriptional activity by blocking H1.2 binding to p53 and thereby attenuating its suppressive effects on p53 transactivation [62]. Moreover, phosphorylation of the linker histones has a role in apoptosis and in DNA damage repair mechanism [38]. As it has been reported, H1 linker histone variants can be post-translationally acetylated [63]. Some of them, such as human H1.0 and H5 in avian cells, exhibit acetylation of the second residue of the N-terminus [63]. Since H1.0 variant is known to be associated with differentiation processes and it is abundant in differentiating cells, a correlation between acetylation of this histone variant and differentiation was suggested [63]. Interestingly, the study of Garcia *et al*. [64] showed that other human linker histone variants H1.2, H1.3 and H1.4 display just one acetylation site at Lys 64. In contrast, another group [65] found nine acetylation sites of human H1.4 histone variant. Most of this acetylation sites are localised to globular domain and they are thought to be involved in DNA binding.

More recent proteomic approaches uncovered additional and more specific histone modifications, such as lysine methylation [27], ubiquitination [27], and formylation [66]. Methylation combined with other post-translational modification of human H1 linker histone has been reported form many residues. For example, experiments performed by the Garcia group showed that methylation of human H1.4 variant at Lys26 was followed by simultaneous phosphorylation of Ser27 [64]. Remarkably, similar methylation and phosphorylation at Lys9-Ser10 and Lys27-Ser28 was observed within H3 core histone and is associated with transcription regulation. Putative methylation sites were also identified at Lys169 of H1.4 and H1.5, Lys170 in H1.3 variant [64]. The study performed by the Reinberg group showed that the mono- and di-methylation of the H1 variant at Lys26 leads to binding of different chromatin condensing proteins, such as L3MBTL1 at Rb-regulated genes [41]. This observation revealed a link between post-translational modifications of the linker histone and H1-mediated protein-protein interactions. The crosstalk between H1 modifications and interaction with other factors was also observed by the Schneider laboratory, where they identified specific interaction between methylated Lys26 of H1.4 histone variant and chromodomain of the protein HP1. Remarkably, phosphorylation of the adjacent serine 27 blocked binding of HP1 [42]. Such a specific recruitment of heterochromatin-specific proteins like HP1 by post-translationally modified H1 histone suggests other function for the linker histones than only DNA binding.

Another modification found in H1 histone is ubiquitination, a post-translational modification carried out by a set of three enzymes, E1, E2 and E3. First ubiquitination of H1 linker histone was identified at Ly46 in H1.2, H1.3 and H1.4 variants in human HeLa cells [65]. Moreover, this post-translational modification was also detected at Lys116 in H1.1 variant as well as at Lys46 in H1.2 and H1.3 linker histone variants from mouse tissues [65]. Except mentioned modifications, recently formylation was discovered as a novel post-translational modification of H1 histones [66]. N-formylation takes place at multiple lysine residues located both in the tails and globular domains of the linker histones [66]. Interestingly, the study of Jiang *et al*. [67] demonstrated that lysine N-formylation can arise from oxidative damage of DNA. Interestingly, the H1 linker histones are the most formylated class of histones. Studies of Wisniewski *et al.*, revealed that the H1 histone possesses thirteen formylated lysine residues, among which some were important for DNA binding [66].

The last identified modification of the H1 linker histones was the poly(ADP)-ribosylation. It is a transient modification of many nuclear proteins, including histones, transcription factors and RNA polymerase II, which regulates their binding to DNA [68]. Recent studies of the Carrión laboratory showed that poly(ADP)-ribosylation of H1 may be associated with the memory coding at the genomic level [68]. This post-translational modification results in histone H1 release and seems to promote local chromatin alterations at specific promoters [68]. Additionally, poly(ADP)-ribosylation of H1.4 histone variant was reported to display an inhibitory effect on DNA methylation [69].

1.5 Association of the H1 linker histones with DNA methylation and transcription processes

As previously mentioned (1.2.2), H1c, H1d, H1e triple null mouse embryonic stem cells displayed several alterations in chromatin folding [29]. Surprisingly, despite those changes in structure, only a small number of genes were affected. Remarkably, expression of one-third of these genes was also regulated by DNA methylation [29]. As it was observed, some of the analysed loci indeed exhibited reduced level of this modification but the global DNA methylation was unchanged [29]. For example, the effect of H1 depletion on DNA methylation was observed within the imprinting control regions of *Gtl2-Dlk1* and *H19-Igf2* loci, but the level of CpG methylation was unchanged within the satellite DNA sequences and endogenous C type retrovirus repeats [70]. These results indicated that mammalian H1 linker is involved in transcriptional regulation of genes through an influence on DNA methylation [71]. Importantly, parallel studies performed on *Arabidopsis thaliana* also showed correlation between the H1 level and DNA methylation [72]. The down-regulation of H1 histone levels was reported to result in minor changes in the methylation patterns of repetitive and single-copy sequences [72]. The results suggested a regulatory role of H1 variant in methylation of DNA that occurs both in animals and plants.

In contrast, deletion of an H1-like gene in the *Ascolobus immerses* fungus did not show any effect on methylation-related gene silencing, although it resulted in global methylation, which was not observed in mammalian cells [73].

Interestingly, recent study performed by Wilkinson and colleagues pointed again on a mechanism of genes expression regulation by the H1 linker histones and DNA methylation in the context of the *Rhox* homeobox genes transcription [74]. Despite the fact that *Rhox* genes possess a homeobox, they differ in both sequence and evolutionary origin from the well-characterised *Hox* genes. While *Hox* genes are rather organized in an ancient gene cluster, the *Rhox* cluster seems to have arisen relatively recent in mammals from an ancestral homeobox gene related to the single copy *Drosophila melanogaster aristaless* gene [75, 76]. The newly discovered homeobox gene cluster on the mouse X chromosome was reported to be a major target of H1-mediated repression in mouse ES cells. The results revealed that H1 promotes site-specific methylation of a key regulatory region in *Rhox5* what causes the inhibition of transcription from one of *Rhox5* alternative promoters. As it was demonstrated, H1 depletion results in demethylation and transcriptional induction of a *Pd Rhox5* promoter [74]. Moreover, other genes from *Rhox* cluster were also identified as targets of H1-dependent methylation [74].

Taken together, all these studies suggest more specific roles for the H1 linker histones than being a structural protein. Apart from an essential role in the chromatin compaction, the H1 linker histones are also involved in regulation of gene transcription. Surprisingly, studies of H1 deletion revealed that the linker histones are not general repressors of transcription but rather the transcription regulators of specific genes [29, 73]. Microarray studies performed on *Tetrahymena thermophile* and in yeast organisms, carrying deletion of the H1 linker histone, revealed that only a small number of transcripts displayed up- and down-regulation [29, 77]. This suggested that H1 should not be considered as a protein, which globally represses gene expression.

1.6 Diverse functions of the H1 linker histone variants

As described above, H1 linker histone variants are involved in the chromatin condensation and modulation of the local accessibility of DNA for other proteins which are involved in transcriptional regulation of genes thus in functional state of chromatin.

A specific role for a H1 histone variant was found in studies of myogenic gene *myoD* regulation by the Msx homeoprotein family (Figure 1.4) [35, 78]. The studies revealed that mouse H1b histone variant is recruited to the core enhancer region of *myoD* gene via a specific interaction with the Msx1 protein. This binding is essential for the inhibition of the muscle cell differentiation by the activation and control of the *myoD* gene expression during embryogenesis. These data suggest contribution of particular linker histone subtype to the control of a specific gene locus by the interaction with a transcriptional regulator protein. Another example of the H1functions in transcriptional regulation comes from the studies of mouse *H3.2* histone locus (Figure 1.4) [79]. Murine H1b variant binds specifically to a *cis* regulatory region within the *H3.2* locus where the linker histone variant is required for correct transcriptional repression of the gene [79].

The targeting of H1 linker histones to specific chromatin regions was also observed by the Wilson group that discovered a specific association between H1.1 linker histone and a barrier to the autointegration factor (BAF) [80]. BAF is a DNA binding protein that regulates the chromatin structure presumably by direct and specific binding to the C-terminal domain of the H1.1 histone variant [80].

The interaction of H1 histone variants with transcription regulators appears to be a common mechanism of gene expression regulation. For example, recent studies revealed that one of the human H1 histone variants, H1.5 binds the forkhead box transcription factor FoxP3 that controls the development and function of CD4+CD25+ regulatory T cells [81]. The FoxP3 associates with H1.5 through its zipper domain and this interaction specifically enhances the FoxP3 association at the interleukin-2 (IL-2) promoter and transcriptional repression of the gene in human T cells [81]. Remarkably, the H1.5 depletion inhibits the ability of FoxP3 to repress IL-2 expression in human T regulatory cells and impaired their function in T cells suppression. This indicates that interaction between linker histone H1.5 and FoxP3 is important for the FoxP3-mediated gene expression and in maintaining T regulatory cell functions [81].

Beyond the transcriptional regulation, H1 linker histones can also be associated to other biological processes (Figure 1.4). As mentioned earlier (1.4), H1.2 histone variant showed direct involvement in apoptosis process induced by double strand break DNA damage. Irradiation with X-ray causes dissociation of H1.2 from the chromatin and its translocation into the cytoplasm. The form of histone H1.2 released from the nucleus during X-ray-induced apoptosis seemed to be chemically identical to the nuclear form of this histone. As it is suggested, H1.2 is normally associated with chromatin in the nucleus, but DNA double-strand breaks followed by the p53-dependent repair process may result in its release into the nucleoplasm and then into the cytoplasm [38]. The cytoplasmic fraction of H1.2 variant entails permeabilization of the mitochondrial membrane and in turn release of apoptotic factors [38]. Consistently with these results, the chicken variant H1R was found to be involved in the cellular response to DNA damage [82]. The Hashimoto group presented that chicken DT40 cells which were deficient for the H1R histone variant exhibited increased sensitivity to factors causing DNA damage, but the molecular mechanism still needs to be elucidated [82].
Remarkably, the non-transcription related functions were also assigned to human H1X variant. Studies of Fukui laboratory, which applied RNA interference experiments, revealed that H1X is required for chromosome alignment and segregation as well as for the morphology of spindle [83]. In particular, depletion of H1X histone variant was found to distract attachment of microtubule to the kinetochores [83]. In general, the H1.X is thought to play important functions in mitotic progression [83].
Interestingly, a role of particular H1 histone variants was also described in the context of DNA replication [84]. Studies of De *et al.*, performed on *Xenopus* egg extracts, showed inhibition of DNA replication in response to the presence of H1c, H1t or H1.0 variants [84]. Importantly, earlier studies have already demonstrated that somatic H1 histones are able to inhibit the DNA replication in sperm nuclei by regulation of the pre-replication complexes assembly on chromatin [85]. Molecular analysis revealed that the carboxyl-terminal domain of H1 histones is responsible for the differential binding and inhibition of DNA replication [84].
Furthermore, a recent study of the histone methyltransferase Ezh2 distribution in the round spermatids of mice demonstrated additional function of H1t2 variant during spermiogenesis [86]. Ezh2 was shown to co-localise with H1t2 at the apical pole of round spermatids. Moreover, the H1t2 histone presented specific binding to the histone methyltransferase Ezh2 [86]. These together indicate that in the apical region of the round spermatids methylation of histones influence the spermiogenic chromatin remodeling and probably Ezh2 protein is an essential effector of this event.

Although the H1 linker histones have been shown to interact with many different non-histone nuclear and cytosolic proteins, the majority of studies describing H1-dependent protein-protein interaction have not identified a domain responsible for the interaction. As it has been suggested, both N- and C-terminal tail can be involved in H1 interactions. The N-terminal domain can form a non-amphipathic α-helix motif [70] that may be a site of H1-protein interactions, as it was proposed for HP1 protein [42]. On the other hand, the C-terminal tail may form an amphipathic α-helix motif that creates a hydrophobic surface which can serve as an interaction place [12].

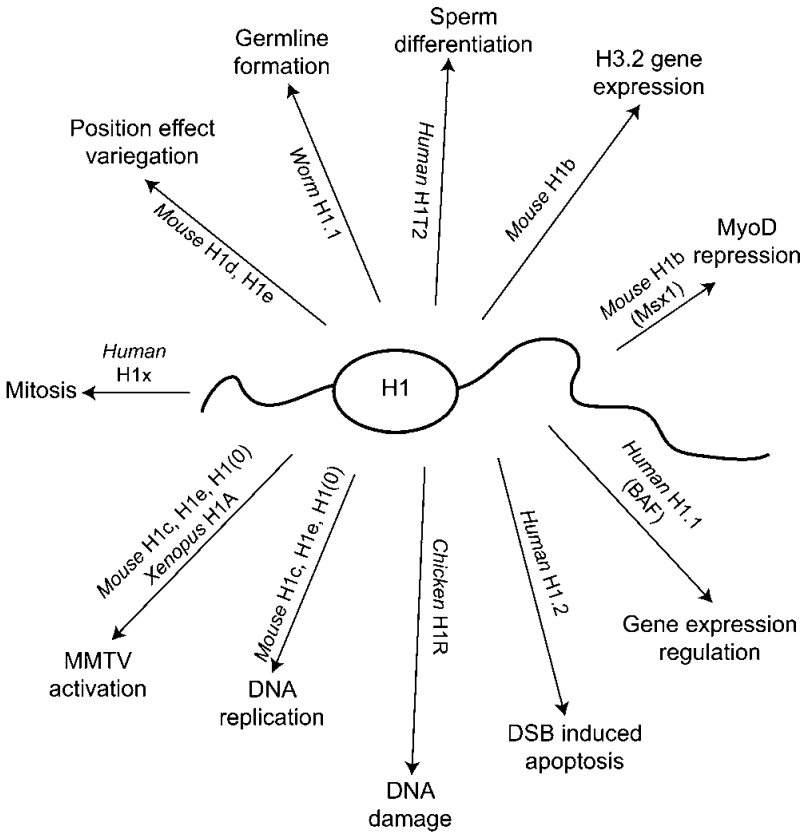

Figure 1.4 Summary of the H1 linker histone functions. Illustration taken from [6].

1.7 A specific chromatin structure and genome organization of *C. elegans*

Studies of the linker histones, performed in lower eukaryotes such as protozoans and yeasts, provided important insights into the biological processes regulated by the H1. While in single-celled organisms, and also in some multicellular eukaryotes the biological functions of H1 are relatively well described, the role of the linker histones in *Caenorhabditis elegans* organism remains unexplained. One reasons for this is the specific chromatin organization across the *C. elegans* chromosomes. The distinct structure of chromatin present in nematode entails suspiciousness with regard to the epigenetic studies performed on this organism.

Caenorhabditis elegans genome is formed in approximately 80% of the single-copy sequences and the remaining 20% account for repetitive sequences that are present in two to ten copies [87, 88, 89]. The metaphase karyotype of the wild type *C. elegans* hermaphrodite contains 12 chromosomes, five pairs of autosomes and one pair of sex chromosomes. *C. elegans* males possess 11 chromosomes with only one sex chromosome [87, 90]. The six chromosomes are almost equal in size, both in terms of DNA content and of recombinational length [91]. Each of the five autosomes exhibit two characteristic regions: a central cluster containing a higher density of more conserved and essential genes, which is flanked by arms with relatively lower number of genes [92, 93]. The arm regions can also be distinguished

from the clusters by a different distribution of repeat sequences [90]. In contrast, the X chromosome does not exhibit such a substantial diversity across its length, in particular, it does not have a gene cluster and it has a significantly lower gene density (6.54 kb per gene) [91]. The most important feature of *C. elegans* chromosomes is that they do not have a single centromere with the localised kinetochores, as it has been observed in mammalian cells (Figure 1.5). Instead, *C. elegans* possesses chromosomes with diffuse kinetochores, which are described as holocentric or holokinetic (Figure 1.5) [93, 94, 95].

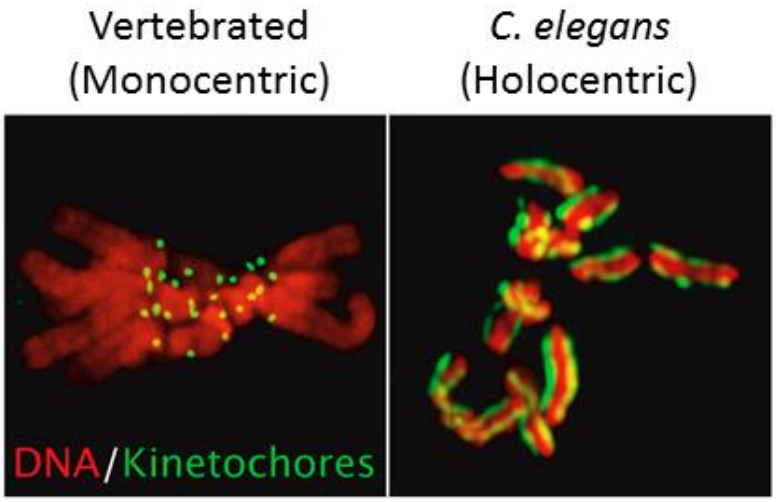

Figure 1.5 Comparison of the structure of mammalian and *C. elegans* metaphase chromosomes. Images presenting the monocentric chromosomes with the localised kinetochores of a vertebrate cell, and the holocentric chromosomes with the diffuse kinetochores present in a *C. elegans* embryo. Illustration taken from [96].

The telomeres of *C. elegans* form 4-9 kb long blocks of the tandemly repeated hexanucleotide sequences TTAGGC which are closely related to the vertebrate repeat TTAGGG [87, 97, 98]. Additionally, the blocks of TTAGGC repeats may also be present in the internal part of the *C. elegans* genome [87, 99]. In contrast to other species, *C. elegans* do not have specific subtelomeric regions. Each of these regions has its unique subtelomeric sequence and many of them possess repetitive DNA, such as satellite-like tandem repeats [87].

1.8 *C. elegans* histones

Despite significant differences in the chromatin structure, *C. elegans* is a good model organism for the study of the function of particular core and linker histone variants and their influence on the nematodes development.

The genes of *C. elegans* core histone are organized in pairs, H3-H4 and H2A-H2B, and contain two 5′ conserved sequences in the common spacer regions [100]. Importantly, these two sequence elements are not present in other organisms. They are also not found in non-histone genes of *C. elegans*. However, these sequences, which are thought to be regulatory elements of *C. elegans* core histone genes, are similar to the regulatory elements of both

higher and lower eukaryotes. The *C. elegans* core histones display very high similarity in structure (no less than 80% identical amino acid sequence) when compared to the human histones but also to other organisms [101-104]. For example, *C. elegans* N-terminus of the H2B histone shows high degree of sequence homology to the corresponding region in H2B from *Drosophila melanogaster*, mollusc *Patella* and from starfish *Asterias* [101]. Furthermore, H3 and H4 proteins exhibit respectively 97% and 98% similarity to their human orthologs at the level of the amino acid sequences.

Consequently, the properties and the protein sequences of genes encoding histone H1 proteins are similar to histone H1 proteins of higher eukaryotes. A family of *C. elegans* linker histone H1 consists of eight single copy genes: *hil-1*, *hil-2*, *hil-3*, *hil-4*, *hil-5*, *hil-6*, *hil-7* and *his-24* [100]. Unlike the majority of mammalian linker histone genes, all *C. elegans* histone genes contain introns and encode polyadenylated mRNAs [35, 56, 106]. Additionally, the linker histone variant genes of *C. elegans* are dispersed individually in the genome, in contrast to clustered somatic H1 variants presented in mammals [35, 106]. As it was observed in mammalian histone paralogs [6], *C. elegans* linker histone variants display highly conserved globular domain (85% sequence similarity among variants), but the N- and C-terminal tails show strong variability (about 46% similarity in sequence encodes for C-terminal end) (Figure 1.7) [107].

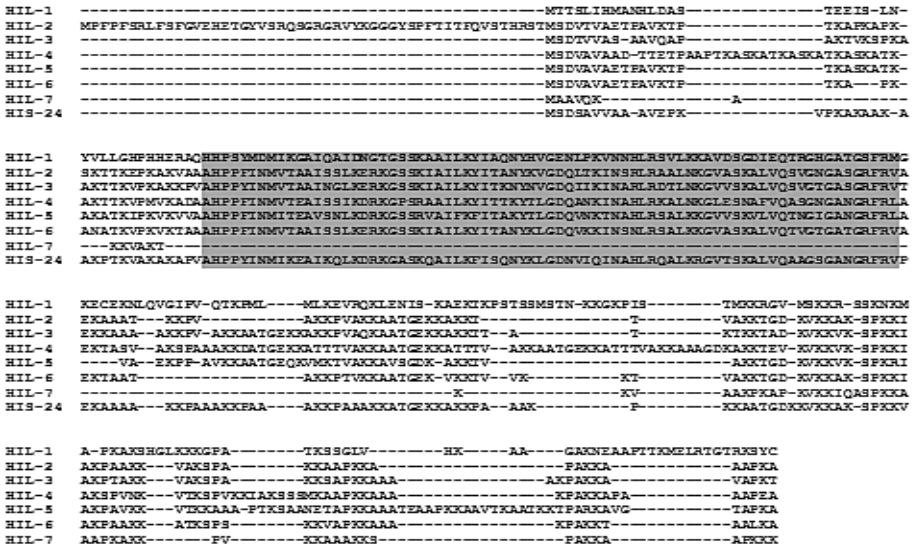

Figure 1.6 Alignment of all the *C. elegans* H1 variants. Alignment of amino-acid sequence by the ClustalW method followed by manual editing. The conserved globular domain is highlighted in grey.

Despite the fact that the first two histone H1 proteins, HIS-24 and HIL-2, were described for the first time more than twenty years ago, still very little is known about the function of all *C. elegans* linker histone variants [108, 109].

Linker histone protein HIL-1, also known as H1.X variant, was initially identified and described by the Jedrusik M.A. and Schulze E. [107]. This histone exhibits a three-domain structure with the conserved globular motif and highly divergent terminal ends (Figure 1.6) [107, 110]. Remarkably, unlike other *C. elegans* variants, HIL-1 does not possess

characteristic lysine-rich N-terminal domain. Instead, the HIL-1 external domains contain highly hydrophobic amino acid residues: tyrosine and leucine [110]. These amino acids are involved in hydrophobic interactions, which are not characteristic for linker histone variants. As it was suggested by the Schulze group, the terminal domains of HIL-1 variant may display different folding and it may be responsible for distinct biochemical interaction than N- and C-terminus of other histones [110]. Interestingly, HIL-1 protein is mainly expressed in the cytoplasm of a several cell types, such as the marginal cells, epithelial cells of pharynx, the body-wall and vulva muscle cells as well as in some head neurons and excretory cells [110]. The observation of HIL-1 expression in the marginal cells revealed that this protein is associated with intermediate filaments, in particular with the tonofilaments [110]. Moreover, since HIL-1 depletion results in a decreased number of the marginal cells and the elongated pharynx phenotype, this histone variant is thought to be involved in the development of muscles and in the basic muscular function [109]. Additionally, *C. elegans* HIL-1 protein was found to be associated with the nucleolus, where it co-localises with fibrillarin [110].

HIL-2 linker histone is the one of the first identified *C. elegans* variants that also exhibits three-domain structure [109]. In HIL-2 protein, the central globular motif and most of the C-the terminus are relatively conserved contrary to the N-terminal end which is strongly diverged in comparison to other variants [109]. Moreover, HIL-2 C-terminal end exhibits two potential phosphorylation sites [109]. Analysis of the secondary-structure prediction revealed a high potential for α-helix formation in the C-terminal region of HIL-2 [109]. Although primary and secondary structure of this linker histone variant is relatively well described, its localisation and function in *C. elegans* still needs to be examined.

Histone HIS-24, apart from HIL-2, was the first purified and sequenced linker variant [108, 109]. It is also the most characterised one among all *C. elegans* linker histones [108, 109, 110]. Despite the fact that the nematode *his-24* gene shares a relatively small sequence identity with genes of the H1 family derived from other organisms, the main structure of HIS-24 protein has been well conserved [108, 109]. A tripartite domain structure consists of a central hydrophobic core with about 80 residues, flanked by an N-terminal domain which is slightly acidic at the very N-terminus, but very basic further on, and a lysine-, alanine- and proline-rich C-terminus (Figure 1.7) [108]. Another characteristic feature of the HIS-24 linker histone is the occurrence of repetitive motifs in the C-terminal domain, such as AAAKKP, KKPAAA, and AKPAA (Figure 1.7) [108].

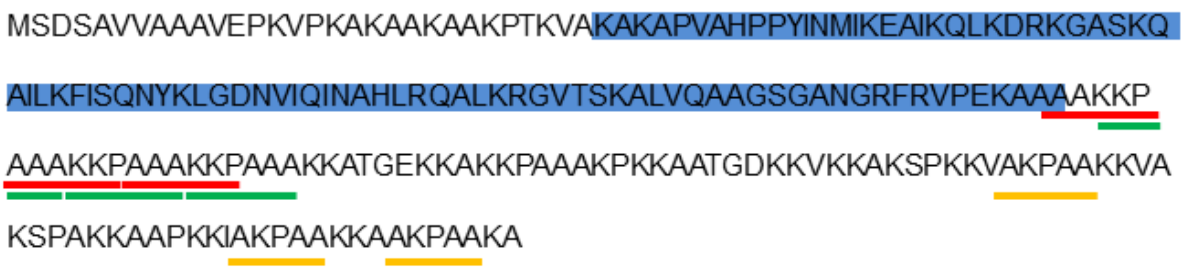

Figure 1.7 Amino acid sequence of the *C. elegans* HIS-24 linker histone variant. The globular domain is highlighted in blue. Individual repeated sequences are underlined with different line colors.

Interestingly, the HIS-24 histone variant is the most abundant in *C. elegans* organism. The majority of expressed sequence tags among the H1 gene family belong to *his-24* gene (24% of all H1) [110]. Expression of HIS-24 protein is observed in all somatic cells from the eight-cell stage embryo, but this protein is also detected in the germline of both hermaphrodites and males [110, 111]. Germline HIS-24 expression starts at late L3 larva stage of hermaphrodite, at the same time as gonad development [111]. Surprisingly, germline HIS-24 protein does not have a nuclear expression at that stage, but instead, it associates with cytoplasmic peculiar granular structures surrounding the nuclei [111]. Cytoplasmic HIS-24 variant is observed during most developmental stages of the germline and only during late pachytene stage a small fraction of HIS-24 associates with chromatin [111]. It is, however, absent in the primordial germ cells Z2 and Z3 [111]. Additionally, cytoplasmic HIS-24 protein is also detected in germline of *C. elegans* males [111]. Importantly, right after the fertilization HIS-24 variant translocates to the germline nuclei and associates with chromatin [111]. Remarkably, the HIS-24 linker histone variant was found to be essential for chromatin silencing and for *C. elegans* germline development. As it was observed by the Schulze group, depletion of *his-24* by double stranded RNA-mediated interference (RNAi) resulted in loss of gene silencing in the germline [111]. Similarly, *his-24(ok1024)* mutant animals showed de-silencing of the germline genes that was characterised by an increased level of the activating H3K4 methylation mark and by a decrease of the repressive H3K9 methylation [111]. Furthermore, hermaphrodites either with knockdown of *his-24* gene or *his-24* deletion displayed substantial abnormalities in gonad structure as well as in germline proliferation and differentiation, such as lack of differentiated oocytes [110]. These observed defects resulted in reduced fertility of *C. elegans* [110]. Interestingly, similar phenotype is observed in *C. elegans* with deletion of *mes* genes encoding for histone methyltransferase for H3K27me3 [110, 111, 112]. Moreover, the cytoplasmic retention of HIS-24 was found to be lost in animals with mutation of a single *mes* gene: *mes-2*, *mes-3*, *mes-4* or *mes-6* as well as in *sir-2.1* mutant animals, lacking histone deacetylase [111]. In particular, the germline of *his-24(ok1024); mes-3(bn35)* double mutant animals exhibited more reduced level of the repressive H3K27 methylated than in the respective *mes* single mutant [111]. Importantly, further studies performed by the Jedrusik-Bode group demonstrated that HIS-24 histone variant specifically interacts with the H3K27 region, when unmodified or tri-methylated [113, 114]. In addition, recent analysis of the HIS-24 linker histone biology revealed that this variant possesses a single methylation site at lysine 14. Remarkably, HIS-24 is the only linker histone in *C. elegans* that can be methylated, but the function of this post-translational modification is still unknown.

1.9 *C. elegans* heterochromatin protein 1 (HP1)

Recent studies of the HIS-24 linker histone functions pointed at two homologs of mammalian heterochromatin protein 1 (HP1), HPL-1 and HPL2, as a potential interaction partners of *C. elegans* H1 protein [115].

HP1 proteins are essential components of the heterochromatin and contribute to the transcriptional repression of genes [116, 117]. All HP1 proteins are characterised by the presence of two highly conserved domains, chromodomain (CD) and chromo shadow domain (CSD), which are separated by the variable hinge region (Figure 1.8 A, B), [118]. Chromo domain is localised at the N-terminal region and it is essential for the association with the methylated lysine 9 on the histone H3, whereas chromo shadow domain is present at the C-terminal end promoting homodimerization and protein-protein interactions in the nucleus [116, 118, 119].

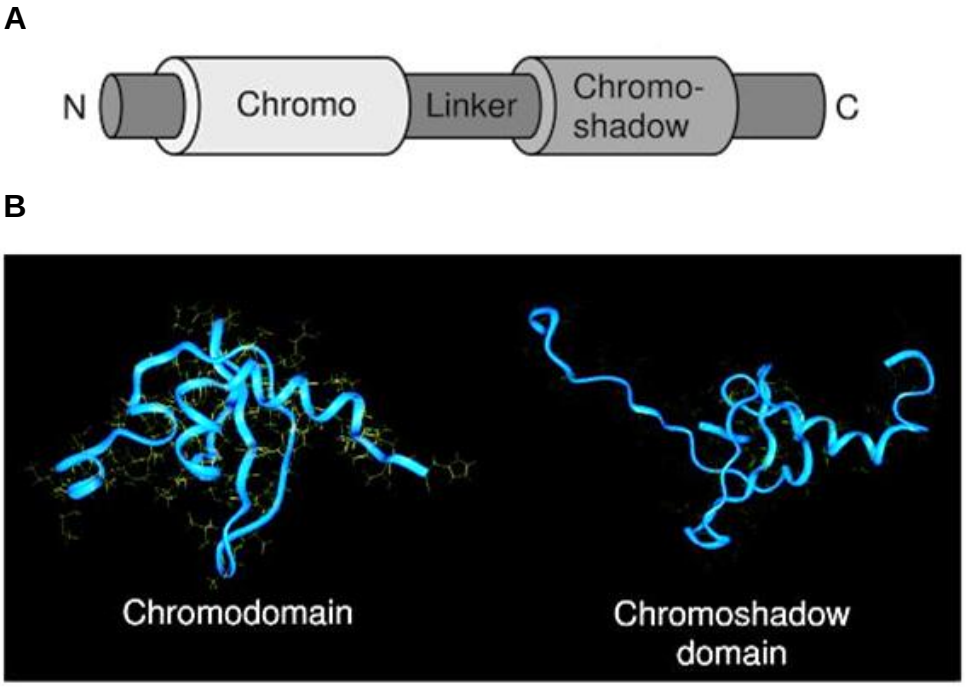

Figure 1.8 Structure of the HP1 protein. The conserved linear structure of HP1 proteins with N-terminal chromodomain and C-terminal chromo shadow domain **(A)**. The three-dimensional structures of the chromodomain and chromo shadow domain of murine HP1β **(B)**. Figure taken from [120].

All metazoan usually possess several members of the HP1 family that differ in their distribution and function. For example, the mammalian HP1 family consists of at least three members, H1α which is predominantly localised to centromeres, H1β which exhibits wide distribution along chromosomes, and H1γ which associates with euchromatin regions [116, 119].

C. elegans has two HP1 homologues, HPL-1 and HPL-2, that exhibit a conserved two-domain protein structure. Both proteins show 48% of similarity at the amino acid level with very high homology within the chromo and chromo shadow domains [121]. Localisation studies show that both HPL-1 and HPL-2 are ubiquitously expressed nuclear proteins [116,121]. However, HPL-1 and HPL-2 expression patterns do not overlap completely. Expression of HPL-1 starts in 50-cell stage embryo and stays through larval and adult stages. HPL-1 protein is present in most, but not all, cells and its expression is strong in the head and tail hypodermal and

neuronal nuclei [121]. HPL-2 protein is presented in nuclei through the all life cycles with expression also observed in the germline and developing oocytes [121]. While the exact function of HPL-1 protein still needs to be elucidated, HPL-2 is known to be involved in both somatic and germline development [121]. In the somatic cells, *hpl-2* gene is essential for the vulva cell fate specification as a member of the synMuv (synthetic multivulva) pathway [112, 120]. In the germline, HPL-2 protein is important for the proper development of germ cells and for the chromatin based silencing mechanism [116, 119, 121]. Moreover, *hpl-2* negatively regulates RNA-mediated interference (RNAi) probably through the repression of RNAi genes in the somatic cells [122]. Studies of Palladino and colleagues show that, although *hpl-1* alone has no attributed role, it appears to have a redundant function with *hpl-2* in larval development as well as in somatic gonad and germline development [116].

1.10 Open questions and objective of PhD thesis

In the last years the chromatin field has focused on the biology of core histones, in particular on their modifiers and the influence on chromatin organization. Hence the linker histone H1 has been somehow found beyond the main field of interest and therefore we currently begin to understand its biological role.

Recent studies pointed to post-translational modifications (PTM) as an essential mechanism of regulation of the H1 linker histone functions [27, 60-69]. Although the analysis of H1 protein in mammals has provided key insights into the role of post-translational modifications, still little is known about the functionality of most of modification sites, their modifiers, and putative interaction partners. Furthermore, it is not known whether the post-translational modifications of H1 are dynamic during the development of a multicellular organism or the changes are linked to certain functions.
Caenorhabditis elegans is a simple, multicellular organism and an outstanding model to study chromatin regulation in cellular and developmental processes. It possesses a family of linker histones whose covalent post-translational modifications are just being discovered. As mentioned in section 1.7, *C. elegans* HIS-24 protein exhibits one methylation site at lysine position 14. Currently, it is not known whether this post-translational modification is essential for the proper function of HIS-24 protein and if so, what the biological consequences of this biochemical change are.
Furthermore, as described in section 1.4, mammalian HP1 was found to bind specifically to linker histone H1.4K26me2 [42]. Despite the fact that *C. elegans* HPL proteins, homologs of mammalian HP1, were identified as putative interaction partners of HIS-24, there is no indication to date for the eventual function of the HIS-24-HPL interplay.

The aim of my PhD thesis was to elucidate the influence of post-translational modifications on the biology of the HIS-24 linker histone in the context of gene regulation. A further goal was to characterise the physiological nature of HIS-24-HPL interaction and the mechanism through which these proteins regulate the transcription of genes.

2 Materials and methods

2.1 Materials

2.1.1 Laboratory equipment

Generally used laboratory equipment is summarized in Table 2.1.

Table 2.1 Generally used laboratory equipment.

Equipment	Manufacturer
AGFA Curix 60 Film Processor	Agfa HealthCare, Bonn
Beckman Centrifuge, Model CS-15R	Beckman, Krefeld
Biofuge pico	Heraeus, Hanau
Biofuge primo R	Heraeus, Hanau
Bio Rad Criturion blotter	Bio Rad, München
Bio Rad Power Pac 300, power supply	Bio Rad, München
Bio Rad Sub-Cell® Model 192	Bio Rad, München
Branson Digital Sonifier	Branson Ultrasonics, Danbury (USA)
Eppendorf Centrifuge, Model 5417R	Eppendorf AG, Hamburg
Eppendorf Centrifuge, Model 5430	Eppendorf AG, Hamburg
Eppendorf Research pipettes	Eppendorf AG, Hamburg
Freezer -20°C Liebherr	Liebherr, Bulle Switzerland
Freezer -20°C Liebherr Comfort	Liebherr, Bulle Switzerland
Freezer -80°C Profiline	National Lab GmbH, Mölln
Gel iX Imager	Intas, Göttingen
GFL Water Bath	LAT, Garbseb Berenbostel
Heraeus BBD 6220 incubator	Thermo Scientific, Braunschweig
Heraeus kelvitron ® t incubator	Thermo Scientific, Braunschweig
Heraeus herasafe sterile hood	Thermo Scientific, Braunschweig
Horizontal Mixer RM5-V	CAT Ingenieurbüro, Staufen
HulaMixer™ Sample Mixer	Invitrogen, Karlsruhe
Hypercassette™ (18x24)	GE Healthcare, Buckinghamshire (UK)
iCycler Optical Module 584BR	Bio Rad, München
Laboratory balance TP-3002	Denver Instrument, Göttingen
Leica DM IRB microscope	Leica, Wetzlar
Leica DMI 6000 B microscope	Leica, Wetzlar

Mastercycler® gradient	Eppendorf AG, Hamburg
Multitron 2 incubator shaker	Infors AG, Bottmingen/Basel Switzerland
NanoDrop® ND-100 Spectrophotometer	PeqLab, Erlangen
Pipetus®	Hirschmann Laborgeräte GmbH & Co.KG, Eberstadt
pH/Pt 1000-Sensor SE 100 N	Knick, Berlin
SANYO MIR-154 incubator	SANYO E&E Europe, The Hague The Netherlands
Thermomixer comfort	Eppendorf AG, Hamburg
Wild M5 Stereomicroscope	Wild Heerbrugg AG, Gais Switzerland
Vortex Top-Mix 94323	Bioblock Scientific, Frenkendorf
XCell SureLock™ Mini-Cell	Invitrogen, Karlsruhe

2.1.2 Chemicals

Chemicals used for buffers, solutions, and media are summarized in Table 2.2.

Table 2.2 Generally used chemicals.

Chemicals	Manufacturer
1,4-Piperazinediethanesulfonic acid (PIPES)	Sigma-Aldrich GmbH, Steinheim
Acetic acid	Merck, Mannheim
Agarose NEEO Ultra-Qualität	Carl Roth GmbH, Karlsruhe
Albumin, bovine serum (BSA)	Sigma-Aldrich GmbH, Steinheim
Ampicillin sodium salt	ApliChem GmbH, Darmstadt
Calcium chloride ($CaCl_2$)	Merck, Mannheim
Chloroform	Merck, Mannheim
Cholesterol	Sigma-Aldrich GmbH, Steinheim
Citric acid	Merck, Mannheim
Cooper (II) sulfate pentahydrate ($CuSO_4 \cdot 5H_2O$)	Sigma-Aldrich GmbH, Steinheim
Complete EDTA-free Coctail Tablets	Roche, Mannheim
Dimethylsulfoxid (DMSO)	Sigma-Aldrich GmbH, Steinheim
Disodium hydrogen phosphate (Na_2HPO_4)	Merck, Mannheim
DL-Dithiothreitol (DTT)	Alexis Biochemicals, Lörrach
Ethanol (EtOH)	Merck, Mannheim

Ethylenediaminetetraacetate (EDTA)	Carl Roth GmbH, Karlsruhe
Ethylenediaminetetraacetic acid disodium salt dihydrate (Na_2EDTA)	Sigma-Aldrich GmbH, Steinheim
Gelatin	Sigma-Aldrich GmbH, Steinheim
Glucose	ApliChem GmbH, Darmstadt
Glycerol	Merck, Mannheim
Glycine	Merck, Mannheim
Hepes	Sigma-Aldrich GmbH, Steinheim
Hydrochloric acid fuming 37% (HCl)	Merck, Mannheim
Iron (II) sulfate heptahydrate ($Fe_2SO_4 \cdot 7H_2O$)	Sigma-Aldrich GmbH, Steinheim
Isopropanol	Merck, Mannheim
Isopropyl-β-D-thiogalactopyranosid (IPTG)	Carl Roth GmbH, Karlsruhe
Lithiumchlorid	Carl Roth GmbH, Karlsruhe
Kanamycin sulfate	ApliChem GmbH, Darmstadt
Magnesium chloride ($MgCl_2$)	Merck, Mannheim
Magnesium sulfate ($MgSO_4$)	Merck, Mannheim
Manganese (II) chloride tetrahydrate ($MnCl_2 \cdot 4H_2O$)	Sigma-Aldrich GmbH, Steinheim
Methanol (MeOH)	Merck, Mannheim
Methylviologen dichloride hydrate (Paraquat)	Sigma-Aldrich GmbH, Steinheim
N- Lauroylsarcosine sodium salt solution	Sigma-Aldrich GmbH, Steinheim
Nonfat dried milk powder	ApliChem GmbH, Darmstadt
Nonidet™ P 40 Substitute (NP40)	Sigma-Aldrich GmbH, Steinheim
N-Z-amine A	Sigma-Aldrich GmbH, Steinheim
Paraformaldehyde (PFA)	Carl Roth GmbH, Karlsruhe
Peptone	Carl Roth GmbH, Karlsruhe
peqGOLD Low Melt Agarose	PEQLAB Biotechnologie GmbH, Erlangen
Phenol/Chloroform/Isoamyl alcohol	Carl Roth GmbH, Karlsruhe
Potassium chloride (KCl)	Merck, Mannheim
Potassium hydroxide (KOH)	Carl Roth GmbH, Karlsruhe
Potassium dihydrogen phosphate (KH_2PO_4)	Merck, Mannheim
Select Agar®	Invitrogen, Karlsruhe

Sodium Acetate	Merck, Mannheim
Sodium chloride (NaCl)	Merck, Mannheim
Sodium deoxycholate	Sigma-Aldrich GmbH, Steinheim
Sodium dodecyl sulfate (SDS)	SERVA Electrophoresis GmbH, Heidelberg
Sodium hydroxide (NaOH)	Merck, Mannheim
Sodium hypochlorite solution	Merck, Mannheim
Tris(hydroxymethyl)aminomethan (Tris)	VWR International, Hannover
Triton® X-100	Merck, Mannheim
Tween 20	Sigma-Aldrich GmbH, Steinheim
Yeast extract	Life Technologies, Karlsruhe
Zinc sulfate heptahydrate	Sigma-Aldrich GmbH, Steinheim

2.1.3 Consumables and reagents

Generally used consumables and reagents are listed in Table 2.3.

Table 2.3 Generally used consumables and reagents.

Consumables and reagents	Supplier
0.05% Trypsin-EDTA (1x)	Gibco, München
0.2 ml PCR Tubes	Eppendorf AG, Hamburg
4',6-diamidino-2-phenylindole (DAPI)	Molecular Probes®, Karlsruhe
6x Mass Ruler Loading Dye	Fermentas, St. Leon-Rot
Abgene® PCR Plates	Thermo Fisher Scientific, Rockford (USA)
Acrodisc Sterile Syringe Filters	Pall GmbH, Dreieich
Amersham Hybond™ ECL™	GE Healthcare, Buckinghamshire (UK)
Amersham Hyperfilm ECL (18x24)	GE Healthcare, Buckinghamshire (UK)
ATX Ponceau S red staining solution	Fluka Analytical, Seelze
Centrifuge Tubes 50 ml	Vwr, Batavia (USA)
Complete, EDTA-free, Protease Inhibitor Cocktail Tablets	Roche, Mannheim
Costar® 2ml, 5ml,10mL, 25ml, 50ml Stripette® Serological Pipets	Corning Incorporated, Lowell (USA)
Cryogenic Vials	Nalge Nunc, Rochester (USA)
Dulbecco's Modified Eagle Medium (DMEM) GlutaMAX™, high glucose, pyruvate	Gibco, München

Dulbecco's Phosphate-Buffered Saline (DPBS)	Gibco, München
Eppendorf Tubes 1.5 ml	Eppendorf AG, Hamburg
Fetal Bovine Serum (Heat Inactivated) (FBS)	Gibco, München
FuGENE® HD Transfection Reagent	Roche, Mannheim
GeneRuler™ 100bp DNA Ladder	Fermentas, St. Leon-Rot
GeneRuler™ 100 bp Plus DNA Ladder	Fermentas, St. Leon-Rot
GFP-Trap®-A beads	Chromotek, Planegg-Martinsried
Glycogen	Fermentas, St. Leon-Rot
GR safe DNA stain	Excellgen, Rockville (USA)
Lab-Tek™ II - CC2™ Chamber Slide™	Thermo Fisher Scientific, Rockford (USA)
Opti-MEM® Reduced Serum Medium, GlutaMAX™	Gibco, München
LumiGLO® and Peroxide	Cell Signaling Technology, Frankfurt am Main
Microscope Cover Glasses 22 x 22 mm	Menzel, Braunschweig
Mowiol® 4-88	Polysciences Europe GmbH, Eppelheim
Nunc EasYFlasks™ Nunclon™Δ	Nunc GmbH & Co. KG, Wiesbaden
NuPAGE® LDS Sample Buffer	Invitrogen, Karlsruhe
NuPAGE® MOPS SDS Running Buffer	Invitrogen, Karlsruhe
NuPAGE® Novex® 4–12% Bis-Tris Gels	Invitrogen, Karlsruhe
NuPAGE® Sample Reducin Agent	Invitrogen, Karlsruhe
Nystatin (100x)	Sigma-Aldrich GmbH, Steinheim
Penicillin- Streptomycin-Neomycin solution (100x)	Gibco, München
Petri dishes Ø 55 mm, Ø 90 mm, Ø 140 mm	VWR International, Hannover
Pierce® Protein G Agarose	Thermo Scientific, Rockford (USA)
Pierce® Streptavidin Agarose Resin	Thermo Scientific, Rockford (USA)
Polystyrene Round-Bottom Tubes 14 ml	Becton Dickinson Labware, Franklin Lakes (USA)
Proteinase K	Fermentas, St. Leon-Rot
Restore™ Western Blot Stripping Buffer	Thermo Scientific, Rockford (USA)
SeeBlue® Plus2 Pre-Stained Standard	Invitrogen, Karlsruhe
VECTASHIELD® Mounting Medium	Vector Laboratories, Burlingame (Canada)
Western Blotting Filter Paper	Thermo Scientific, Rockford (USA)

2.1.4 Media and stocks

Generally used media and stocks are described below.

Ampicillin stock solution (100 mg/ml)

Dissolve 1g of ampicillin in 10 ml of ddH_2O. Filter through a 0.22 µm filter to sterilize. Aliquot and store at -20°C.

Cholesterol stock solution (5 mg/ml)

Dissolve 50 g of cholesterol in 10 ml in 95% ethanol. Do not sterilize.

IPTG stock solution (1M)

Dissolve 2.38 g of IPTG in 8 ml ddH_2O. Bring to a final volume of 10ml. Filter through a 0.22 µm filter to sterilize. Aliquot and store at -20°C.

Kanamycin stock solution (50 mg/ml)

Dissolve 0.5 g of ampicillin in 10 ml of ddH_2O. Filter through a 0.22 µm filter to sterilize. Aliquot and store at -20°C.

Lysogen broth (LB) agar (1L)

Peptone	10 g
Yeast extract	5 g
NaCl	10 g
Agar	15 g

Adjust volume to 1 liter with dH_2O and autoclave.

Lysogen broth (LB) medium (1L)

Peptone	10 g
Yeast extract	5 g
NaCl	10 g

Adjust volume to 1 liter with dH_2O and autoclave.

NZY^+ broth medium (1L)

NZ amine (casein hydrolysate)	10 g
Yeast extract	5 g
NaCl	5 g

Adjust volume to 1 liter with H_2O, bring the pH to 7.5 and autoclave. Add the following, sterilized supplements prior to use

1M $CaCl_2$	12.5 ml
1M $MgSO_4$	12.5 ml
20% (w/v) glucose	20 ml

Standard worm Nematode Growth Medium (NGM) agar (1L)

NaCl	3 g
Agar	17 g
Peptone	2.5 g
Cholesterol (5 mg/ml in ethanol)	1 ml
dH_2O	973 ml

Autoclave and add the following sterilized supplements prior to use:

1M $CaCl_2$	1 ml
1M $MgSO_4$	1 ml
1M KPO_4, pH 6.0	25 ml

2.1.5 Buffers and solutions

Commonly used buffers and solutions are described below.

Buffers and solutions used in *C. elegans* culturing

Freezing Solution (1L)

NaCl	5.85 g
KH_2PO_4	6.8 g
Glycerol	300 g
1 M NaOH	5.6 ml

Adjust volume to 1 liter with dH_2O and autoclave. Using sterile technique add 1M $MgSO_4$.

Lysis buffer for Single Worm PCR

Tris-HCl, pH 8.3	10 mM
KCl	50 mM
MgCl2	2.5 mM
NP40	0.45 %
Tween 20	0.45 %
Gelatin	0.01 %

Autoclave and freeze at -20°C.

M9 buffer (1L)

KH_2PO_4	3 g
Na_2HPO_4	6 g
NaCl	5 g
1M $MgSO_4$	1 ml

Adjust volume to 1 liter with dH_2O and autoclave.

K phosphate buffer (KPO_4), pH 6.0 (1L)

KH_2PO_4	136.1 g
KOH	17.9 g

Adjust volume to ~750 ml with dH_2O, bring the pH to 6.0 and autoclave.

S Basal (1L)

NaCl	0.1 M
K phosphate, pH 6.0	50 ml
Cholesterol (5 mg/ml in ethanol)	1ml

Adjust volume to 1 liter with dH_2O and autoclave.

Trace metals solution 100x (500ml)

$Fe_2SO_4 \cdot 7H_2O$	0.346 g
Na_2EDTA	0.93 g

$MnCl_2 \cdot 4H_2O$	0.098 g
$ZnSO_4 \cdot 7H_2O$	0.144 g
$CuSO_4 \cdot 5H_2O$	0.012 g

Adjust volume to 1 liter with dH_2O. Autoclave and keep in the dark.

S medium for *C. elegans* liquid culture

S basal	1 liter
1M potassium citrate pH 6	10 ml
Trace metals solution	10 ml
1M $CaCl_2$	3 ml
1M $MgSO_4$	3 ml
Penicillin/Streptomycin/Neomycin	1 x
Nystatin	1 x

Salts solution

PIPES pH 7.0	50 mM
KCl	25 mM
$MgSO_4$	1 mM
NaCl	45 mM
$CaCl_2$	2 mM

Buffer for agarose gel electrophoresis

TAE buffer 50x (1L)

Tris base	242 g
Acetic acid	57.1 ml
0.5 M EDTA pH 8.0	100 ml
dH_2O	800 ml

Adjust the pH to 8.5. Add H_2O to 1 liter.

Buffers used for western blot assay

Phosphate- buffered saline (PBS) buffer 10x (1L)

NaCl	80 g
KCl	2 g
Na_2HPO_4	14.4 g
KH_2PO_4	2.4 g
dH_2O	800 ml

Adjust the pH to 7.4. Add H_2O to 1 liter.

PBS-T buffer

PBS	1x
Tween 20	0.1%

Transfer buffer 10x (TB)

Tris base	30.3 g
Glycine	144.1 g

Adjust volume to 1 liter with dH_2O.

Buffers used for peptide pull-down assay

C Buffer

Hepes, pH 7.9	20 mM
KCl	420 mM
$MgCl_2$	1.5 mM
EDTA	0.2 mM
Glycerol (v/v)	25 %
protease inhibitors (freshly added)	
DTT to 1 mM (freshly added)	

PD 150 buffer

Hepes, pH 7.9	20 mM
KCl	150 mM
Triton X-100	0.2 %
Glycerol (v/v)	20 %

Buffers used for chromatin immunoprecipitation assay

FA buffer

Hepes/KOH pH 7.5	50 mM
EDTA	1 mM
NaCl	150 mM
Triton X-100	1 %
Sodium deoxycholate	0.1 %

FA-1 M NaCl buffer

Hepes/KOH pH 7.5	50 mM
EDTA	1 mM
NaCl	1 M
Triton X-100	1 %
Sodium deoxycholate	0.1 %

FA-500 mM NaCl buffer

Hepes/KOH pH 7.5	50 mM
EDTA	1 mM
NaCl	500 mM
Triton X-100	1 %
Sodium deoxycholate	0.1 %

TEL buffer

LiCl	0.25 M
EDTA	1 mM
Tris-HCl, pH 8.0	10 mM
NP-40	1 %
Sodium deoxycholate	1 %

TE buffer

Tris-Cl, pH 7.5	10 mM
EDTA	1 mM

Elution buffer

NaCl	250 mM
SDS in TE	1 %

Solution for fixation of cells

PFA solution 4%

Paraformaldehyde	10 g
10 N NaOH	50 µl
PBS 10x	25 ml
ddH_2O	200 ml

2.1.6 Kits

Generally used kits are listed in Table 2.4.

Table 2.4 Generally used kits.

Kits	Supplier
QuikChange XL Site-Detected Mutagenesis Kit	Stratagene, La Jolla (USA)
QIAquick gel Extraction Kit	Qiagen, Hilden
Zero Blunt® TOPO® PCR Cloning Kit for Sequencing	Invitrogen, Karlsruhe
MSB® Spin PCRapace	Stratec Molecular GmbH, Berlin
Wizard® Plus SV Minipreps DNA Purification System	Promega, Madison (USA)
EndoFree® Plasmid Maxi Kit	Qiagen, Hilden

2.1.7 Enzymes

Generally used enzymes are listed in Table 2.5.

Table 2.5 Generally used enzymes.

Enzyme	Supplier
Antarctic phosphatase	New England Biolabs (NEB), Ibswich (USA)
*Dpn*I, *Hind*III, *Kpn*I	New England Biolabs (NEB), Ibswich (USA)
KOD DNA Polymerase	Novagen, Darmstadt
iQ™ SYBR® Green Supermix	Bio Rad, München
Pwo DNA Polymerase	Roche, Mannheim
T4 DNA Ligase	New England Biolabs (NEB), Ibswich (USA)
T4 DNA Ligase	Roche, Mannheim
T4 DNA Poymerase	New England Biolabs (NEB), Ibswich (USA)
Taq DNA Polymerase (recombinant), LC	Fermentas, St. Leon-Rot

2.1.8 Antibodies

Generally used antibodies are listed in Table 2.6.

Table 2.6 Generally used antibodies.

Name	Manufacturer, catalog number	Host species	Applications	Dilution
Primary antibodies:				
anti-GFP	Abcam, ab 6556	rabbit, polyclonal	WB	1:2500
anti-GFP	Roche	mouse, monoclonal	ChIP IP WB	1 µg 10 µg 1:1000
anti-EGL-5	S.W. Emmons	rabbit, polyclonal	WB	1:100
anti-HIS-24	Charles River Laboratories International	rabbit, polyclonal	IF IP WB ChIP	1:800 1 µg 1:20000 3 µg
anti-HIS-24me1	Charles River Laboratories International	rabbit, polyclonal	IF EM IF WB	1:500 1:80 1:10000
anti-HPL-1	F. Palladino	rabbit, polyclonal	WB	1:2000
anti-HPL-2	F. Palladino	rabbit, polyclonal	WB	1:2000
anti-H3	Abcam,ab 1791	rabbit, polyclonal	ChIP IP WB	1.5 µg 1.5 µg 1:10000
anti-H3K4me3	Abcam, ab 1012	mouse, monoclonal	ChIP IF IP WB	10 µg 1:100 10 µg 1:1000
anti-H3K9me2	Abcam, ab 1220	mouse, monoclonal	ChIP IP WB	4 µg 3 µg 1:1000
anti-H3K9me3	Abcam, ab 8898	rabbit, polyclonal	IP WB	5 µg 1:1000
anti-H3K27me2	Upstate, 07-322	rabbit, polyclonal	ChIP IP WB	3 µg 12 µg 1:500
anti-H3K27me3	T. Jenuwein	rabbit, polyclonal	ChIP IP WB	3 µg 3 µg 1:20000
anti-H4K20me3	Abcam, ab 9053	rabbit, polyclonal	IP	2.5 µg
Secondary antibodies:				
Alexa Fluor® 488 anti-rabbit	Molecular Probes	goat	IF	1:500
Alexa Fluor® 555	Invitrogen A21422	goat	IF	1:500

anti-mouse IgG				
Alexa Fluor® 555 anti-rabbit IgG	Invitrogen, A21428	goat	IF	1:500
anti-rabbit IgG, HRP-linked	Cell signaling #7074	goat	WB	1:5000
anti-mouse IgG, HRP-linked	Cell signaling #7076	horse	WB	1:2500
Chromeo™ 488 anti-rabbit IgG	Active Motif 15041	goat	IF	1:500
DyLight® 488, anti-rabbit IgG	Thermo Scientific #35553	goat	IF	1:500
Tertiary antibody:				
Fc-FITC, anti-rabbit IgG	Dianova 111095008	goat	IF	1:500

2.1.9 Peptides

Generally used peptides are listed in Table 2.7.

Table 2.7 Generally used peptides.

Name	Peptide	Amino acid sequence	Modification	Supplier
HIS-24K14me0	HIS-24 (2-22)	N-CSDSAVVAAAVEP-K-VPKAKAAK-C	-	Squarix, Marl
HIS-24K14me1	HIS-24 (2-22)	N-CSDSAVVAAAVEP-K_{14me}-VPKAKAAK-C	mono-methylation	Squarix, Marl
H3K9me0	H3 (1-20C)	N- ARTKQTAR-K-STGGKAPRKQL-C	-	Squarix, Marl
H3K9me1	H3 (1-20C)	N- ARTKQTAR-K_{9me}-STGGKAPRKQL-C	mono-methylation	Squarix, Marl
H3K9me2	H3 (1-20C)	N- ARTKQTAR-K_{9me}-STGGKAPRKQL-C	di-methylation	Squarix, Marl
H3K9me3	H3 (1-20C)	N- ARTKQTAR-K_{9me}-STGGKAPRKQL-C	tri-methylation	Squarix, Marl
H3K27me0	H3 (18-39C)	H-QLATKAAR-K-SAPATGGUKKP-K(biot)-NH2	-	Squarix, Marl
H3K27me1	H3 (18-39C)	H-QLATKAAR-K_{27me}-SAPATGGUKKP-K(biot)-NH2	mono-methylation	Squarix, Marl
H3K27me2	H3 (18-39C)	H-QLATKAAR-K_{27me}-SAPATGGUKKP-K(biot)-NH2	di-methylation	Squarix, Marl
H3K27me3	H3 (18-39C)	H-QLATKAAR-K_{27me}-SAPATGGUKKP-K(biot)-NH2	tri-methylation	Squarix, Marl

2.1.10 Oligonucleotides

Primer sequences were designed using Primer3 Input program and verified with respect to their homology by BLAST (WormBase) suite. Designed primers were used for cloning, genotyping or quantitative PCR (Table 2.8). Mutated nucleotides are in bold type and underlined sequences indicate restriction sites.

Table 2.8 Generally used primers.

Name	Sequence	Application
ESPCR 124_hpl1_for	ATGTCACGTCAAAACCCTG	genotyping
ESPCR 125_hpl1_rev	TTGAAGGCCGAATTTGCTCG	genotyping
HIS-24_1	GAGGACTCGCACAGTCATCA	genotyping
HIS-24_2	CTGACGGAGATGAGCATTGA	genotyping
HIS-24_4	CCTCCATCCGTGCAAAGTTTCTT	genotyping
MJ192_Hpl2(tm1489)_for2	GACAGTATAAGTTCCCCGAC	genotyping
MJ193_Hpl2(tm1489)_rev	GTTTACCAGCTTTTCCGTGTG	genotyping
MJ224_His24 MUT_F	CGAGCCA**G**AGGTCCCAAAGGCTAAGGC	mutagenesis
MJ225_His24 MUT_R	GGGACCT**C**TGGCTCGACAGCGGC	mutagenesis
MJ214_HPL1_for_HindIII_mcherry	CCCAAGCTTATGTCACGTCAAAACCCTGTCCG	cloning
MJ215_HPL1_rev_KpnI_mcherry	GGGGTACCCGGCTCATTCCTCCTGGGATGGTTG	cloning
MJ222_HPL2a_for_HindIII_GFP	CCCAAGCTTATGCGAGCAAATCAACAAAGCG	cloning
MJ223_HPL2a_rev_KpnI_GFP	GGGGTACCCGAAGCTCGTCGGCTTTTGGG	cloning
MJ224_His24_for_HindIII_GFP	CCCAAGCTTATGTCTGATTCCGCTGTTGTTGC	cloning
MJ224_His24_rev_KpnI_GFP	GGGGTACCCGGGCCTTGGCGGCTGGC	cloning
MS_ceh2_1f	GGGTAAGTTGATTTCCCAAATG	qPCR
MS_ceh2_1r	ACCTTATCGGCTACTGTGTCC	qPCR
MS_egl5_1f	TCCGGTTAGCCAGTCACTTT	qPCR
MS_egl5_1r	AGCAGAGGCCTACAACTGGA	qPCR
MS_egl5_2f	GCACAAAATCTAGCTACAACATGC	qPCR
MS_egl5_2r	ATCTCCCTCCCCATTTAAGGTAT	qPCR
MS_mab5_1f	CATCCAGGATACATGCTCATTTG	qPCR
MS_mab5_1r	CGTGCTCCCTACTTTTTCTCTATC	qPCR
MS_mab5_4f	AAACATCCGATGCTCAGGTC	qPCR
MS_mab5_4r	AATTCGAGCCCTAAGCACAA	qPCR

2.1.11 Plasmids

Plasmids used for cloning are listed in Table 2.9

Table 2.9 Generally used plasmids.

Name	Type	Promoter	Resistance	Tag	Source
pCR®4Blunt-TOPO®	bacterial expression vector	*lac*	ampicillin, kanamycin	-	Invitrogen, Karlsruhe
pEGFP-N1	mammalian expression vector	CMV	kanamycin	C- terminal EGFP-tag	Clontech, Mountain View (USA)
pmCherry-N1	mammalian expression vector	CMV	kanamycin	C- terminal mCherry-tag	Schulze E, University of Freiburg, Germany

2.1.12 Bacterial strains

Bacterial strains used during the study are listed in Table 2.10

Table 2.10 Generally used bacterial strains.

Strain	Genotype	Application	Source
DSM 350	*B. thuringiensis* non-pathogenic	Survival assay for *C. elegans*	Nakad R, Christian Albrechts-Universität Kiel
DH5α	*E. coli* F-φ80*lac*ZΔM15 Δ(*lac*ZYA-*arg*F)U169 *rec*A1 *end*A1 *hsd*R17(r_k^-, m_k^+) *pho*A*sup*E44 *thi*-1 *gyr*A96 *rel*A1 λ^-	cloning; plasmids amplification	Invitrogen, Karlsruhe
DSM 1099	*E. coli*, Lysine-requiring auxotroph. Lacks meso-Dap decarboxylase	SILAC	German Collection of Microorganisms and Cell Cultures (DSMZ)
HB101	*E. coli* [supE44 hsdS20(rB-mB-) recA13 ara-14 proA2 lacY1 galK2 rpsL20 xyl-5 mtl-1]	*C. elegans* food (liquid culture)	Avery L, University of Texas Southwestern Medical Center, Dallas (USA); distributed by the CGC
HT115	*E. coli* [*F*⁻, *mcrA, mcrB, IN(rrnD-rrnE)1, lambda*⁻, *rnc14::Tn10(DE3 lysogen:lacUV5 promoter-T7 polymerase*)]	RNA interference by feeding	Sanger Institute (UK)/CGC (USA)
OP-50	*E. coli* B, streptomycin resistant, uracil auxotroph	*C. elegans* food	Hodgkin J, Oxford University, Oxford, England; distributed by the CGC
PS80JJ1 NRRL B-18679	*B. thuringiensis* very pathogenic	Survival assay for *C. elegans*	Nakad R, Christian Albrechts-Universität Kiel
XL10-Gold®	TetR Δ(*mcrA*)*183* Δ(*mcrCB-hsdSMR-mrr*)*173 endA1 supE44 thi-1 recA1 gyrA96 relA1 lac* Hhe [F´ *proAB lacI*qZΔ*M15* Tn*10* (TetR) Amy CamR]	mutagenesis	Stratagene, La Jolla (USA)

2.1.13 *C. elegans* strains

C. elegans strains generated during the study or obtained from different sources are listed in Table 2.11

Table 2.11 *C. elegans* strains used in the study.

Strain	Genotype	Source	Reference
N2	wild-type	Hodgkin J, Oxford University, Oxford, England; distributed by the CGC	[123]
RB1067	*his-24(ok1024)* X	*C. elegans* Gene Knockout Consortium	[111]
RB1371	*hil-3(ok1556)* X	Barstead R, Oklahoma Med Research Foundation, Oklahoma; distributed by the CGC	-
PFR60	*hpl-1(tm1624)* X	Palladino F, Ecole Normale Superieure de Lyon, Lyon, France; distributed by the CGC	[116]
PFR40	*hpl-2(tm1489)* III	Palladino F, Ecole Normale Superieure de Lyon, Lyon, France; distributed by the CGC	[116]
EC624	*his-24(ok1024)* X *hpl-1(tm1624)* X	Monika Jedrusik-Bode (MAJ), MPI for Biophysical Chemistry, Göttingen, Germany	-
EC629	*his-24(ok1024)* X; *hpl-2(tm1489)* III	Monika Jedrusik-Bode (MAJ), MPI for Biophysical Chemistry, Göttingen, Germany	-
EC630	*his-24(ok1024)* X *hpl-1(tm1624)* X; *hpl-2(tm1489)* III	Monika Jedrusik-Bode (MAJ), MPI for Biophysical Chemistry, Göttingen, Germany	-
EC602	[*unc-119*(*ed3*)III; *eels602[unc-119*(+) *his-24*::*gfp]*	Schulze E, University of Freiburg, Germany	[111]
MAJ17	[*unc-119*(*ed3*)III; *eels602[unc-119*(+)*his-2414KA::gfp]*	Monika Jedrusik-Bode (MAJ), MPI for Biophysical Chemistry, Göttingen, Germany	[115]
FR463	*swIs14[Ex218(rol-6(su10006)+hpl-2::GFP]*	Palladino F, Ecole Normale Superieure de Lyon, Lyon, France	[121]
PFR6	*qaIS1[Ex2(rol-6(su10006)+hpl-1::GFP]* *hpl-2::gfp;hpl-1(tm1624)*	Palladino F, Ecole Normale Superieure de Lyon, Lyon, France Palladino F, Ecole Normale Superieure de Lyon, Lyon, France	[121] [121]
EM599	*bxls13 [egl-5::gfp; him-5(e1490)* V*; lin-15B(n765)* X*]*	Emmons S, Albert Einstein University, Bronx, NY; distributed by the CGC	[124, 125]
HZ111	*muIs16[mab-5::gfp ; sor-1(bp1)/qC1 dpy-19(e1259) glp-1(q339)* III; *him-5(e1490)* V]	Zhang H, National Institute of Biological Sciences, Beijing, China; distributed by the CGC	[125, 126]

MAJ18	*his-24::gfp; his-24(ok1024)* X	Monika Jedrusik-Bode (MAJ), MPI for Biophysical Chemistry, Göttingen, Germany	-
MAJ19	*his-24::gfp; hpl-2(tm1489)* III; *his-24(ok1024)* X	Monika Jedrusik-Bode (MAJ), MPI for Biophysical Chemistry, Göttingen, Germany	-
MAJ20	*his-2414KA::gfp; hpl-2(tm1489)* III; *his-24(ok1024)* X	Monika Jedrusik-Bode (MAJ), MPI for Biophysical Chemistry, Göttingen, Germany	-
MAJ21	*egl-5::gfp; hpl-2(tm1489)* III	Monika Jedrusik-Bode (MAJ), MPI for Biophysical Chemistry, Göttingen, Germany	-
MAJ22	*egl-5::gfp; his-24(ok1024)* X	Monika Jedrusik-Bode (MAJ), MPI for Biophysical Chemistry, Göttingen, Germany	-
MAJ23	*egl-5::gfp; hpl-2(tm1489)* III; *his-24(ok1024)* X	Monika Jedrusik-Bode (MAJ), MPI for Biophysical Chemistry, Göttingen, Germany	-
MAJ24	*mab-5::gfp; hpl-2(tm1489)* III	Monika Jedrusik-Bode (MAJ), MPI for Biophysical Chemistry, Göttingen, Germany	-
MAJ25	*mab-5::gfp; his-24(ok1024)* X	Monika Jedrusik-Bode (MAJ), MPI for Biophysical Chemistry, Göttingen, Germany	-
MAJ26	*mab-5::gfp; hpl-2(tm1489)* III; *his-24(ok1024)* X	Monika Jedrusik-Bode (MAJ), MPI for Biophysical Chemistry, Göttingen, Germany	-

2.1.14 Cell lines

Cell line used for protein expression is described in Table 2.12

Table 2.12 Cell line used in the study.

Cell line	Cell type	Organism	Medium	Source
NIH-3T3	Embryonic fibroblast	mouse	90% DMEM+ 10% FBS	Deutsche Sammlung von Mikroorganismen und Zellkulturen *(*DSMZ)

The NIH3T3 cell line, used for transfection and immunofluorescence assays, originally generated by Deutsche Sammlung von Mikroorganismen und Zellkulturen *(*DSMZ), was kindly provided by Dr. Gabriela Whelan.

2.2 Molecular methods

2.2.1 Preparation of plasmid DNA

Chemically competent DH5α bacteria were transformed with the plasmid of interest and grown in LB medium at 37°C with constant shaking, overnight. For small-scale plasmid isolation, bacteria were grown in 5 ml of medium whereas for more efficient isolation bacteria were cultured in 50 ml of medium. Plasmid DNA was isolated using either the Wizard® Plus SV Minipreps DNA Purification System or the EndoFree® Plasmid Maxi Kit according to the manufacturer's protocol. Concentration of the plasmid DNA was determined using the NanoDrop® ND-100 Spectrophotometer.

2.2.2 Restriction enzyme digestion of DNA

Plasmid DNA and PCR products were digested using appropriate restriction enzymes (New England Biolabs (NEB)) according to manufacturer's description.

2.2.3 Polymerase chain reaction (PCR)

Respective DNA sequences were amplified using polymerase chain reaction (PCR) according to the manufacturer's instructions (Roche, Mannheim). A PCR reaction mix (50 µl) contained 200 µM of dNTP mix (10 mM), 600 nM of each primer, 0.75 µg of template DNA, 1 x PCR buffer with 20 mM $MgSO_4$, 2.5 U of Pwo DNA Polymerase and sterile H_2O (up to 50 µl). PCR reactions were performed in the Mastercycler gradient (Eppendorf) using the following program:

	Temperature	Time	Cycle No.
Initial denaturation	95°C	2 min	1 x
Denaturation	95°C	30 s	
Annealing	56°C	1 min	5 x
Elongation	68°C	3 min	
Denaturation	95°C	30 s	
Annealing	58°C	1 min	25 x
Elongation	68°C	3 min	
Final elongation	68°C	4 min	1 x

2.2.4 Site-Directed Mutagenesis

Mutagenesis was performed using the QuikChange XL Site-Detected Mutagenesis Kit (Stratagene). The mutagenic oligonucleotide primers were designed according to the "Primer Design Guidelines" (Stratagene) and are listed in Table 2.8. Plasmid DNA that served as a template was amplified with KOD DNA Polymerase (Novagen) according to the

manufacturer's protocol. Briefly, a 50 µl PCR reaction mix contained 200 µM of dNTP mix (2 mM each), 400 nM of each primer, 5 ng of template plasmid DNA, 1 x buffer (10 x) for KOD DNA Polymerase, 1.5 mM $MgCl_2$, 1 U of KOD DNA Polymerase and PCR Grade Water (up to 50 µl). PCR reactions were performed using the following program:

	Temperature	Time	Cycle No.
Initial denaturation	94°C	30 s	1 x
Denaturation	94°C	30 s	
Annealing	58°C	30 s	25 x
Elongation	72°C	60 s	
Final elongation	68°C	7 min	1 x

5 µl of the obtained PCR product were separated by agarose gel electrophoresis (2.2.5). The rest of the amplified DNA was treated with 1 µl of *Dpn*I enzyme (NEB) that specifically digests the parental, methylated DNA template. The vector DNA carrying the desired mutation was transformed into or XL10-Gold® competent cells (2.2.6) isolated using Wizard® Plus SV Minipreps DNA Purification System (2.2.7) and sequenced by SeqLab (Göttingen).

2.2.5 Separation and isolation of DNA fragments from the agarose gel

DNA fragments were separated with respect to their size by agarose gel electrophoresis. The DNA was mixed with 6 x Mass Ruler Loading Dye and then loaded into the gel pockets. Samples were separated either on 0.7% or 1% agarose gels (x% (w/v) agarose, 1x TAE buffer, 0.01% GR safe DNA stain) using the Bio Rad Sub-Cell® electrophoresis chamber (Bio Rad, München). The gel was electrophoresed at 90-120 V until the required separation has been achieved which usually occurred after 30 min. The DNA fragments were visualised by Gel iX Imager (UV light- 365 nm wavelength) and their sizes were determined by comparing to the bands of the DNA ladder (100bp/Plus DNA ladder, Fermentas). If necessary, DNA fragments were isolated from the agarose gel using the QIAquick gel Extraction Kit (Qiagen, Hilden).

2.2.6 Transformation of plasmid DNA into chemically competent bacteria

Plasmid DNA was transformed using DH5α chemically competent bacteria. One vial (50 µl) of competent cells was thawed on ice and mixed gently with 0.5-2 µl (1-10 ng) of plasmid DNA. The sample was incubated on ice for 20 min. Bacterial cells were heat shocked for 45 sec in 42°C and immediately put back on ice for 2 min. After incubation, transformed bacteria were mixed with 950 µl of pre-warmed LB medium and cultured at 37°C for 1 hour at 225

rpm. Bacteria were spread on a pre-warmed selective (ampicillin 100 µg/ml or kanamycin 50 µg/ml) LB plate and incubated overnight at 37°C.

Plasmid DNA, obtained after mutagenesis procedure, was transformed into XL10-Gold® ultracompetent cells. Transformation was performed according to manufacturer description. Briefly, thawed XL10-Gold® ultracompetent cells were transferred to a prechilled 14 ml falcon polypropylene round-bottom tube and mixed with 2 µl of β-Mercaptoethanol (provided by the manufacturer). The content of the tube was incubated on ice for 10 min and gently swirled every 2 min. Bacterial cells were then mixed with 2 µl of *Dpn*I-digested plasmid DNA, swirled gently and incubated on ice for 30 min. The tube with bacteria was heat-pulsed for 30 sec in a 42°C water bath and then incubated on ice for 2 min. Transformation reaction was mixed with 500 µl of pre-warmed NZY$^+$ broth and cultured at 37°C for 1 hour with shaking at 225 rpm. Bacteria were plated on pre-warmed selective (ampicillin 100 µg/ml or kanamycin 50 µg/ml) LB plates and incubated overnight at 37°C.

2.2.7 Cloning procedure

The DNA sequences used for cloning into target vectors were amplified by PCR reaction with primer pairs described in Table 2.8. All primers contained sequences of restriction sites recognised by endonucleases used for cloning procedure. The amplified cDNAs were purified by the MSB® Spin PCRapace purification kit (Stratec Molecular GmbH, Berlin). Every PCR product was cloned first into the pCR®4Blunt-TOPO® bacterial expressed vector using blunt-ends cloning procedure (Fig. 2.1). In order to add blunt ends to each purified PCR products, cDNA was incubated with 10x T4 DNA polymerase buffer, 0.24 mM dNTP and 1U of T4 DNA polymerase (New England Biolabs (NEB), Ibswich (USA)). Blunt-end cDNA was then loaded into 0.7% (w/v) peqGOLD Low Melt Agarose (PEQLAB Biotechnologie GmbH, Erlangen) gel (2.2.5). A proper DNA fragment was cut out of the gel and melted down in 65°C. Ligation was performed in a total volume of 6 µl containing 4 µl of DNA, 1 µl of Salt solution and 1 µl of TOPO® vector (all reagents provided by the manufacturer). After incubation at RT for 25 min, all ligation mixture was remelted again at 65°C and transformed into the DH5α bacteria (2.2.6). Transformed bacteria were put on pre-warmed LB plates with corresponding antibiotic and incubated overnight at 37°C. Single, well isolated colonies from LB agar plate were used to inoculate 5 ml of LB medium (containing the same antibiotic) on the next day. Inoculated bacterial colonies were grown at 37°C overnight. Afterward, plasmid DNA was isolated from the bacteria culture (2.2.1) and digested with restriction enzymes corresponding to flanking sites of the insert DNA. The same endonucleases were used for the restriction digestion of the target vector. 1 µg of the vector DNA was dephosphorylated with 5 U of Antarctic Phosphatase (New England Biolabs (NEB), Ibswich (USA)) in a presence of 10x Antarctic Phosphatase Reaction Buffer (provided by the manufacturer) . After incubation with enzymes the cDNA fragments and the targeted vector were separated by gel electrophoresis with peqGOLD Low Melt Agarose (PEQLAB Biotechnologie GmbH, Erlangen) gel (2.2.5) and the proper bands were cut out of the gel. Ligation was performed in a total volume of 20 µl containing 1 µg of digested DNA, 2 µl of 10x ligation buffer (provided by the manufacturer) and 2 U of T4 DNA ligase (Roche, Mannheim or New

England Biolabs (NEB), Ibswich (USA)). The ligation mixture was incubated at 15°C overnight, transformed into DH5α competent cells and put on LB agar plates with antibiotic corresponding to the used vector. Single colonies were transferred from the plates to 5 ml of the LB medium and grown at 37°C overnight. Plasmid DNA was isolated from each bacteria culture, digested with restriction endonucleases and loaded into 1% (w/v) agarose gel. Plasmids that exhibited the correct size of insert were sequenced by SeqLab (Germany).

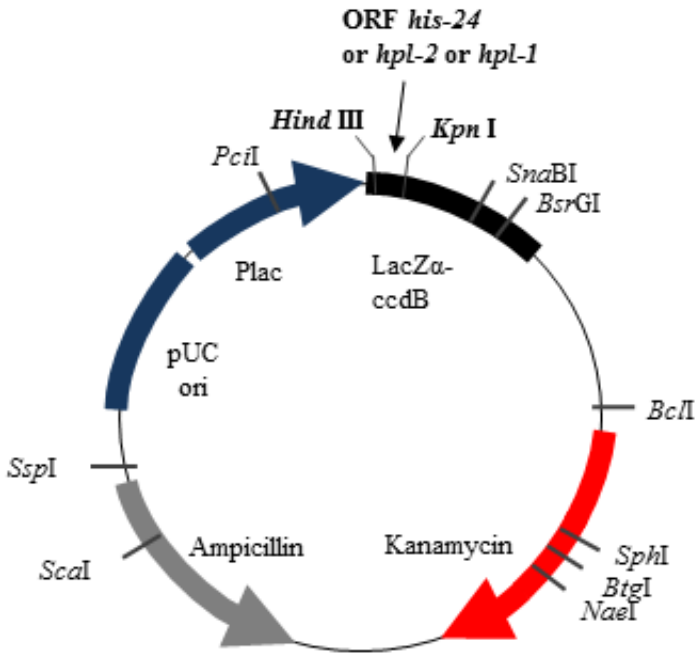

Figure 2.1 Restriction map of the pCR®4Blunt-TOPO® bacterial expressed vector. Restriction sites are labelled to visualise the actual cleavage site.

2.2.8 Summary of cloned plasmid vector constructs

2.2.8.1 pEGFP-N1 mammalian expression vector based constructs

In order to express *C. elegans* proteins tagged to C-terminal EGFP-tag in the NIH3T3 cells (Table 2.11), cDNA sequences were cloned into the mammalian expression vector pEGFP-N1 (Clontech, USA) (Figure 2.2).

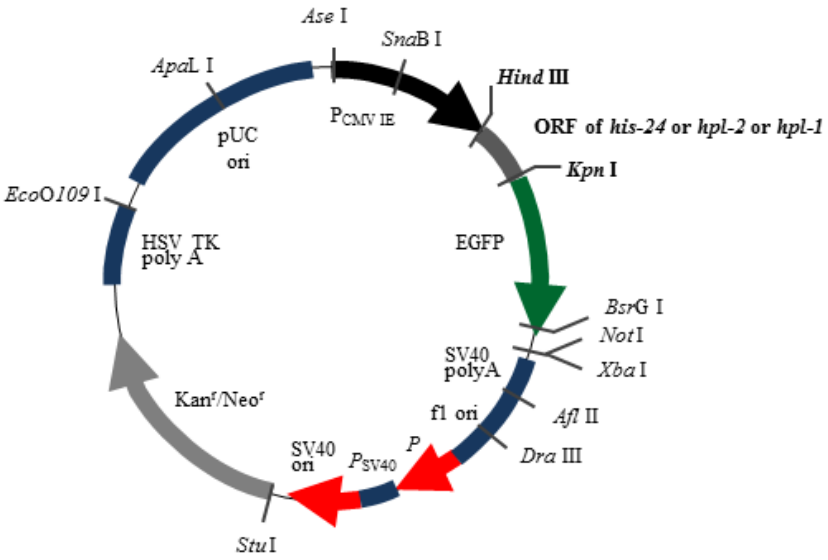

Figure 2.2 Restriction map of the pEGFP-N1 vector for NIH3T3 cells transfection. Restriction sites are labelled to visualise the actual cleavage site.

The *hpl-1* and *hpl-2a* cDNA sequences of *C. elegans* genes (Appendix A.1) were amplified by PCR (2.2.3) from pGEX-HPL-1, pGEX-HPL-2a plasmids, kindly provided by Dr. Francesca Palladino (Ecole Normale Superieure de Lyon, Lyon, France). Following primer pairs were used for the amplification (DNA sequences in Table 2.8):

MJ214_HPL1_for_HindIII_mcherry
MJ215_HPL1_rev_KpnI_mcherr

MJ222_HPL2a_for_HindIII_GFP
MJ223_HPL2a_rev_KpnI_GFP

C. elegans his-24 cDNA (Appendix A.1) was amplified from the plasmid pET3a-HIS-24, kindly provided by Dr. Monika Jedrusik-Bode (Max-Planck Institute for Biophysical Chemistry, Göttingen, Germany) using following primer pair (DNA sequences in Table 2.8):

MJ224_His24_for_HindIII_GFP
MJ224_His24_rev_KpnI_GFP

The *gfp-his-24* plasmid DNA, kindly provided by Dr. Monika Jedrusik-Bode (Max-Planck Institute for Biophysical Chemistry, Göttingen, Germany), was used as a template for the side directed mutagenesis PCR (2.2.4) to generate the *C. elegans gfp::his-24K14A* transgenic

strain. The plasmid contained the promoter and the complete genomic coding sequence of *his-24*, which fused to *gfp*. Mutagenesis was performed to generate HIS-24 protein that carries one point mutation in amino acid residue that is methylated and responsible for proper functioning of the protein. The lysine (K) residue 14 was mutated to alanine (A) using following primer pair (DNA sequences in Table 2.8):

MJ224_His24 MUT_F
MJ225_His24 MUT_R

2.2.8.2 pmCherry-N1 mammalian expression vector based constructs

The same *C. elegans* DNA sequences were alternatively cloned into the pmCherry-N1 vector (Figure 2.3). This enabled the expression of proteins with a C-terminal mCherry-tag in NIH3T3 mammalian cells.

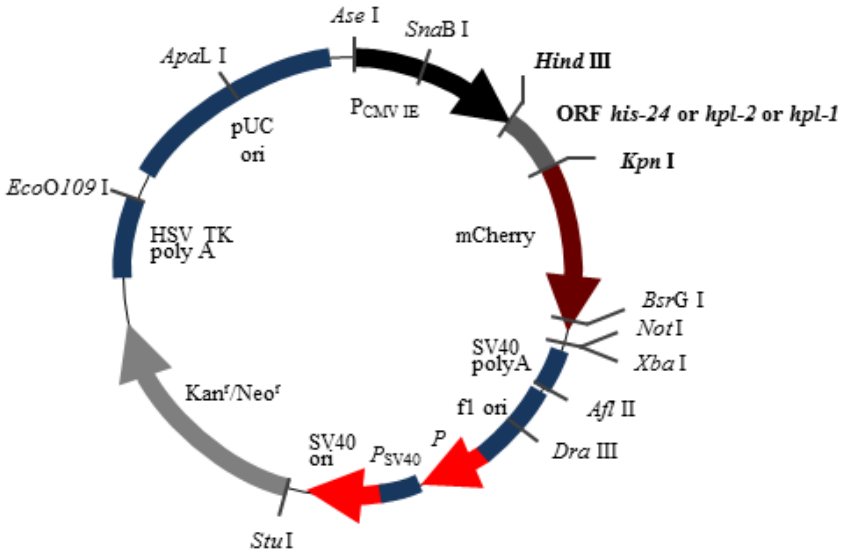

Figure 2.3 Restriction map of the pmCherry-N1 vector for NIH3T3 cells transfection. Restriction sites are labelled to visualise the actual cleavage site.

2.3 Protein biochemical methods

2.3.1 SDS polyacrylamide gel electrophoresis (NuPAGE® SDS-PAGE)

Proteins were separated with respect to their molecular weight using NuPAGE® SDS-PAGE (Invitrogen, Karlsruhe) polyacrylamide gel electrophoresis, according to the manufacturer's protocol. Briefly, proteins were mixed with NuPAGE® LDS Sample Buffer (4x), with NuPAGE® Sample Reducin Agent (10x), boiled for 5 min and spun down shortly. Protein samples were loaded on the NuPAGE® Bis-Tris Gel 4–12% gels using the XCell *SureLock*® Mini-Cell electrophoresis system (Invitrogen, Karlsruhe). The samples were separated at a constant voltage of 120 V in NuPAGE® MOPS SDS Running Buffer 1x (Invitrogen, Karlsruhe). Protein sizes were determined by comparing them to the bands of the SeeBlue® Plus2 Pre-Stained Standard (Invitrogen, Karlsruhe).

2.3.2 Techniques of protein detection

2.3.2.1 Western blotting

To identify specific proteins by antibody-based detection, samples were first separated on NuPAGE® SDS-PAGE gel (2.3.1) and then transferred to a nitrocellulose membrane Amersham Hybond™ ECL™ (GE Healthcare, Buckinghamshire (UK)). The nitrocellulose membrane was equilibrated before transfer in the 1x protein transfer buffer (10% (v/v) 10x transfer buffer (2.1.5), 10% (v/v) methanol, and distilled water) for 10 min. Electrotransfer was run in the 1x protein transfer buffer for 60 min at 4°C and constant current of 100 mA using the Bio Rad Sub-Cell® blotting system (Bio Rad, München). To prevent nonspecific binding of the detection antibodies during subsequent steps, the membrane was blocked in PBS-T buffer (2.1.5) either with 5% (w/v) nonfat dried milk or 5% albumin, bovine serum (BSA) for 30-60 min at RT with gentle rocking. After blocking, membrane was probed overnight at 4°C with primary antibodies (for dilutions see Table 2.1.8) diluted in PBS-T with milk or BSA. The probed membrane was washed three times with PBS-T buffer for 5 min each and then incubated for 60 min at RT with the corresponding horseradish peroxidase (HRP) conjugated secondary antibodies, diluted in PBS-T with milk or BSA. The membrane was washed again with PBS-T three times for 5 min each. Proteins of interest were detected using Lumi®GLO Reagent (20x) and Peroxydase (20x) (Cell Signaling Technology, Frankfurt am Main) according to the manufacturer's instructions. Amersham Hyperfilm ECL films (GE Healthcare, Buckinghamshire (UK)) were developed using the AGFA Curix 60 Film Processor (Agfa HealthCare, Bonn).

2.3.2.2 Peptide competition assay (PCA)

Peptide competition assay was performed in order to confirm the specific band reactivity of the antibodies used for further experiments (2.4.14-16). Peptides (Table 2.7) at concentrations of 50 ug/ml were plotted on the nitrocellulose membrane, left to dry and shortly washed with PBS-T buffer (2.1.5). Additionally, BSA solution was plotted on the membrane that served as a negative control. The membrane was then blocked with BPS-T with 5% (w/v) milk buffer for 60 min at RT with gentle rocking and incubated overnight at 4°C with primary antibodies (for dilutions see Table 2.1.8). The rest of the experiment was performed in the same way as in the western blotting procedure.

2.4 *C. elegans* based methods

2.4.1. Culturing *C. elegans* on agar plates

C. elegans was maintained on Nematode Growth Medium (NGM) agar plates (2.1.4) carrying a lawn of OP50 strain of *Escherichia coli* (Table 2.10). For general purpose, Ø 90 mm Petri dishes were used for growing. *C. elegans* worms were cultured at 15°C, 20°C or 25°C. For experiments, which required larger quantities of animals, worms were cultured on Ø 140 mm

plates. The nematodes were transferred to a new plate by means of a platinum wire pick, sealed to a Pasteur pipette, or by cutting out a piece of agar from the old plate and putting it on the new plate.

2.4.2 Liquid culture of *C. elegans*

For biochemical experiments that required larger quantities of the nematode, animals were cultured in liquid medium. Liquid cultures of *C. elegans* were grown in S Medium (2.1.5) using concentrated HB101 strain of *Escherichia coli* (Table 2.10) as a food source. Animals used for inoculation of the S medium were previously rinsed off the NGM agar plates with M9 buffer (2.1.5) and washed three times using the same buffer. Worms of about 5 NGM plates (Ø 90 mm) were used for inoculation of 200 ml of S medium. The worm cultures were incubated at 20°C with constant shaking at 120 rpm for about seven days until the required density of culture was reached. The worm cultures were monitored by checking a drop of the culture under the microscope, and additional *Escherichia coli* HB101 were added as needed. Before the harvesting of *C. elegans*, the flask with culture was put on ice for 15 min to allow the worms to settle. Most of the liquid was removed from the flask and the remaining culture was transferred to a 50 ml centrifuge tube and spun at 4°C for 2 min at 2800 rpm to pellet the worms. The pellet was washed with cold M9 buffer (2.1.5) until the supernatant was clear. *C. elegans* pellet was stored at -80°C.
For quantitative proteome analysis by SILAC (stable isotope labelling by amino acids), *C. elegans* worms were cultured in S medium using DSM1099 strain of *Escherichia coli* (Table 2.10). The nematodes were fed with two types of [$^{13}C_6$] lysine labelled strain of bacteria: "light" *Escherichia coli* (labelled with [$^{12}C_6$, $^{14}N_2$] Lys) and "heavy" *Escherichia coli* (labelled with [$^{13}C_6$, $^{12}N_2$] Lys). The worm cultures were incubated at 20°C with constant shaking at 120 rpm for two weeks to obtain incorporation rates of approximately 90%. The worm cultures were monitored every single day. After harvesting, *C. elegans* pellet was stored at -80°C.

2.4.3 Decontamination of *C. elegans* stocks

To decontaminate *C. elegans* strain from foreign bacteria, yeasts or mold, animals were treated with a hypochlorite solution (2 vol. 4 M NaOH : 3 vol. 10-20% NaOCl, fresh mixed). 10 µl of the hypochlorite solution was plotted on the edge of the Ø 40 mm NGM plate with OP50 bacterial strain. Adult, gravid hermaphrodites were transferred to the hypochlorite solution and left overnight at RT. Next day, when hatched nematodes crowed to bacteria, a part of the agar with the rest of contaminants was cut out.

2.4.4 Freezing and recovery of *C. elegans* stocks

C. elegans can be frozen and stored indefinitely in -80°C. For freezing, two Ø 90 mm NGM plates with just starving animals at L1 and L2 larva stage were taken. Worms were rinsed off

the plates with about 1 ml of M9 buffer (2.1.5) and collected in the freezing vials. After adding an equal amount of freezing solution (2.1.5), the worms' suspension was mixed and immediately placed in a Styrofoam box at -80°C. For recovery of a *C. elegans*, a frozen stock was thawed at RT and transferred immediately on NGM agar plate.

2.4.5 Crossing of *C. elegans*

Crosses between hermaphrodites and males were carried out by placing three young adult hermaphrodites together with an excess of males (e.g. eight males) on a small Ø 40 mm NGM plate with OP50. Plates were incubated for 2-3 days at 20°C. After that time, hermaphrodites were separated from males and were left until eggs laying. L4 stage hermaphrodites of the F1 generation, from the successful mating (~ 50% of male progeny), were placed separately on new NGM plates and were left until eggs laying. F2 L4 stage hermaphrodites were again put on new NGM plates and after eggs laying they were genotyped by single worm PCR reaction (2.4.6). In the case of mating with strain carrying integrated GFP protein, only F1 and F2 L4 stage hermaphrodites expressing green fluorescence protein were selected for further crossing. Generated strains (MAJ17- MAJ25) are described in Table 2.11.

2.4.6 Single worm PCR

Single worm PCR genotyping was performed in order to determine if worms from certain strain are heterozygous or homozygous with respect to a particular deletion allele. A single hermaphrodite was transferred to a 0.2 ml PCR tube with 2.5 µl of lysis buffer (2.1.5) supplemented with Proteinase K (100 µg/ml). The tube was frozen at -80°C for 30 min. Worms were then lysed in the Mastercycler gradient (Eppendorf) at 65°C for 1 hour and incubated at 95°C for 15 min to inactivate Proteinase K. A PCR reaction mix (22.5 µl) contained 1X *Taq* Buffer with $(NH_4)_2SO_4$ (provided by the manufacturer), 3 mM $MgCl_2$ (provided by the manufacturer), 250 µM of each dNTP (provided by the manufacturer), 0.2 U Taq DNA polymerase (Fermentas, St. Leon-Rot), 500 nM of each primer (Table 2.8) and sterile H_2O (up to 22.5 µl). PCR reactions were performed using the following program:

	Temperature	Time	Cycle No.
Initial denaturation	95°C	30 sec	1 x
Denaturation	95°C	3 min	
Annealing	50°C	30 s	5 x
Elongation	72°C	30 s	
Denaturation	95°C	40 s	
Annealing	51°C	30 s	25 x
Elongation	72°C	30 s	
Final elongation	72°C	1 min	1 x

2.4.7 Double-stranded RNA-mediated interference (RNAi) by feeding

RNA interference was used to obtain animals display a phenotype that results from the depletion of the target gene but without generation of knockout animals. RNA interference was achieved by feeding worms with transgenic *Escherichia coli* strain HT115 (2.10) producing specific dsRNA. *E. coli* strain, carrying feeding vector L4440 with specific gene sequence, was cultured in 5 ml of LB medium containing ampicillin (100 µg/ml) and incubated at 37°C overnight with constant shaking. 100 µl of the bacteria culture were plated on Ø 40 mm NGM feeding plates (NGM plate with 100 µg/ml ampicillin and 1 mM IPTG) and incubated for 5 hours at RT to induce expression of dsRNA. After the incubation time, *C. elegans* worms at early L4 stage were transferred on the NGM feeding plates and incubated at 25°C. Animals from the F1 generation were examined for phenotypic alterations using Wild M5 dissecting microscope (Wild Heerbrugg AG, Gais Switzerland) and Leica DMI 6000 B microscope (Leica, Wetzlar). Following *E. coli* HT115 bacteria clones were used in the study: *him-14* (RNAi), *hpl-1* (RNAi), *hpl-2* (RNAi), *mes-2* (RNAi), *mes-3* (RNAi) and *sop-2* (RNAi).

2.4.8 Immunohistochemistry of *C. elegans*

For staining of *C. elegans*, 20-50 adult worms were placed in 10 µl of salts solution (2.1.5) on a microscope glass slide. Every single worm was incised between the pharynx and gonad to release the embryos and the gonad arms. Salts solution with worms was mixed with 10 µl of 4% PFA and incubated at RT for 5 min. After incubation, a coverslip slide was placed on the top and the microscope glass slide was frozen in the liquid nitrogen for 10 min. The coverslip was quickly removed using a blade and the slide was transferred immediately into 96% ethanol for 1 minute. After incubation the slide was wiped from below to remove residual ethanol and it was placed in PBS-T buffer (1% Triton X-100) for 10 min. Incubation with PBS-T was repeated two more times and after that the buffer was wiped off the slide. 70 µl of primary antibody (for dilutions see Table 2.6) diluted in PBS-T was placed onto the slide with worms and incubated in a humid chamber at 4°C overnight. On the next day, the slide was washed twice in PBS-T buffer for 10 min each and incubated with 70 µl of secondary antibody (for dilutions see Table 2.6) at 4°C overnight. After the incubation, 70 µl of DAPI solution (Molecular Probes, Karlsruhe) was placed on the slide for 10 min and then washed off three times with PBS-T buffer for 10 min each. The slide was wiped, closed with coverslip using VECTASHIELD® Mounting Medium (Vector Laboratories, Canada) and stored at 4°C.
C. elegans immunohistochemistry analysed by simulated emission depletion (STED) microscopy was performed in the same way with some modifications. After secondary antibodies (for dilutions see Table 2.6) incubation, the slide was washed three times with PBS-T buffer and incubated at RT for 1 hour with Fc-FITC, anti-rabbit IgG tertiary antibody (for dilution see Table 2.6). After that the slide was washed again three times with PBS-T buffer and mounted with Mowiol® 4-88 mounting medium (Polysciences Europe GmbH, Eppelheim).

2.4.9 DAPI staining of *C. elegans*

For DAPI staining of *C. elegans*, 20-50 adult worms were placed in 10 µl of salts solution (2.1.5) on a microscope glass slide. After the transfer of worms, excess of the liquid was removed and animals were incubated with a drop of DAPI solution in ethanol (150 ng/ml) at RT for 30 min. Then the worms were transferred on the new glass slide to 10 µl of M9 buffer (2.1.5) and left for 20 min for re-hydration. After incubation, excess of the buffer was removed and the slide was closed with VECTASHIELD® Mounting Medium (Vector Laboratories, Canada) and stored at 4°C.

2.4.10 Microscopy analysis of *C. elegans*

Phenotypes of all *C. elegans* strains were monitored on NGM agar plates using Wild M5 dissecting microscope (Wild Heerbrugg AG, Gais Switzerland). For differential interference contrast microscopy or fluorescence microscopy the Leica DMI 6000 B microscope (Leica, Wetzlar) was used. Analysed worms were placed on 2% (w/v) agarose pads with 10 µl of 2% sodium azide that causes *C. elegans* immobility.
Immunoelectron microscopy analysis was performed by Dirk Wenzel at the Electron Microscopy group of the Max Planck Institute for Biophysical Chemistry, Göttingen. Briefly, ultrathin cryosections were stained with an antibody and examined using a Philips CM120 electron microscope and a TVIPS charge-coupled-device camera system.
Stimulated emission depletion (STED) microscopy analysis was performed by Dr. Gael Moneron at the Department of NanoBiophotonics of the Max Planck Institute for Biophysical Chemistry, Göttingen. STED microscopy of *C. elegans* was performed using a custom-build fast-beam-scanning setup based on a continuous-wave (CW) fiber laser.

2.4.11 Behavioral tests of *C. elegans*

2.4.11.1 Survival assay of *C. elegans* after infection with *Bacillus thuringiensis*

To test susceptibility of *C. elegans* strains to infection, a total of 120 worms at the L4 stage were placed on small Ø 40 mm NGM plates (without peptone) and infected with *Bacillus thuringiensis* very pathogenic strain BT-18679 (Table 2.10). The stock of *Bacillus thuringiensis* was diluted 1:50 with an *Escherichia coli* OP50 culture and spread on NGM plates. Infected worms were incubated at 21°C for 24 hours. Survived animals were scored after incubation. Simultaneously, worms were also incubated on plates with non-pathogenic strain (DSM-350) of *Bacillus thuringiensis* (Table 2.10) that served as a control.

2.4.11.2 Thermotolerance assay

C. elegans behaviour analysis upon heat stress conditions was performed according to the protocol from Lithgow G.J. *et al.* [127]. A total of 100 animals at L4 stage were transferred on small, pre-warmed Ø 40 mm NGM plates and incubated at 35°C for 13 hours. The survival of

worms was scored every hour at 22°C as the number of animals that showed touch-provoked movement. Animals that failed to display motility or pharyngeal pumping were scored as dead. Statistical significance between strains was determining using the Log-Rank Test.

2.4.11.3 Osmotic stress assay

Adaptation of *C. elegans* to extreme concentration of salt was examined by placing worms on small NGM plates (Ø 40 mm) with very high (500 mM) NaCl concentration. One day before an experiment, high-salted plates were seeded with *Escherichia coli* OP50 and incubated at RT overnight. 60 worms at L4 stage were transferred on NGM plates and survival was scored in every 10 min. Animals that did not respond to touch were found as dead. Statistical significance between strains was determining using the two-tailed *t*-test.

2.4.11.4 Oxidative stress assay

The survival of *C. elegans* worms in the presence of oxidative stress conditions was performed according to protocol from Solomon *et al.* [128]. To determine the susceptibility of worms to oxidative stress conditions within the time range, cleaned worm strains were incubated on small NGM plates containing 0.25 mM or 0.5 mM of Methylviologen dichloride hydrate (Paraquat). A day before the experiment, plates were seeded with *Escherichia coli* OP50 and incubated at RT overnight. Three hermaphrodites were transferred on each, paraquat containing, NGM plate and were left until eggs lying. New hatched worms were incubated at 20°C and survival, based on motility, was monitored every day.

2.4.12 Preparation of *C. elegans* lysate for western blot analysis

C. elegans worms were rinsed off the NGM plates with M9 buffer (2.1.5) and collected in a 1.5 ml Eppendorf Tube. Suspension of worms was shortly incubated on ice to allow the worms to settle and centrifuged at 3000 rpm for 3 min. The worm pellet was washed with M9 buffer until the supernatant was clear. Then the pellet was mixed with the NuPAGE® LDS Sample Buffer (4x), with NuPAGE® Sample Reducing Agent (10x) and boiled for 5 min. Worms extract was centrifuged at 13000 rmp for 5 min. Obtained supernatant was loaded on the NuPAGE® Bis-Tris Gel 4–12% gel for Western blot analysis (2.3.2.1).

2.4.13 Preparation of total *C. elegans* protein extracts

C. elegans worms obtained by liquid culture (2.4.2) were used for preparation of total worm protein extract according to protocol from Cheeseman *et al.* [129]. A frozen pellet of worms (approximately 5 g) was thawed and ground with a mortar and pestle using liquid N_2. Ground worms were mixed with equal volume of C buffer (Immunoprecipitation/Peptide pull-down assays) or with M9 buffer (Chromatin immunoprecipitation assay**)** (2.1.5) supplemented with

protease inhibitors (Roche, Mannheim), thawed on ice and sonicated using a Branson Digital Sonifier (Branson Ultrasonics, USA). Sonication was performed with following settings: 30% amplitude for 3 min (15 sec on, 45 sec off) and 40% amplitude for 45 sec (15 sec on, 45 sec off). Sonicated worm lysate was transferred to 1.5 ml Eppendorf Tubes and centrifuged at 4°C and 13000 rpm for 10 min. The obtained supernatant was collected in a fresh 1.5 ml tubes and used for further biochemical analysis (see sections 2.4.14-16).

2.4.14 Protein immunoprecipitation from *C. elegans* extract

Protein immunoprecipitation experiments were performed by using total worm protein extracts (2.4.13). 50 µl of settled Protein G Agarose (70 µl resin slurry) were transferred to a 1.5 ml Eppendorf Tube and equilibrated by washing three times with 1 ml of cold 1x PBS buffer (2.1.5). Beads were centrifuged for 3 min at 2500 rpm and 4°C between every washing. Proper antibody (for concentrations see Table 2.6) was bound to the equilibrated beads during 3 hours of incubation at 4°C with constant rotation. After coupling, beads were washed again for three times with PD 150 buffer (2.1.5) and incubated with constant rotation at 4°C overnight with the worm protein extract to immunoprecipitate protein of interests. On the next day, beads were washed three times with PD 150 buffer (supplemented with protease inhibitors) and boiled for 5 min with NuPAGE® LDS Sample Buffer (4x), with NuPAGE® Sample Reducin Agent (10x).
For immunoprecipitation with GFP-Trap®-A beads (GFP-binding protein coupled to protein A agarose), 50 µl of resin slurry were equilibrated by washing with 1x PBS and then incubated with the worm protein extract at 4°C for 4 hours with constant rotation.

2.4.15 Peptide pull-down assay from *C. elegans* extract

Total worm protein extracts (2.4.13) were also used for peptide-binding experiments. 80 µl of Streptavidin Agarose beads were equilibrated by washing three times with 1ml of 1x PBS buffer (0.2% Triton X-100 and protease inhibitor). 10 µg of the biotinylated peptide (Table 2.7) were coupled to the equilibrated beads during 3 hours of incubation at RT and shaking at 1400 rpm. Beads-bound peptides were incubated with the worm protein extract at 4°C overnight with constant rotation. After incubation, streptavidin beads were washed seven times with PD 150 buffer (supplemented with protease inhibitors), boiled for 5 min with NuPAGE® LDS Sample Buffer (4x), with NuPAGE® Sample Reducin Agent (10x) and loaded on the NuPAGE® Bis-Tris Gel 4–12% gel for Western blot analysis (2.3.2.1).

2.4.16 Chromatin immunoprecipitation (ChIP) from *C. elegans* extract

C. elegans worms obtained by liquid culture (2.4.2) were used for ChIP experiments. A frozen pellet of worms (approximately 5 g) was thawed and resuspended in 47 ml of M9 buffer (2.1.5). To crosslink the proteins with DNA, the worms suspension was mixed with 2.8 ml of 37% formaldehyde (PFA) solution and incubated for 30 min at RT with constant

rotation. After incubation, the worms were washed once with 50 ml of 100 mM Tris-HCl pH 7.5 to quench excess of PFA, two times with 50 ml of M9 buffer and once with 10 ml of FA buffer (2.1.5) supplemented with protease inhibitor (Roche, Mannheim). The suspension was spun down at 4°C for 2 min at 2800 rpm, the worms pellet was resuspended in the equal volume of FA buffer (supplemented with protease inhibitor) and used for the total worm protein extract isolation (2.4.13). 10% of each sample was transferred to a new tube and stored at -20°C until it was used for the input DNA preparation. The *C. elegans* protein extract was then mixed with the 20% N-Lauroylsarcosine sodium salt solution to purify natively folded proteins from inclusion bodies and centrifuged at 13000 rpm for 5 min at 4°C. Obtained supernatant was transferred to new 1.5 ml Eppendorf Tubes and incubated with proper antibodies (for concentrations see Table 2.6) overnight at 4°C with constant rotation. On the next day, 50 µl of settled Protein G Agarose per ChIP sample were transferred to 1.5 ml Eppendorf Tube and equilibrated by washing four times with 1 ml of cold FA buffer (2.1.5). After the washes, the beads were suspended in one bead volume with FA buffer. ~100 µl of the bead slurry were added to each ChIP sample and continued to rotate at 4°C for 3 hours. After incubation, the beads were washed at RT by adding 1 ml of each of following buffers: twice with FA buffer for 5 min, once with FA-1 M NaCl buffer for 5 min, once with FA-500 mM NaCl for 10 min, once with TEL buffer for 10 min and twice with TE buffer for 5 min (2.1.5). During washing, beads were incubated on a rotator and collected by spinning at 2800 rpm for 2 min. To elute the immunocomplexes from the beads, 150 µl of Elution buffer (2.1.5) was added to each sample and the Eppendorf tubes were incubated for 15 min at 65°C. The samples were mixed on vortex in every 5 min. After incubation, the beads were spun down at 2800 rpm for 2 min and the supernatants containing DNA were collected in new tubes. The elution procedure was repeated a second time. 2 µl of Proteinase K (10 mg/ml) was added to each eluted supernatant and also to the thawed input DNA samples and incubated for 2 hours at 55°C. To reverse crosslinks, samples were transferred to 65°C and incubated for 20 hours. Phenol-chloroform extraction technique was used for DNA isolation from the ChIP sample. Supernatant from each sample was mixed with equal volume of phenol/chloroform/isoamyl alcohol and spun down for 3 min at 10000 rpm. The upper phase of each sample was transferred to a new 1.5 ml tube, mixed with an equal volume of chloroform/isoamyl (96:4) and spun down with the same settings. Again, the upper phase was transferred to a new microfuge tube, mixed with 3 M NaAc pH 5.0 (1/10 vol.), with an equal volume of isopropanol and with 1 µl of glycogen (20mg/ml). The solution was incubated overnight at -20°C. After the precipitation, each sample was centrifuged for 45 min at 4°C and 13000 rpm. DNA pellet obtained after isolation was washed once with 70% ethanol, dried at 37°C and dissolved in TE buffer (2.1.5).

The ChIP samples were then used for a qPCR reaction. A reaction mix (50 µl) contained 1 µl of the ChIP DNA, 300 nM of each primer, 25 µl of the iQ™ SYBR® Green Supermix **(**Bio Rad, München) and sterile H_2O (up to 50 µl). All qPCR samples were done in triplicates. qPCR reactions were performed in the iCycler Optical Module 584BR (Bio Rad, München) using the following program:

	Temperature	Time	Cycle No.
Activation	50°C	2 min	1x
Initial denaturation	94°C	10 min	1 x
Denaturation	95°C	15 s	
Annealing	60°C	30 s	40 x
Elongation	72°C	30 s	
Final elongation	72°C	10 min	1 x

qPCR results were normalized to the negative pre-immunized IgG ChIP sample.

2.4.17 Microarray data analysis

C. elegans RNA samples, isolated by Dr. Monika Jedrusik-Bode, from the wild type, single: *hpl-1(tm1624)* X, *his-24(ok1024)* X, *hpl-2(tm1489)* III; double: *hpl-1(tm1624)* X *his-24(ok1024)* X, *his-24(ok1024)* X; *hpl-2(tm1489)* III, *hpl-1(tm1624)* X; *hpl-2(tm1489)* III and triple: *hpl-1(tm1624)* X *his-24(ok1024)* X; *hpl-2(tm1489)* III knockout strains, were analysed using microarray approach by the group of Lennart Optiz at the Georg-August-Univeristy (Göttingen). The microarray data analysis consisted of clustering the genes with significant (logFC < 1.3) expression changes between the groups. For the profiling of considerably up- or down-regulated genes, Wormbase (http://www.wormbase.org) and The Gene Ontology (http://www.geneontology.org/) web pages were used.

2.5 Cell culture based methods

2.5.1 Cultivation of cells

NIH3T3 cell line (Table 2.12) was cultured in plastic flasks with the Dulbecco's MEM (DMEM) medium formulated with 10% Fetal Bovine Serum (FBS) at 37°C with 5% CO_2. Cell culture was split every 3-5 days when the confluence reached approximately 80%. NIH3T3 cells were subcultured by washing them once with 10 ml of Dulbecco's PBS (DPBS) and incubating for 5 min with 0.05% Trypsin-EDTA. When cells began to disperse, trypsin activity was stopped by addition of DMEM culture medium. Cells were seeded out to a new flask at a concentration of 1x 10^4 cells/cm^2 and incubated at 37°C.

2.5.2 Freezing of cells

Cryogenic preservation of cell cultures was used to maintain reserves of cells. The DMEM medium was changed for fresh the day before the freezing of cells. As cells became confluent they were rinsed with 0.05% Trypsin-EDTA solution and incubated for 5 minutes at 37°C.

Once all of the cells were rounded up they were collected with medium in a 15 ml centrifuge tube and spun for 5 min at 1000 rpm. After centrifugation, the supernatant was removed and the cell pellet was resuspended in the cryoprotective medium containing 70% DMSO, 20% FBS and 10% DMSO to give a final cell concentration of about 4x 10^6 cells/ml. Cell suspension was transferred to the cryogenic vials and stored in a Styrofoam box at -80°C. After 24 hours, the cells were transferred to a liquid nitrogen freezer for permanent storage.

2.5.3 Transient transfection of cells

In order to express *C. elegans* proteins in mammalian system NIH3T3, cells were transfected with plasmid DNA carrying sequences of worm's genes. Cells were transiently transfected with the FuGENE® HD Transfection Reagent (Roche, Mannheim) according to manufacturer's protocol. Briefly, the day before the transfection NIH3T3 cells were seeded on a chamber slides (Thermo Fisher Scientific, USA) at a concentration of 8x10^4 cells/ml and incubated with 1 ml of DMEM medium at 37°C with 5% CO_2. On the next day, plasmid DNA was diluted with Opti-MEM I Reduced Serum Medium (Gibco, München) to a concentration of 1µg DNA/50 µl Opti-MEM. FuGENE® HD Transfection Reagent was pipetted into the medium containing diluted DNA, mixed by vigorous tapping the tube and incubated for 15 min at RT. After incubation, the transfection solution was added to the cells in a drop-wise manner. To obtain optimal expression of *C. elegans* proteins, cells were incubated for 24 hours at 37°C with 5% CO_2.

2.5.4 Immunofluorescence staining of cells

NIH3T3 proteins either normally expressed or upon transient transfection were identified by the immunofluorescence staining of cells. Before the antibody-based labelling, cells cultured in chamber slides were washed three times with 1 ml Dulbecco's PBS (DPBS) for 5 min each and fixed at RT for 15 min using 4% PFA solution (2.1.5). After fixation process, cells were washed again three times with DPBS and incubated for 15 min with 600 µl of 0.1% Triton X-100 in DPBS solution to permeabilize the cell membrane. Subsequently, NIH3T3 cells were incubated for one hour with 600 µl of 5% BSA in DPBS solution and then for two hours with 500 µl of primary antibody diluted in 1% BSA in DPBS (for antibodies dilutions see Table 2.6). After incubation, the primary antibody was discarded and cells were washed three times with 600 µl of DPBS. Next, cells were incubated for 1 hour with 500 µl of fluorochrome-conjugated secondary antibody diluted in 1% BSA in DPBS (for antibodies dilutions see Table 2.6) and then washed once with DPBS. To stain nuclear DNA, cells were additionally incubated for 10 min with 300 µl of DAPI solution diluted 1:1000 in 1% BSA in DPBS. Afterwards, stained cells were washed three times with DPBS, closed with coverslip using VECTASHIELD® Mounting Medium (Vector Laboratories, Canada) and stored at 4°C.

2.5.5 Microscopy analysis of transfected cells

The distribution of *C. elegans* proteins expressed in the mammalian NIH3T3 cells was examined on slides used previously for transient transfection (2.5.3). For the fluorescence microscopy, a Leica DMI 6000 B microscope (Leica, Wetzlar) was used.

3 Results

3. 1 Analysis of HIS-24 protein expression and localisation in *C. elegans*

Histone proteins, both linker and core histones, are known to be post-translationally modified. Although modifications of the core histones are relatively well described, still little is known about post-translational modifications of H1. On the basis of the previous report showing post-translational methylation of the human H1.4 linker histone variant at lysine position 26 (K26) [42], *C. elegans* linker histones were analysed with regard to their potential post-translational modifications. Mass spectrometry analysis, performed by Prof. Dr. Jacek R. Wisniewski (Max-Planck-Institute for Biochemistry, Martinsried, Germany) revealed several modification sites of *C. elegans* H1 variants. Only two of eight linker histone variants, HIS-24 and HIL-4, exhibited post-translational modification among which phosphorylation, acetylation and methylation were found (Figure 3.1). Interestingly, the post-translational methylation site was identified only on HIS-24 linker histone that exhibits a single methylation at lysine 14 (Figure 3.1) [115].

Figure 3.1 Study of *C. elegans* H1 Proteomics. HIS-24 as the only one linker histone variant exhibits mono-methylation site at lysine position 14. Apart from methylation, *C. elegans* H1 histones are phosphorylated and acetylated. Figure taken from [115] and modified.

Since HIS-24 mono-methylation was identified, it was of great interest to elucidate the expression pattern of this modified protein. To investigate the differences in distribution and localisation of unmodified and mono-methylated HIS-24, I performed immunohistochemistry of *C. elegans* worms. For the analysis I used αHIS-24 that recognises both the unmodified and the modified histone variant as well as αHIS-24K14me1 antibody provided by Monika Jedrusik-Bode that shows a specificity for the modified state of the linker histone. Microscopy analysis of HIS-24 distribution in the gonad arms of wild type hermaphrodites revealed that the mono-methylated form of linker histone is a predominantly nuclear protein that co-localises with chromatin regions (Figure 3.2 A). While unmodified, HIS-24 is presented in nuclei, together with chromatin, but can be also found in cytoplasm of the germline (Figure 3.2 B), in contrast to somatic cells where it is exclusively nuclear.

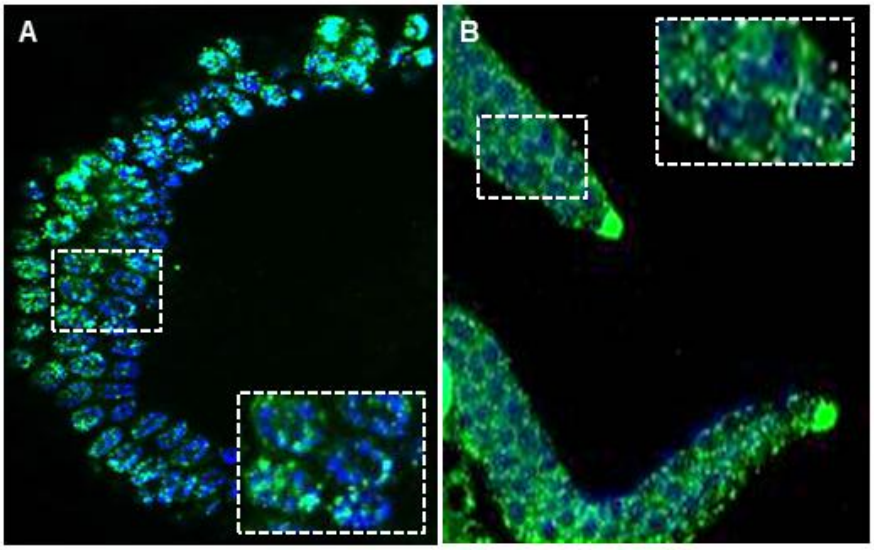

Figure 3.2 Expression pattern of unmodified and mono-methylated linker histone HIS-24 protein in *C. elegans* wild type animals. Immunofluorescence showing association of mono-methylated HIS-24 with chromatin of germline nuclei **(A)** and partially cytoplasmic distribution of unmodified HIS-24 in germ cells of *C. elegans* gonad arms **(B)**.

Since I observed that the mono-methylated form of HIS-24 exhibited predominantly nuclear expression, I was interested in subnuclear localisation of this linker histone variant. *C. elegans* wild type animals stained with αHIS-24K14me1 antibody were first analysed by the STED (**ST**imulated **E**mission **D**epletion) microscopy, what enabled observation on the nuclear interior with high resolution. Strong expression of mono-methylated HIS-24 was detected around nucleolus and in areas closed to the nuclear membrane (Figure 3.3 A). HIS-24K14me1 was also detected already in embryonic nuclei (Figure 3.3 B). The expression pattern was consistent with previously published results showing HIS-24 expression in all somatic cells from the eight-cell stage embryo [107]. Furthermore, as linker histone HIS-24 is a DNA associated protein, I was interested in its subcellular distribution among chromatin domains. In particular, I wanted to verify the potential differences in localisation with chromatin between unmodified and mono-methylated linker histone since both forms displayed diverse distribution in germline of *C. elegans*. Therefore the immunoelectron microscopy was performed in collaboration with Dirk Wenzel (Electron microscopy facility of the Max Planck Institute for Biophysical Chemistry, Göttingen). Immunogold labelling using αHIS-24K14me1 revealed that mono-methylated HIS-24 localises to electro-dense regions, representing heterochromatin, but also to less electro-dense regions that demonstrate euchromatin (Figure 3.3 C, E, F). Consistently with immunofluorescence analysis results, *C. elegans* cells labelled with αHIS-24 antibody, recognizing also unmodified linker histone, exhibited cytoplasmic expression of the analysed linker histone in germline nuclei(Figure 3.3 D, G).

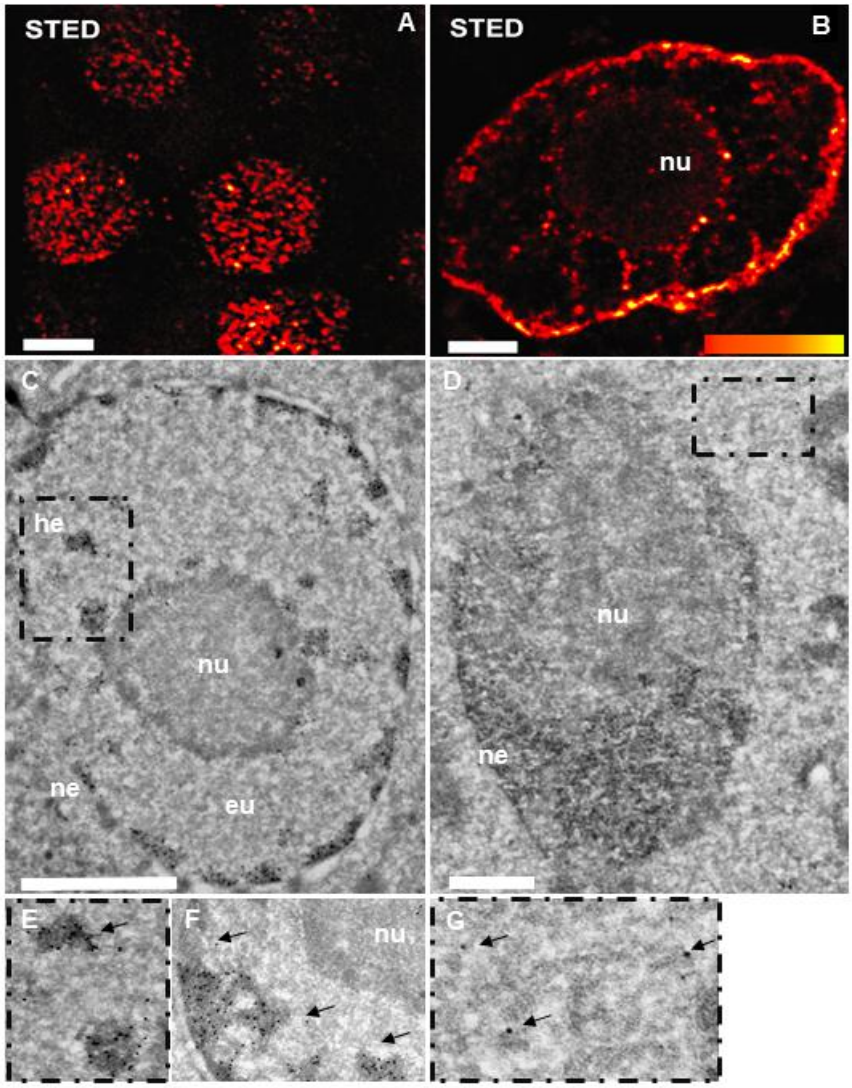

Figure 3.3 The expression pattern of HIS-24 and HIS-24K14me1 protein in *C. elegans* wild type worms. STED microscopy picture showing distribution of HIS-24K14me1 in nucleus of embryonic nuclei **(A)** and in the polyploidal intestine cell **(B)**. Scale bar 2 µm. Electron micrograph of HIS-24K14me1 localisation in electro-dense regions **(C, E)** and less electro-dense regions **(F)** of somatic cells. Electron micrograph of HIS-24 localisation in the cytoplasm **(D, G)**. Arrows indicate HIS-24K14me1 localisation in the nucleus. eu-euchromatin, he-heterochromatin, ne- nuclear envelop, nu-nucleolus. Scale bar 1 µm. Figure taken from [115] and modified

3.2 Identification of HIS-24 interaction partners

3.2.1 HPL heterochromatin like proteins as interaction partners of linker histone HIS-24

Factors interacting with HIS-24 protein were initially identified by Dr. Monika Jedrusik-Bode, using peptide pull- down analysis followed by mass spectrometry study. Proteins bound to mono-methylated lysine 14 and unmethylated HIS-24 peptides were loaded in polyacrylamide SDS gel and complete lanes were analysed by mass spectrometry performed

in collaboration with Prof. Dr. Henning Urlaub (Bioanalytical Mass Spectrometry Group of the Max Planck Institute for Biophysical Chemistry, Göttingen). Between peptides identified by mass spectrometry analysis, two homologs of mammalian heterochromatin protein 1 (HP1), HPL-1 and HPL-2, were identified (Figure 3.4).

Figure 3.4 Homology between human heterochromatin protein 1 and *C. elegans* HPL variants. Alignment of amino-acid sequences of the HP1 proteins from human (HP1α, -β and -γ) and *C. elegans* (HPL-1, -2a and -2b) by the ClustalW method followed by manual editing. The conserved chromo domain (CD) and chromo shadow domain (CSD) are highlighted in grey and red, respectively.

Since it was reported that mammalian HP1 binds specifically to linker histone H1.4K26me2 [42], it was of great interest to elucidate, if *C. elegans* HP1 homologs interact with HIS-24 variant when modified. Immunoprecipitation analysis performed with αHIS-24 as well as αHIS-24K14me1 antibody and with total worm extracts from *hpl-1::gfp* and *hpl-2::gfp* strains, kindly provided by Dr. Francesca Palladino (Ecole Normale Superieure de Lyon, Lyon, France)**,** showed that HPL-1 and HPL-2 protein co-immunoprecipitated with the modified but also with the unmodified form of HIS-24 (Figure 3.5 A, B) [115]. The both αHIS-24 antibodies were used in order to visualise the level of mono-methylated HIS-24 among whole HIS-24 fraction that associates with HPL proteins. The experiment revealed that HPL-1 co-immunoprecipitated with HPL-2 protein (Figure 3.5 C) [115]. The interaction between HIS-24 and HPL proteins was verified by peptide pull-down assay with synthetic peptide of HIS-24 mono-methylated at lysine 14 and with unmodified peptide [115]. The experiment was performed using bacterially (*Escherichia coli*) expressed HPL proteins. HPL-1 protein bound specifically HIS-24K14me1 peptide but HPL-2 failed to bind either modified or unmodified peptide (Figure 3.5 E, F). In contrast, HPL-2 did bind to di- and tri-methylated H3K9 peptides that were used as a positive control [113, 130]**.** To exclude the possibility that interplay between HPL-2 and HIS-24 takes place via binding to HPL-1 protein, the immunoprecipitation experiment was carried out using worm lysate from *hpl-2::gfp; hpl-1(tm1624)* transgenic line, expressing GFP tagged HPL-2 protein on the *hpl-1(tm1624)* knockout background [115]. Remarkably, the immunoprecipitation experiment did not show HPL-2::GFP binding to HIS-24K14me1 (Figure 3.5 D). To summarize, mass spectrometry

analysis, immunoprecipitation and peptide pull-down experiments revealed that HPL-1 protein specifically binds to mono-methylated histone HIS-24 whereas HPL-2 protein associates with linker histone only through HPL-1 protein.

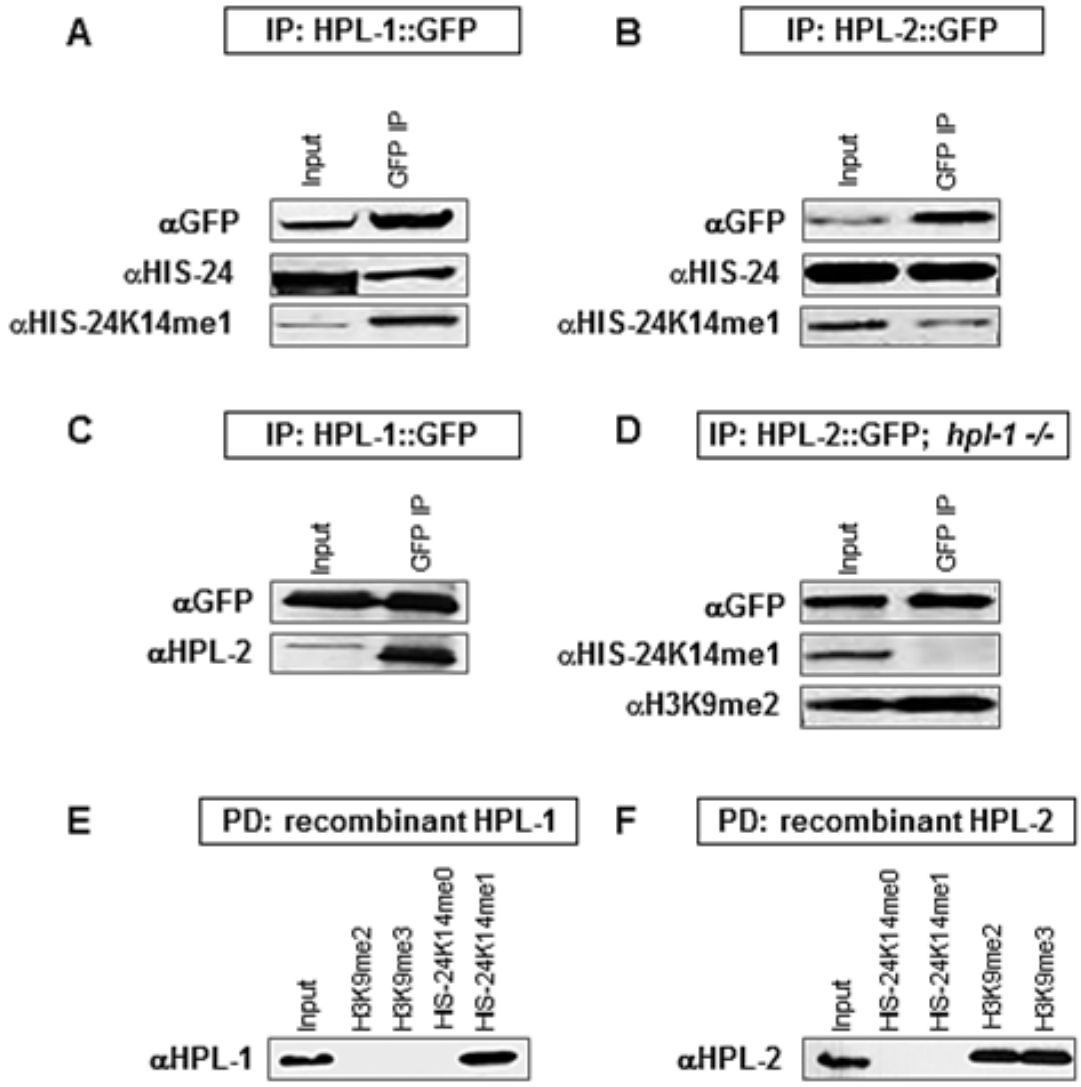

Figure 3.5 Analysis of specific binding of HPL-1 protein to mono-methylated HIS-24. HPL-1 and HPL-2 proteins co-immunoprecipitated with both, the modified HIS-24K14me1 and the unmodified linker histone **(A, B)**. HPL-2 protein bound to lys14-methylated HIS-24 **(A).** HPL-1 precipitated together with HPL-2 protein **(C)** but HPL-2 did not bind to HIS-24 variant in the absence of HPL-1 protein **(D).** Recombinant HPL-1 protein specifically recognised methylated form of HIS-24 **(E)** whereas recombinant HPL-2 protein did not show binding to HIS-24 peptides **(F)**. Input 5%, α-antibody, IP- immunoprecipitated protein fraction, PD- pulled down protein. Figure taken from [115] and modified.

3.3 Characterisation and consequences of *his-24, hpl-1* and *hpl-2* deletion in *C. elegans*

To analyse the biological function of linker histone HIS-24 and heterochromatin protein HPL in *C. elegans*, I characterised *his-24(ok1024)*X, *hpl-1(tm1624)*X**,** *hpl-2(tm1489)*III single, *his-*

*24(ok1024)*X *hpl-1(tm1624)*X, *his-24(ok1024)*X*; hpl-2(tm1489)*III, and *hpl-1(tm1624)*X; *hpl-2(tm1489)*III double as well as *his-24(ok1024)*X *hpl-1(tm1624)*X; *hpl-2(tm1489)*III triple mutant strains (Table 2.11).

3.3.1 Description of *his-24, hpl-1* and *hpl-2* depleted *C. elegans* strains used in the study

Single gene deletion mutants *his-24(ok1024)*X were generated by the *C. elegans* Gene Knockout Consortium. The strain was outcrossed five times with N2 line that is considered as a wild type strain [123]. *his-24(ok1024)*X mutant animals carry partial deletion in genomic sequence of *his-24* gene that results in partial loss of exon 1 and 2 (Figure 3.6A). *C. elegans hpl-1(tm1624)*X and *hpl-2(tm1489)*III mutant animals were generated by Dr. Shohei Mitani (Core Facility PI, Tokyo Women's Medical University) and kindly provided by Dr. Francesca Palladino (Ecole Normale Superieure de Lyon, Lyon, France). Both strains were outcrossed four times with N2 strain to eliminate background mutations. A 496 bp deletion in the genomic sequence of *hpl-1* gene in *hpl-1(tm1624)* X strain results in a loss of exon 2 (part), exon 3 and 4 (Figure 3.6 B). *hpl-2(tm1489)* III knockout strain exhibits deletion of 672 bp from the genomic sequence that causes complete loss of exon 3 and 4 or exon 5 and 6 in *hpl-2a* or *hpl-2b* gene, respectively (Figure 3.6 C). Single mutant strains showed mild phenotype under standard growth conditions at 20°C. Double and triple mutant strains (Table 2.11) were generated by crossing and were genotyped for the carried deletions. Primers used for genotyping are listed in Table 2.8.

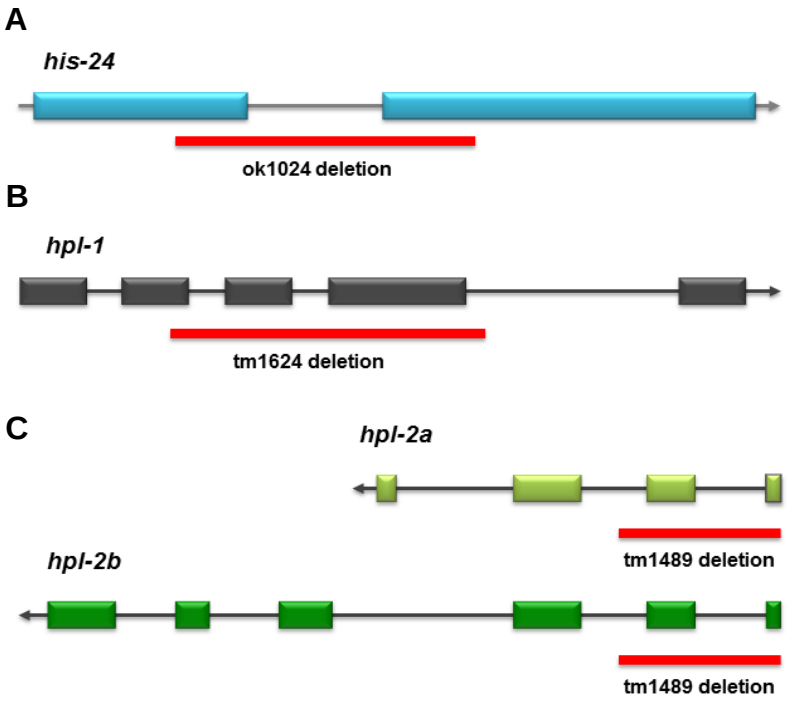

Figure 3.6 Localisation of *his-24, hpl-1* and *hpl-2* genes deletions. Red bars indicate deleted regions in particular gene.

3.3.2 Knockout of *his-24* together with *hpl* genes results in several developmental defects in *C. elegans* hermaphrodites

To investigate the biological function of the HIS-24 linker histone and heterochromatin proteins HPL as well as the potential synergism between them, I analysed single, double and triple mutant animals in relation to their morphological defects. In particular, I concentrated on the germline development, the vulva cells differentiation and the somatic patterning of the male tail since these tissues are known to be affected by mutations in chromatin factors [107, 131]. Moreover, HPL-2 protein is known to play a crucial role during the vulva cell fate specification process in the synthetic multivulva (synMuv) pathway of *C. elegans* [121]. I observed that single deletion of either *his-24* or *hpl-2* gene resulted in low percentage of sterile worms in population (7% and 5% respectively) at 20°C (Table 3.1). As it has been suggested by Jedrusik and Schulze [107], sterility of *his-24(ok1024)*X hermaphrodites probably resulted from the observed substantial defects in the gonad structure as well as of aberrant germline proliferation and differentiation (lack of differentiated oocytes and sperm). Remarkably single *hpl-2(tm1489)*III mutant animals exhibited significant increase of sterility at 25°C (Table 3.1). Surprisingly, the knockout of *hpl-1* gene did not caused visible developmental defects. Interestingly, I found that the deletion of *his-24(ok1024)*X combined with *hpl-2(tm1489)*III mutation caused synergistic defects in vulva cell fate specification, which was manifested by everted vulva or multivulva phenotype (Table 3.1). Furthermore, *his-24(ok1024)*X*; hpl-2(tm1489)*III double mutant hermaphrodites exhibited sterility both at 20°C and 25°C (Table 3.1). Microscopic analysis of *his-24(ok1024)*X*; hpl-2(tm1489)*III hermaphrodites gonads revealed that observed sterility may be an effect of reduced oocyte number and the presence of the oocyte DNA endoreduplication phenotype (Figure 3.7 A, B), which presence has been also reported in hermaphrodites with mutation of homeobox gene *ceh-18* [132]. All substantial morphological aberrations observed in animals with double and triple mutations suggested that HIS-24 and HPL proteins may play a synergistic role during *C. elegans* development.

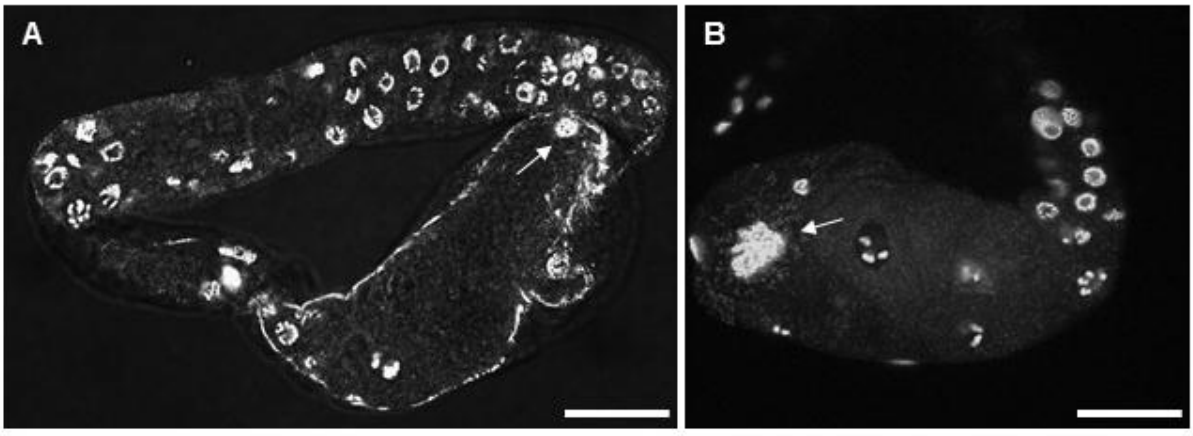

Figure 3.7 Analysis of the gonad morphology in *his-24(ok1024)*X*; hpl-2(tm1489)*III double mutant hermaphrodites. DAPI stained gonad arms with a reduced number of oocytes and the DNA reduplication **(A, B).** Arrows point to oocytes that exhibit endoreduplication of DNA. Scale bar 25 μm

Table 3.1 Genetic interaction of *his-24*, *hpl-2* and *hpl-1* genes.

Genotype	% sterility		% multivulva		% everted vulva	
	20°C	25°C	20°C	25°C	20°C	25°C
wild type	0	0	0	0	0	0
***his-24(ok1024)*X**	7	8	0	0	0	0
***hpl-1(tm1624)*X**	0	0	0	0	0	0
***hpl-2(tm1489)*III**	5	66	5	22	0	32
***his-24(ok1024)*X *hpl-1(tm1624)* X**	0	0	0	0	0	2
***his-24(ok1024)*X;*hpl-2(tm1489)*III**	11	88	9	28	12	62
***hpl-1(tm1624)* X; *hpl-2(tm1489)*III**	0	L2/L3 arrest	4	L2/L3 arrest	5	L2/L3 arrest
***his-24(ok1024)* X *hpl-1(tm1624)* X; *hpl-2(tm1489)*III**	11	L2/L3 arrest	12	L2/L3 arrest	28	L2/L3 arrest

Further analysis revealed severe defects in the somatic gonad morphology of *his-24(ok1024)*X *hpl-1(tm1624)*X mutants grown at 20°C. In wild type, in single mutant animals and in *his-24(ok1024)*X*; hpl-2(tm1489)*III mutant strain, the gonad arm has an U-shaped form (Figure 3.8 A, B, C), while approximately 25% of *his-24(ok1024)*X *hpl-1(tm1624)*X animals exhibited a loop form of gonad arm (Figure 3.8 D).

In addition, animals were also examined with regard to the size of their brood. Interestingly, the brood size of the *his-24(ok1024)*X*; hpl-2(tm1489)*III hermaphrodites was decreased to 35% of wild type worms, and was further decreased to 50% in *his-24(ok1024)*X *hpl-1(tm1624)*X; *hpl-2(tm1489)*III triple mutant animals (figure 3.8 E).

In summary, the results of the analysis suggested that HIS-24 and HPL-1 proteins are involved in the somatic gonad development while HIS-24 together with HPL-2 has a synergistic effect on the vulva cell fate specification and reproduction.

Figure 3.8 Analysis of the somatic gonad development and the brood size in *his-24* and *hpl* deficient animals. *his-24(ok1024)*X **(A)** or *hpl-1(tm1624)*X **(B)** single, and *his-24(ok1024)*X*; hpl-2(tm1489)*III double mutant animals exhibit normal, U-shaped form of gonad arm **(C).** *his-24(ok1024)*X *hpl-1(tm1624)*X double mutant hermaphrodite demonstrates a loop form of the gonad arm **(D)**. The graph shows the number of embryos (± SEM) in individual strains of *C. elegans*. Stars point to statistically significant changes in the brood size ($p < 0.0001$) versus wild type strain.

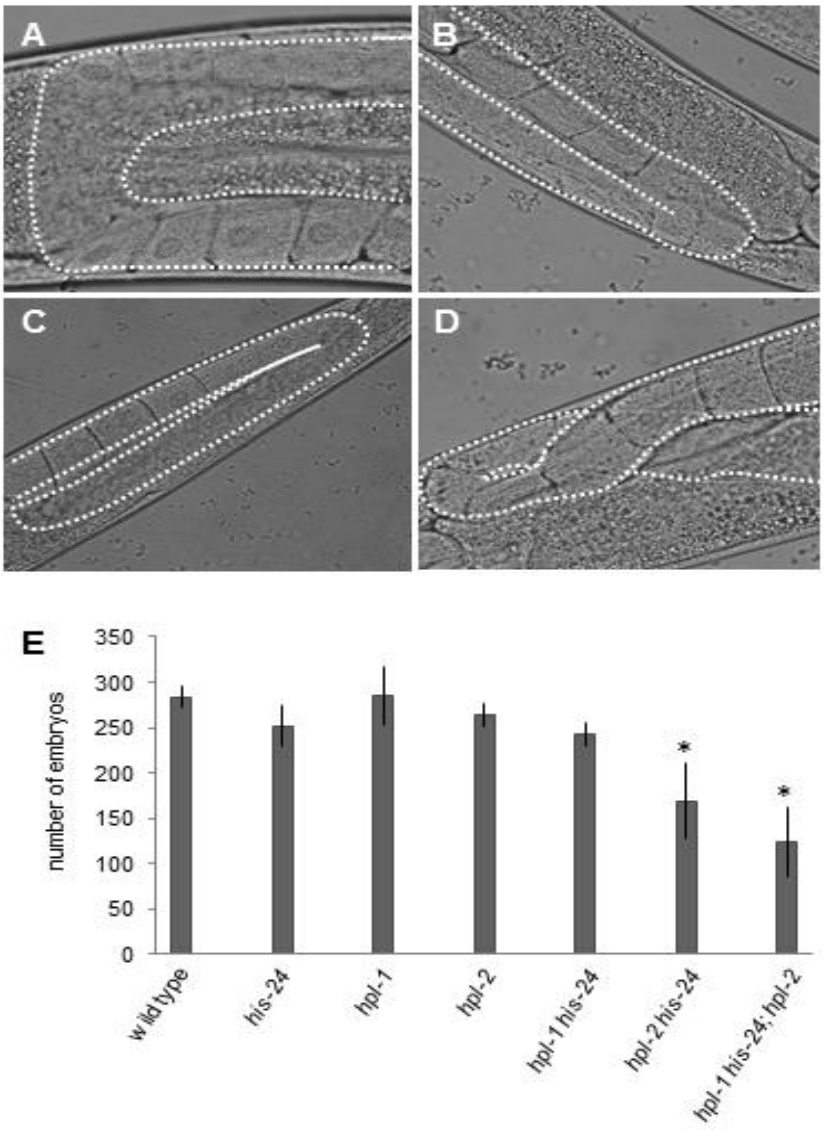

3.3.3 Deletion of *his-24* with *hpl-2* gene leads to reduction of chromatin compaction

As has been reported, HIS-24 and HPL-2 proteins are essential in the chromatin-based repression of germline transgenes and they are also indispensable for the proper germline development [107, 121]. To elucidate if these both factors have an influence on the nuclei structure, I performed DAPI staining (see section 2.4.9) of dissected *C. elegans* gonads from *his-24(ok1024)*X and *hpl-2(tm1489)*III single as well as *his-24(ok1024)*X*; hpl-2(tm1489)*III double mutants, and looked on the germline nuclei morphology. Thorough analysis revealed substantial differences in size and morphology of nuclei among *C. elegans* strains. In particular, I observed that *his-24(ok1024)*X*; hpl-2(tm1489)*III double mutant worms had a significantly bigger germline nuclei when compared to *his-24(ok1024)*X, *hpl-2(tm1489)*III single mutants and to wild type animals grown at 20°C (Figure 3.9 A-D). Furthermore, the observed chromatin in 86% of *his-24(ok1024)*X*; hpl-2(tm1489)*III individuals had a more open, less condensed structure (Figure 3.9 E). These results suggested that HIS-24 together with HPL-2 protein may be important for the chromatin condensation.

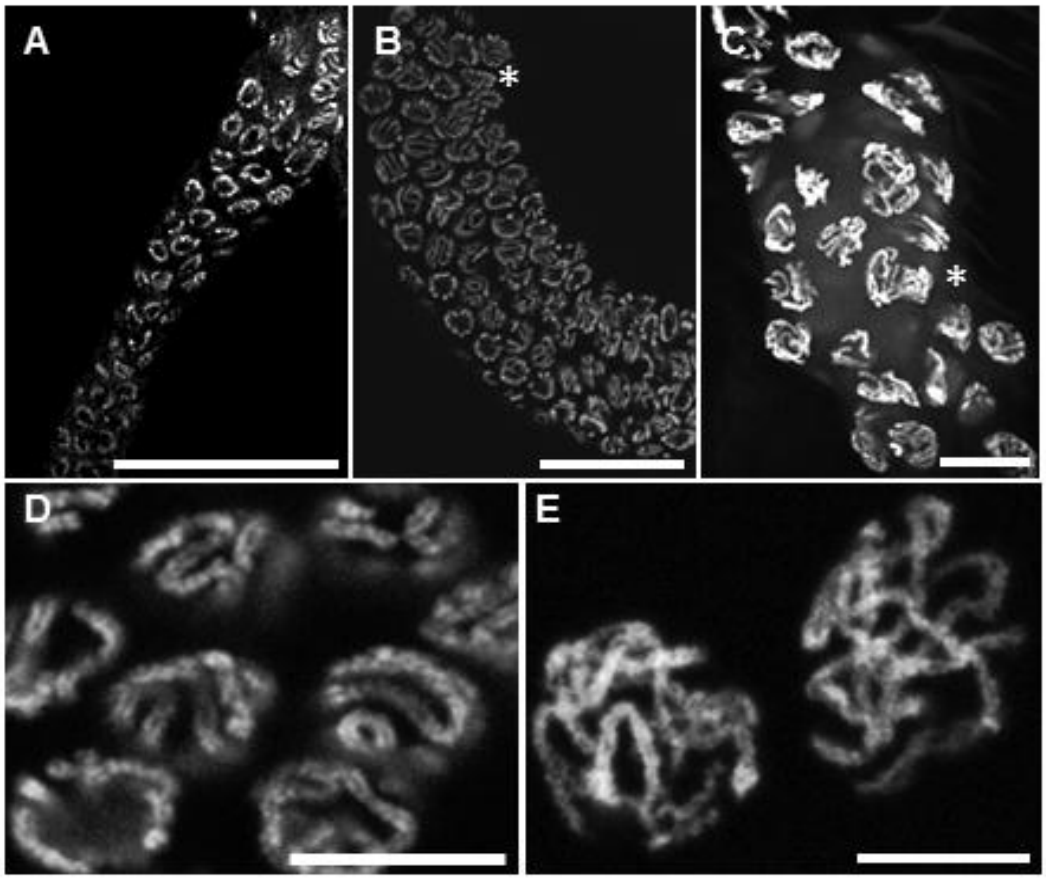

Figure 3.9 Chromatin structure analyses in germ cells of *his-24* and *hpl* deficient animals. DAPI stained gonad arms of *his-24(ok1024)*X **(A)** or *hpl-2(tm1489)*III single **(B)** and *his-24(ok1024)*X*; hpl-2(tm1489)*III double mutants **(C)**. Stars point to pachytene stage germ nuclei. Scale bar: 50 µm. Morphology of pachytene stage nuclei of the germline of *hpl-2(tm1489)*III mutant animals **(D)** compared to the nuclei of *his-24(ok1024)*X*; hpl-2(tm1489)*III double mutants **(E)**. Scale bar: 7.5 µm.

To gain more insight into the role of HIS-24 and HPL proteins in chromatin condensation process, I decided to investigate the heterochromatin distribution in *his-24* and *hpl* deficient *C. elegans* worms. For this reason I analysed the immunoelectron microscopy pictures that were taken by Dr. Dirk Wenzel at the Electron Microscopy group of the Max Planck Institute for Biophysical Chemistry, Göttingen. The analysis revealed that single and double mutant animals did not exhibit any changes in heterochromatin distribution in comparison to the wild type animals (Figure 3.10 A-F). In contrast, nuclei of *his-24(ok1024)*X *hpl-1(tm1624)*X**;** *hpl-2(tm1489)*III triple mutant worms showed substantial reduction of heterochromatin regions (electro-dense regions), indicating that deletion of three chromatin associated proteins influences the heterochromatinisation process (Figure 3.10 G). Remarkably, *his-24(ok1024)*X *hpl-1(tm1624)*X**;** *hpl-2(tm1489)*III triple mutant animals are viable at 25°C in spite of such a substantial changes in the heterochromatin level.

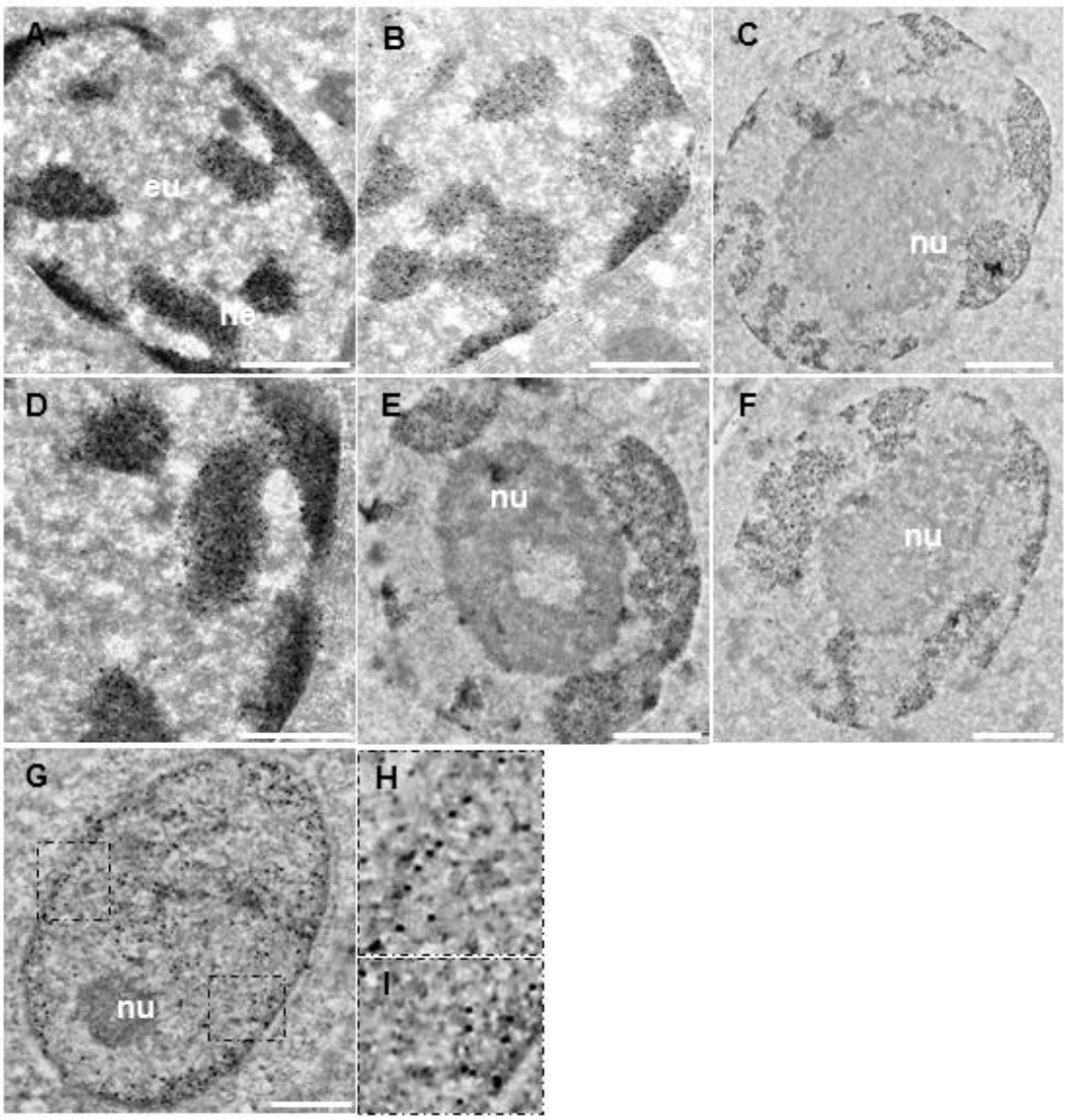

Figure 3.10 Analysis of heterochromatinzation in nuclei of *his-24* and *hpl* deficient worms. Nuclei of *C. elegans* worms from *his-24(ok1024)*X **(A)**, *hpl-1(tm1624)*X **(B)**, *hpl-2(tm1489)*III **(C),** *his-24(ok1024)*X *hpl-1(tm1624)* X **(D),** *his-24(ok1024)*X*; hpl-2(tm1489)*III **(E)** and *hpl-1(tm1624)*X*; hpl-2(tm1489)*III **(F)** strains, presenting heterochromatin regions (electro-dense regions). Nucleus of *his-24(ok1024)*X *hpl-1(tm1624)*X; *hpl-2(tm1489)*III triple mutant worm with strongly reduced areas of heterochromatin **(G- I)**. Black dots indicate H3K27me3 localisation in the nucleus. eu-euchromatin, he-heterochromatin, nu-nucleolus. Scale bar 0.5 µm.

A more relaxed structure of chromatin in the absence of HIS-24 and HPL-2 proteins and affected heterochromatinisation in triple mutant animals let me expect to observe significant changes of the histone modifications. In particular, I concentrated on two repressive heterochromatin marks: H3K9me3 and H3K27me3. I performed western blot analysis of chromatin modification levels of all mutant strains using antibodies specific for H3K9me3, H3K27me3 modifications and an antibody for H3 histone level. Surprisingly, I did not find considerable alternations of histone modification levels in *C. elegans* single, double and triple mutant worms (Figure 3.11). The result implied that apparently the observed aberration in heterochromatinisation is not a result of changes in the level of core histones modifications.

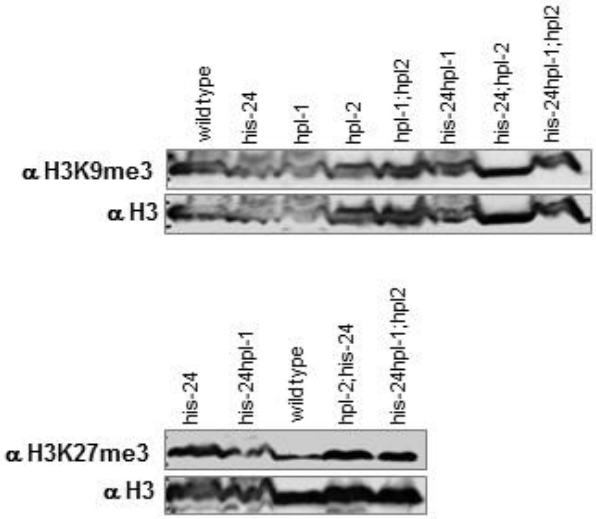

Figure 3.11 The levels of heterochromatin marks are not altered in the *hpls, his-24* mutant animals. No changes of the H3K27me3, H3K9me3 and H3 levels were observed in single, double and triple mutant animals.

3.4 Genome-expression profile analysis of *his-24*, *hpl-1* and *hpl-2* mutant *C. elegans* worms

3.4.1 Identification of mis-regulated genes in *his-24*, *hpl-1* and *hpl-2* mutant animals

The alternation of chromatin compaction observed in germline nuclei of *his-24(ok1024)*X*; hpl-2(tm1489)*III double mutants suggested that significant changes in transcription of genes may occur. To analyse the influence of *his-24* and *hpl* deletion on the gene transcription process, the whole genome expression profiling of each mutant strain was performed in collaboration with Lennart Optiz and Dr. Gabriela Salinas-Riester (Georg-August University, DNA Microarray Facility, Göttingen, Germany). I compared the gene expression profiles of single, double and triple mutant animals of L4 larva stage, grown at 20°C. The L4 larvae were used for the microarray approach since it was determined by Prof. Dr. Jacek R. Wisniewski that HIS-24 is the most abundant linker histone variant at that stage (Appendix A.2). The genome profiling was compared to the transcription profile of wild type animals that served as a control. Surprisingly, the analysis of approximately 16 000 microarray target probes revealed that only a small number of transcripts displayed slight changes in expression (Table 3.2). The majority of those transcripts showed up-regulation (7.1%) in response to deletion of three chromatin factors HIS-24, HPL-2 and HPL-1, whereas two times less of transcripts exhibited down-regulation. To summarize, results of the analysis suggested that HIS-24 and HPL are not global repressors of the transcription (Table 3.2).

Table 3.2 Summary of microarray analysis of gene expression in mutant animals versus wild type.

Genotype	Up-regulated genes (%)	Down-regulated genes (%)
	FDR<0.05; |log$_2$-fold change| > 1 (total)	
*his-24(ok1024)*X	1.5 (15458)	2.0 (15719)
*hpl-1(tm1624)*X	2.6 (15458)	2.1 (15719)
*hpl-2(tm1489)*III	4.7 (14718)	2.1 (15612)
*hpl-1(tm1624)*X*; hpl-2(tm1489)*III	4.9 (15013)	2.2 (15521)
*hpl-1(tm1624)*X *his-24(ok1024)*X	3.6 (15458)	1.0 (15719)
*hpl-2(tm1489)*III*; his-24(ok1024)*X	8.1 (14718)	2.2 (15612)
*hpl-1(tm1624)*X *his-24(ok1024)*X*; hpl-2(tm1489)*III	7.1 (14941)	3.9 (15540)

Given the physical interaction of HPL-1 with mono-methylated lysine 14 of HIS-24, and the role of heterochromatin proteins HPL in the *C. elegans* development [115, 116], it was of great interest to elucidate whether HIS-24 and HPL variants regulate the expression of common genes. At first, I compared mis-regulated transcripts of single mutant animals and I found 273 transcripts that displayed mis-regulation in the absence of either HIS-24, HPL-1 or HPL-2 proteins (Figure 3.12 A). After the analysis of double and triple mutant strains, I found 464 transcripts that were commonly up-regulated in *hpl-1(tm1624) hpl-2(tm1489)*III and *his-24(ok1024)*X *hpl-1(tm1624)*X; *hpl-2(tm1489)*III mutants, and 195 commonly down-regulated transcripts (FDR<0.05) (Figure 3.12 B). Additionally, to gain more insight into the function of genes mis-regulated in single, double and triple mutant animals, I performed a gene ontology study. The analysis of the set of transcripts common for *his-24(ok1024)*X, *hpl-1(tm1624)*X and *hpl-2(tm1489)*III single mutant worms revealed a presence of a significant number of genes induced by bacterial or fungal infection (Figure 3.13 A). On the other hand, the verification of the genes which were up-regulated or down-regulated in *his-24(ok1024)*X *hpl-1(tm1624)*X, *hpl-2(tm1489)*III mutant animals showed few sets of genes with some link to reproduction, lipid storage, protein metabolic processes, embryonic development, determination of adult lifespan, transmembrane transport as well as regulation of cellular transcription (Figure 3.13 B). Interestingly, among mis-regulated transcripts that presented association to the transcriptional regulation, the majority belonged to the hormone receptor family genes (*nhr*), but I identified also some genes with homeodomain sequences (*ceh-33*, *ceh-39* and *ceh-43*) (Appendix A.3).

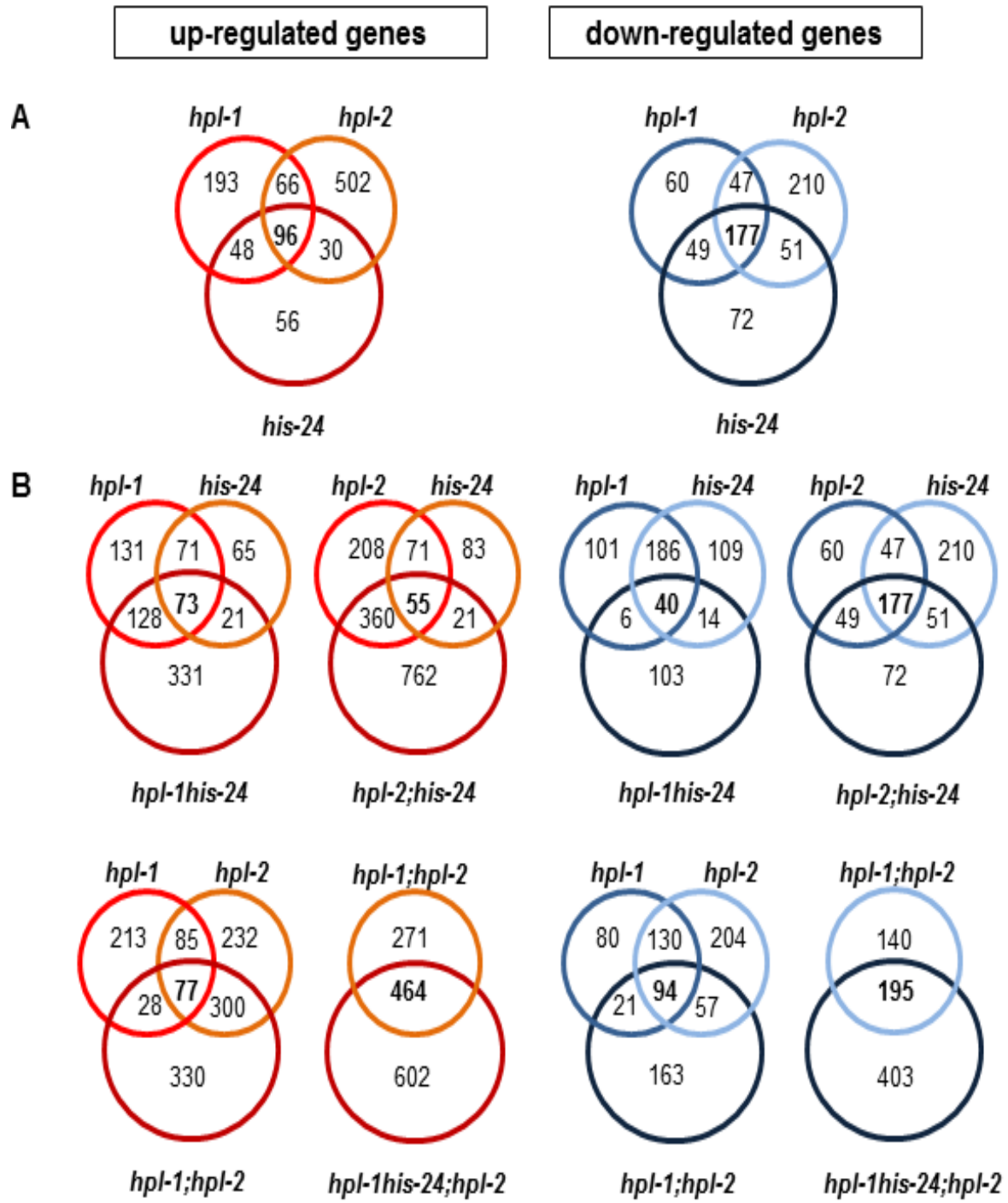

Figure 3.12 Genome-expression profile analyses of *his-24*, *hpl-1* and *hpl-2* mutant *C. elegans* worms. Venn diagrams on the basis of whole genome microarray showing the extent of overlap among genes that are associated with HIS-24 and HPLs activity. Values for fold change are the average from two independent biological replicates (FDR<0.05; $|\log_2$-fold change$| > 1$). Figure taken from [115] and modified.

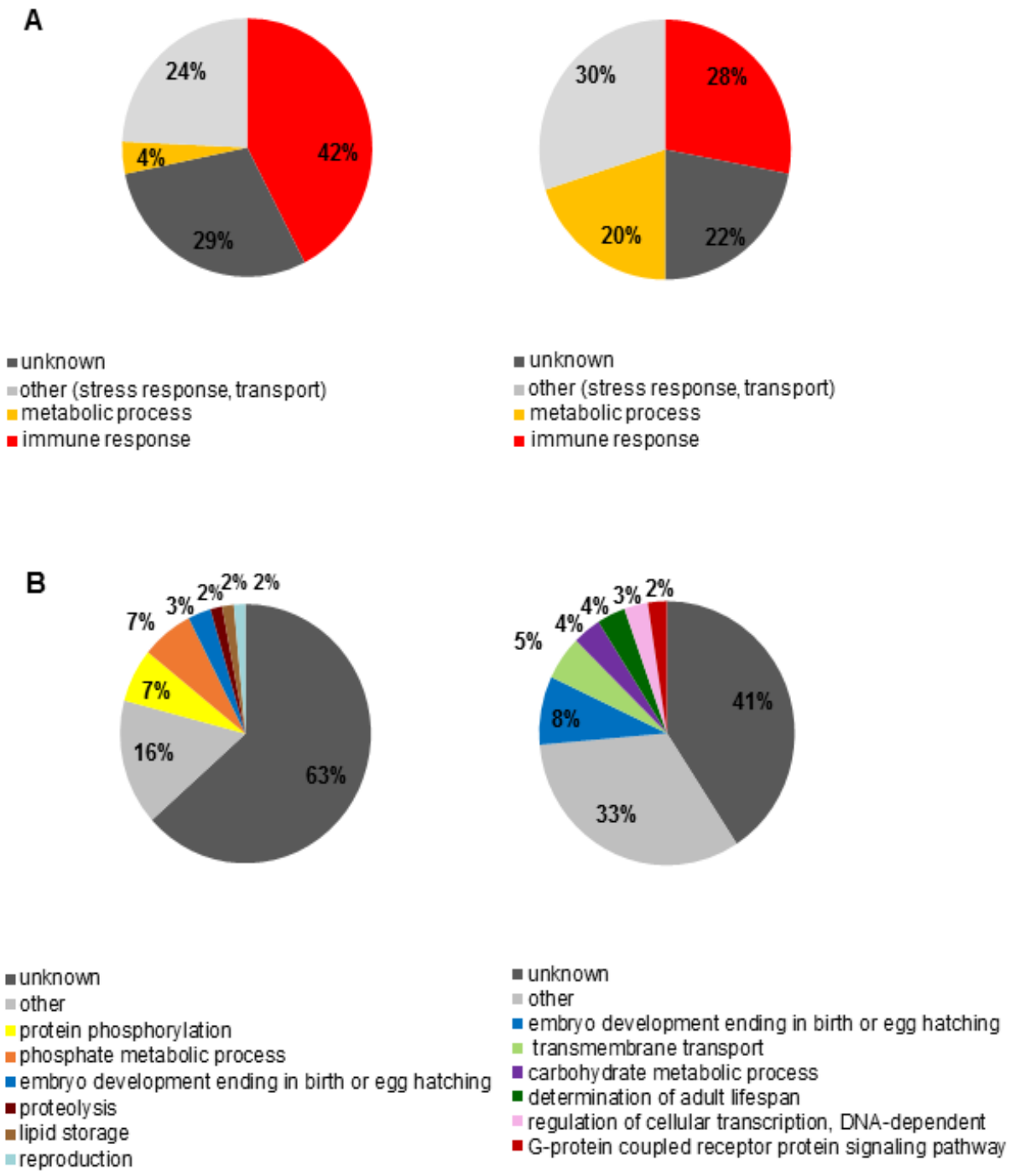

Figure 3.13 Summary of the gene ontology profiling of up- and down-regulated genes in *his-24, hpl-1* and *hpl-2 C. elegans* mutants. Functional clusters of genes up-regulated (graphs on the left) and down-regulated (graphs on the right) in *his-24(ok1024)*X, *hpl-1(tm1624)*X and *hpl-2(tm1489)*III single mutants **(A)** and in *his-24(ok1024)*X *hpl-1(tm1624)*X, *hpl-2(tm1489)*III triple mutant animals **(B)**. The molecular functions and the percentage of the total for each group are indicated. Gene Ontology (GO) terms taken from The Gene Ontology web page (http://www.geneontology.org/). Figure taken from [115] and modified.

3.5 Analysis of tail homeotic-like transformations observed in *C. elegans* males with *his-24*; *hpl-2* deletion

3.5.1 Deletion of *his-24* and *hpl-2* cause male tail defects

As it was observed in genome expression profiling, loss of *his-24* and *hpl-2* function resulted in transcriptional de-repression of several homeobox genes (Appendix A.3). Interestingly, HPL-2 protein is known to be involved in the regulation of *lin-39 Hox* gene expression in vulva precursor cells of *C. elegans* [133]. Both observations led me to expect the presence of homeotic transformations in *C. elegans* mutant strains with *his-24* and *hpl* deletion. In my study I concentrated on the male tail development since it provides an ideal model for analysis of homeotic alterations in *C. elegans* [134].
The wild type *C. elegans* male tail consists of nine pairs of rays that are generated during post-embryonic development by the three most posterior pairs of seam cells (lateral hypodermal cells) V5, V6 and T (Figure 3.14 A). Each of the lateral seam cells give rise to different subset of rays. The V5 cell is programmed to form ray 1, V6 forms rays 2-6, while T cell give rise to rays 7, 8 and 9 (Figure 3.14 B) [125, 126, 131].

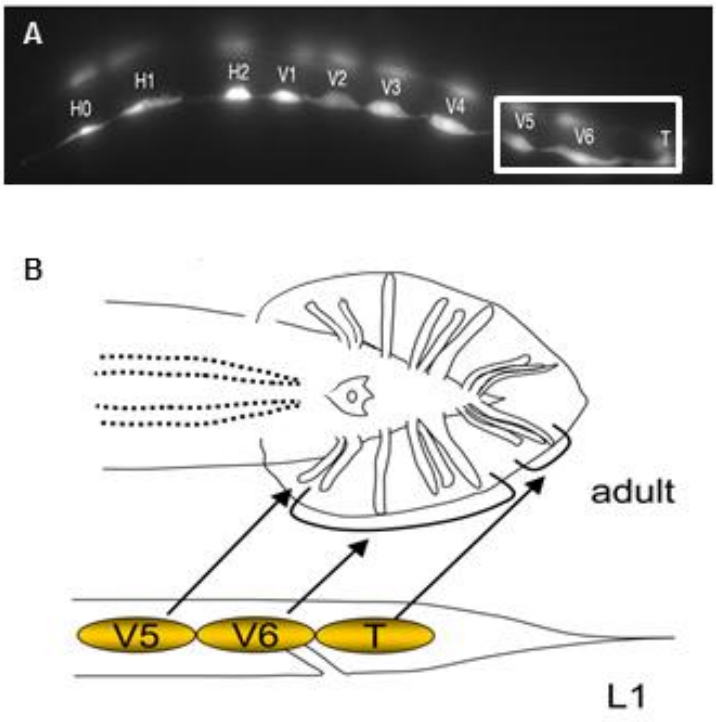

Figure 3.14 Origin of the hypodermal mating structures during postembryonic development. Epifluorescent image of early-L1-stage transgenic animal expressing the *ajm-1::gfp* reporter in epithelial cells (seam cells). Frame mark area of three posterior seam cells that give origin to the mating structures in *C. elegans* **(A)**. Figure taken from the Worm Atlas (http://www.wormatlas.org/). Illustration of the blast cells locations in the posterior of an L1 larval male are shown in a lateral view. Seam cells V5, V6 and T each give rise to a subset of the rays **(B)**. Illustration taken from [134].

For examination of *C. elegans* mating structures, worms were grown of *him-14* (**H**igh **I**ncidence of **M**ales) (RNAi) feeding plates in order to generate representative population of

males in every mutant line. In phenotype analysis, I found that *his-24(ok1024)*X, *hpl-1(tm1624)*X and *hpl-2(tm1489)*III single mutants as well as *his-24(ok1024)*X *hpl-1(tm1624)*X and *hpl-1(tm1624)*X*; hpl-2(tm1489)*III double mutant worms exhibited normal development of mating structures (Table 3.3, Figure 3.15 A-E, H). In contrast, double mutant males, carried mutations in *his-24* and *hpl-2* as well as triple mutant males, displayed abnormalities in development of V-deriving cells. 37% of *his-24(ok1024)*X*; hpl-2(tm1489)*III and 83% of *his-24(ok1024)*X *hpl-1(tm1624)*X; *hpl-2(tm1489)*III mutants exhibited following aberrations of rays morphology: underdeveloped ray, ectopic rays (present anteriorly to normal rays), rays fusions or complete lack of rays in some areas (Table 3.3, Figure 3.15 F, G, H). Interestingly, *hpl-1* deletion had no visible effect on the male tail development however it appeared to have synergistic effect in combination with *his-24* and *hpl-2* double mutation. As presented in Table 3.2, the number of underdeveloped and fused rays was increased up to 46% in the *his-24(ok1024)*X *hpl-1(tm1624)*X; *hpl-2(tm1489)*III triple mutant animals when compared with *his-24(ok1024)*X; *hpl-2(tm1489)*III double mutant males (Table 3.3). This suggested that *hpl-1* plays an important function in rays development but only in combination with *his-24*, *hpl-2* double mutation.

Table 3.3 Ray defects associated with *hpl-1*, *hpl-2* or *his-24* mutations.

Genotype	Ectopic rays (%)	Fused/ missing rays (%)	Underdeveloped rays 1 and 2 (%)	Number of worms scored
wild type*	0	0	0	72
*his-24(ok1024)*X*	0	0	0	54
hpl-1(tm1624) X *	0	0	0	48
hpl-2(tm1489) III *	0	0	0	67
***his-24(ok1024)* X; *hpl-2(tm1489)* III ***	**0**	**24**	**13**	**73**
hil-3(ok1556) on *hpl-2* feeding*	0	0	0	78
his-24(ok1024 X)*hpl-1(tm1624)* X *	0	0	0	54
***his-24(ok1024)* X *hpl-1(tm1624)* X *; hpl-2(tm1489)* III ***	**4**	**37**	**42**	**107**
hpl-1(tm1624) X*; hpl-2(tm1489)*III*	0	0	0	58

* on *him-14* feeding plates at 20°C

To evaluate obtained results as a specific for the linker histone *his-24* depletion, I also tested male tail phenotype of a *hil-3(ok1556)*X mutant strain. Remarkably, I did not observe any aberration of male tail development in *hil-3(ok1556)*X males growing on *hpl-2* (RNAi) feeding plates (Table 3.3, Figure 3.15 H), indicating that HIS-24 together with HPL-2 specifically affects the formation of rays in *C. elegans* males.

Interestingly, the presence of ectopic rays and ray fusions in *his-24(ok1024)*X; *hpl-2(tm1489)*III mutants was consistent with phenotype described for *C. elegans* males with mis-regulation of *mab-5* and *egl-5 Hox* genes in the V-derived ray lineage [131].

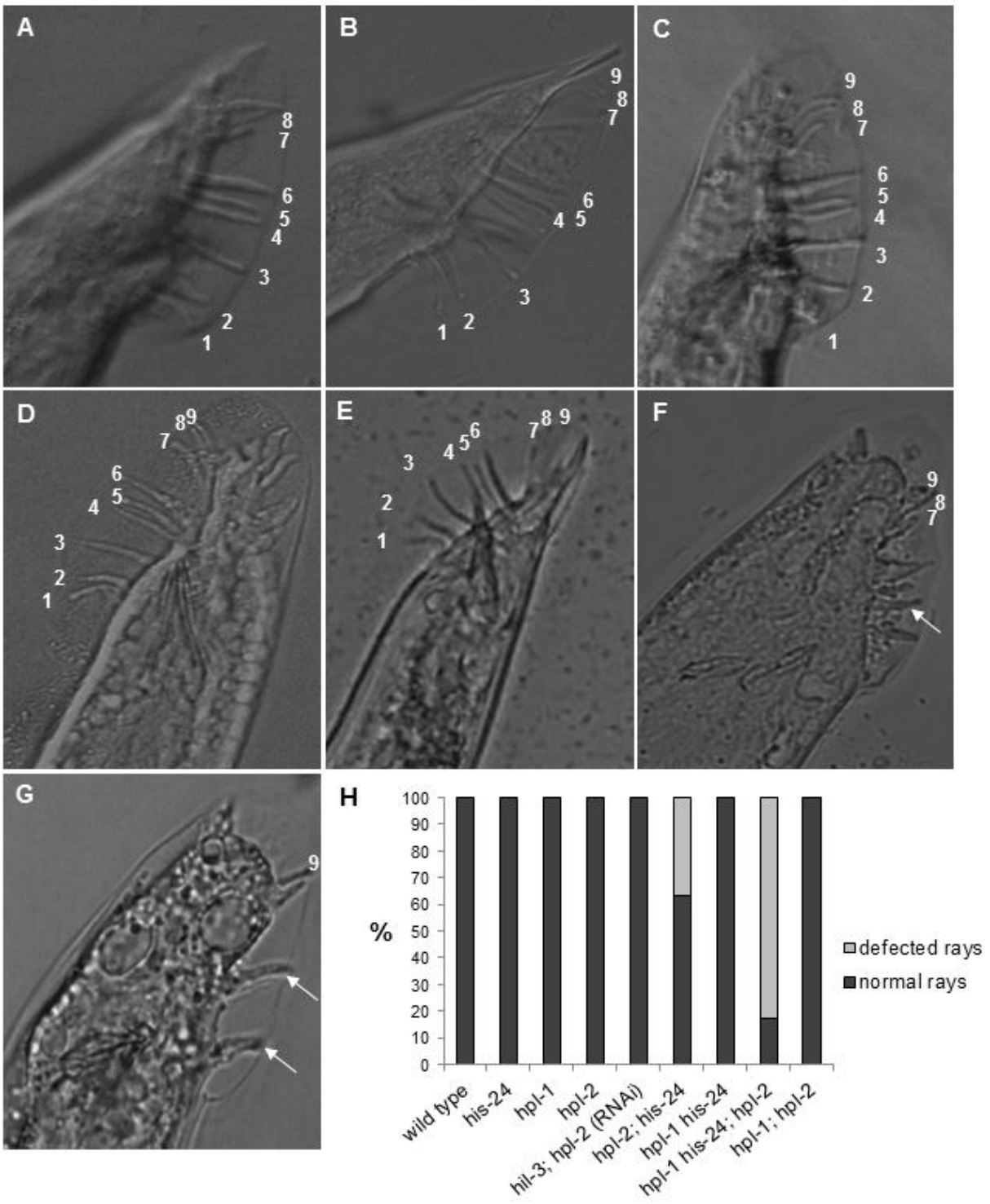

Figure 3.15 Analysis of postembryonic development of male-specific structures in *his-24* and *hpl* deficient animals. All nine rays are formed normally in *his-24(ok1024)*X **(A)**, *hpl-1(tm1624)*X **(B)** or *hpl-2(tm1489)*III **(C)** single mutants as well as in *his-24(ok1024)*X *hpl-1(tm1624)*X **(D)** and *hpl-1(tm1624)*X; *hpl-2(tm1489)*III **(E)** double mutant males. Abnormal male tails of *his-24(ok1024)*X; *hpl-2(tm1489)*III **(F)** and *his-24(ok1024)*X *hpl-1(tm1624)*X; *hpl-2(tm1489)*III **(G)** mutant animals. Arrows point to ray fusions. Quantifications of ray defects observed in single, double and triple mutant males **(H)**. All animals were growing on *him-14* (RNAi) feeding plates at 20°C.

3.5.2 Lack of *his-24* and *hpl-2* genes activity cause ectopic expression of *mab-5* and *egl-5 Hox* genes

As previously mentioned, deletion of *his-24* together with *hpl* resulted in aberrant pattering of mating structures in *C. elegans* males. Remarkably, these abnormalities were similar to phenotype associated with mis-regulation of *mab-5* and *egl-5 Hox* gene [131]. Interestingly, microarray data revealed that *mab-5* gene was slightly up-regulated in *his-24(ok1024)*X; *hpl-2(tm1489)*III mutant males. The *Hox* genes *mab-5* (**M**ale **Ab**normal, an ortholog of human *HOXB7*) and *egl-5* (**EG**g **L**aying defective, an ortholog of human *HOXB9-13*) are localised on III chromosome and expressed from the same gene cluster (homolog of human HOM-C) (Figure 3.16) [90]. Both are involved in proper development of V-derived rays [131, 135]. Within the posterior body region, *mab-5* activity controls epidermal, neuronal, and mesodermal cell differentiation whereas *egl-5* is required for specification of the HSN (hermaphrodite specific neuron) cell fate and also for cell fates specification within the tail region.

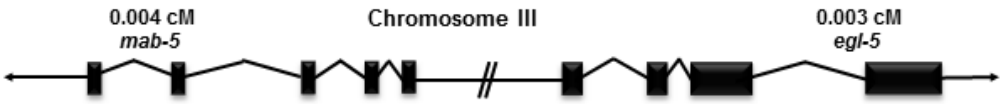

Figure 3.16 Chromosomal localisation of the *mab-5* and *egl-5 Hox* genes. The *mab-5* and *egl-5* are found in the Hox genes cluster on chromosome III.

In order to verify possible regulation of *mab-5* and *egl-5 Hox* genes by HIS-24 and HPL proteins, I crossed single, double and triple mutant hermaphrodites with males carrying *mab-5::gfp* or *egl-5::gfp* reporter (for strains description see Table 2.11). Then I analysed the expression pattern of MAB-5::GFP and EGL-5::GFP proteins in wild type animals and in combination with *his-24(ok1024)*X, *hpl-1(tm1624)*X and *hpl-2(tm1489)*III mutations. Because both *Hox* genes reporters have the strongest expression at L3 larva stage of *C. elegans* development, I examined males mainly at that stage but I also looked at the expression in adult animals. Interestingly, I observed that MAB-5::GFP protein was ectopically expressed in approximately 30% of early L3 stage *his-24(ok1024)*X; *hpl-2(tm1489)*III double mutant males (Figure 3.17 A, B). Altered expression of this reporter was also detected in adult males. Similarly, about 80% of *his-24(ok1024)*X; *hpl-2(tm1489)*III double mutant males at L3 larva stage displayed an ectopic expression of *egl-5::gfp* reporter (Figure 3.17 E). In the wild type animals, EGL-5::GFP expression was present only in the two daughters of R4, R5 and R6 ray precursor cells (Figure 3.17 C), while *his-24(ok1024)*X; *hpl-2(tm1489)*III double mutant males exhibited ectopic expression of reporter protein in descendants of ray precursor cells anterior to R4, R5 and R6 (Figure 3.17 D). Surprisingly, I did not observe significant enhancement of the *mab-5* and *egl-5* ectopic expression in *hpl-1* depleted *his-24(ok1024)*; *hpl-2(tm1489)* double mutant animals, suggesting that only HIS-24 and HPL-2 are essential for silencing of the *Hox* gene cluster. To ensure that *Hox* genes regulation requires the activity of both HIS-24 and HPL-2, I looked at the MAB-5::GFP and

EGL-5::GFP reporters in *his-24(ok1024)* and *hpl-2(tm1489)* single mutant strains. I did not observe an ectopic expression of the analysed HOX proteins (Figure 3.17 B, E) indicating that only double deletion of *his-24* together with *hpl-2* results in mis-regulation of *mab-5* and *egl-5* genes.

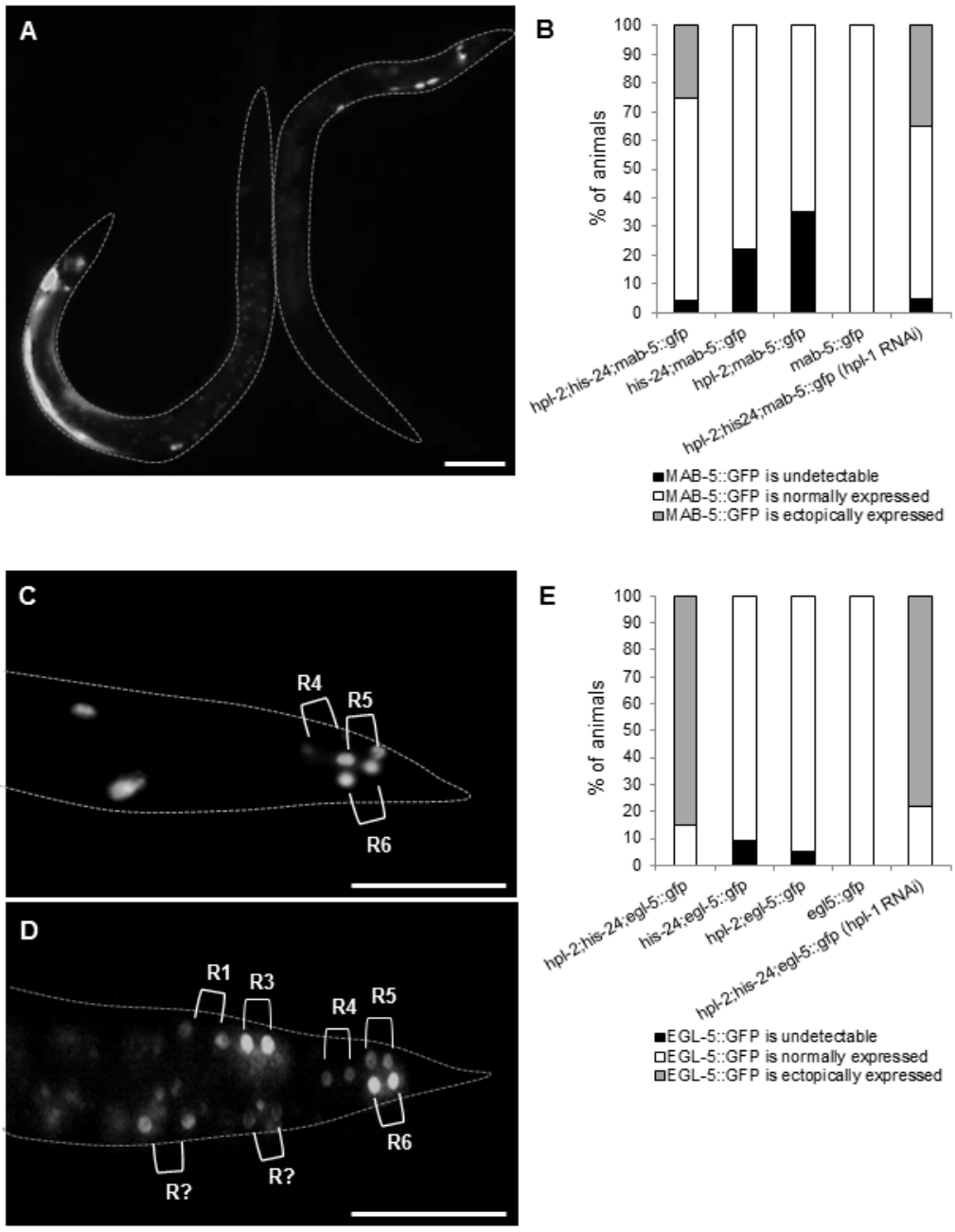

Figure 3.17 Analysis of *mab-5* and *egl-5* ectopic expression in *his-24* and *hpl* deficient *C. elegans* males. A *his-24(ok1024)*X; *hpl-2(tm1489)*III early L3 mutant male with ectopically expression of *mab-5::gfp* in ventral cord nerve and hypodermal syncytium cell ((hyp7); animal on the left side) **(A)**. Expression of *mab-5::gfp* in a wild type early L3 male marks very few cells at the posterior (animal on the right side) **(A)**. Scale bar: 25 µm. Quantification of progeny of single, double and triple mutant hermaphrodites with males carrying *mab-5::gfp* reporter compared to progeny of wild type males **(B)**. In a wild type L3 male, expression of *egl-5::gfp* is limited to the daughters of the ray precursor cells R4, R5 and R6 which give rise to rays 3-6 **(C)**. In *hpl-2*; *his-24* L3 mutant male the reporter is expressed in additional ray sublineages **(D)**. Scale bar: 25 µm. Quantification of progeny of single, double and triple mutant hermaphrodites with males carrying *egl-5::gfp* reporter compared to wild type males **(E)**.

Additionally, since HIS-24 and HPL proteins are known to be involved in the silencing mechanisms of *gfp*-reporter genes [107, 136], I decided to validate obtained results by analysis of the EGL-5 protein level in *C. elegans* mutant males. For that reason I performed western blot analysis with wild type, *his-24(ok1024)*; *hpl-2(tm1489)* double mutants as well as *egl-5::gfp C. elegans* males using αEGL-5 antibody, kindly provided by Prof. Scott W. Emmons (Albert Einstein College of Medicine, USA) (for concentrations see Table 2.6). Interestingly, I observed that males carrying *his-24(ok1024)*; *hpl-2(tm1489)* double mutation exhibited an increased level of endogenous EGL-5 protein in comparison to the wild type and *egl-5::gfp* males (Figure 3.18 A, B). This suggested that absence of HIS-24 and HPL-2 results in de-repression of *egl-5* gene and in turn in increased expression of EGL-5 protein. Unfortunately, I could not perform the same experiment for the *mab-5::gfp*; *his-24(ok1024)*; *hpl-2(tm1489)* mutant strain due to lack of available antibody for MAB-5 protein.

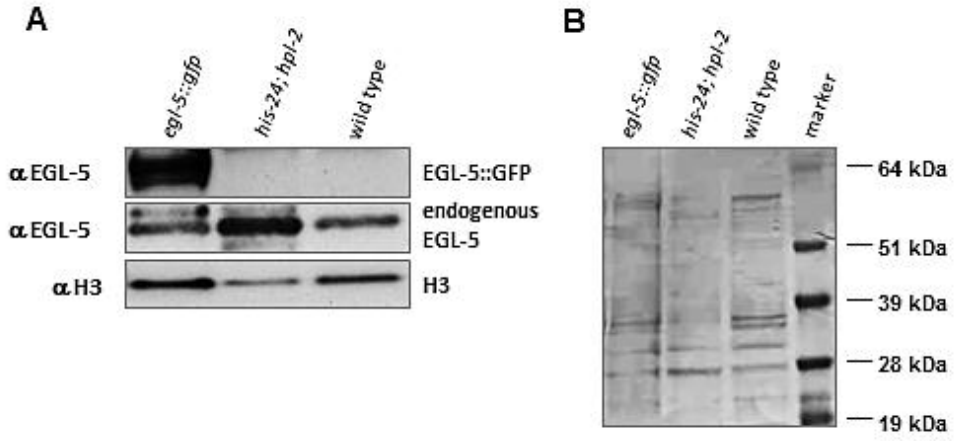

Figure 3.18 Verification of EGL-5 protein level in males lacking *his-24* and *hpl-2* expression. Western blot of protein extracts (150 males) from wild type, *his-24(ok1024)*X; *hpl-2(tm1489)*III double mutant and *egl-5::gfp* transgenic strain **(A)**. The blot was probed with an antibody raised against EGL-5 that recognised endogenous EGL-5 and the EGL-5::GFP fusion protein in *egl-5::gfp* transgenic strain. Protein loading was confirmed by probing with an αH3 antibody and by staining of the western blot with Ponceau S **(B)**.

3.5.3 Identification of *mab-5* and *egl-5 Hox* genes as downstream targets of HIS-24 protein

As HIS-24 and HPL-2 protein turned out to be required for inhibition of *mab-5* and *egl-5* ectopic expression, I was interested if these proteins could regulate the *Hox* genes expression by direct binding to the regulatory sites *in vivo*. For that purpose I performed chromatin immunoprecipitation experiments (ChIP) followed by qPCR reactions using primer sets directed to the promoters and intragenic regions of *mab-5* and *egl-5* genes (for primer sequence see Table 2.8). For the control I used primers set directed to the promoter of *ceh-2*, a homeobox gene. As mentioned earlier (see section 3.5.2), *mab-5* and *egl-5* are tightly clustered on chromosome III (Figure 3.16), indicating that the expression of these genes can be coordinately regulated. In contrast, *ceh-2* gene is located on chromosome I. ChIP

experiments were carried out by using total worm extracts isolated from synchronous cohorts of *his-24::gfp* or *hpl-2::gfp* animals at L2/L3 larva stage and with specific ChIP-grade antibodies (for concentrations see Table 2.6). Remarkably, ChIP-qPCR analyses of *his-24::gfp* worms extract revealed association of HIS-24 protein with the promoters and also with intragenic regions of *mab-5* and *egl-5* (Figure 3.19 A, B, Appendix A.4a, b). Moreover, qPCR showed HIS-24 binding to the *mab-5* and *egl-5* gene promoters with a 20-fold and 25-fold increase respectively in comparison to binding to the *ceh-2* promoter region (Appendix A.4a). In contrast, I did not observe significant differences of H3 occupancy at the *mab-5* and *egl-5* and *ceh-2* promoters (Figure 3.21, Appendix A.4e) what implicated that HIS-24 may be specifically enriched at *mab-5* and *egl-5 Hox* gene promoters. The results suggested that most likely, HIS-24 binds to *mab-5* and *egl-5* genes in order to repress transcription in majority of *C. elegans* tissues.

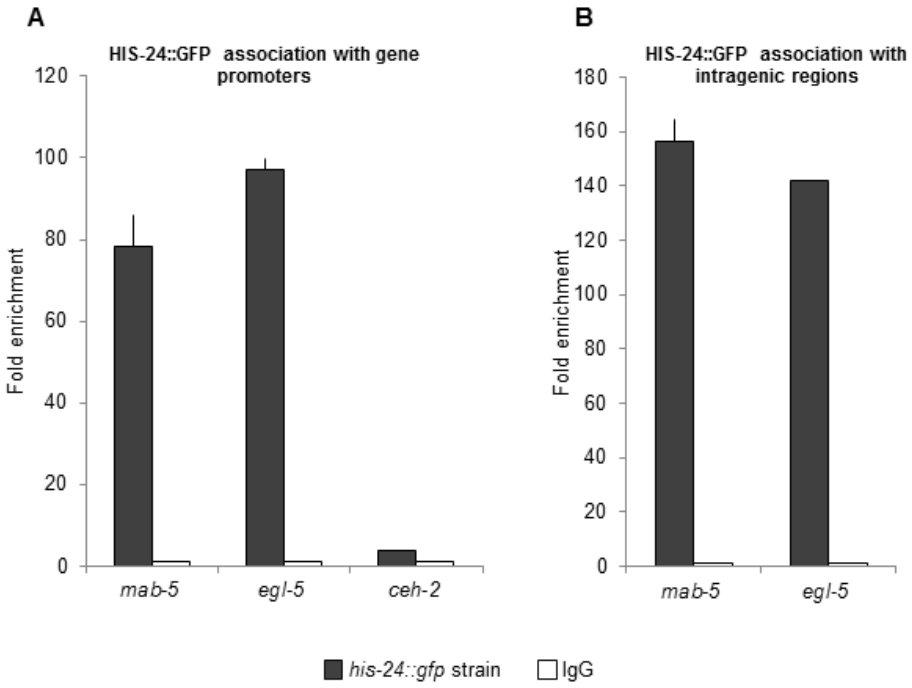

Figure 3.19 Investigation of the linker histone HIS-24::GFP binding to the regulatory regions of *mab-5*, *egl-5* and *ceh-2* genes. Quantitative chromatin immunoprecipitation assay determining HIS-24::GFP fusion protein occupancy at the *mab-5*, *ceh-2* or *egl-5* promoters **(A)** and at the intragenic regions **(B)** of *mab-5* and *egl-5* genes. ChIP was performed using an antibody raised against GFP and extracts prepared from *his-24::gfp* transgenic worms. All results were normalized to binding by control IgG antibody and performed in triplicates. Error bars indicate ±SD.

Furthermore, to ascertain that HIS-24 protein is associated with the *Hox* genes only during their repressive state, I performed the chromatin immunoprecipitation analysis using the *mab-5::gfp* strain that exhibits an ectopic expression of the *mab-5 Hox* gene. This specific *mab-5::gfp* line expresses the *Hox* gene reporter on a background with depletion of *sor-1*, a gene that encodes SOR-1 protein, which is one of the factors involved in the transcriptional repression of *mab-5* [137]. For that ChIP-qPCR experiment I used αHIS-24 antibody that recognises both, the mono-methylated and the unmodified form of HIS-24 protein. I observed

that in the *mab-5::gfp* strain, occupancy of HIS-24 protein was reduced at the *mab-5* gene promoter and intragenic region by 3.5-fold (43%) and 2-fold (32%) respectively in comparison to the binding in wild type animals (Figure 3.20 A, B, Appendix A.4c). This implied that ectopic expression of the *Hox* genes may occur when HIS-24 protein is not associated with regulatory regions. Interestingly, these results were consistent with a previous western blot analysis that showed strong expression of EGL-5 protein in *his-24(ok1024)*; *hpl-2(tm1489)* mutant males.

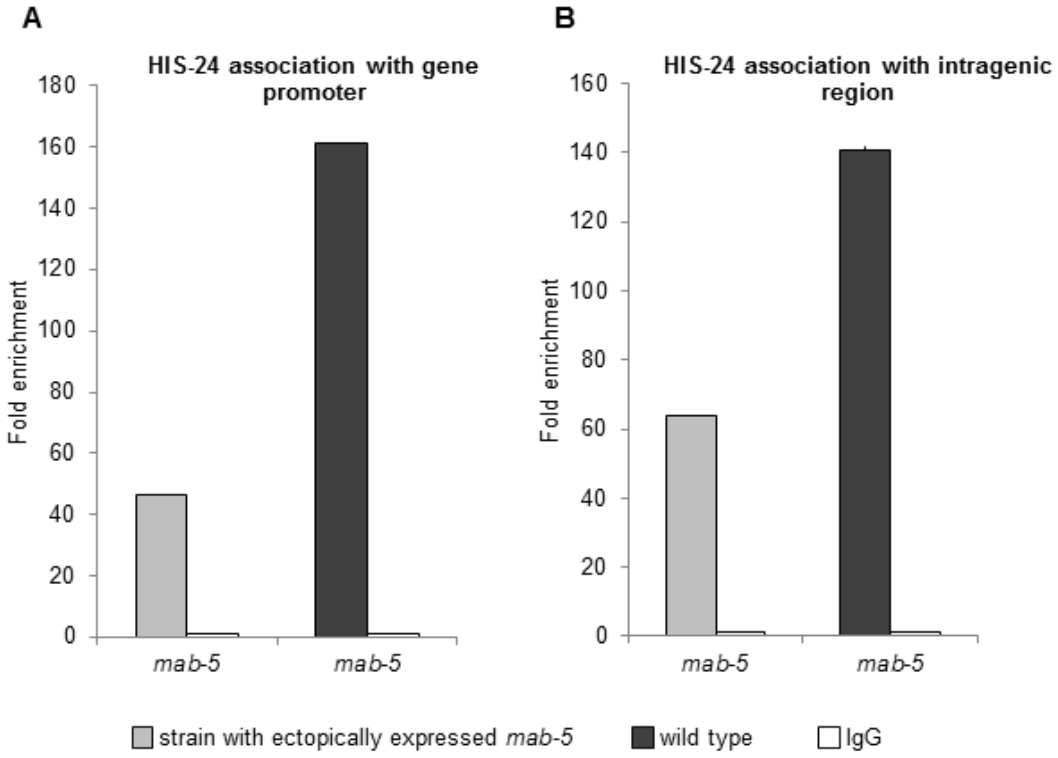

Figure 3.20 Analysis of HIS-24 enrichment at regulatory region of the *mab-5 Hox* gene. Quantitative chromatin immunoprecipitation assay determining decreased level of the linker histone HIS-24 at the *mab-5* promoter **(A)** and at the intragenic region **(B)** in *mab-5::gfp* transgenic strain, where *mab-5* is ectopically expressed. The results were confronted with the HIS-24 enrichment in wild type strain. ChIP was performed using αHIS-24 antibody. All results were normalized to binding by control IgG antibody and performed in triplicates. Error bars indicate ±SD.

To elucidate the function of HPL-2 protein in regulation of the *mab-5* and *egl-5 Hox* genes, I performed the ChIP-qPCR experiment by using total worm extract isolated from *hpl-2::gfp* strain. Unfortunately, I failed to detect binding of HPL-2 protein to the *mab-5* and *egl-5 Hox* genes. I concluded that HPL-2 protein may not be directly associated with the promoters of *mab-5* and *egl-5*, however it seems to play a crucial role in their transcriptional repression.

3.5.4 Association of H3K27me3 chromatin mark with the *mab-5* and *egl-5 Hox* genes transcriptional activity

As it has been reported by Schwartz and Pirrotta [138], H3K27me3 chromatin mark is known to be associated with the repression of *Hox* genes transcription. In my study, I was interested in tri-methylated H3K27 mark occupancy at the promoters and intragenic regions of *mab-5* and *egl-5* genes in the wild type organism and in the absence of *his-24* and *hpl-2* genes expression. By ChIP-qPCR analysis I first investigated the status of H3K27 tri-methylation in wild type animals. Additionally, I examined levels of H3K4me3, a mark for active transcription of genes, as well as of H3K9me2 and H3K27me2. I found that H3K27me3 was abundantly present at the promoters of *mab-5* and *egl-5* and *ceh-2* genes and at intragenic regions, in contrast to H3K4me3 mark (Figure 3.21 A, B, Appendix A.4d). Furthermore, I did not detect an increased level of H3K9me2 and H3K27me2 chromatin marks, what suggested a specific enrichment of H3K27me3 at *mab-5* and *egl-5* (Figure 3.21 A, B, Appendix A.4d).

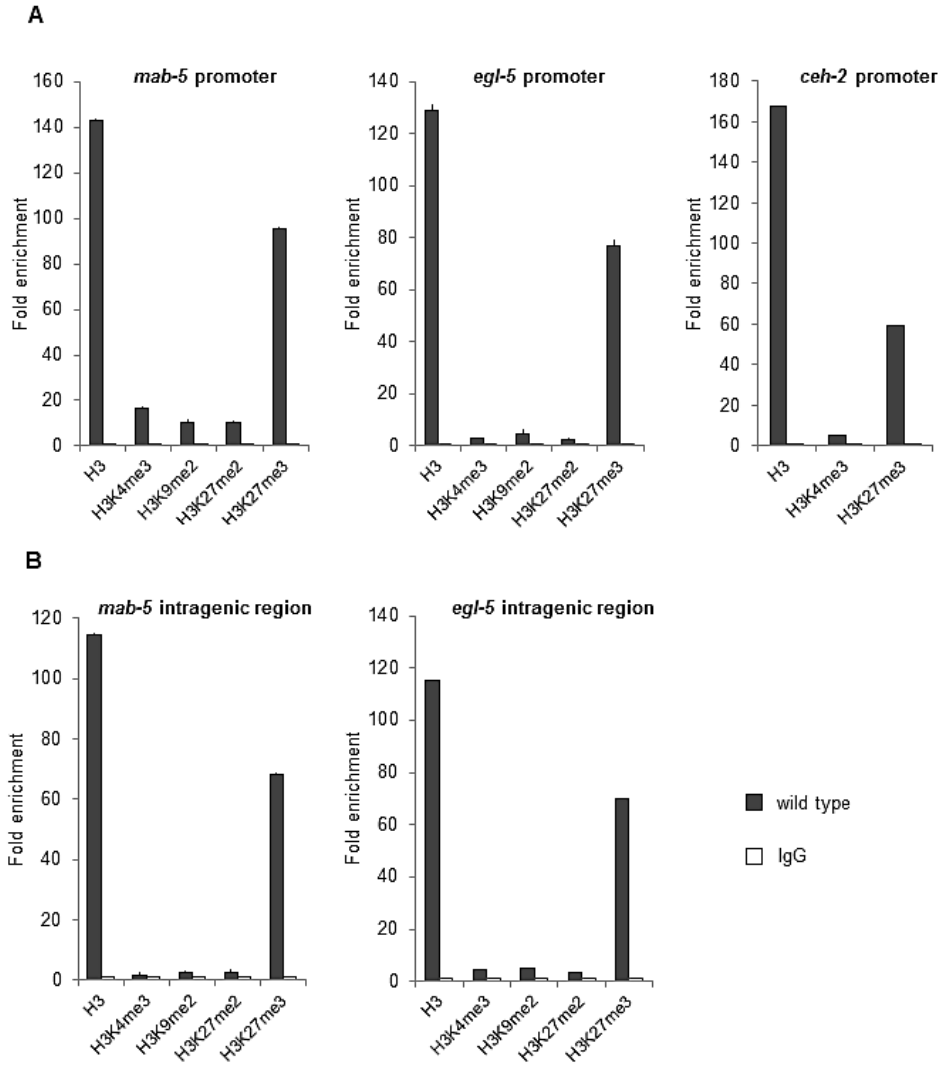

Figure 3.21 Study of H3K27me3 mark occupancy at regulatory regions of *mab-5*, *egl-5* and *ceh-2* genes. Quantitative ChIP performed from total protein of wild type worms. The H3K27me3 mark is abundantly enriched at *mab-5*, *egl-5* and *ceh-2* promoters **(A)** and at the intragenic regions **(B)** of *mab-5*, *egl-5* genes. All results were normalized to binding by control IgG antibody and performed in triplicates. Error bars indicate ±SD.

I also verified the level of H3K27me3 chromatin mark in *mab-5::gfp* strain with ectopic expression of the *mab-5 Hox* gene in *sor-1* knockout background. Interestingly, the ChIP-qPCR analysis revealed a significant reduction of H3K27 tri-methylation level at the *mab-5 Hox* gene, similarly to previously observed reduction of HIS-24 binding (see section 2.5.3). The level was decreased 5-fold (63%) at the promoter and 3-fold (56%) at the intragenic region in comparison to wild type (Figure 3.22 A, B, Appendix A.4e).

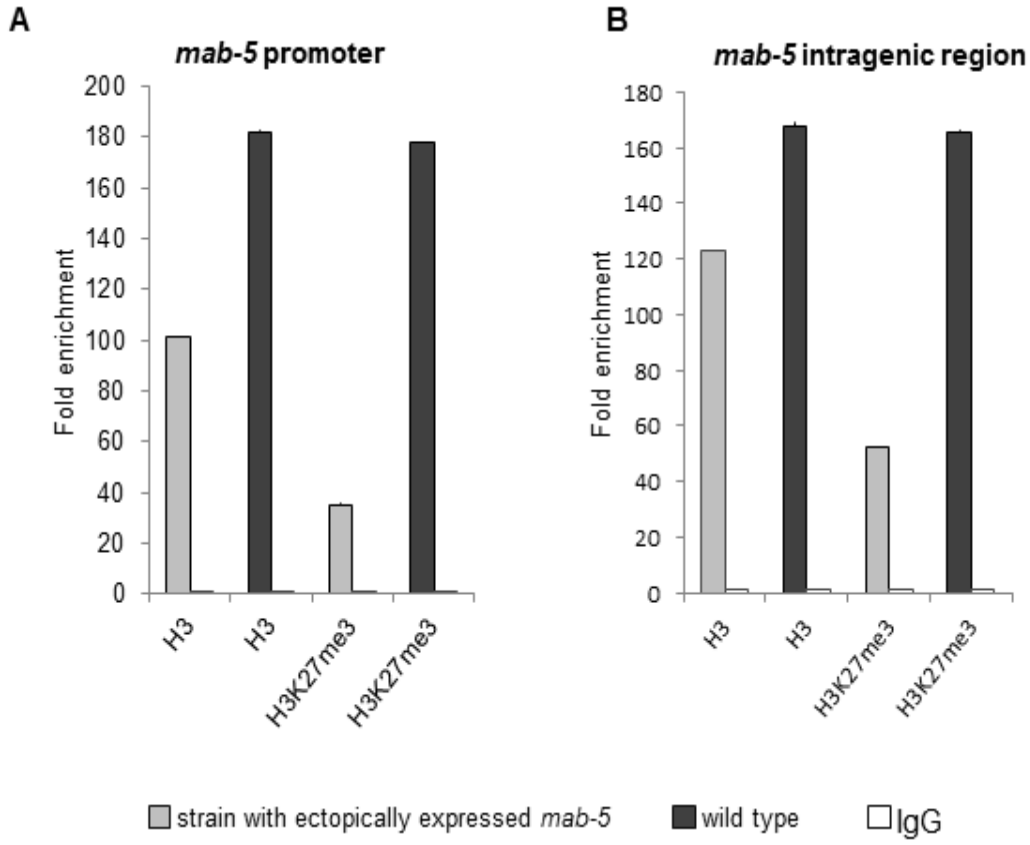

Figure 3.22 Study of H3K27me3 mark occupancy at regulatory region of the *mab-5 Hox* gene. Quantitative ChIP performed from total protein of *mab-5::gfp* transgenic worms with ectopically expressed *mab-5* in *sor-1* background. Decreased level of H3K27me3 observed at the promoter **(A)** and at the intragenic region **(B)** of ectopically expressed (active) *mab-5* gene. All results were normalized to binding by control IgG antibody and performed in triplicates. Error bars indicate ±SD.

3.5.5 HIS-24 and HPL proteins associate with the H3K27me3 chromatin mark

The performed ChIP-qPCR experiments revealed strong correlation between levels of H3K27me3 chromatin mark and of HIS-24 protein associated with regulatory regions of the *mab-5* and *egl-5 Hox* genes. In further study, I was interested whether HIS-24 regulates the transcriptional repression of *mab-5* and *egl-5* genes through the binding to the tri-methylated H3K27 mark. I wanted also to elucidate the function of HPL-2 protein in the *Hox* genes regulation since only double *his-24(ok1024)*; *hpl-2(tm1489)* mutation causes mis-regulation

of *mab-5* and *egl-5*. At first, I performed the peptide pull-down analysis from wild type *C. elegans* extracts where I used biotinylated mono-, di-, tri- methylated or unmodified H3K27 peptides and αHIS-24K14me1 antibody that recognises the modified form of linker histone HIS-24. Obtained results showed that mono-methylated HIS-24 interacted preferentially with H3K27me3 when compared to the unmodified, mono- and di-methylated H3K27 peptides (Figure 3.23 A). I also did the peptide pull-down experiment using unmodified and mono-methylated peptides of HIS-24 and the H3K27me3 antibody. Consistently, I found specific binding of H3K27me3 to the methylated form of linker histone (Figure 3.23 A). Parallel, I analysed the potential interaction of HPL-2 protein with the H3K27me3 mark using the same approaches. Additionally I used di-, tri-methylated and unmodified H3K9 peptides as a positive control [113, 130]. The peptide pull-down experiment with αHPL-2 antibody revealed strong preference in binding of HPL-2 to the tri-methylated form of H3K27 peptide and to the H3K9me2/3 chromatin mark but I also found a weak interaction with H3K27me2 mark (Figure 3.23 A). These results were verified by immunoprecipitation experiments with wild type lysates and antibodies directed to following chromatin marks: H3K4me3, H3K9me2, H3K9me3, H3K27me2, H3K27me3, and H4K20me3. Again, I detected specific preferences of HIS-24 to the H3K27me3, but also a weak interaction with H3K27me2 mark (Figure 3.23 B). In the case of HPL-2, once more I found an association with di- and tri-methylated H3K9 as well as with di- and tri-methylated H3K27me3 (Figure 3.23 B). Moreover, by immunoprecipitation from *hpl-2::gfp C. elegans* extract I confirmed that HPL-2 protein binds tri-methylated H3K27 (Figure 3.23 C). All these results suggested that both HIS-24 and HPL-2 bind to H3K27me3 repressive mark. To exclude the possibility that interplay between HPL-2 and H3K27me3 takes place via binding to HIS-24 protein, I carried out immunoprecipitation and peptide pull-down experiments with extracts obtained from *his-24(ok1024)*X mutant animals expressing GFP tagged HPL-2 protein. I found that the HPL-2 association to H3K27me3 does not depend on the presence of the linker histone HIS-24 (Figure 3.23 D).

Additionally, the binding analysis of recombinant HIS-24 protein (expressed in *Escherichia coli*), performed by Dr. Monika Jedrusik-Bode, revealed that bacterially expressed linker histone bound both, the unmodified and the modified H3K27 mark. (Figure 3.23 E). The differences between the specificity of H3K27me3 binding by native and recombinant HIS-24 could arise from the fact that bacterially expressed protein could not be methylated. Surprisingly, recombinant HPL-2 protein did not show association with H3K27me3 chromatin mark, indicating that a mediator protein or unknown post-translational modifications of HPL-2 must be involved in this binding (Figure 3.23 E).

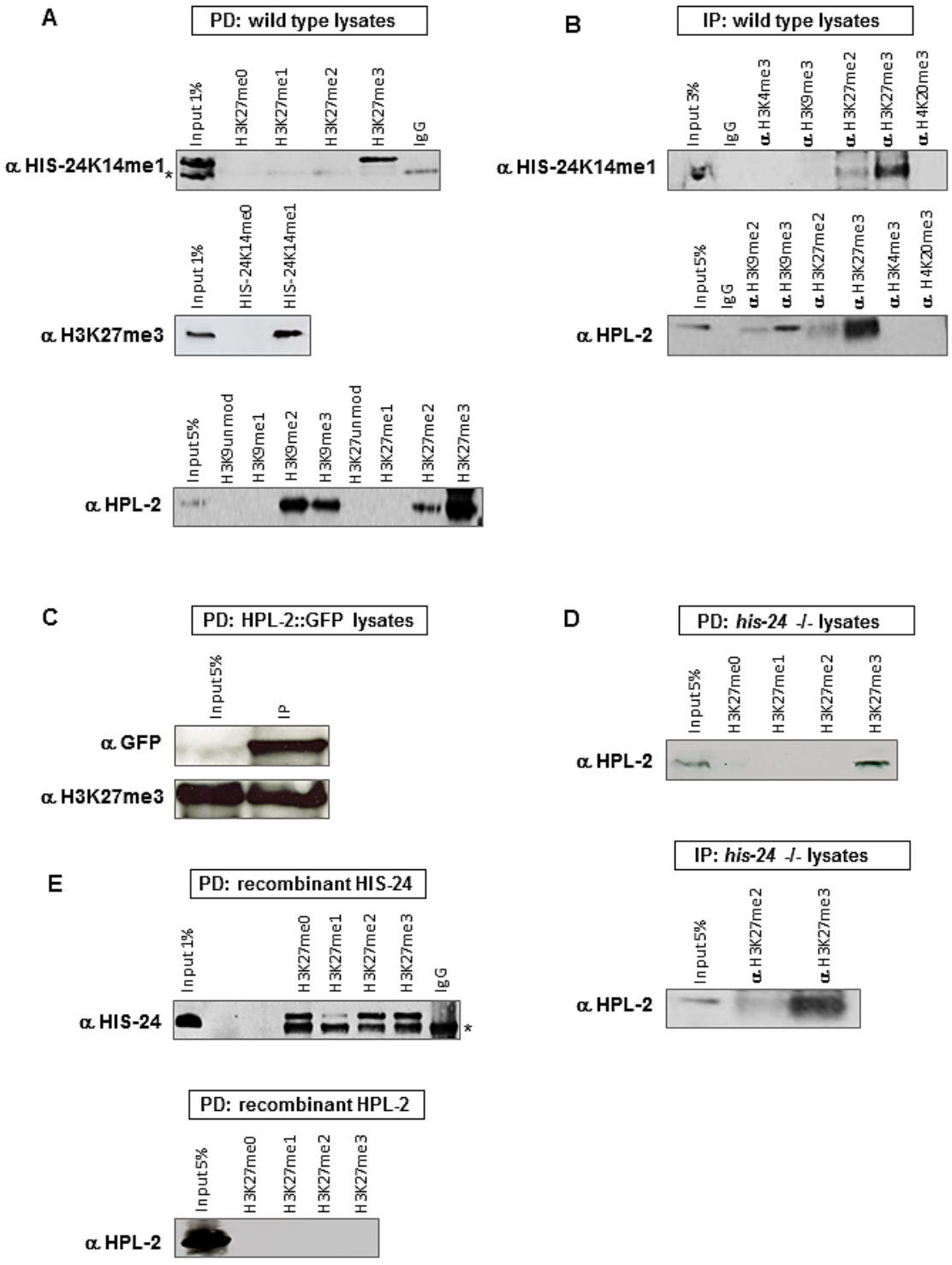

Figure 3.23 Verification of HIS-24K14me1 and HPL-2 bind to the H3K27me3 chromatin mark. HIS-24K14me1 protein co-immunoprecipitated with H3K27me3 chromatin mark and HPL-2 bound H3K27me2/me3 as well as H3K9me2/me3 **(A, B)**. GFP-tagged HPL-2 protein showed specific binding to H3K27me3 **(C)**. Deficiency of HIS-24 did not influence the binding of HPL-2 to H3K27me3 **(D)**. Recombinant HIS-24 protein recognised H3K27me0/2/3 in contrast to recombinant HPL-2 **(E)**. α-antibody, IP-immunoprecipitated protein fraction, PD-pulled down protein. Non-specific bindings are indicated by a star.

3.5.6 Expression and localisation analysis of HIS-24, HPL-1 and HPL-2 in mammalian system

To gain more insight into the localisation of the heterochromatin proteins HPL and the linker histone HIS-24 with the repressive H3K9me3 and H3K27me3 chromatin marks, I performed the distribution studies in *C. elegans* tissues. The analysis of immunofluorescence results did not provide clear evidences for co-localisation of HPL and HIS-24 with repressive chromatin marks, mostly due to difficulties with high resolution imaging of chromatin in *C. elegans* cells. Alternatively, I decided to express these *C. elegans* proteins in the mammalian cells. For that reason I cloned *his-24*, *hpl-1* and *hpl-2* genes into the pEGFP-N1 or pmCherry-N1 mammalian expression vectors and I used them for transient transfection of mouse fibroblast cell line (NIH3T3). After optimization of transfection conditions I decided to use only the pmCherry-N1 vector due to a smaller background noise observed in cells in comparison to the pEGFP-N1 vector. In particular, I concentrated on the analysis of HIS-24 and HPL association with chromatin in mouse fibroblast and their localisation in relation to the H3K4me3, H3K9me3 and H3K27me3 chromatin marks. As described previously, HIS-24 is a chromatin associated protein that can be found within the nucleus (see section 3.1.2). Transient transfection of mouse fibroblasts with *his-24-pmCherry-N1* plasmid revealed that mCherry-tagged HIS-24 was indeed expressed in nuclei of NIH3T3 cells but *C. elegans* protein displayed an aberrant distribution pattern (Figure 3.24 A-C). Transfected cells were additionally immunolabelled using antibodies directed against H3K4me3, H3K9me3 and H3K27me3 chromatin marks. Surprisingly, HIS-24-mCherry did not show an association with chromatin and co-localisation with chromatin mark but instead, it was assembled in large aggregates within the nucleus (Figure 3.24 A). In parallel, I performed transient transfection of NIH3T3 cells with pmCherry-N1 plasmid carrying either *hpl-1* or *hpl-2* sequence. Transfected cells presented diffused nuclear expression of both mCherry-tagged *C. elegans* HPL-1 and HPL-2 proteins (Figure 3.24 B, C). Unfortunately, none of the proteins exhibited association with bulk chromatin structure and co-localisation with analysed chromatin marks (Figure 3.24 B, C).

To summarize, HIS-24 and HPL proteins expressed in mammalian system did not show the expected chromatin localisation and association with either H3K9me3 or H3K27me marks. Moreover, unusual behaviour of these proteins in mouse cells suggested that environmental conditions specific for cell culture (e.g. to high temperature) may entail difficulties with the expression of *C. elegans* proteins, such as incorrect folding.

Figure 3.24 Analysis of HIS-24, HPL-1 and HPL-2 subcellular localisation in mouse fibroblast cells. Exogenous mCherry-tagged HIS-24 protein (red) exhibited aberrant nuclear expression pattern and did not show co-localisation with chromatin (blue), nor with H3K4me3, H3K9me3 and H3K27me3 chromatin marks (green) **(A)**. mCherry-tagged HPL-1 **(B)** or HPL-2 **(C)** also did not display co-localisation with any chromatin marks in NIH3T3 cells. Immunofluorescence performed 24 hours after transfection using antibodies directed against active chromatin mark H3K4me3 and repressive chromatin marks H3K9me3 and H3K27me3. Scale bar, 10 μm.

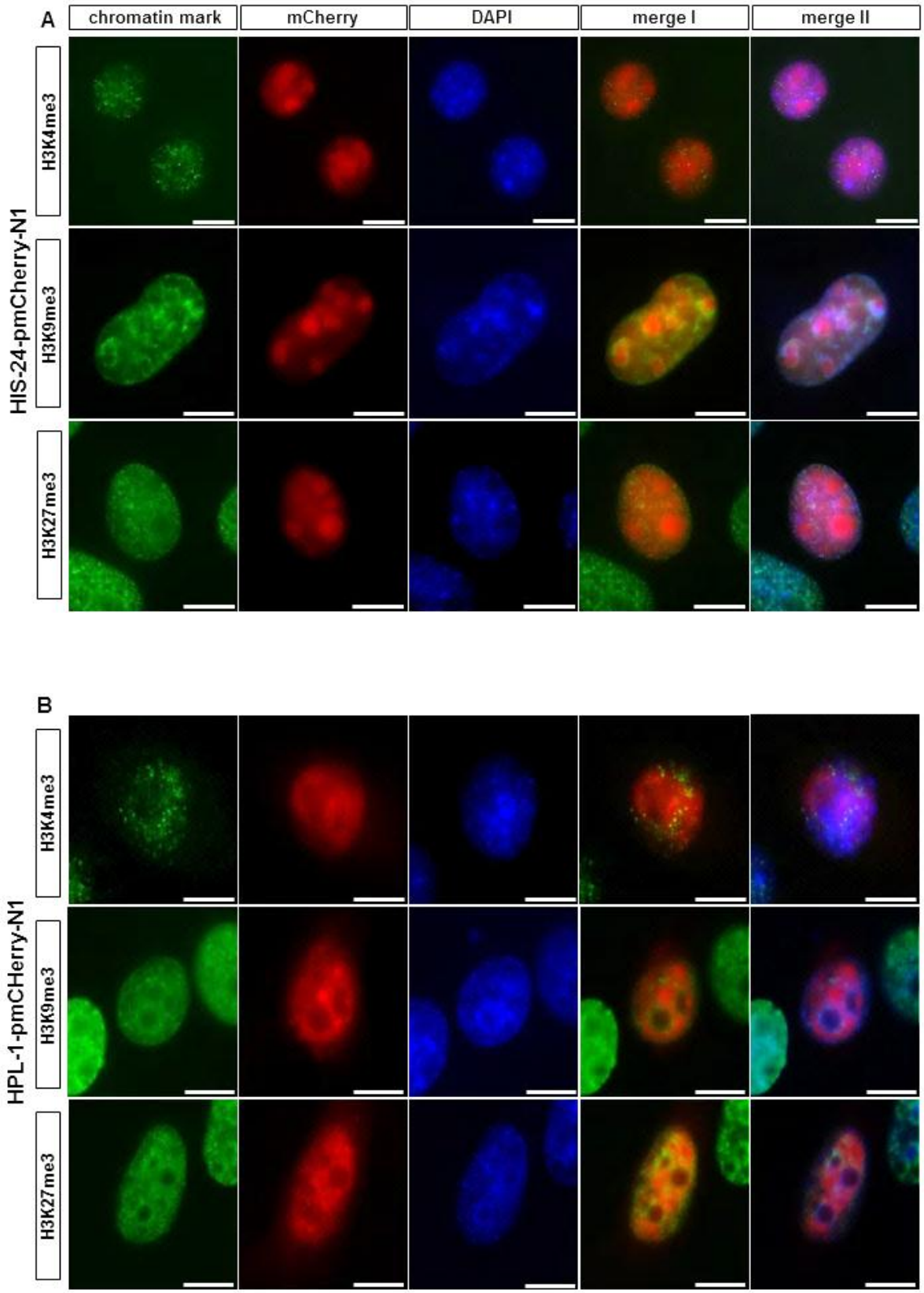
A
chromatin mark
mCherry
DAPI
merge I
merge II
HIS-24-pmCherry-N1
H3K4me3
H3K9me3
H3K27me3
B
HPL-1-pmCHerry-N1
H3K4me3
H3K9me3
H3K27me3

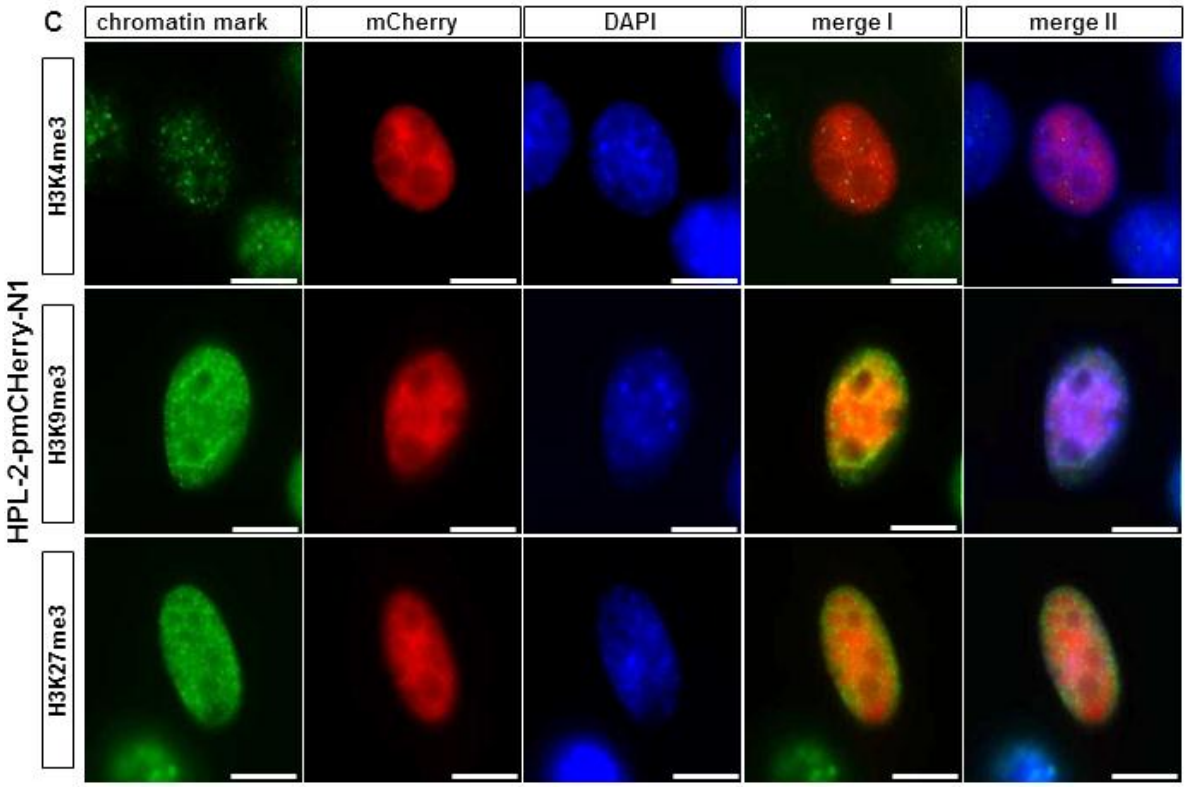

3.5.7 Genetic epistasis analysis of potential co-relation between the Polycomb group proteins (PcG) and HIS-24 activity in contexts of *C. elegans* male tail development

Expression of *Hox* genes is dependent on activity of the Polycomb group proteins (PcG) [131]. In mammals, they form two main evolutionary conserved complexes: Polycomb repressive complex 1 (PRC1) and 2 (PRC2). The PRC1 complex is responsible for monoubiquitylation of histone H2A and for chromatin compaction [138]. PRC2 catalyzes the methylation of histone H3 at lysine 27 which results in transcriptional repression of homeobox genes in a lineage specific fashion [139, 140, 141]. Interestingly, *C. elegans* appears to lack any homologs of the core components of PRC1 [126], Polycomb group proteins are represented by MES complex, a homolog of mammalian PRC2. MES (**M**aternal **E**ffect **S**terile) complex is consisted of MES-2, MES-3 and MES-6 protein [142]. MES-2 constitutes a homolog of mammalian EZH2 that methylates the H3 core histone at lysine 27. MES-6 is a homolog of the embryonic ectoderm development (EED) whereas MES-3 forms novel protein that does not provide any immediate insights into the function of MES complex [143]. Remarkably, mutation in *mes-2* and *mes-6* results in ectopic expression of *Hox* genes and causes male tail defects in *C. elegans* [131].

To elucidate a crosstalk between HIS-24, HPL and MES proteins, I performed the genetic epistasis analysis of *mes-2* and *mes-3* depleted *his-24(ok1024)*X; *hpl-2(tm1489)*III and *his-24(ok1024)*X *hpl-1(tm1624)*X; *hpl-2(tm1489)*III mutant animals and I analysed rays development. Interestingly, I found that double and triple mutant males exhibited slight enhancement of phenotype. Depletion of *mes* genes resulted in 18% and 27% increase of

underdeveloped rays amount in *mes-2* and *mes-3* depleted double mutant animals respectively (Table 3.4, Figure 3.25 A, B, E). Additionally, *his-24(ok1024)*X; *hpl-2(tm1489)*III males with knockdown of *mes-2* and *mes-3* genes displayed appearance of ectopic rays (respectively 5% and 12% of animals) that were not present in control, double mutants (Table 3.4, Figure 3.25 C, D, E). Similarly, *his-24(ok1024)*X *hpl-1(tm1624)*X; *hpl-2(tm1489)*III triple mutant males exhibited respectively two times and three times more ectopic rays in the absence of *mes-2* and *mes-3* expression, but the percentage of fused and underdeveloped rays did not change significantly (Table 3.4). The enhancement of phenotype in double and triple mutants in the absence of MES expression suggested that *his-24* and *hpl* genes act downstream of the Polycomb group proteins: MES-2 and MES-3.

Table 3.4 Rays defects associated with *hpl-1, hpl-2* and *his-24* mutations in *mes-2* or *mes-3* depleted worms.

Genotype	Ectopic rays (%)	Fused/ missing rays (%)	Underdeveloped rays 1 and 2 (%)	Number of worms scored
wild type*	0	0	0	72
wild type on *mes-2* feeding*	3	1	0	86
wild type on *mes-3* feeding*	5	1	0	85
*his-24(ok1024)*X; *hpl-2(tm1489)*III*	0	24	13	73
*his-24(ok1024)*X*; hpl-2(tm1489)*III on *mes-2* feeding*	5	23	31	82
*his-24(ok1024)*X*; hpl-2(tm1489)*III on *mes-3* feeding*	12	44	40	96
*his-24(ok1024)*X *hpl-1(tm1624)*X*; hpl-2(tm1489)*III *	4	37	42	107
*his-24(ok1024)*X *hpl-1(tm1624)*X*; hpl-2(tm1489)*III on *mes-2* feeding*	10	43	41	102
*his-24(ok1024)*X *hpl-1(tm1624)*X*; hpl-2(tm1489)*III on *mes-3* feeding*	13	45	46	107

* on *him-14* feeding plates at 20°C

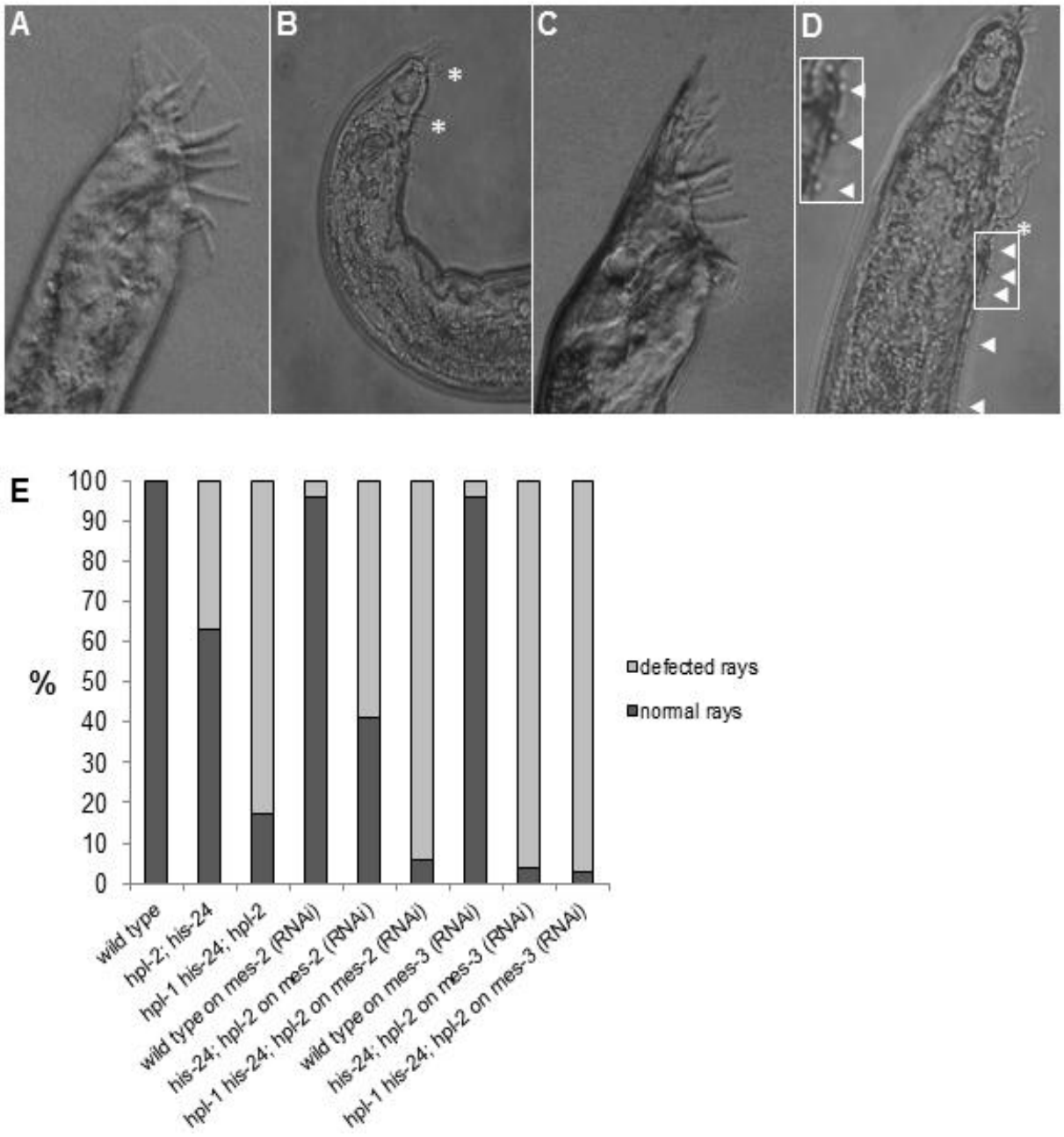

Figure 3.25 Phenotype analyses of *his-24(ok1024)*X *hpl-1(tm1624)*X; *hpl-2(tm1489)*III *C. elegans* mutant males with *mes-2* or *mes-3* depletion. Lack of MES-2 **(A)** or MES-3 **(C)** proteins in wild type animals did not influence the mating structures development. *his-24(ok1024)*X *hpl-1(tm1624)*X**;** *hpl-2(tm1489)*III mutant males with knockdown of *mes-2* **(B)** or *mes-3* **(D)** exhibited increased number of defected rays. Ectopic rays are indicated with arrowheads and under-developed rays by a star. Quantification of ray defects associated with *hpl-2; his-24* double and *hpl-2*; *hpl-1his-24* triple mutations **(E)**. The animals were growing on *him-14* and *mes-2* or *mes-3* feeding plates at 20°C.

Apart of transcriptional repression of the *Hox* genes by MES proteins, their activity can be also regulated by worm-specific SOP-2 and SOR proteins [137]. Both proteins are members of a novel PcG-like complex exclusively present in *C. elegans* and involved in regulation of *Hox* genes expression [125]. To explicate a potential correlation in function between PcG-like complex, HIS-24 and HPL proteins I analysed the phenotype of double and triple mutant

males with knockdown of *sop-2* gene. Remarkably, I did not observe any influence of *sop-2* depletion in *his-24(ok1024)*X; *hpl-2(tm1489)*III and *his-24(ok1024)*X *hpl-1(tm1624)*X; *hpl-2(tm1489)*III mutant background, indicating that HIS-24 and HPL proteins are involved in the same *Hox* genes regulation pathway as MES proteins which is different from the PcG-like pathway.

3.5.8 Analysis of HIS-24K14 mono-methylation: an essential post-translational modification for the proper function of the linker histone during male tail development

The obtained results suggested that only the mono-methylated form of HIS-24 protein binds to tri-methylated H3K27 chromatin mark and through this interaction regulates *mab-5* and *egl-5 Hox* genes expression and in turn proper male tail development. To assess whether the methylated form of HIS-24 has a crucial role in the observed changes of the male tail morphology, I analysed the phenotype of *his-24::gfp* and *his-24K14A::gfp* transgenic worms in the *his-24(ok1024)*X; *hpl-2(tm1489)*III mutant background. The *his-24K14A::gfp* transgenic strain, carrying a point mutation at position 14, where lysine amino acid was replaced with nonmethylatable alanine residue. I found that the expression of the wild type form of GFP-tagged HIS-24 restored a normal development of the male tail in 97% of *his-24(ok1024)*X; *hpl-2(tm1489)*III mutant animals, suggesting that HIS-24 is involved in establishing or maintaining the repression state of the *Hox* genes (Table 3.5, Figure 3.26 A, C). Importantly, the nonmethylatable HIS-24K14A::GFP mutant protein failed to rescue the wild type rays development in *his-24(ok1024)*X; *hpl-2(tm1489)*III males, indicating that methylation of HIS-24 at lysine 14 is essential and sufficient to regulate mail tail development (Table 3.5, Figure 3.26 B, C).

Table 3.5 Summary of ray defects found in *his-24::gfp* and *his-24K14A::gfp* transgenic lines generated on *his-24(ok1024)* X; *hpl-2(tm1489)* III double mutant background.

Genotype	Ectopic rays (%)	Fused/ missing rays (%)	Underdeveloped rays 1 and 2 (%)	Number of worms scored
his-24(ok1024) X ;*hpl-2(tm1489)* III *	0	24	13	73
his-24(ok1024) X; *hpl-2(tm1489)* III *	0	0	3	100
rescue *his-24::gfp*				
his-24(ok1024) X ;*hpl-2(tm1489)* III *	2	0	42	42
rescue *his-24K14A::gfp*				

* on *him-14* feeding plates at 20°C

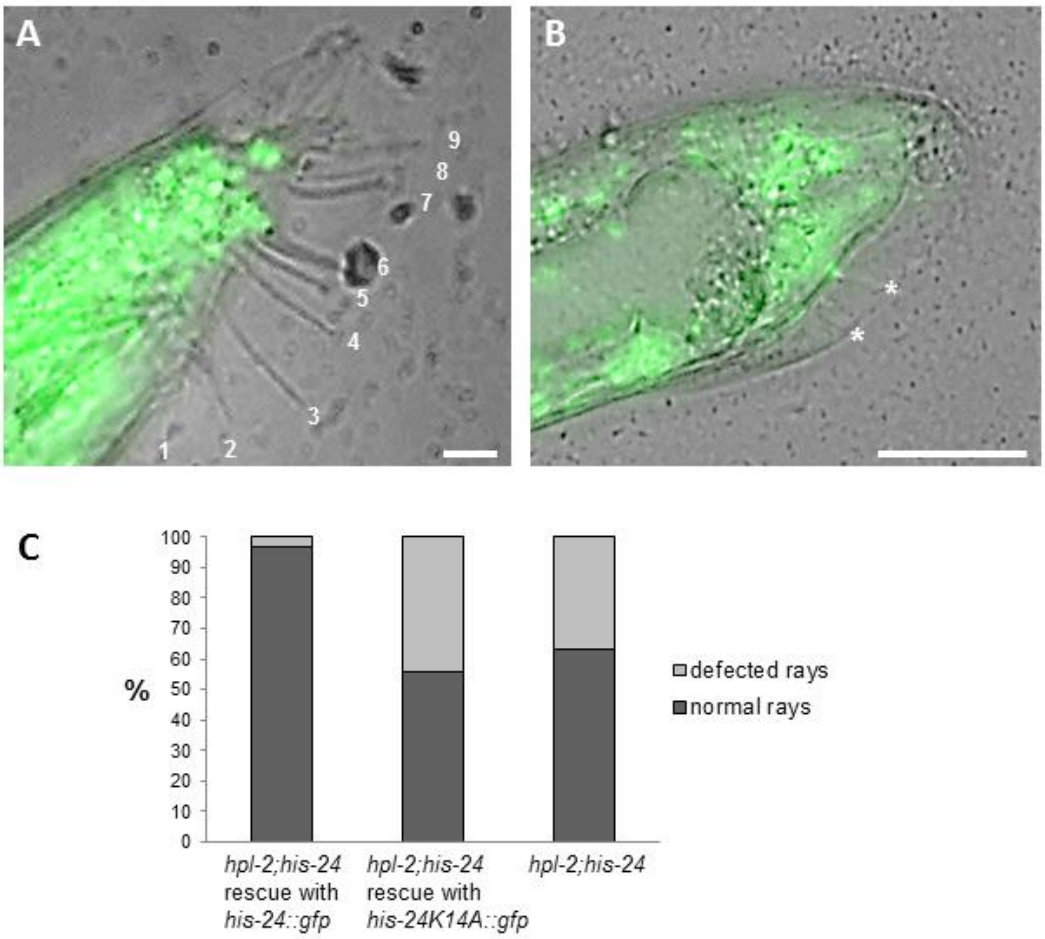

Figure 3.26 HIS-24::GFP and HIS-24K14A::GFP expression analyses in *his-24(ok1024)*X; *hpl-2(tm1489)*III mutant males. Expression of GFP-tagged wild type form of HIS-24 restores normal male tail development in animals lacking *his-24* and *hpl-2* expression **(A)** in contrast to mutated HIS-24K14A::GFP protein **(B)**. The exogenous, mutated form of HIS-24K14A::GFP is expressed at the level comparable to that in animals carrying HIS-24::GFP wild type form **(A, B)**. Scale bar 10 µm **(A)**. Scale bar 25 µm **(B)**. Stars point to under-developed rays. Quantification of ray defects associated with *his-24K14A::gfp* and *his-24::gfp* in *hpl-2; his-24* background mutation **(C)**. The animals were growing on *him-14* feeding plates at 20°C.

3.6 Role of HIS-24 and HPL proteins in the regulation of *C. elegans* immune response

3.6.1 Lack of HIS-24 protein results in the induction of infection-inducible proteins

As previously mentioned, the analysis of microarray experiment using *his-24(ok1024)*X, *hpl-1(tm1624)*X, and *hpl-2(tm1489)*III single mutant animals, revealed that mutant worms displayed a mis-regulation of significant number of genes induced by infection with either gram-negative bacteria (like *Pseudomonas aeruginosa)* or gram-positive bacteria (*Microbacterium nematophilum)* as well as by fungal infection (*Drechmeria coniospora*), (Figure 3.13 A) [115, 144-148]. In particular, an altered expression was observed in genes encoding for immune response-related proteins, such as C-type lectin domain-(CTLD) containing proteins [149], antimicrobial effectors like lysozymes (LYS) [149], thaumatin

family members (THN) [147] and some antimicrobial peptides (AMPs) [146]. Additionally, mis-expression was also detected in genes involved in stress response, e.g. superoxide dismutase (*sod-3*), and methionine sulfoxide reductase A (*msra-1*), which are involved in the oxidative stress response (Appendix A.5), [115, 150, 151].

To assess whether HIS-24 can be involved in modulation of defense-response genes, I decided to verify the results of the genome-expression profile analysis of *his-24(ok1024)*X mutants. In particular, I analysed the level of protein mis-expressed in this strain and I confronted them with the transcriptome results. For that reason, I prepared wild type and *his-24(ok1024)*X mutant animals for the quantitative proteome analysis by SILAC (stable isotope labelling by amino acids). The worms were fed with heavy- or light-lysine labelled *Escherichia coli* that resulted in lysine isotope incorporation with *C. elegans* proteins and enabled quantitative study (see section 2.4.2). All SILAC approaches were performed by Dr. Marcus Krüger and Anne Konzer (Max Planck Institute for Heart and Lung Research, Department of Cardiac Development and Remodeling, Bad Nauheim, Germany). By the quantitative proteome analysis more than one thousand proteins (1,217) were quantified (detection by at least two peptides). Interestingly, about 30% of proteins ($P < 0.05$) detected in *his-24(ok1024)* mutant animals showed a distinct expression level when compared to the wild type. Importantly, the lack of HIS-24 protein in the *C. elegans* organism did not result in increased expression of other linker histone variants, suggesting a lack of a compensatory effect.

The SILAC quantification followed by a gene ontology study showed that among these 30% of differentially expressed proteins were some, which are known to play a role in metabolic processes, transport, embryonic development and in stress response. Moreover, about one third of proteins, which showed a changed expression level, represent factors associated with the immune and stress response (Appendix A.6) [144, 145, 147, 148]. This set of proteins contained some gene products previously identified in microarray analysis, such as MAO-C-like dehydratase domain protein (MAOC-1), which is known to be related to immune response processes [148], a member of galectin family (LEC-2), associated with stress response processes [152] as well as, mentioned above, methionine sulfoxide reductase A (*msra-1*) [151] (Appendix A.6, A.7). Apart from that, some other defense-related factors were identified, e.g. members of the Hsp90 family of molecular chaperones (HSP and DAF-21/HSP-90), protein that belongs to the sorbitol dehydrogenase family (SODH-1) [152], and a member of Saposin-like protein family (SPP-14), [153], (Appendix A.6).

The comparison of both SILAC and microarray analysis revealed that the number of proteins with altered expression, which were also mis-regulated at the transcriptional level in the of the *his-24(ok1024)*X mutant animals, is very low (169 common gene products) (Figure 3.27). This can be explained by the fact that not all transcribed mRNA is translated into protein. Besides mRNAs have a much shorter half-life than proteins which can be cumulated in the cell. Importantly, 30% (50) from these 169 common proteins found in the SILAC and detected by microarray at the transcriptional level are known to be induced by infection (Appendix A.7).

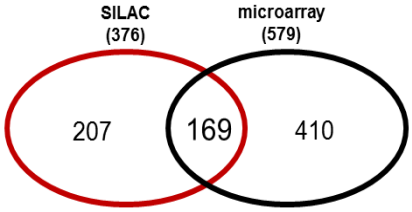

Figure 3.27 Comparison of data obtained from the genome-expression profile analysis and quantitative proteome analysis. A Venn diagram of the gene products obtained from the microarray analysis corresponding to the results of the quantitative proteome analysis. Figure taken from [115] and modified.

3.6.2 Analysis of sensitivity to infection with gram-positive bacteria of single, double and triple mutant strains of *C. elegans*

SILAC as well as microarray approaches pointed to HIS-24 and HPL proteins as those, which are required for regulation of immune response genes transcription. Interestingly, ChIP-qPCR analyses, performed by Dr. Monika Jedrusik-Bode, revealed that this regulation takes place through direct binding of HIS-24 and HPL to the regulatory sites of antimicrobial genes [115].

Since the ChIP analysis revealed that immune response genes are direct targets of the linker histone HIS-24 and HPL proteins, it was of great interest to investigate the biological influence of this transcriptional regulation. Therefore I tested the resistance of single *his-24(ok1024)*X, *hpl-1(tm1624)*X, *hpl-2(tm1489)*III, *hil-3(ok1556)*X, double *his-24(ok1024)*X *hpl-1(tm1624)*X, *his-24(ok1024)*X*; hpl-2(tm1489)*III, *hpl-1(tm1624)*X; *hpl-2(tm1489)*III and triple *his-24(ok1024)*X *hpl-1(tm1624)*X; *hpl-2(tm1489)*III mutant worms to infection with the gram-positive bacterium *Bacillus thuringiensis*. After a 24-hour incubation with bacteria, I scored a surviving fraction of animals and I found that *his-24(ok1024)*X mutant animals showed significantly increased sensitivity to the infection (Figure 3.28). Only 31% of *his-24(ok1024)*X animals were alive after infection in comparison to 42% wild type animals that survived. Interestingly, the lack of *hil-3* histone variant in *hil-3(ok1556)*X mutant strain did not cause decreased survival upon infection (41% of survived animals), suggesting that observed sensitivity is specific for the *his-24* linker histone deletion (Figure 3.28). Surprisingly, *hpl-1(tm1624)*X and *hpl-2(tm1489)*III mutant animals exhibited decreased sensitivity to infection (54% and 53% respectively) in comparison to the *his-24(ok1024)*X mutants and to wild type animals (Figure 3.28). Analysis of double and triple mutant strains revealed that all of them had increased resistance to the infection with *B. thuringiensis* in comparison to the single mutants and wild type animals (Figure 3.28). I found that fraction of survived *his-24(ok1024)*X *hpl-1(tm1624)*X animals (87%) was twice as much as fraction of wild type animals (Figure 3.28). Similarly, 66% of *hpl-1(tm1624)*X; *hpl-2(tm1489)*III and 71% of *his-24(ok1024)*X *hpl-1(tm1624)*X; *hpl-2(tm1489)*III triple mutants were viable 24 hours after infection (Figure 3.28). In the light of these findings, it is possible that the absence of HPL proteins in *his-24(ok1024)*X may neutralise the negative effect of *his-24* deletion during infection with *Bacillus thuringiensis*.

Additionally, all mutant strains were infected in parallel with non-pathogenic strain of *Bacillus thuringiensis* and scored for survival 24 hour later. In that case 100% of animals from each strain were alive after infection, indicating that the results obtained for the pathogenic *Bacillus thuringiensis* bacteria strain were specific.

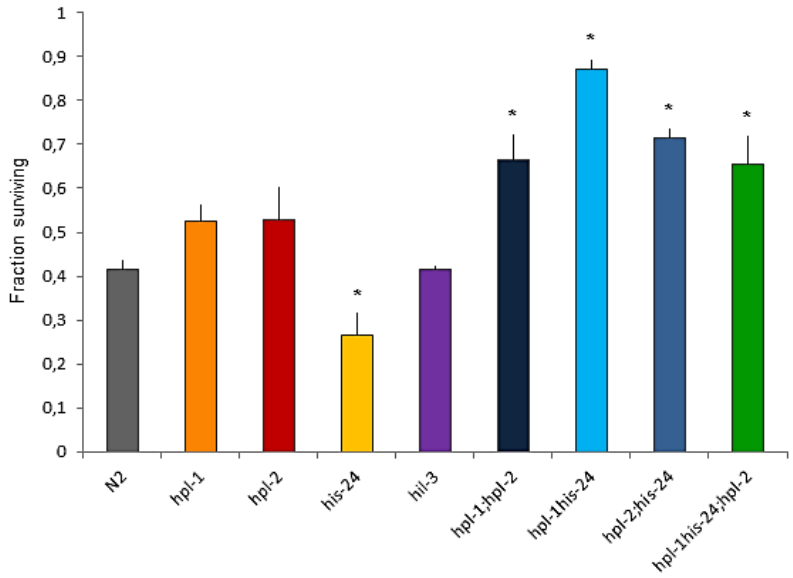

Figure 3.28 Investigation of HIS-24 and HPL roles in control of microbial resistance. Quantification of mutant animals survived infection with the gram-positive bacterium *B. thuringiensis* (BT). Error bars indicate ±SD, stars point to statistically significant changes ($p<0.0001$, vs. wild type). Figure taken from [115].

3.6.3 Analysis of sensitivity to infection with gram-positive bacteria of transgenic strains of *C. elegans*

As the lack of HIS-24 resulted in decreased resistance of *C. elegans* to gram-positive bacterium, in my further study, I was interested in the influence of HIS-24 and HPL overexpression on the survival of worms upon *Bacillus thuringiensis* infection. For that reason I analysed the resistance of animals overexpressing GFP-tagged HIS-24, HPL-1 and HPL-2 proteins. Importantly, the presence of GFP-tagged HIS-24 protein on both wild type background and *his-24(ok1024)*X resulted in substantial reduction of sensitivity to the *Bacillus thuringiensis* infection (by 50% more of survived worms). As it turned out, this effect was dependent on HIS-24 methylation at lysine 14 because *his-24K14A::gfp* transgenic animals, carrying a nonmethylatable form of the linker histone, showed increased sensitivity to bacterial infection (Figure 3.29). Importantly, I found that the expression of GFP-tagged HIS-24 together with endogenous linker histone HIS-24 resulted in survival of more animals (92%) than in the absence of the endogenous protein (75% of survived worms) (Figure 3.29). In further analysis I found that *hpl-1::gfp* and *hpl-2::gfp* did not exhibit significant differences in survival (41% and 40% of survived animals respectively) in comparison to wild type animals (45%) (Figure 3.29). Nevertheless, the absence of the linker histone HIS-24 decreased the resistance of *hpl-1::gfp* and *hpl-2::gfp* worms by approximately 10% (28% and 30% of viable animals) (Figure 3.29).

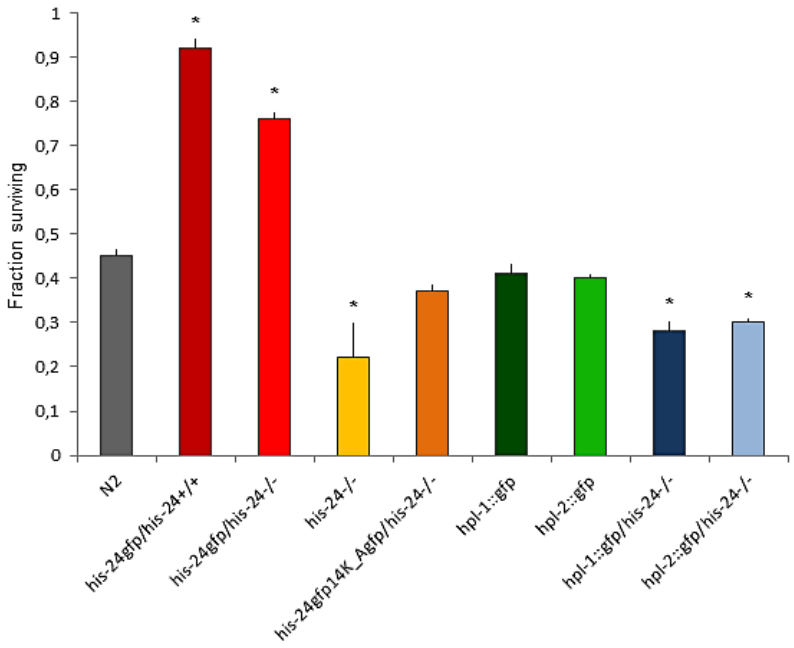

Figure 3.29 Analysis of sensitivity of *his-24* and *hpl* transgenic lines to bacterial infection. Quantification of survived transgenic animals after infection with the gram-positive bacterium *B. thuringiensis* (BT). The presence of the mutated form of HIS-24::GFP (HIS 24A14::GFP) did not increase the survival of *his-24-/-* mutant animals on BT plates in contrast to the wild type form of HIS-24. Error bars indicate ±SD, stars point to statistically significant changes ($p<0.0001$, vs. wild type).Figure taken from [115] and modified.

3.6.4 Analysis of HIS-24 distribution and the methylation level after infection with *Bacillus thuringiensis*

Because the analysis of *C. elegans* transgenic lines implied that the overexpression of HIS-24 increases the resistance to *Bacillus thuringiensis* infection, I was concerned with the behaviour of this protein in the *C. elegans* organism. To investigate the biological role of HIS-24 in innate immune response, I looked at the cellular localisation of the linker histone before and after bacterial infection in *his-24::gfp* and *his-24K14A::gfp* strains, which lack endogenous HIS-24. In particular, I concentrated on intestinal cells since they are the most exposed to bacteria and therefore compose the first barrier for microorganisms. I observed that in uninfected worms HIS-24::GFP had diffuse distribution in nucleoplasm of intestinal cells (Figure 3.30 A) while after infection, 45% of animals displayed both nuclear and cytoplasmic expression of HIS-24::GFP (Figure 3.30 B). Half of these 45% of infected animals presented only a cytoplasmic distribution of GFP-tagged HIS-24 (Figure 3.30 C). Interestingly, animals from the *his-24K14A::gfp* transgenic line did not exhibit cytoplasmic localisation of mutated HIS-24K14A::GFP after infection with *Bacillus thuringiensis* (Figure 3.30 D, E). This suggested that mono-methylation of HIS-24 at lysine 14 is crucial for changes of their subcellular localisation and it seems to be important for the function of HIS-24 during defense response.

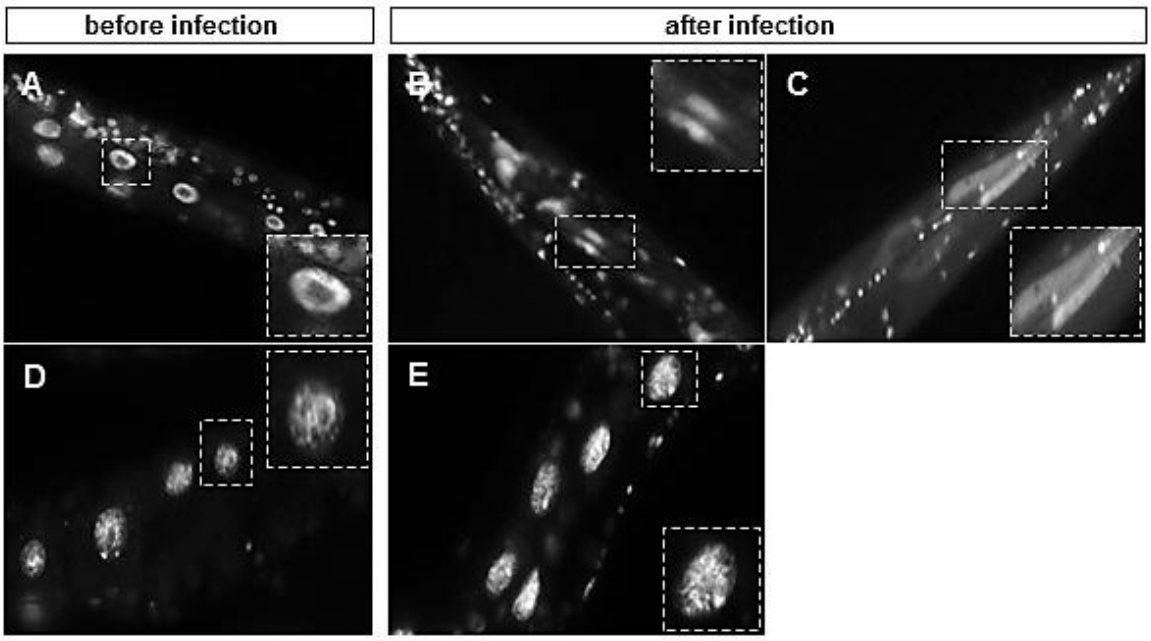

Figure 3.30 Analysis of HIS-24::GFP and HIS-24K14A::GFP distribution after *Bacillus thuringiensis* infection in intestinal cells of *C. elegans* carrying *his-24-/-* background mutations. Before infection GFP-tagged HIS-24 exhibited nuclear expression in intestinal cells **(A)**. 12 hour after infection, except nuclear expression pattern, some fraction of the exogenous HIS-24::GFP protein displayed cytoplasmic localisation **(B)**. In some intestinal cells, HIS-24::GFP protein was found only in the cytoplasm of the intestine cells **(C)**. In contrast, nonmethylatable HIS-24K14A::GFP showed nuclear expression before and after infection **(D, E)**. Figure taken from [115] and modified.

3.6.5 Role of the HIS-24 and HPL proteins in the stress response

As it has been reported, immune response of *C. elegans* can be controlled by many stress conditions (e.g. heat/cold, oxygen lack, desiccation, food limitation, etc.) [154]. Interestingly, the genome expression profiling and the quantitative proteome analysis of *his-24* and *hpl* deletion mutants detected many transcripts predicted to protect from stress. Among them several genes involved in oxidative stress were found, such as *sod-3* superoxide dismutase gene, *cyp* genes, *mtl-1* methallothionein gene but also *hsp* genes encoding heat shock proteins that play a role in tolerance of *C. elegans* to the non-permissive temperature. Since the results showed that *his-24* and *hpl-2* loss of function influences immune response, I was interested if this could also cause general stress response. To answer the question I performed three behavioral tests where I used different sources of stress. I exposed single *his-24(ok1024)*X, *hpl-1(tm1624)*X, *hpl-2(tm1489)*III, *hil-3(ok1556)*X, double *his-24(ok1024)*X *hpl-1(tm1624)*X, *his-24(ok1024)*X*; hpl-2(tm1489)*III, *hpl-1(tm1624)*X; *hpl-2(tm1489)* III and triple *his-24(ok1024)*X *hpl-1(tm1624)*X; *hpl-2(tm1489)*III mutant animals to oxidative stress (0.5 mM), osmotic stress (500mM NaCl) and heat stress (35°C). I found that *his-24(ok1024)*X mutant strain displayed a significantly increased sensitivity to osmotic and heat stress. Worms with deletion of *his-24* gene died two times faster on plates with 500mM of salt but also in temperature of 35°C in comparison to the wild type animals (Figure 31 A, B). This strain also proved to be slightly more sensitive to the oxidative stress conditions than wild type worms (Figure 31 C). In general, double and triple mutant worms were less resistant to all types of

stress I performed but in the case of tolerance to oxidative and heat stress, the absence of *hpl-1* gene on the *his-24(ok1024)* background seemed to neutralise the negative effect of HIS-24 deficiency (Figure 31 B, C). From the other hand, deletion of both *hpl* genes in *hpl-1(tm1624)*X; *hpl-2(tm1489)* III mutant strain resulted in death of worms five days earlier (8 days) than the control animals (13 days) when maintained in oxidative stress conditions (Figure 31 C). Altogether, the results indicate that the absence of HIS-24 and HPL proteins may also influence the response to different stress conditions which in turn can affect expression of immunity related antimicrobial genes.

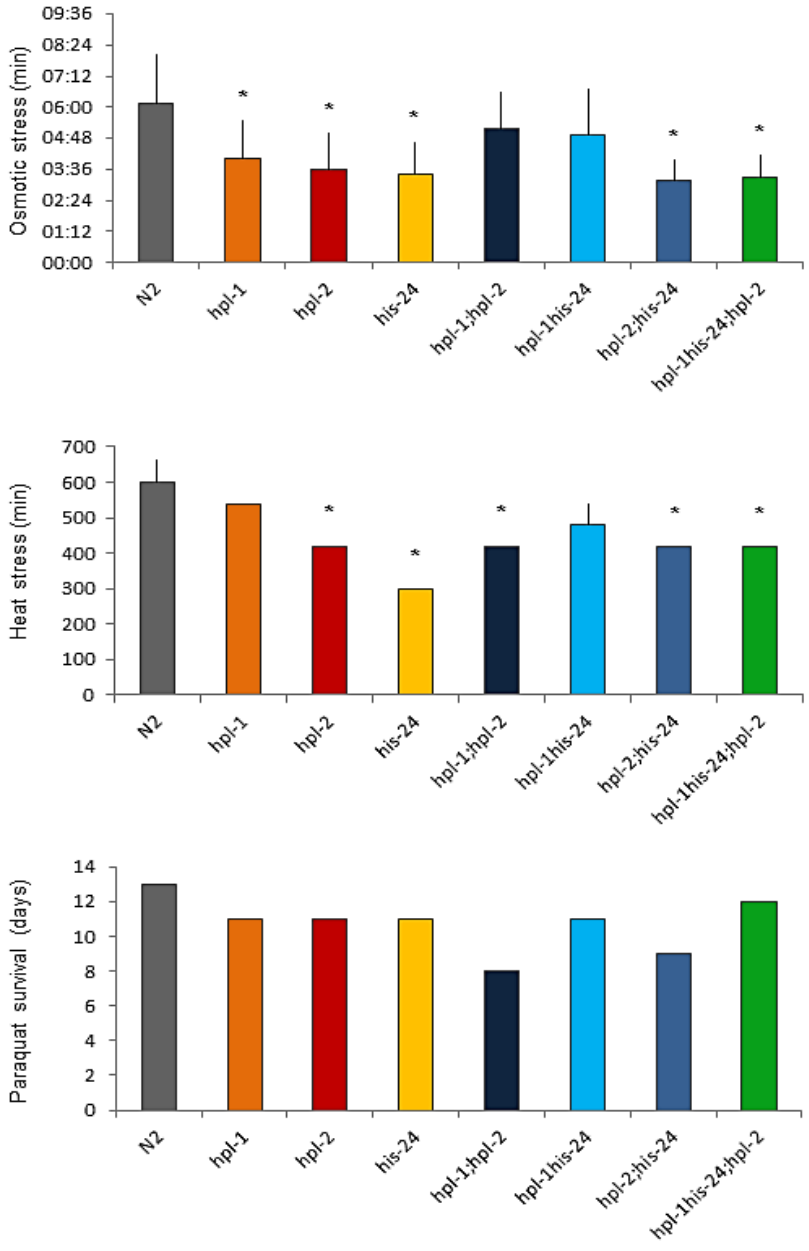

Figure 3.31 Study of the influence of the *his-24* and *hpl* deletion on *C. elegans* stress response. Graphs presenting the fraction of survived animals after the osmotic, heat shock and oxidative stress assay. Error bars indicate ±SD, stars point to statistically significant changes (P<0.0001, vs. wild type). Figure taken from [115] and modified.

4 Discussion

4.1 HIS-24 is a mono-methylated protein associated with chromatin

The linker histones (H1) form a highly conserved family of proteins which are essential for the proper chromatin condensation and modulation of the genes transcription [3-8]. Extensive biochemical studies on mammalian H1 variants revealed that the linker histones can be post-translationally modified. Although many types of H1 post-translational modifications have been identified in mammals, still little is known about the expression pattern of modified linker histones and about their function [60-67]. The roundworm *C. elegans*, with its simple genetics and relatively well described development, is an ideal organism for the study of biological effects of the H1 post-translational modification. *C. elegans* possesses eight different H1 variants, which are encoded by single copy genes with relatively high sequence conservation in comparison to mammalian linker histones [96]. Although the studies of H1 function in *C. elegans* have generally concentrated on the HIS-24 linker histone variant, its role still has remained elusive [98, 99]. Recent mass spectrometry analysis of H1 post-translational modification revealed that HIS-24 is the only *C. elegans* H1 histone variant that possesses a single methylation site at lysine 14 [115]. Since the mono-methylation site was identified, it was of great interests to determine the potential differences between cellular distributions of unmodified as well as modified HIS-24 and to distinguish between the functions of these two forms of protein. In this study, for the first time I investigated the localisation pattern of HIS-24K14me1 using the antibody that specifically recognises the mono-methylated state of *C. elegans* H1. Immunofluorescence analysis of the germ line showed that mono-methylated HIS-24 is predominantly associated with chromatin whereas the unmodified form of linker histone can be also found in the cytoplasm. The results were consistent with previously published analysis of HIS-24 distribution, where the cytoplasmic HIS-24 variant was observed during most developmental stages of the germline and only during late pachytene stage a small fraction of HIS-24 was associated with chromatin [101]. Interestingly, the results of immunofluorescence experiment were supported by the STED and electron microscopy study. The electron microscopy pictures revealed that HIS-24K14me1 is not only presented in the heterochromatin regions but can be also found among euchromatin. This would suggest that the HIS-24 linker histone variant should be perceived not only as a protein involved in the transcriptional repression, but also as a factor that may potentially be involved in the activation of genes transcription. The role of H1 variant as a gene-specific positive regulator of expression was previously presented in the *in vivo* study of *Tetrahymena thermophila* cells [155]. The analysis of H1 function revealed that the linker histone is required for the activation of *BC11* (also known as *CyP*) gene that encodes cysteine protease and in the absence of H1 activity the BC11 transcription is reduced [155, 156].
Interestingly, modified HIS-24 variant was also identified inside of the nucleolus region what indicated that it may be involved in the regulation of transcription of rRNA genes. In fact, H1-dependent regulation of rRNA genes transcription has been already shown in the *Xenopus* oocytes, where H1 is responsible for the specific repression of the 5S rRNA genes [157, 158]. Furthermore, a later study performed on *Drosophila melanogaster* revealed an association of ribosomal proteins with linker histone H1 [159]. Although HIS-24 participation in the rRNA

genes transcription has not been described yet, it is possible that mono-methylated form of this histone variant is involved in the repression of rRNA genes.

4.2 Specific binding of HPL-1 protein to the mono-methylated HIS-24 linker histone

Linker histone, post-translationally methylated at some of its residues, can be specifically bound by several interacting proteins. One of the well-described proteins that bind to H1 is heterochromatin protein 1 (HP1) [39, 62, 160]. The chromodomain of HP1 specifically recognises the linker histone H1.4 methylated at Lys 26 (H1.4K26), but the role of this methylation in biological processes remains unknown [39]. It has been suggested that methylation of H1.4K26 could have a role in HP1 association with chromatin, which in turn influences transcription of downstream targets [39].
Analysis of the *C. elegans* H1 putative interaction partners confirmed that the binding of HIS-24 with HPL-1, a homolog of mammalian HP1, is indeed evolutionary conserved. However the precise mechanism of HPL-1 attachment to HIS-24 is noticeably different from the well-studied binding of human HP1 to H1K26me2. In mammals, the chromodomain of HP1 protein is known to bind to di- or tri-methylated lysine residues (Figure 4.1) [161]. In contrast, *C. elegans* HPL-1 protein is able to bind to the mono-methylated lysine residue of the HIS-24 linker histone variant (Figure 4.1).

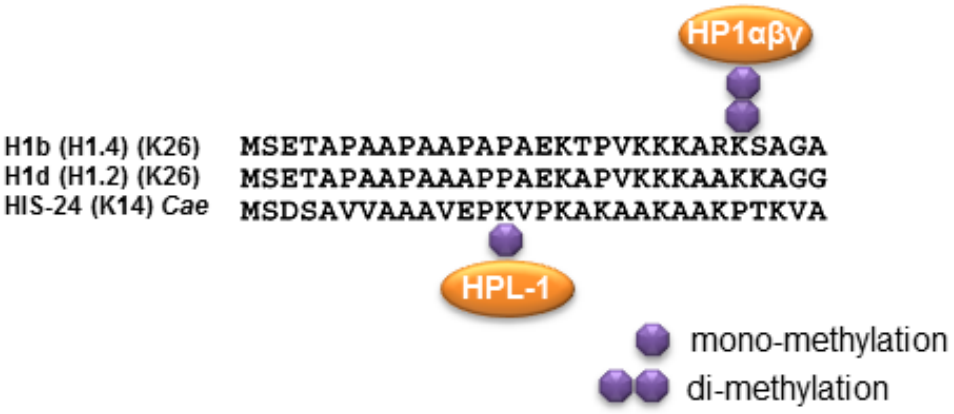

Figure 4.1 Model of HP1/HPL-1 binding to the H1/HIS-24 linker histone. Alignment of amino-acid sequences of the N-terminal end of human H1.2 and H1.4 as well as *C. elegans* HIS-24 linker histone variant created using the ClustalW method and followed by manual editing. Illustration taken from [115] and modified.

Moreover, HPL-1 not only differs from human HP1 in its binding behaviour but also at the sequence level, although the residues directly involved in the binding of methyl groups remain conserved between the species (Figure 3.4, 4.2). For example, the sequence motif of HIS-24K14 (AVEP**K**VPK), which is recognised and bound by the *C. elegans* HPL-1 protein lacks any homology to the sequence of either human H1.4K26 (K**ARKS**AGA) or H3K9 (QT**ARKS**TGG) recognised by chromodomain of the human HP1 protein [160, 161]. Although HPL-1 protein recognises different sequence when compared to the mammalian homologs, the data obtained in this study suggest that the downstream events, such as

regulation of transcriptional activity resulting from the interaction between mono-methylated histone HIS-24 and HPL-1, may be conserved among species.

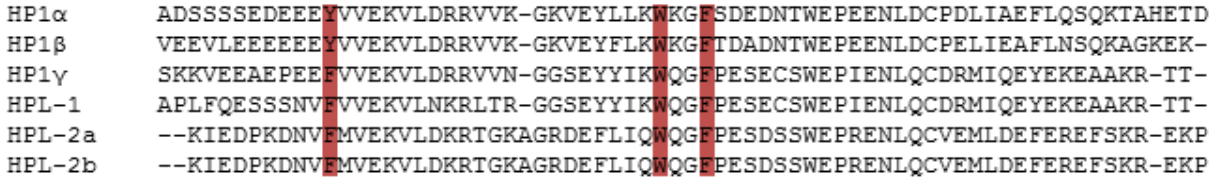

Figure 4.2 Homology between the human and *C. elegans* HP1 proteins. Alignment of chromodomain amino-acid sequence created using the ClustalW method and followed by manual editing. The conserved residues that form the binding site for histone methyl groups are highlighted in red. Illustration taken from [115] and modified.

4.3 The influence of HIS-24 and HPL on chromatin organization

The biological function of the HIS-24 linker histone and heterochromatin proteins HPL as well as the potential synergism between them were investigated in *C. elegans* worms carrying single, double or triple deletion of *his-24*, *hpl-1* and *hpl-2* genes. Under normal growth conditions *his-24(ok1024)*X, *hpl-1(tm1624)*X and *hpl-2(tm1489)*III mutant worms exhibited mild phenotype (low percentage of sterility in the population). Interestingly, a functional redundancy between the HIS-24 linker histone and HPL proteins was well presented in *his-24(ok1024)*X*; hpl-2(tm1489)*III, and *his-24(ok1024)*X*; hpl-1(tm1624)*X double as well as *hpl-1(tm1624)*X *his-24(ok1024)*X*; hpl-2(tm1489)*III triple mutant animals. Deletion of these proteins, associated with chromatin, resulted in significant increase of *C. elegans* sterility as well as in severe defects in gonads and vulva development of hermaphrodites. The observed phenotype was consistent with the previously described role of HIS-24 and HPL in the germline development and vulva cell fate specification [96, 121]. Chromatin structure studies of *his-24(ok1024)*X*; hpl-2(tm1489)*III double and *hpl-1(tm1624)*X *his-24(ok1024)*X*; hpl-2(tm1489)*III triple mutant animals using either DAPI staining or immunogold labelling for electron microscopy showed enlarged nuclei with uncondensed chromatin. Since HIS-24 and HPL proteins are known to be crucial for the chromatin folding and repression of genes expression in germline, it was conceivable that the knockout of *his-24* and *hpl* results in significant deregulation of transcription of the downstream targets important for the *C. elegans* germline development [96, 101, 106, 111]. Nevertheless the magnitude of observed decrease in heterochromatin regions, visualised by electron microscopy, let to expect more serious developmental defects or even embryonic lethality seeing that these animal displayed a complete lack of two basic structural chromatin proteins. Since the deletion of three H1 isoforms (H1c, H1d and H1e) in mice or *Su(var)205* (also called *HP1*) in *Drosophila melanogaster* results in lethal defects in development, it is surprising that *C. elegans* worms are viable without one linker histone variant (HIS-24) and both heterochromatin proteins HPL [29, 162]. Especially in the light of recently performed mass spectrometry analysis showing that HIS-24 is the most abundant linker histone variant in the *C. elegans* organism. Although the synergistic effects of *his-24* and *hpl* deletion observed in *C. elegans* hermaphrodites agree with the reported role for HIS-24 and HPL in the development, the

substantial defects of mating structures of *C. elegans* were not reported before for none of these genes [96, 121, 131]. Despite the fact that several chromatin remodelling factors were reported to be involved in formation of *C. elegans* rays, such as Polycomb group proteins and Polycomb-like complex, there is no information about HIS-24 or HPL association with male tail development [125, 126, 131]. Besides, the observed abnormalities in the rays formation suggest more specific regulation of genes transcription and disagree with the common accepted theory about H1 and HP1 as general repressors of transcription. All substantial morphological aberrations observed in animals with double and triple mutations of *his-24* and *hpl* suggest that HIS-24 and HPL proteins play rather a regulatory role of a gene-specific transcription. However, it is impossible to exclude that additional global changes in chromatin structure and/or chromatin stability, resulting from deficiency of *C. elegans* H1 and HP1 proteins, may also affect the worm development.

4.4 HIS-24 and HPL are not global repressors of transcription

HP1 and H1 are heterochromatin components that are believed to be associated with global repression of transcriptional activity [163, 164]. Although the linker histone and the heterochromatin protein 1 are key regulators of chromatin folding, few studies have investigated their function as gene-specific transcription factors [77, 155].

Consistently with the observed phenotype of *his-24* and *hpl* mutant worms and previous assumptions, the performed microarray analysis revealed that H1 and HP1 play subtle and gene-specific roles in the roundworm *C. elegans*. Moreover, the results of analyses support a more precise role of the HIS-24 and HPL in specific gene regulation, rather than a general repressive function [63, 165, 166]. Despite global changes in chromatin compaction, observed in *his-24(ok1024)*X*; hpl-2(tm1489)*III and in *hpl-1(tm1624)*X *his-24(ok1024)*X*; hpl-2(tm1489)*III mutant animals, I found slight variations in the gene expression profile of mutants when compared with wild type animals. Furthermore, I identified a set of genes that were commonly regulated by HIS-24 and HPL proteins. Among them were both up- and down-regulated genes indicating redundant roles for the linker histone variant HIS-24 and HPL proteins. Remarkably, the redundancy in function was already suggested by the synergistic effects of HIS-24 and HPL deletion observed in several developmental processes of *C. elegans*. Importantly, the rather small number of mis-regulated genes presented in triple mutant animals once more denies the function of H1 and HP1 as global repressors. However, *C. elegans* is not the only organism that does not display substantial gene expression changes in response to H1 deletion. Elimination of H1 in *Tetrahymena thermophile* and in yeast did not affect global transcription, but resulted in up- and down-regulation of small number of specific genes [77, 155]. The slight changes in gene expression may indicate that HPL proteins and HIS-24 serve as fine tunes of key genes during development and/or differentiation. The subtle variations in gene expression may occur by the dynamic and sequential arrangement of the linker histone HIS-24 and HPL-2 on the chromatin fibre, which in turn might influence higher-order chromatin structure and effect nucleosome positioning, and stability [166]. It is also possible that the properties of the chromatin fiber, which allow for quantitative modulation of gene expression, vary depending on HPL subtypes that together with HIS-24 associate with DNA [63, 165]. Although the observed changes in gene

transcription were subtle, they contributed to the marked phenotypic consequences which were observed in *C. elegans* worms with deletion of *his-24*, *hpl-1* and *hpl-2* genes. In particular, I found that HIS-24 and HPL proteins can regulate some shared targets, such as the homeobox genes and certain immune response-related genes. Despite the fact that changes in the expression of these transcripts were very little, the further analyses revealed that they may have a significant influence of the development and physiology of *C. elegans*. Nevertheless, it cannot be forgotten that the genome-expression profile analysis is a method in which measurements are not strictly quantitative and even inconspicuous changes in transcript levels might in reality stand for serious developmental defects. Therefore obtained results were verified either by qPCR or by quantitative proteome analysis, which revealed again that the linker histone HIS-24 and HPL proteins are transcriptional modulators of only few gene subsets [115].

4.5 Model of transcriptional regulation of *mab-5* and *egl-5 Hox* genes by HIS-24 and HPL proteins

The majority of our understanding of the linker histone and heterochromatin protein 1 biology in mammals, *Drosophila melanogaster* and in *C. elegans* is based on studies of the downstream targets analysis that show mis-expression in response to H1 and HP1 absence. The study of phenotype of *C. elegans* males with *his-24* and *hpl-2* genes deletion suggested that *Hox* genes might be one of the targets for HIS-24 and HPL-2 proteins. Although, HPL-2 protein has been described as a regulatory factor for *lin-39 Hox* gene expression in vulva precursor cells of *C. elegans* [133], there is no evidence for *Hox* gene regulation by *C. elegans* linker histone variants, to date.

The *C. elegans* Hox cluster consists of six genes, which are required for normal developmental patterning (Figure 4.3) [167, 168].

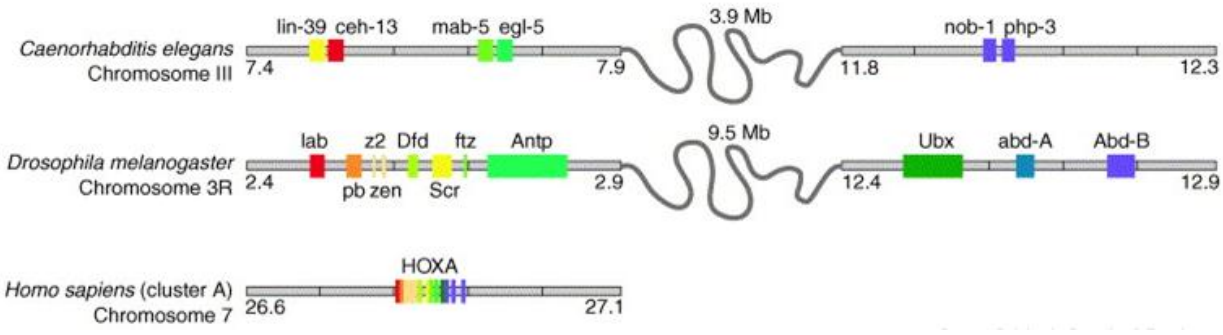

Figure 4.3 Comparisons of the Hox clusters of flies, worms and humans. The clusters were mapped at the same scale, with the colored boxes indicating each Hox gene. The *C. elegans* and *D. melanogaster* found to be broken between *antennapedia*-like genes and more posterior genes, and separated by ~4 Mb and ~10 Mb, respectively. *H. sapiens*, like other vertebrates, has four clusters, which are formed in the same way such as the HOXA cluster presented on the illustration. Distances are given in megabases. Illustration taken from [168] and modified.

In the embryo, the *labial* homolog *ceh-13* is necessary for anterior patterning, while the *Drosophila melanogaster Abdominal-B* (*AbdB*) homologs *nob-1* and *php-3* are required for posterior patterning [169, 170]. The *lin-39 Hox* gene, a homolog of *Sex combs reduced* (*Scr*) in *Drosophila melanogaster*, is expressed in the midbody and is essential for development of the vulva [171, 172, 173]. *mab-5*, a *fushi tarazu* (*ftz*) homolog, and *egl-5*, an *AbdB* homolog, are expressed in partially overlapping posterior domains and are required for development of mating structures in the male [131, 135, 173-177]. Furthermore, the studies of *mab-5* function revealed that it is required to direct posterior cell migrations in both sexes [175]. *C. elegans* Hox genes, like in other organisms, are negatively regulated, which prevents their inappropriate transcription. Anterior expression of *mab-5* as well as *egl-5* genes leads to ectopic differentiation of anterior hypodermal cells into male mating structures, which are normally restricted to the posterior [131, 177].

The expression of *Hox* genes in *C. elegans* organism is known to be regulated by two complexes, the **P**oly**c**omb **g**roup proteins (**PcG**) and the **P**oly**c**omb-like proteins (**PcG-like**) [125, 131]. PcG proteins form a MES (**M**aternal **E**ffect **S**terile) complex in *C. elegans* that consists of four proteins: MES-2, MES-3, MES-4 and MES-6 [141, 142, 178]. The MES proteins are known for their repressive function. As it has been reported, mutation of the *mes-2*, *-3*, *-4* and -6 result in de-repression of high-copy transgenes and X chromosome modifications characteristic for active chromatin, suggesting a role in germline silencing of the X chromosome [136, 178]. Moreover, lack of MES function results in germline degeneration, maternal-effect sterility and male tail defects in *C. elegans* [131, 179]. Interestingly, the Zarkower group showed that the observed male tail defects in *C. elegans* males are the result of an ectopic expression of homeobox genes in the absence of PcG [131].

A similarity between the phenotype of *C. elegans* males with *his-24* and *hpl-2* genes deletion and those with mis-expression of *egl-5* or *mab-5* genes let to assume that HIS-24 and HPL-2 proteins may be involved in the *Hox* gene regulation. The further studies confirmed that indeed HIS-24 and HPL-2 proteins play a regulatory role in the *egl-5* and *mab-5* transcription. In the case of HIS-24 histone variant, I demonstrated that the linker histone represses the *egl-5* and *mab-5* genes transcription by binding to their regulatory regions. Remarkably, when the *Hox* genes are ectopically expressed, the level of HIS-24 associated with the promoters and intragenic regions was reduced (showed for *mab-5::gfp* gene reporter expressed on the *sor-1(bp1)* background). Moreover, peptide pull-down experiments followed by chromatin immunoprecipitation revealed that mono-methylated HIS-24 (HIS-24K14me1) interacts with the H3K27me3 chromatin mark, which is known for its association with the repression of *Hox* genes [137]. This indicated that probably HIS-24K14me1 may serve as an essential protein component in establishing and/or maintaining the repressive chromatin state at the selected *Hox* genes through the interaction with H3K27me3 (Figure 4.3 A).

The performed phenotypic and biochemical studies indicate that loss of the two heterochromatin components, HIS-24K14me1 and HPL-2, probably results in changes of chromatin structure affecting the *Hox* genes expression in *C. elegans*. However, since no interaction of HPL-2 and HIS-24K14me1 was observed in immunoprecipitation experiments, it is tempting to speculate that HPL-2 together with HIS-24K14me1 might be a part of the same protein group involved in the regulation of *Hox* gene expression. The high degree of redundancy between *his-24* and *hpl-2* in *Hox* gene regulation might indicate that these two proteins are only the readers acting in parallel to perform the same role in translating the

effects of histone H3K27 tri-methylation. However, since I have failed so far to detect HPL-2 at the *Hox* gene region using direct ChIP approach, it is possible that the mechanisms by which HPL-2 regulates *mab-5* and *egl-5* might be indirect, involve intermediate factors (RNAi machinery, transcription factors). This model would also explain the lack of direct binding of recombinant HPL-2 to the H3K27me3 chromatin mark (Figure 4.3 A).

Although, the *C. elegans* homeobox genes are silenced by mechanisms involving H3K27 tri-methylation and Polycomb group proteins function, the results indicated that the mono-methylated form of HIS-24 and HPL-2 are also important for the repression of certain *Hox* genes, presumably by their binding to H3K27me3. The genetic epistasis study of potential co-relation between the PcG or PcG-like complex, HIS-24 and HPL-2 proteins as well as tri-methylated H3K27, revealed that probably MES complex is an upstream regulator of HIS-24 and HPL-2 activity during H3K27me3-dependent transcriptional repression of the *Hox* genes. Interestingly, analysis of a putative histone methyltransferase for HIS-24, performed by Dr. Monika Jedrusik-Bode, pointed to MES-2 protein as the one that could methylate lysine residue of this H1 linker histone variant. Remarkably, this histone methyltransferase has been reported to tri-methylate H3K27 chromatin mark. However there are no evidences that MES-2 enzyme is able to attach mono-methylated groups to the lysine residues of the HIS-24 linker histone *in vitro*.

Based on the findings described above, I propose the following model for the regulation of *mab-5* and *egl-5* gene expression by HIS-24 and HPL-2 proteins (Figure 4.4 A, B).

In the wild type *C. elegans* males at the L3 larva stage, the *mab-5* and *egl-5 Hox* genes are transcriptionally active in the posterior part of the body. In the tissues, which are not involved in the formation of sensory rays, H3K27 chromatin mark and the HIS-24 linker histone variant present at the promoter are methylated by the MES-2 enzyme. This interaction may stimulate indirect binding of HPL-2 to the same tri-methylated H3K27 chromatin mark, and finally transcriptional repression of the targeted *Hox* genes (*mab-5* and *egl-5*) (Figure 4.4 A). In the situation when both HIS-24 and HPL-2 proteins are missing, such as in *his-24(ok1024)*X*; hpl-2(tm1489)*III mutant animals, MES-2 protein probably still can methylate lysine 27 of the H3 core histone, but without two heterochromatin proteins the complete silencing is not possible. This may lead to activation of an ectopic *Hox* genes expression (Figure 4.3 4).

Interestingly, recently performed chromatin immunoprecipitation experiment revealed significant reduction of the H3K27 tri-methylation on promoters of the *mab-5* and *egl-5 Hox* genes in *his-24(ok1024)*X*; hpl-2(tm1489)*III mutant animals. This indicates that a decreased level of H3K27me3 can contribute to the observed ectopic expression of both *Hox* genes.

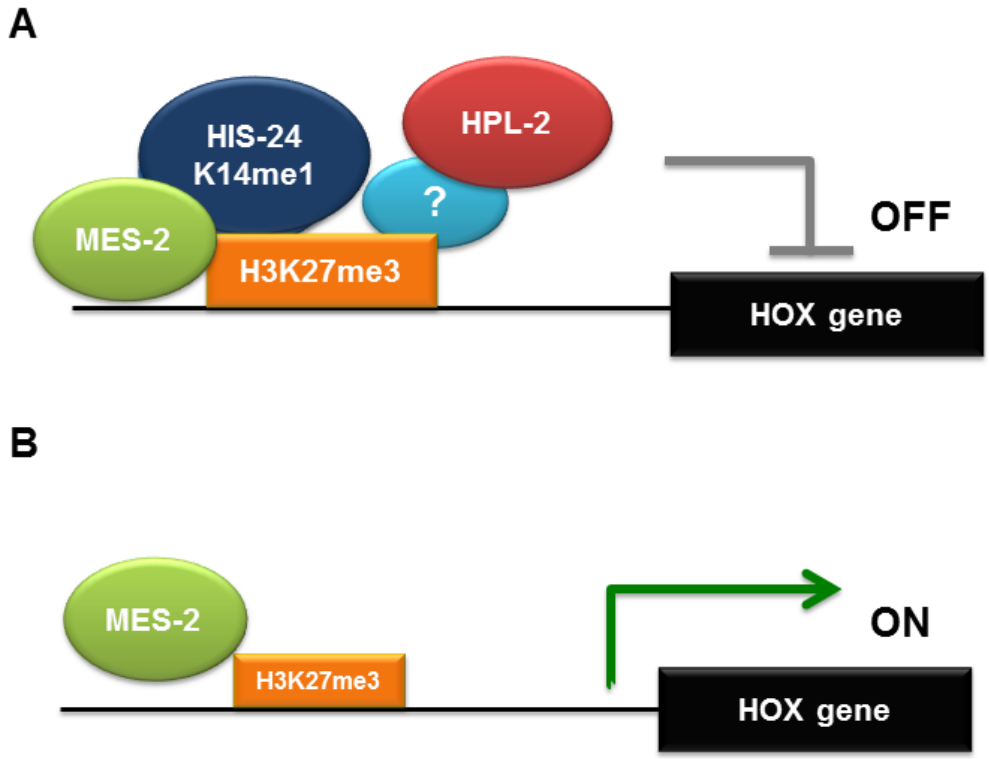

Figure 4.4 Model of the *Hox* genes silencing mediated by HIS-24 and HPL-2 proteins. Methylation of the H3 core histone at lysine 27 and HIS-24 at lysine 14 results in the recruitment of HPL-2 to the promoter of the *Hox* gene and activation of transcription **(A)**. The absence of HIS-24 and HPL-2 proteins causes ectopic expression of the Hox genes despite H3K27me3 occupancy on the promoter **(B)**.

This is the first time when the *C. elegans* H1 histone variant, by mediation with Polycomb group proteins, is reported to interact with H3K27me3 mark in somatic cells of *C. elegans*; however the cross-talk between H1, PcG complex and H3K27 tri-methylation level has been already described in subtelomeric regions of *C. elegans* germ cells as well as in vertebrates [71, 113]. Interestingly, it is suggested that the mammalian linker histone H1 and chromatin structure are important factors in determining substrate preferences of the EZH2 histone methyltransferase complex, a homolog of MES complex in *C. elegans* [180]. Consistently, it was observed that the global H3 Lys-27 methylation is reduced when the levels of H1 are lowered by 50% [71]. Importantly, the reduction of H3K27me3 level was also observed in the germline of *his-24(ok1024); mes-3(bn35)* mutant animals when compared with the respective *mes* single mutant [101]. Taken together, these observations supported a model in which linker histones stimulate H3K27 methylation through the recruitment of the EZH2 complex [101, 181]. If the mechanism present in mammals is conserved in *C. elegans* organism, then HIS-24 will be the one responsible for the recruitment of MES-2 protein, the homolog of EZH2, to the H3 core histone at the *Hox* gene promoter. Nevertheless, it is possible that the MES and HIS-24-dependant repression of the *Hox* genes is a tissue or stage specific phenomenon. As previously mentioned (see section 3.5.7), the *egl-5* and *mab-5 Hox* genes expression is also mediated by newly described PcG-like proteins, SOP-2, SOR-1 and SOR-3 [126, 137]. *sop-2* gene encodes a SAM domain-containing protein that is related to, but not

orthologous with, Polycomb group proteins [126]. During development, SOP-2 activity is required for the proper integration of sexual, spatial, and temporal information during cell fate specification [126]. In particular, SOP-2 is required for maintaining a specific pattern of *Hox* gene expression, such as that of *mab-5* and *egl-5*, to certain cells and tissues like the serotonergic and dopaminergic male tail neurons and the ventral nerve cord [126]. SOP-2 protein interacts directly with other members of PcG-like complex, SOR-1 and SOR-3 [125, 137]. As it was shown by the Zhang group, SOP-2 and SOR-1 are involved in global repression of Hox genes in *C. elegans* [125]. Remarkably, neither SOR-1, SOR-3 nor SOP-2 is conserved in other organisms, not even in the congeneric species *C. briggsae*, suggesting a surprising lack of evolutionary constraint on an ancient regulatory system [125, 137]. The analyses of *C. elegans sop-2(bx91)* mutant strains revealed that the beginning of *Hox* gene expression is normal but it becomes ectopic in diverse body regions in later stages of the development when animals carrying this mutation exhibit the mis-expression of the *mab-5* and *egl-5 Hox* genes [126]. Interestingly, the distribution pattern of ectopically expressed *mab-5* and *egl-5* in *sop-2* deleted worms differs from that observed in the *mes* mutant animals, supporting the hypothesis that these two repressive complexes may be responsible for *Hox* gene expression in distinct tissues of *C. elegans*.

Importantly, the results of phenotypic and biochemical analyses suggest that correct *Hox* gene expression is not only an effect of the crosstalk between the proper H3K27me3 level and the presence of the HIS-24 and HPL-2. The rescue experiment performed on *his-24(ok1024)*X*; hpl-2(tm1489)*III mutant males revealed also the importance of the post-translational modification of HIS-24 protein in the development of males. The presence of HIS-24A14K protein, that is nonmethylatable, is not sufficient to restore a proper formation of male mating structures. While the expression of mono-methylated HIS-24 at lysine 14 positively influences the development of *C. elegans* sensory rays and the function during the transcriptional regulation of gene targets.

In addition, the observed rescue of *C. elegans* male phenotype also indirectly indicated that HPL-2 is not the major factor involved in the regulation of rays formation, since the expression of wild type HIS-24 variant is able to restore the correct sensory rays growth in males with *hpl-2* deletion. It is possible that HPL-2 plays only a modulatory role during transcriptional repression directed by the HIS-24K14me1 histone variant.

4.6 HIS-24K14me1 and HPL-2 as putative members of the PcG repressive complex

As previously mentioned, the *Hox* genes expression is regulated in the mammalian system by the Polycomb group proteins assembled in two complexes, PRC1 and PRC2. Remarkably, there is no evidence to date for the transcriptional regulation of *Hox* genes by any of the mammalian H1 variants. Nevertheless, a recent study of the Wilkinson group discovered a mechanism of gene expression regulation by the linker histones and DNA methylation in the context of the *Rhox* homeobox genes transcription [71]. Although *C. elegans* does not possess methylated DNA, it is still possible that H1 can influence the *Hox* gene regulation in the analogical way as it is observed in *Rhox* genes family. Following this hypothesis, H1 together with HPL-2, could then regulate the *Hox* gene expression as a part of the PcG silencing complex, in particular PRC1 complex which has not yet been identified in *C. elegans*. In

mammals, the PRC1 complex consists of Polycomb (PC) protein, Posterior sex combs (PSC), Polyhomeotic (PH) and RING1 proteins that are responsible for H3K27 recognition and PRC2 recruitment [181, 182]. It is possible that the HIS-24 linker histone variant together with HPL-2 protein, apart from their function as chromatin structural proteins, form a *C. elegans*-specific alternative PRC1complex that interacts with MES (PRC2 homolog) proteins and represses transcription. In particular, I consider the possibility that the interaction of HPL-2 and HIS-24K14me1 with H3K27me3 may regulate the *Hox* gene in PcG (MES) pathway and it may be restricted to specific parts of the genome.
Furthermore, the studies of Sun and Zhang suggest that, like other forms of epigenetic gene silencing, PcG-mediated Hox gene repression might also involve RNA [125, 183]. For example, the PRC1 and PRC2 complexes are essential for the X chromosome inactivation in mammals and they are recruited to the X chromosome in a *Xist* structural RNA-dependent manner [184, 185, 186]. In this context, it is possible that the transcriptional repression of the *mab-5* and *egl-5 Hox* genes, involving HIS-24K14me1 and HPL-2 activity, is mediated by the presence of small RNA molecules.

Surprisingly, the results of this study seem to argue with the well-known 'histone code' theory and indicate that transcriptional regulation is probably more dynamic then it is thought. According to the 'histone code' hypothesis the methylation marks presented on the core histones can be read by proteins that bind them specifically and then regulate downstream events [39]. Heterochromatin protein 1 (HP1), an essential component of chromatin, is known to bind specifically to methylated lysine 9 of histone H3 (H3K9me2/me3) [39]. The theory holds that coordinated patterns of modifications of DNA-packaging histones may be a key factor in turning specific genes "on" or "off". However, as it was observed in mammalian system as well as in this study, HP1/HPL-2 does not always follow the H3K9me2/me3 code and it can by also recruited to chromatin by H3K27me3 mark [187-191]. The association of HPL with H3K27me3 suggests that the chromodomain has sufficient plasticity to recognise and bind both H3K9me2/me3, and H3K27me2/me3 in *C. elegans*. Interestingly, the chromodomain of HP1 protein displays similarity to that found in several protein members of PRC1 complex, such as CBX2 and CBX7, which are known to directly interact with H3K27me3 [192]. Additionally, these two PRC1 proteins also recognise H3 core histone methylated at lysine 9 [192].

Taken together, all these results implicate that HPL and HIS-24 share some common functions even though there are significant structural differences among these proteins. I suggest that the association of HPL-2 and HIS-24K14me1 with H3K27me3 methylation mark may create a major signal for the establishment of repressive pattern on selected homeotic genes. However, it is also conceivable that the function of HIS-24K14me1 in chromatin compaction can be replaced to a certain degree by HPL-2 protein, as *his-24(ok1024)*X males did not show tail defects in comparison to *his-24(ok1024)*X*; hpl-2(tm1489)*III animals. Following this line of thought, the loss of HIS-24K14me1 and HPL-2, two essential components of heterochromatin, probably cause significant changes in the chromatin structure, affecting *Hox* gene expression in *C. elegans*.

4.7 The influence of the HIS-24 linker histone and HPL activity on the innate immune response

The H1 has long been implicated in general repression of transcription. However, recent studies indicate that particular linker histone variants are associated with gene-specific transcriptional regulation [6]. Furthermore, previous reports and this study revealed that beyond regulation of the gene expression H1 histones can also be linked to other biological processes, such as apoptosis induced by double strand break DNA damage or antibacterial defense in *C. elegans* intestine [38, 115]

The results of genome profiling study and quantitative proteome analysis, suggest that linker histone H1 together with HP1 proteins family may act redundantly to coordinate the innate immune response in metazoans. As many as 30% of mis-expressed proteins, found in *his-24(ok1024)*X mutant animals, are known to be induced by infection and showed association with immune response processes, indicating that HIS-24 not only regulates transcription of the *Hox* genes, but it may affect expression of immune response-related genes. The observed interaction of HPL-1 protein with the HIS-24 linker histone variant, through its mono-methylation site at lysine 14, could be an important mechanism of the chromatin compaction and the silencing of immune response-related genes. Indeed, the results of ChIP-qPCR experiments indicate that HIS-24 is the crucial factor in repression of several genes involved in defense response, such as *maoc-1* and *daf-2* [115]. In particular, HIS-24 linker histone showed high enrichment at the *maoc-1* and *daf-2* promoters before infection process, but it was not present at the regulatory gene regions directly after infection. Moreover, the absence of HIS-24 protein resulted in reduction of HPL proteins association with the *maoc-1* and *daf-2* promoters, suggesting that *C. elegans* linker histone and HPL protein family may cooperate in the regulation of the transcription process [115]. Although HIS-24 revealed direct association with the promoters of antimicrobial genes, it cannot be excluded that its role could perhaps by limited only to the structural changes of chromatin, resulting in increased accessibility of DNA to *trans*-acting proteins which may play a causal role in gene expression.

Surprisingly, the functional analysis of the potential regulation of immune response genes by the HIS-24 and HPL proteins, revealed a lack of the synergism between these two proteins. In particular, the investigation of the susceptibility on infection with *Bacillus thuringiensis* showed that while *his-24(ok1024)*X mutant worms live shorter in relation to the wild type animals, the animals with *hpl* deletion display markedly longer survival. One of the possible explanations could be the difference in downstream targets of H1 as well as HPL-1 and HPL-2 proteins. To be exact, in spite of commonly regulated targets, identified by both microarray and SILAC approaches, the other defense-related genes may be separately regulated either by the HIS-24 or by HPL proteins. This would be possible in terms of the differences between chromatin marks with which HIS-24 and HPL are associated. In fact, the performed immunoprecipitation experiments showed that HPL-2 protein predominantly interacts with di- or tri-methylated H3K9 chromatin marks whereas the linker histone HIS-24 associates with tri-methylated H3K27 [115, 130]. Therefore, the expression of genes, exhibiting H3K9me3 on their promoters and regulated by the HPL-2 protein, may result in contradictory effects during immune response of *C. elegans* when compared to HIS-24 impact. Interestingly, the opposite effects of the HIS-24 and HPL deletions result in higher fraction of survived *his-24 (ok1024)*X *; hpl-2(tm1489)*III double and *his-24(ok1024)*X *hpl-1(tm1624)*X; *hpl-2(tm1489)*III

triple mutant animals upon infection with *Bacillus thuringiensis* in comparison to the single *his-24(ok1024)* mutant strain. In this situation it is likely that the negative effect of HIS-24 deletion could be neutralised by the transcriptional up-regulation of HPL targets. In addition, the reduced survival fraction observed in triple mutant animals, in contrary to animals carrying *his-24* 642 *(ok1024)* X *hpl-1(tm1489)* X double mutation, once again suggests that HPL-1 protein appears to have a redundant function with HPL-2 protein.
On the other hand, the analysis of transgenic animals, overexpressing GFP-tagged form of either HIS-24 or HPL proteins, pointed to the significance of post-translational modification of the linker histone for the *C. elegans* resistance to bacterial infection. Since the expression of mutated HIS-24A14K protein, in contrast to the wild type HIS-24, did not restore the survival rate of *his-24(ok1024)* mutant worms to the level observed in the wild type animals, it became clear that mono-methylation must be important for the role of the linker histone in immune response of *C. elegans*.
Remarkably, the significance of HIS-24 post-translational modification at the lysine 14 was confirmed by the linker histone localisation study upon infection. Surprisingly, intestinal cells infected with gram-positive *Bacillus thuringiensis* bacterium, exhibited a cytoplasm fraction of the HIS-24 protein, which was not detected in cells with the mutated HIS-24A14K variant. This indicates that the cytoplasmic fraction of the HIS-24K14me1 linker histone variant may be directly involved in the antibacterial defense in *C. elegans* intestine. Importantly, similar behaviour of the H1 linker histone variant has been already observed by the Mahida group in the human epithelial cells of gastrointestinal tract [193]. They showed that upon infection with *Salmonella typhimurium* the H1 was found to be expressed in the cytoplasm of villus epithelial cells, where it is believed to provide protection against penetration by microorganisms [193]. It appears that the described H1 behaviour constitutes an evolutionary conserved mechanism of immune defense against bacteria. However the precise way of H1 action in terms of interface with pathogenic microorganisms still needs to be determined.
In addition, it is important to remember that immune response should be investigated in the wider context, where antimicrobial defense of organism is linked to stress conditions. Thus the association of the linker histone and HPL proteins with the immune response processes was verified by the behavioral test, with the object of distinction between immune and stress response of *C. elegans*. Remarkably, the analyses revealed that the absence of HIS-24 and HPL proteins influence the response to different stress stimuli in the similar way as it was observed after bacterial infection. This means that the response to the stress conditions may modulate the expression of immunity related antimicrobial genes.

On the basis of the obtained results I suggest a model of HIS-24 and HPL activity, during defense response process in *C. elegans* organism. In the environmental conditions, when the *C. elegans* worm is not exposed to the infection, HIS-24 histone occupies the promoters of some antimicrobial genes and together with HPL proteins represses the transcriptional activity (Figure 4.5 A). However upon the bacterial infection, mono-methylated form of HIS-24 and HPL dissociate from the gene regulatory regions and translocates into the cytoplasm (Figure 4.5 A). This results in transcriptional activation of defense-related genes and subsequent immune response of the *C. elegans* organism.

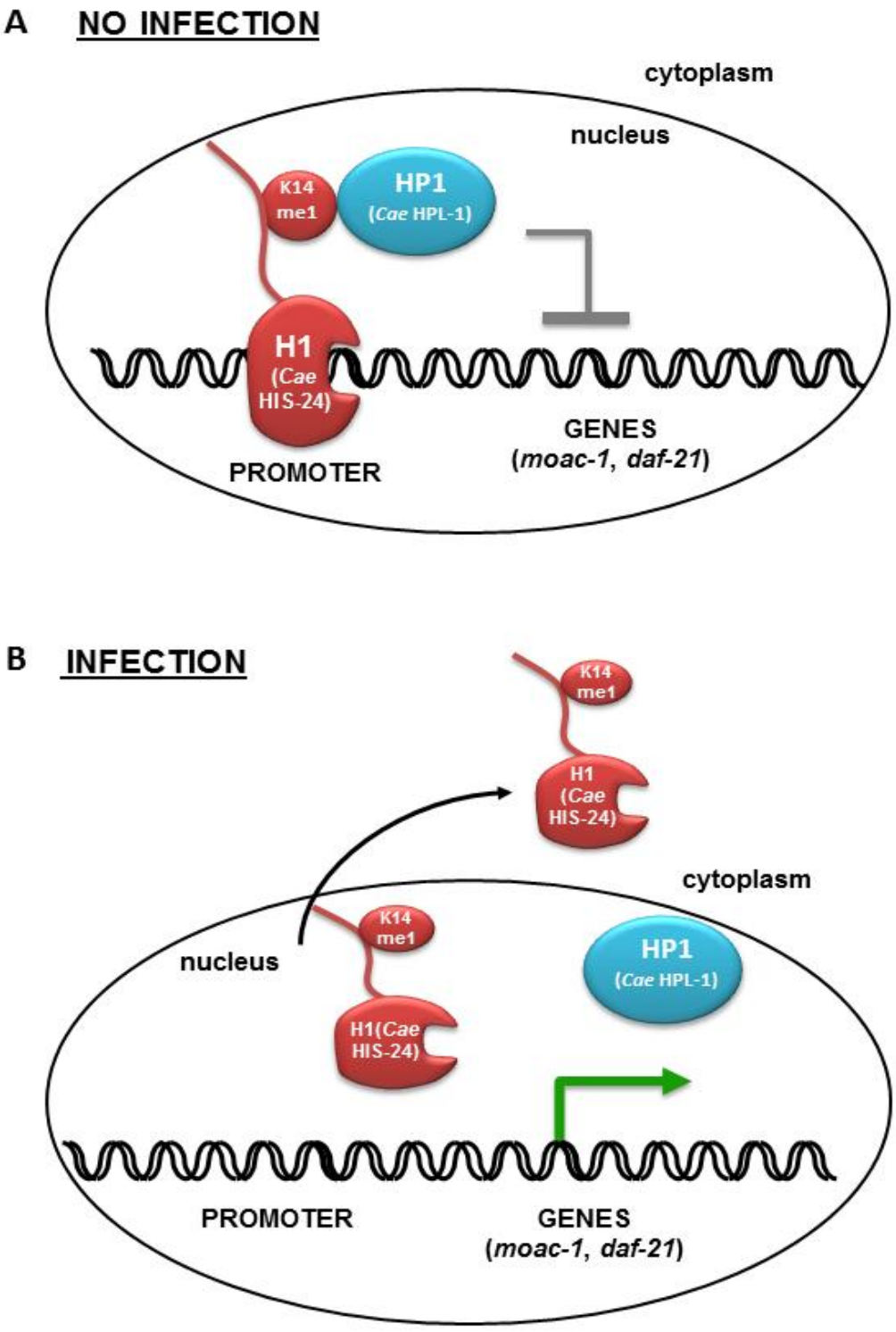

Figure 4.5 Model of H1 and HP1 interaction before and after bacterial infection of *C. elegans* worms. Before infection, mono-methylated HIS-24 together with HPL-1 protein associate with the promoters of antimicrobial genes **(A)**. During the infection process, the HIS-24K14me1 level increases and the majority of mono-methylated fraction together with HPL-1 dissociate from the promoters of antimicrobial genes what causes transcriptional activation. The dissociated HIS-24K14me1 is realized into the cytoplasm, where it is directly involved in the immune defense **(B)**. Illustration taken from [115] and modified.

All in all, in this study I focused on the understanding of the role of post-translational modification of HIS-24 histone variant and how differences in the distribution and function of modified as well as unmodified protein impact on gene expression and development of *C. elegans*. For the first time I report that the HIS-24 linker histone variant together with HPL proteins does not act as a general repressor, but it rather has an impact on the regulation of specific genes. Moreover, mono-methylation of HIS-24 proved to be essential for the proper and tissue specific *Hox* genes repression and also for the transcriptional regulation of immune response-related genes. The observed differences in the subcellular localisation and function of both modified and unmodified linker histones point to a significance of post-translational modification in diverse roles of HIS-24. The results provide new insights and identify additional models of linker histone-based transcriptional regulation in *C. elegans* development and innate immune response.

Additionally, the study demonstrates that it is important to consider the precise function of biochemically modified histones not only in the context of changes in chromatin structure, but also in respect to their functions beyond transcriptional regulation. Understanding the interplay between H1 post-translational modifications in different *C. elegans* tissues may give insights into the other biological processes, in which mono-methylated HIS-24 presumably is involved.

5 Appendix

A.1 cDNA sequences of *his-24, hpl-1* and *hpl-2* genes

his-24 cDNA

```
atgtctgattccgctgttgttgccgccgctgtcgagccaaaggtcccaaaggctaaggccgccaaggccgccaag
ccaaccaaagttgccaaggccaaggctccagtcgctcacccaccatacatcaacatgatcaaggaggccatcaag
cagctcaaggaccgcaaaggagcttccaagcaggcaatcctcaagttcatctcccaaaactacaagctcggagac
aatgtcatccagatcaatgctcatctccgtcaggctctcaagcgtggtgtcaccagcaaggcccttgttcaagcc
gccggatccggagccaacggacgtttccgtgtgccagagaaggccgccgccgccaagaagccagcagcagccaag
aagccagcagcagccaagaaaccagcagccgccaagaaagccactggagagaagaaggcaaagaagccagccgct
gccaagccaaagaaggccgccaccggagataagaaggtcaagaaggccaagagcccaaagaaggttgccaagcca
gctgccaagaaggtcgccaagtctccagccaagaaggccgctccaaagaagatcgccaagccagctgccaagaag
gccgccaagccagccgccaaggcctaa
```

hpl-1 cDNA

```
atgtcacgtcaaaaccctgtccgaagcactcgcgggaattcactcagagctcgggaagctcagcaggcacaagat
gctccgttgtttcaggaatcctccagcaacgtcttcgtggtggaaaaagtgttgaataaacggttgacgcgtggc
ggaagcgagtactatataaaatggcagggattcccagagtccgagtgcagttgggagccaattgagaacctccag
tgcgataggatgattcaggaatacgagaaggaagcggcaaagcgcacaacacgcaaacgtcgatattccccacaa
ccgtcgacttcgtcttctgcagagctccaaccatctaccagcgatgaatgggctgggaaaacactgaagacaatt
attggaatcaccaaggcacccggagaactgcatttcttgtgcaagttcagcgacgactctgtgcatttgattcca
ttgagagaagccaatgttcgttttccaagtcaagtcatcaaattctacgaaacccgtcttgttcttcaaggagtt
tcgccaaccatcccaggaggaatgagctaa
```

hpl-2a cDNA

```
atgtcgagcaaatcaacaaagcgagcaaaaatcgaagatccgaaggacaacgtgttcatggtggaaaa
agtgctggacaagcgaactggaaaagccggcagagacgaatttctcatacagtggcaaggattccccg
agtctgactctagctgggagccgagagagaatctccagtgcgtcgagatgttggacgagtttgagagg
gaattttcaaagagagagaaaccaattcgcaaacgacacagccagaagcccgaaccttccgaagatca
agcggatccagaagaggataaagatgaaaagaaggaaacgaatcaaaatgacaaattctcactggaag
gcaagcagttaaaatgcattgtcgggctcaccaagggacctggggaacttcattttctgtgcaaattc
agtgatgacacggcacggcttcttccagcgaaggaggtgaacagtcgctatccgagccaagttatcag
atactacgaatccaagctaacaatccaagacccaaaagccgacgagctttaa
```

A.2 *C. elegans* H1 proteomics

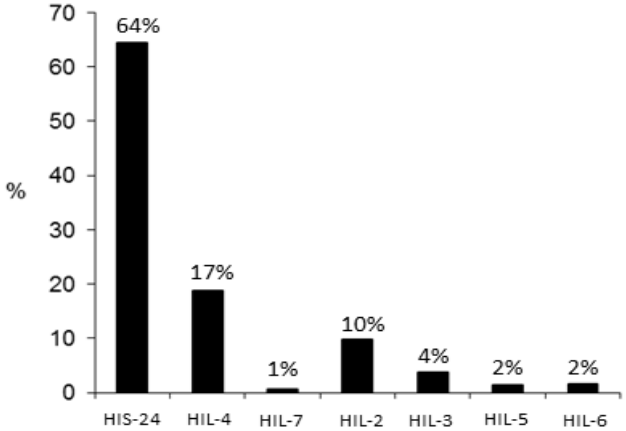

A.3 Transcription factors up- and down-regulated in *his-24(ok1024)*X*; hpl-2(tm1489)*III double mutant animals

Sequence Name	Gene Name	logFC *hpl-1;hpl-2* vs. WT	logFC *hpl-1his-24* vs. WT	logFC *hpl-2;his-24* vs. WT	logFC *hpl-1his-24; hpl-2* vs. WT	logFC *hpl-1* vs. WT	logFC *hpl-2* vs. WT	logFC *his-24* vs. WT
R11G11.14.1	**nhr-132**	**3.9**	0.5	**5.3**	**5.8**	**4.7**	**5.6**	5.2
Y45G5AM.1a.1	**nhr-114**	0.05	0.04	**3.3**	**2.2**	**1.7**	**2.2**	2.0
F46G10.6.2	**mxl-3**	0.4	0.02	1.2	**2.2**	**1.8**	**2.2**	2.2
C25E10.10	-	0.2	0.08	**2.0**	1.3	0.4	0.1	**0.2**
T01G6.7.1	**nhr-55**	0.1	0.2	1.2	**1.3**	0.8	0.6	**0.6**
F21D12.1a	**nhr-21**	0.3	0.9	**1.5**	1.2	1.1	1.1	**0.7**
M02H5.1	**nhr-99**	0.6	0.9	1.3	**2.0**	0.9	1.0	**1.0**
T26C11.7	**ceh-39**	0.5	**1.6**	0.03	1.1	1.0	0.3	**0.7**
C44F1.2	**attf-1**	0.8	0.8	0.4	**-1.7**	0.7	0.1	**-0.3**
H12C20.6.1	**nhr-101**	0.3	0.7	**2.1**	0.9	0.7	0.1	**0.5**
T01G6.4	**nhr-106**	0.7	0.1	1.1	**1.4**	1.0	1.0	**0.8**
H12C20.3	**nhr-68**	0.6	0.7	**3.1**	1.2	0.6	0.7	**0.4**
Y1A5A.1	-	0.6	0.6	0.1	**1.5**	-0.7	0.5	**0.0**
C10G8.7	**ceh-33**	0.7	0.6	0.4	**1.3**	1.0	1.1	**0.7**
ZC410.1.2	**nhr-11**	-0.03	-0.04	**-1.4**	-0.9	0.3	0.1	**-0.0**
T27B7.4	**nhr-115**	-0.2	-0.4	-0.1	**-1.3**	**-1.3**	-1.1	**-0.6**
C04F1.3	**lim-7**	1.1	0.1	**1.3**	**1.6**	0.7	1.1	**0.8**
K06B4.11	**nhr-53**	-0.9	**1.6**	-0.1	-0.6	-0.2	-0.8	**1.2**
R07C12.4	**-**	**2.2**	0.5	**1.8**	1.1	0.1	0.9	**0.7**
R03E9.1	**mdl-1**	0.4	0.8	**1.4**	0.4	-0.4	-0.2	**-0.9**
Y113G7B.14	**-**	0.5	0.2	**1.4**	0.8	-0.0	1.3	**0.3**
C02F12.5	**-**	**-1.6**	0.9	-0.3	-0.7	**-1.6**	-0.3	**-0.1**
F16B4.11	**nhr-179**	-0.8	0.2	**-1.4**	-0.3	-0.2	-0.3	**0.0**
F58H1.2	**-**	0.1	**1.4**	**1.7**	0.3	**1.4**	0.0	**-0.2**
C28A5.4	**ceh-43**	0.6	-0.2	**1.5**	0.5	-0.2	0.7	**-0.9**
R06F6.6	-	**0.6**	**-0.1**	1.6	**-0.2**	**0.1**	**-0.3**	**-0.3**

A.4a HIS-24::GFP fold enrichment at the promoters of the *Hox* genes

Gene name	Fold enrichment	Standard deviation ±SD
mab-5	78.3225	7.605
egl-5	97.0225	2.645
ceh-2	3.8025	0.005

A.4b HIS-24::GFP fold enrichment at the intragenic regions of the *Hox* genes

Gene name	Fold enrichment	Standard deviation ±SD
mab-5	156.25	8
egl-5	141.61	0.32

A.4c HIS-24 binding to the promoter and intragenic region of the *mab-5 Hox* gene in *mab-5::gfp* transgenic strain and in wild type

Gene region	Fold enrichment	Standard deviation ±SD	Strain
mab-5 promoter	161.29	0.18	wild type
	46.24	0.08	*mab-5::gfp*
mab-5 intragenic region	140.423	1.445	wild type
	64	0.02	*mab-5::gfp*

A.4d Chromatin mark occupancy at the regulatory regions of the *Hox* genes in wild type strain

Gene region	Chromatin mark	Fold enrichment	Standard deviation ±SD
***mab-5* promoter**	H3	142.803	0.845
	H3K4me3	16.81	0.08
	H3K9me2	10.5625	0.70817
	H3K27me2	10.1336	0.47461
	H3K27me3	95.7136	0.6367
***mab-5* intragenic region**	H3	144.49	0.72
	H3K4me3	1.5625	0.845
	H3K9me2	2.61361	0.50335
	H3K27me2	2.61361	0.89338
	H3K27me3	68.0625	0.78758
***ceh-2* promoter**	H3	167.7025	0.045
	H3K4me3	4.84	0
	H3K27me3	59.29	0

Gene region	Chromatin mark	Fold enrichment	Standard deviation ±SD
***egl-5* promoter**	H3	128.823	2.205
	H3K4me3	2.7225	0.005
	H3K9me2	4.76674	1.46413
	H3K27me2	2.61361	0.60195
	H3K27me3	77.1469	2.645
***egl-5* intragenic region**	H3	115.563	0.005
	H3K4me3	4.6225	0.125
	H3K9me2	5.0625	0.125
	H3K27me2	3.18028	0.02114
	H3K27me3	70.2803	0.00063

A.4e Chromatin mark occupancy at the regulatory regions of the *mab*-5 *Hox* gene in *mab-5::gfp* transgenic strain and in wild type

Gene region	Chromatin mark	Fold enrichment	Standard deviation ±SD	Strain
***mab-5* promoter**	H3	182.25	6.31E-30	wild type
	H3	101.003	0.245	*mab-5::gfp*
	H3K27me3	178.225	0.005	wild type
	H3K27me3	30.4025	0.245	*mab-5::gfp*
***mab-5* intragenic region**	H3	167.703	1.445	wild type
	H3	123.21	0	*mab-5::gfp*
	H3K27me3	165.123	1.125	wild type
	H3K27me3	52.5625	0.005	*mab-5::gfp*

A.5 Genes regulated by linker histone variant HIS-24 and/or heterochromatinproteins HPL-1, HPL-2 detected by microarray analysis. Table taken from [115] and modified

GO ontology	Genes up-regulated logFC>1.5 (FDR<0.05)	Genes down-regulated logFC<1.5 (FDR<0.05)
GO:0006508 **PROTEOLYSIS**		F40B5.1 (gene encodes a neprilysin)
GO:0005488 **BINDING**	*clec-4* (C-type LECtin), *clec-66, clec-67, clec-68, clec-190*[a]	*clec-9, clec-4, clec-48, clec-210, clec-227,bclec-258*
GO:0003796 **LYSOZYME ACTIVITY**	*lys-2* (LYSozyme)	W03D2.7, *lys-6 (*LYSozyme), *lys-5, lys-4, ilys-3* (Invertebrate LYSozyme)
GO:0006952 **DEFENSE RESPONSE**		*thn1* (Thaumatin), *thn-2, thn-3*
GO:0003824 **CATALYTIC ACTIVITY**		F25D1.5, C33C12.8, C30G12.2, *cth-1* (CystaTHionine gamma lyase), C50B6.7, F44G3.2.1, *pho-6* (intestinal acid PHOsphatase), *pho-13*
GO:0006355 **REGULATION OF TRANSCRIPTION**		*mxl-3* (MaX-Like), *nhr*-114 (Nuclear Hormone Receptor family)
GO:0055114 **OXIDATION REDUCTION**	***sod-3* (SuperOxide Dismutase)**[b]	***cyp-34A10* (CYtochrome P450 family), *cyp-13A4, cyp-13A5, cyp-33D, cyp-13A7, cyp-34A9 (dod-16), cyp-13A12, msra-1*(Methionine Sulfoxide Reductase A), *sodh-1(dod-11)* (SOrbitol DeHydrogenase family)**
GO:0006629 **LIPID METABOLIC PROCESS**		*fat-3* (FATty acid desaturase), ZK593.3, W03D8.8, C40H1.8, K04A8.5, F54F3.3, acs-2 - (fatty Acid CoA Synthetase family), *far-3* - (Fatty Acid/Retinol binding protein)), *far-7*, F54F3.3
GO:0008152 **METABOLIC PROCESS**	*nlp-4* (Neuropeptide-Like Protein)	*ugt-15*(UDP-Glucuronosyl Transferase), *stdh-2 (dod-10)* (STeroid DeHydrogenase family),C23G10.6, *acdh-2* (Acyl CoA DeHydrogenase), *alh-5*- (ALdehyde deHydrogenase), F21C10.10.2, K12D9.1, R05D8.9, ech-9 - (Enoyl-CoA Hydratase)
GO:0009790 **EMBRYONIC DEVELOPMENT**	*nit-1*(NITrilase)	F42A10.7.1, Y41C4A.11, C23G10.11
GO:0006810 **TRANSPORT**	*acd-1*(ACid-sensitive Degenerin)	F47E1.4.1, *pmp-5* (Peroxisomal Membrane Protein related), *pgp-1* P-GlycoProtein related) B0222.3.1, *hrg-4* (Heme Responsive Gene), *aqp-1-* (AQuaPorin or aquaglyceroporin related)
GO:0016021 **INTEGRAL TO MEMBRANE**	*col-43* (COLlagen), *col-88, col-127, col-128, col-137*, Y9C9A.8, *bus-1* (Bacterially Un-Swollen), F57G8.7, *bah-1*(Biofilm Absent on Head), F44G3.10, *dct-5* (DAF-16/FOXO Controlled, germline Tumor affecting)	*col-74, col-121*, Y38H6C.21, C45B2.3, *dct-7*, Y34F4.2, B0564.3.1, M02D8.4a.1, C35C5.8a, C18H7.1.2, K03h6.4, F07C3.9, R09H10.7, F57B1.6, T04C12.1, F10F2.4 , C49G7.7 (CUB-like domain), F55G11.2, F55G11.7, F55G11.8, C17H12.6, F08G5.6, F35E12.5, C32H11.4

[a] Genes involved in immune response are highlight in gray

[b] Stress response genes in bold tape

A.6 Selected functional infection-inducible proteins regulated by HIS-24[a]. Table taken from [115] and modified.

Group and Wormbase cosmid ID	Gene symbol	Description	Expression site(s)	*P* value (SILAC)	Fold induction (microarray) [FDR <0.05]	Pathogen(s)[b]
Up-regulated proteins						
Y48E1B.10	*gst-20*	predicted glutathione *S*-transferase	Muscle, hypodermis, neurons	0.04044	1.0	*E. carotovora*, *P. luminescens*
F11G11.2	*gst-7*		Intestine	0.00276	0.4	*P. aeruginosa*
Y39B6A.20	*asp-1*	Aspartyl protease	Intestine	0.00162	0.5	*E. carotovora*, *E. faecalis*, *P. luminescens*
T18H9.2	*asp-2*		ND[d]	0.00294	0.0	*E. carotovora*, *E. faecalis*, *P. luminescens*
K09F5.3	*spp-14*	Saposin-like protein	ND	0.04032	0.5	*E. carotovora*, *P. luminescens*
F35C5.6	*clec-63*	C-type lectin	ND	0.00068	0.0	*M. nematophilum*, *E. carotovora*, *E. faecalis*, *P. luminescens*
ZC434.8	NA[c]	Probable kinase	ND	0.00171	0.2	*S. marcescens*
ZK1055.7	NA		Intestine	0.00238	0.4	*P. aeruginosa*
E04F6.3	*maoc-1*	MAO-C-like dehydratase domain	Intestine	0.00620	0.5	*P. aeruginosa*, *E. carotovora*, *E. faecalis*, *S. marcescens*
ZK6.10	*daf-19*	Abnormal Dauer formation	Muscles, intestine	0.00895	1.2	*P. aeruginosa*
C47E8.5	*daf-21/ hsp90*		Intestine	0.00783	0.5	*P. aeruginosa*
Down-regulated proteins						
F41C3.3	*acs-11*	Fatty acid-CoA synthetase	Hypodermis, intestine	0.01479	0.8	ND
C46F4.2	*acs-17*		Hypodermis, intestine	0.00342	1.0	*P. aeruginosa*
K05B2.3	*if-a4*	Intermediate filament protein	Rectum, some neurons, excretory cell	0.00622	1.4	*M. nematophilum*
K01A2.2	a *far-7*	Fatty acid/retinol binding protein	Hypodermis, excretory cells	0.00727	1.3	*M. nematophilum*
K12G11.3	*sodh-1*	Sorbitol/alcohol dehydrogenase	ND	0.02172	2.5	*M. nematophilum*, *P. aeruginosa*
C05E4.9	*gei-7 (icl-1)*	Isocitrate lyase/malate synthase	ND	0.00419	1.1	*E. carotovora*, *E. faecalis*

F54D8.3	*alh-1*	Aldehyde dehydrogenase	Intestine, nervous system	0.00017	0.3	*P. aeruginosa*, *E. carotovora*, *E. faecalis*, *S. marcescens*
F36H1.6	*alh-3*		ND	0.00259	0.1	*P. aeruginosa*, *E. carotovora*, *E. faecalis*, *S. marcescens*
T08B1.3	*alh-5*		ND	0.04017	1.9	*P. aeruginosa*
F43E2.5	*msra-1*	Methionine sulfoxide-*S*-reductase	Intestine, hypodermis, neurons	0.02069	2.2	*P. aeruginosa*, *E. carotovora*, *E. faecalis*, *S. marcescens*
T10H9.5	*pmp-5*	Peroxisomal membrane protein	Intestine, hypodermis	0.02343	2.6	*P. aeruginosa*
F52H3.7	*lec-2*	Galectin family member	Muscle	0.01086	0.8	*E. faecalis*
Y38F1A.6	NA	Probable alcohol dehydrogenase	Muscle, intestine	0.00423	1.2	*P. aeruginosa*, *E. carotovora*, *E. faecalis*, *S. marcescens*
C55F2.1b	NA	Putative AICAR transformylase	ND	0.00090	0.8	*P. aeruginosa*, *E. faecalis*, *S. marcescens*

[a] Short information about selected response proteins detected in *his-24*(*ok1024*) mutant strain by the SILAC approach. The data are confronted with the fold induction of genes obtained using microarray analysis.

[b] The list of pathogens that affect expression of the particular genes (taken from WormBase).

[c] NA, not available.

[d] ND, not determined.

A.7 Proteins regulated by the linker histone HIS-24, found by SILAC and microarray analyses. Table taken from [115] and modified.

Protein description	his24/WT (log)	SILAC p-value	Microarray (FDR<0.05)	Pathogens
GRounDhog (hedgehog-like family) family member (GRD-10) F09D12.1	-0.70	0.000684576	-0.5	*P. aeruginosa*
Hypothetical protein C55F2.1b	-1.28	0.00090653	-0.8	*P. aeruginosa*, *E. faecalis*, *S. marcescens*
inorganic PYroPhosphatase (PYP-1) C47E12.4b	-0.36	0.001482243	-0.5	*P. aeruginosa*
ASpartyl Protease family member (ASP-1) protease 1 (transcribed exclusively in intestinal cells) Y39B6A.20	1.24	0.00162171	0.5	*E. carotovora*, *E. faecalis*, *S. marcescens*, *P. luminescens*
MAO-C-like dehydratase domain (MAOC-1) E04F6.3	0.41	0.006206456	0.5	*P. aeruginosa*, *E. carotovora*, *E. faecalis*, *S. marcescens*
abnormal dauer formation (DAF-21)	0.25	0.00783	0.5	*P. aeruginosa*
Glycerol-3-Phosphate DeHydrogenase (GPDH-2) K11H3.1b	-0.47	0.002536335	-0.5	*P. aeruginosa*
ALdehyde deHydrogenase family member (ALH-12) Y69F12A.2	-0.13	0.003934963	-1	*P. aeruginosa*
GEX Interacting protein family member (GEI-7) C05E4.9	-1.27	0.00419057	-1.1	*E. carotovora*, *E. faecalis*
fatty Acid CoA Synthetase family member (ACS-17) C46F4.2	-0.50	0.003420956	-1	*P. aeruginosa*
GEX Interacting protein family member (gei-7) C05E4.9	-1.27	0.00419057	-1.1	*E. carotovora*, *E. faecalis*
Hypothetical protein Y38F1A.6	-0.59	0.004237102	-1.2	*E. carotovora*, *E. faecalis*, *P. aeruginosa*, *S. marcescens*
Hypothetical protein Y38F1A.6	-0.59	0.004237102	-1.2	*E. carotovora*, *E. faecalis*, *P. aeruginosa*, *S. marcescens*
GEI-4(Four) Interacting protein family member (GFI-1) F57F4.3	-0.49	0.004870596	-0.7	*E. faecalis*, *S. marcescens*
Hypothetical protein W04B5.3a (sugar binding)	0.87	0.005489211	0.5	*E. faecalis*, *P. luminescens*
Cytoplasmic intermediate filament (IF) protein (IF-A4) K05B2.3	-0.94	0.006224154	-1.4	*M. nematophilium*

VAB-10A protein intestine enriched ZK1151.1	-0.50	0.006981555	-0.9	*P. luminescens*
Fatty Acid/Retinol binding protein family member (FAR-7) K01A2.2	-1.11	0.007272455	-1.3	*M. nematophilium, P. aeruginosa*
Downstream of daf-16 (regulated by daf-16) protein 19 (DAF19) ZK6.10	0.99	0.008950146	1.2	*P. aeruginosa*
Hypothetical protein (Acetyl-CoA acetyltransferase) T02G5.7	-0.91	0.010487264	-0.6	*E. faecalis*
Hypothetical protein F52H3.7a gaLECtin family member (LEC-2) F52H3.7	-0.67	0.010867072	-0.8	*E. faecalis*
Hypothetical protein C04F12.1	1.48	0.012263878	0.5	*P. luminescens*
C.Elegans Y-box family member (CEY-4) Y39A1C.3	0.26	0.012846437	0.5	*E. faecalis*
Hypothetical protein C31C9.2	-0.39	0.013688887	-0.5	*E. faecalis*
Hypothetical protein F21D5.7	0.44	0.014245015	0.5	*E. carotovora.*
fatty Acid CoA Synthetase family member (ACS-11) F41C3.3	-0.94	0.014795401	-0.8	*E. carotovora*
MUscle Attachment abnormal family member (MUA-6) W10G6.3	-0.22	0.015388721	-0.7	*P. aeruginosa*
Hypothetical protein protein KINase family member (KIN-1) ZK909.2l	-0.55	0.017533111	-0.4	*S. marcescens, E. faecalis*
Hypothetical protein (PAT-2) F54F2.1	-0.20	0.01764769	-0.5	*P. luminescens*
hypothetical protein TropoNin T family member (TNT-2) F53A9.10	-0.39	0.018056902	-0.5	*P. luminescens*
Hypothetical protein T13F3.6	-0.56	0.019464802	-0.5	*P. aeruginosa, S. marcescens*
CCT-2 T21B10.7	0.16	0.019952227	0.5	*H.bacteriophoa*
Hypothetical protein (MSRA-1) F43E2.5	-0.70	0.020693581	-2.2	*P. aeruginosa, S. marcescens, E. carotovora, P. luminescens*
SOrbitol DeHydrogenase family member (SODH-1) K12G11.3	-1.42	0.021723915	-2.5	*M. nematophilium, P. aeruginosa*
Peroxisomal membrane protein related protein 5, isoform b (PMP-5) T10H9.5	-0.57	0.023430349	-2.6	*P. aeruginosa, Y. pestis*
Hypothetical protein Y53H1B.2	0.48	0.025552485	0.5	*E. faecalis, E. carotovora.*
AQuaPorin or aquaglyceroporin related family member (AQP-2) C01G6.1a	-0.50	0.025702823	-0.5	*S. marcescens*

Hypothetical protein F52H3.7b gaLECtin family member (LEC-2)	-0.38	0.03070475	-0.8	*E. faecalis*
Hypothetical protein R11A5.4a	-0.30	0.034833293	-0.5	*E. faecalis*
Transthyretin-related family domain protein 8 (TTR-8) R13A5.6	0.42	0.036369773	0.5	*P. luminescens*
Lipid binding protein protein 6 (LBP-6) W02D3.5	-0.33	0.038747996	-0.5	*E. faecalis*
AQuaPorin or aquaglyceroporin related family member (AQP-7) M02F4.8	-0.28	0.039923843	-0.5	*P. luminescens*
F30A10.5 STomatin-Like family member (STL-1)	0.40	0.039942758	0.5	*E. faecalis*
ALdehyde deHydrogenase family member (ALH-5) T08B1.3	-0.29	0.04017301	-1.9	*P. aeruginosa*
SaPosin-like Protein family member (SPP-14)	1.03	0.040326687	0.5	*E. carotovora*, *E. faecalis*
Glutathione S-Transferase family member (GST-20) Y48E1B.10	0.52	0.040440405	1	*E. carotovora*, *P. luminescens*
Hypothetical protein VF13D12L.3	-0.30	0.043745014	-0.5	*E. faecalis*, *P. luminescens*
GRounDhog (hedgehog-like family) family member (GRD-5) F41E6.2	-0.39	0.044779738	-0.5	*P. luminescens*
Intermediate filament, d protein 2 (IFD-2) F25E2.4	-0.35	0.044908487	-0.5	*P. aeruginosa*, *E. faecalis*
Hypothetical protein Y57A10A.23 (intestine enriched)	1.07	0.047944421	0.7	*P. aeruginosa*

6 References

1. Luger K., Mader A.W., Richmond R.K., Sargent D.F., Richmond T.J. (1997). Crystal structure of the nucleosome core particle at 2.8 A resolution. Nature 389, 251–260.

2. Burlingame R.W., Love W.E., Wang B.C., Hamlin R., Nguyen H.X., Moudrianakis E.N. (1985). Crystallographic structure of the octameric histone core of the nucleosome at a resolution of 3.3 A. Science 228, 546–553.

3. Noll M. and Kornberg R.D. (1977). Action of micrococcal nuclease on chromatin and the location of histone H1. J. Mol. Biol. 109, 393–404.

4. Allan J., Hartman P.G., Crane-Robinson C., and Aviles F.X. (1980). The structure of histone H1 and its location in chromatin. Nature 288, 675–679.

5. Zhou Y.B., Gerchman S.E., Ramakrishnan V., Travers A., and Muyldermans S. (1998). Position and orientation of the globular domain of linker histone H5 on the nucleosome. Nature 395, 402–405.

6. Izzo A., Kamieniarz K., Schneider R. (2008). The histone H1 family: specific members, specific functions? Biol Chem. 389(4), 333-43.

7. Robinson P.J., Rhodes D. (2006). Structure of the '30 nm' chromatin fiber: a key role for the linker histone. Curr Opin Struct Biol. 16(3), 336-43.

8. Chapman G.E., Hartman P.G., Bradbury E.M. (1976). Studies on the role and mode of operation of the very-lysine-rich histone H1 in eukaryote chromatin. The isolation of the globular and non-globular regions of the histone H1 molecule. Eur. J. Biochem. 61, 69–75.

9. Allan J., Staynov D.Z., Gould H. (1980). Reversible dissociation of linker histone from chromatin with preservation of internucleosomal repeat. Proc Natl Acad Sci U S A 77(2), 885-9.

10. Ramakrishnan V., Finch J.T., Graziano V., Lee P.L., Sweet R.M. (1993). Crystal structure of globular domain of histone H5 and its implications for nucleosome binding. Nature 362, 219–223.

11. Thomas J.O., Rees C., Finch J.T. (1992). Cooperative binding of the globular domains of histones H1 and H5 to DNA. Nucleic Acids Res 20, 187–194.

12. Groft C.M., Uljon S.N., Wang R., Werner M.H. (1998). Structural homology between the Rap30 DNA-binding domain and linker histone H5: implications for preinitiation complex assembly. Proc Natl Acad Sci U S A 95(16), 9117-22.

13. McBryant S.J., Lu X., Hansen J.C. (2010). Multifunctionality of the linker histones: an emerging role for protein-protein interactions. Cell Res. 20(5), 519-28.

14. Lu X., Hamkalo B., Parseghian M.H., Hansen J.C. (2009). Chromatin condensing functions of the linker histone C-terminal domain are mediated by specific amino acid composition and intrinsic protein disorder. Biochemistry 48, 164-172.

15. Lu X., Hansen J.C. (2004). Identification of specific functional subdomains within the linker histone H10 C-terminal domain. J Biol Chem 279, 8701–8707.

16. Hansen J.C., Lu X., Ross E.D., Woody R.W. (2006). Intrinsic protein disorder, amino acid composition, and histone terminal domains. J Biol Chem 281, 1853–1856.

17. Caterino T.L., Fang H., Hayes J.J. (2011). Nucleosome linker DNA contacts and induces specific folding of the intrinsically disordered h1 carboxyl-terminal domain. Mol. Cell. Biol. 31, 2341-2348.

18. Ponte I., Vila R., Suau P. (2002). Expression, structure and evolution of H1 linker histones. Contribution to Science 2 (2), 225-235.

19. Allan, J., Mitchell, T., Harborne, N., Bohm, L., Crane-Robinson, C. (1986). Roles of H1 domains determining higher order chromatin structure and H1 location. J. Mol. Biol. 187, 591-60.

20. Lennard A.C., Thomas J.O. (1985). The arrangement of histone H5 molecules in extended and condensed chicken erythrocyte chromatin. EMBO J. 4, 3455-3462.

21. Arents G., Moudrianakis E.N. (1995). The histone fold: a ubiquitous architectural motif utilized in DNA compaction and protein dimerization. Proc Natl Acad Sci U S A 92(24), 11170-4.

22. Kasinsky H.E., Lewis J.D., Dacks J.B., Ausió J. (2001). Origin of H1 linker histones. FASEB J. 15(1), 34-42.

23. Bult C.J., White O., Olsen G.J., Zhou L., Fleischmann R.D., Sutton G.G., Blake J.A., FitzGerald L.M., Clayton R.A., Gocayne J.D., Kerlavage A.R., Dougherty B.A., Tomb J.F., Adams M.D., Reich C.I., Overbeek R., Kirkness E.F., Weinstock K.G., Merrick J.M., Glodek A., Scott J.L., Geoghagen N.S., Venter J.C. (1996). Complete genome sequence of the methanogenic archaeon, Methanococcus jannaschii. Science 273(5278), 1058-73.

24. Multigner L., Gagnon J., Van Dorsselaer A., Job D. (1992). Stabilization of sea urchin flagellar microtubules by histone H1. Nature 360(6399), 33-9.

25. Jerzmanowski A., Cole R.D. (1992). Partial displacement of histone H1 from chromatin is required before it can be phosphorylated by mitotic H1 kinase in vitro. J Biol Chem. 267(12), 8514-20.

26. Kaczanowski S., Jerzmanowski A. (2001). Evolutionary correlation between linker histones and microtubular structures. J Mol Evol. 53(1), 19-30.

27. Wood C., Snijders A., Williamson J., Reynolds C., Baldwin J., Dickman M. (2009). Post-translational modifications of the linker histone variants and their association with cell mechanisms. FEBS J. 276(14), 3685-97.

28. Ausió J. (2000). Are linker histones (histone H1) dispensable for survival? Bioessays. 22(10), 873-7.

29. Shen X., Yu L., Wei J.W., Gorovsky M.A. (1996). Linker histones are not essential and affect chromatin condensation in vivo. Cell 82, 47-56.

30. Fan Y., Sirotkin A., Russell R.G., Ayala J., and Skoultchi A.I. (2001). Individual somatic H1 subtypes are dispensable for mouse development even in mice lacking the H1(0) replacement subtype. Mol. Cell. Biol. 21, 7933–7943.

31. Lin Q., Sirotkin A., Skoultchi A.I. (2000). Normal spermatogenesis in mice lacking the testis-specific linker histone H1t. Mol Cell Biol. 20(6), 2122-8.

32. Fan Y., Nikitina T., Morin-Kensicki E.M., Zhao J., Magnuson T.R., Woodcock C.L., Skoultchi A.I. (2003). H1 linker histones are essential for mouse development and affect nucleosome spacing *in vivo*. Mol. Cell. Biol. 23, 4559–4572.

33. Neelin J. M., Callahan P. X., Lamb D. C., Murray K. (1964). The histones of chicken erythrocyte nuclei. Can. J. Biochem. 42,1743-1752.

34. Ausió, J. (1999). Histone H1 and the evolution of the sperm nuclear basic proteins. J. Biol. Chem. 274, 31115-31118.

35. Happel N., Doenecke D. (2009). Histone H1 and its isoforms: contribution to chromatin structure and function. Gene 431(1-2), 1-12.

36. Lever M.A., Th'ng J.P., Sun X., Hendzel M.J. (2000). Rapid exchange of histone H1.1 on chromatin in living human cells. Nature 408(6814), 873-6.

37. Hendzel M.J., Lever M.A., Crawford E., Th'ng J.P. (2004). The C-terminal domain is the primary determinant of histone H1 binding to chromatin in vivo. J Biol Chem. 279(19), 20028-34.

38. Konishi A., Shimizu S., Hirota J., Takao T., Fan Y., Matsuoka Y., Zhang L., Yoneda Y., Fujii Y., Skoultchi A.I., Tsujimoto Y. (2003). Involvement of histone H1.2 in apoptosis induced by DNA double-strand breaks. Cell 114, 673–688.

39. Albig W., Kardalinou E., Drabent B., Zimmer A., Doenecke D. (1991). Isolation and characterization of two human H1 histone genes within clusters of core histone genes. Genomics 10(4), 940-8.

40. Terme J.M., Sesé B., Millán-Ariño L., Mayor R., Belmonte J.C., Barrero M.J., Jordan A. (2011). Histone H1 variants are differentially expressed and incorporated into chromatin during differentiation and reprogramming to pluripotency. J Biol Chem. 286(41), 35347-57.

41. Trojer P., Reinberg D. (2007). Facultative heterochromatin: is there a distinctive molecular signature? Mol Cell. 28(1), 1-13.

42. Daujat S., Zeissler U., Waldmann T., Happel N., Schneider R. (2005). HP1 binds specifically to Lys26-methylated histone H1.4, whereas simultaneous Ser27 phosphorylation blocks HP1 binding. J Biol Chem. 280(45), 38090-5.

43. Hale T.K., Contreras A., Morrison A.J., Herrera R.E. (2006). Phosphorylation of the linker histone H1 by CDK regulates its binding to HP1alpha. Mol Cell. 22(5), 693-9.

44. Parseghian M.H., Clark R.F., Hauser L.J., Dvorkin N., Harris D.A., Hamkalo B.A. (1993). Fractionation of human H1 subtypes and characterization of a subtype-specific antibody exhibiting non-uniform nuclear staining. Chromosome Res. 1, 127–139.

45. Parseghian M.H., Newcomb R.L., Winokur S.T., Hamkalo B.A. (2000). The distribution of somatic H1 subtypes is nonrandom on active vs. inactive chromatin: distribution in human fetal fibroblasts. Chromosome Res. 8, 405–424.

46. Th'ng J.P., Sung R., Ye M., Hendzel M.J. (2005). H1 family histones in the nucleus. Control of binding and localization by the C-terminal domain. J. Biol. Chem. 280, 27809–27814.

47. Seyedin S.M., Kistler W.S. (1980). Isolation and characterization of rat testis H1t. An H1 histone variant associated with spermatogenesis. J Biol Chem. 255(12), 5949-54.

48. Koppel D.A., Wolfe S.A., Fogelfeld L.A., Merchant P.S., Prouty L., Grimes S.R. (1994). Primate testicular histone H1t are highly conserved and the human H1t gene is located on chromosome 6. J Cell Biochem. 54(2), 219-30.

49. Drabent B., Bode C., Bramlage B., Doenecke D. (1996). Expression of the mouse testicular histone gene H1t during spermatogenesis. Histochem Cell Biol. 106(2), 247-51.

50. Steger K., Klonisch T., Gavenis K., Drabent B., Doenecke D., Bergmann M. (1998). Expression of mRNA and protein of nucleoproteins during human spermiogenesis. Mol Hum Reprod. 4(10), 939-45.

51. Cavalcanti M.C., Rizgalla M., Geyer J., Failing K., Litzke L.F., Bergmann M. (2009). Expression of histone 1 (H1) and testis-specific histone 1 (H1t) genes during stallion spermatogenesis. Anim Reprod Sci. 111(2-4), 220-34.

52. Tanaka H., Iguchi N., Isotani A., Kitamura K., Toyama Y., Matsuoka Y., Onishi M., Masai K., Maekawa M., Toshimori K., Okabe M., Nishimune Y. (2005). HANP1/H1T2, a novel histone H1-like protein involved in nuclear formation and sperm fertility. Mol Cell Biol. 25(16), 7107-19.

53. Martianov I., Brancorsini S., Catena R., Gansmuller A., Kotaja N., Parvinen M., Sassone-Corsi P., Davidson I. (2005). Polar nuclear localization of H1T2, a histone H1 variant, required for spermatid elongation and DNA condensation during spermiogenesis. Proc Natl Acad Sci U S A 102(8), 2808-13.

54. Yan W., Ma L., Burns K.H., Matzuk M.M. (2003). HILS1 is a spermatid-specific linker histone H1-like protein implicated in chromatin remodeling during mammalian spermiogenesis. Proc Natl Acad Sci U S A 100(18), 10546-51.

55. Fu G., Ghadam P., Sirotkin A., Khochbin S., Skoultchi A.I., Clarke H.J. (2003). Mouse oocytes and early embryos express multiple histone H1 subtypes. Biol Reprod. 68(5), 1569-76.

56. Tanaka M., Hennebold J.D., Macfarlane J., Adashi E.Y. (2001). A mammalian oocyte-specific linker histone gene H1oo: homology with the genes for the oocyte-specific cleavage stage histone (cs-H1) of sea urchin and the B4/H1M histone of the frog. Development 128(5), 655-64.

57. Lea, M.A. (1987). Relationship of H1o histone to differentiation and cancer. Cancer Biochem. Biophys. 9, 199–209.

58. Girardot V., Rabilloud T., Yoshida M., Beppu T., Lawrence J.J., Khochbin S. (1994). Relationship between core histone acetylation and histone H1o gene activity. Eur. J. Biochem. 224, 885–892.

59. Stoldt S., Wenzel D., Schulze E., Doenecke D., Happel N. (2007). G1 phase-dependent nucleolar accumulation of human histone H1x. Biol Cell. 99(10), 541-52.

60. Roth S.Y., Allis C.D. (1992). Chromatin condensation: does histone H1 dephosphorylation play a role? Trends Biochem. Sci. 17, 93–98.

61. Dou Y., Mizzen C.A., Abrams M., Allis C.D., Gorovsky M.A. (1999). Phosphorylation of linker histone H1 regulates gene expression *in vivo* by mimicking H1 removal. Mol. Cell 4, 641–647.

62. Kim K., Jeong K.W., Kim H., Choi J., Lu W., Stallcup M.R., An W. (2012). Functional interplay between p53 acetylation and H1.2 phosphorylation in p53-regulated transcription. Oncogene. 10.1038/onc.2011.605.

63. Alami R., Fan Y., Pack S., Sonbuchner T.M., Besse A., Lin Q., Greally J.M., Skoultchi A.I., Bouhassira E.E. (2003). Mammalian linker-histone subtypes differentially affect gene expression *in vivo*. Proc. Natl. Acad. Sci. USA 100, 5920–5925.

64. Garcia B.A., Busby S.A., Barber C.M., Shabanowitz J., Allis C.D., Hunt D.F. (2004). Characterization of phosphorylation sites on histone H1 isoforms by tandem mass spectrometry. J Proteome Res 3, 1219–1227.

65. Wisniewski J.R., Zougman A., Krüger S., Mann M. (2007). Mass spectrometric mapping of linker histone H1 variants reveals multiple acetylations, methylations, and phosphorylation as well as differences between cell culture and tissue. Mol Cell Proteomics 6, 72–87.

66. Wisniewski J.R., Zougman A., Krüger S., Mann M. (2008). Nepsilon-formylation of lysine is a widespread post-translational modification of nuclear proteins occurring at residues involved in regulation of chromatin function. Nucleic Acids Res. 36(2), 570-7.

67. Jiang T., Zhou X., Taghizadeh K., Dong M., Dedon P.C. (2007). N-formylation of lysine in histone proteins as a secondary modification arising from oxidative DNA damage. Proc. Natl Acad. Sci. USA 104, 60-65.

68. Fontán-Lozano A., Suárez-Pereira I., Horrillo A., del-Pozo-Martín Y., Hmadcha A., Carrión AM. (2010). Histone H1 poly[ADP]-ribosylation regulates the chromatin alterations required for learning consolidation. J Neurosci. 30(40), 13305-13.

69. Zardo G., Marenzi S., Caiafa P. (1998). H1 histone as a trans-acting factor involved in protecting genomic DNA from full methylation. Biol Chem. 379(6), 647-54.

70. Vila R., Ponte I., Collado M., Arrondo J.L., Jiménez M.A., Rico M., Suau P. (2001). DNA-induced alpha-helical structure in the NH2-terminal domain of histone H1. J Biol Chem. 276(49), 46429-35.

71. Fan Y., Nikitina T., Zhao J., Fleury T.J., Bhattacharyya R., Bouhassira E.E., Stein A., Woodcock C.L., Skoultchi A.I. (2005). Histone H1 depletion in mammals alters global chromatin structure but causes specific changes in gene regulation. Cell 123(7), 1199-212.

72. Wierzbicki A.T., Jerzmanowski A. (2005). Suppression of histone H1 genes in Arabidopsis results in heritable developmental defects and stochastic changes in DNA methylation. Genetics 169(2), 997-1008.

73. Barra J.L., Rhounim L., Rossignol J.L., Faugeron G. (2000). Histone H1 is dispensable for methylation-associated gene silencing in Ascolobus immersus and essential for long life span. Mol Cell Biol. 20(1), 61-9.

74. Maclean J.A., Bettegowda A., Kim B.J., Lou C.H., Yang S.M., Bhardwaj A., Shanker S., Hu Z., Fan Y., Eckardt S., McLaughlin K.J., Skoultchi A.I., Wilkinson M.F. (2011). The rhox homeobox gene cluster is imprinted and selectively targeted for regulation by histone h1 and DNA methylation. Mol Cell Biol. 31(6), 1275-87.

75. Ferrier D.E., Holland P.W. (2001). Ancient origin of the Hox gene cluster. Nat Rev Genet. 2(1), 33-8.

76. MacLean J.A. 2nd, Lorenzetti D., Hu Z., Salerno W.J., Miller J., Wilkinson M.F. (2006). Rhox homeobox gene cluster: recent duplication of three family members. Genesis 44(3), 122-9.

77. Hellauer K., Sirard E., Turcotte B. (2001). Decreased expression of specific genes in yeast cells lacking histone H1. J Biol Chem. 276(17), 13587-92.

78. Lee H., Habas R., Abate-Shen C. (2004). MSX1 cooperates with histone H1b for inhibition of transcription and myogenesis. Science 304(5677), 1675-8.

79. Kaludov N.K., Pabón-Peña L., Seavy M., Robinson G., Hurt M.M. (1997). A mouse histone H1 variant, H1b, binds preferentially to a regulatory sequence within a mouse H3.2 replication-dependent histone gene. J Biol Chem. 272(24), 15120-7.

80. Montes de Oca R., Lee K.K., Wilson K.L. (2005). Binding of barrier to autointegration factor (BAF) to histone H3 and selected linker histones including H1.1. J Biol Chem. 280(51), 42252-62.

81. Mackey-Cushman S.L., Gao J., Holmes D.A., Nunoya J.I., Wang R., Unutmaz D., Su L. (2011). FoxP3 interacts with linker histone H1.5 to modulate gene expression and program Treg cell activity. Genes Immun. 12(7), 559-67.

82. Hashimoto H., Sonoda E., Takami Y., Kimura H., Nakayama T., Tachibana M., Takeda S., Shinkai Y. (2007). Histone H1 variant, H1R is involved in DNA damage response. DNA Repair (Amst). 6(11), 1584-95.

83. Takata H., Matsunaga S., Morimoto A., Ono-Maniwa R., Uchiyama S., Fukui K. (2007). H1.X with different properties from other linker histones is required for mitotic progression. FEBS Lett. 581(20), 3783-8.

84. De S., Brown D.T., Lu Z.H., Leno G.H., Wellman S.E., Sittman D.B. (2002). Histone H1 variants differentially inhibit DNA replication through an affinity for chromatin mediated by their carboxyl-terminal domains. Gene 292(1-2), 173-81.

85. Lu Z.H., Sittman D.B., Romanowski P., Leno G.H. (1998). Histone H1 reduces the frequency of initiation in Xenopus egg extract by limiting the assembly of prereplication complexes on sperm chromatin. Mol Biol Cell. 9(5), 1163-76.

86. Lambrot R., Jones S., Saint-Phar S., Kimmins S. (2012). Specialized Distribution of the Histone Methyltransferase Ezh2 in the Nuclear Apical Region of Round Spermatids and Its Interaction with the Histone Variant H1t2. J Androl. [Epub ahead of print]

87. Wood W.B. and the Community of C. elegans Researchers. (1988). The nematode Caenorhabditis elegans. Cold Spring Harbor Monograph Series, Volume 17.

88. Kamath R.S., Fraser A.G., Dong Y., Poulin G., Durbin R., Gotta M., Kanapin A., Le Bot N., Moreno S., Sohrmann M., Welchman D.P., Zipperlen P., Ahringer J. (2003). Systematic functional analysis of the Caenorhabditis elegans genome using RNAi. Nature 421(6920), 231-7.

89. Barrière A., Yang S.P., Pekarek E., Thomas C.G., Haag E.S., Ruvinsky I. (2009). Detecting heterozygosity in shotgun genome assemblies: Lessons from obligately outcrossing nematodes. Genome Res. 19(3), 470-80.

90. Riddle D.L., Blumenthal T., Meyer B.J., Priess J.R., editors. (1997). C. elegans II. 2nd edition. Cold Spring Harbor (NY): Cold Spring Harbor Laboratory Press.

91. Hodgkin J. (2005). Karyotype, ploidy and gene dosage. WormBook, ed. The C. elegans Research Community, WormBook, doi/10.1895/wormbook.1.3.1, http://www.wormbook.org.

92. Hutter H., Vogel B.E., Plenefisch J.D., Norris C.R., Proenca R.B., Spieth J., Guo C., Mastwal S., Zhu X., Scheel J., Hedgecock EM. (2000). Conservation and novelty in the evolution of cell adhesion and extracellular matrix genes. Science 287, 989–994.

93. Maddox P.S., Oegema K., Desai A., Cheeseman I.M. (2004). "Holo"er than thou: chromosome segregation and kinetochore function in C. elegans. Chromosome Res. 12(6), 641-53.

94. Albertson D.G., Thomson J.N. (1993). Segregation of holocentric chromosomes at meiosis in the nematode, Caenorhabditis elegans. Chromosome Res. 1(1), 15-26.

95. Dernburg A.F. (2001). Here, there, and everywhere: kinetochore function on holocentric chromosomes. J Cell Biol. 153(6), F33-8.

96. Oegema K., Desai A., Rybina S., Kirkham M., and Hyman A.A. (2001). Functional analysis of kinetochore assembly in Caenorhabditis elegans. J. Cell Biol. 153, 1209–1226.

97. Wicky C., Villeneuve A.M., Lauper N., Codourey L., Tobler H., and Muller F. (1996). Telomeric repeats (TTAGGC)n are sufficient for chromosome capping function in Caenorhabditis elegans. Proc. Natl. Acad. Sci. USA 93, 8983–8988.

98. Zakian V.A. (1989). Structure and function of telomeres. Annu Rev Genet. 23, 579-604.

99. Cangiano G., La Volpe A. (1993). Repetitive DNA sequences located in the terminal portion of the Caenorhabditis elegans chromosomes. Nucleic Acids Res. 21(5), 1133-9.

100. Roberts S.B., Emmons S.W., Childs G. (1989). Nucleotide sequences of Caenorhabditis elegans core histone genes. Genes for different histone classes share common flanking sequence elements. J Mol Biol. 206(4), 567-77.

101. Vanfleteren J.R., Van Bun S.M., Delcambe L.L., Van Beeumen J.J. (1986). Multiple forms of histone H2B from the nematode *Caenorhabditis elegans*. Biochem.J. 235, 769–773.

102. Vanfleteren J.R., Van Bun S.M., Van Beeumen J.J. (1987a). The primary structure of histone H2A from the nematode *Caenorhabditis elegans*. Biochem.J. 243, 297–300.

103. Vanfleteren J.R., Van Bun S.M., Van Beeumen J.J. (1987b). The primary structure of histone H3 from the nematode *Caenorhabditis elegans*. FEBS Lett. 211, 59–63.

104. Vanfleteren J.R., Van Bun S.M., Van Beeumen J.J. (1987c). The primary structure of histone H4 from the nematode *Caenorhabditis elegans*. Comp. Biochem. Physiol. B 87, 847–849.

105. Vanfleteren J.R., Van Bun S.M., Van Beeumen J.J. (1989). The histones of *Caenorhabditis elegans*: no evidence of stage-specific isoforms: an overview. FEBS Lett. 257, 233–237.

106. Sanicola M., Ward S., Childs G., Emmons S.W. (1990). Identification of a Caenorhabditis elegans histone H1 gene family. Characterization of a family member containing an intron and encoding a poly(A)+ mRNA. J Mol Biol. 212(2), 259-68.

107. Jedrusik M.A., Schulze E. (2001). A single histone H1 isoform (H1.1) is essential for chromatin silencing and germline development in Caenorhabditis elegans. Development 128(7), 1069-80.

108. Vanfleteren J.R., Van Bun S.M., Van Beeumen J.J. (1988). The primary structure of the major isoform (H1.1) of histone H1 from the nematode Caenorhabditis elegans. Biochem J. 255(2), 647-52.

109. Vanfleteren J.R., Van Bun S.M., De Baere I., Van Beeumen J.J. (1990). The primary structure of a minor isoform (H1.2) of histone H1 from the nematode Caenorhabditis elegans. Biochem J. 265(3), 739-46.

110. Jedrusik M.A., Vogt S., Claus P., Schulze E. (2002). A novel linker histone-like protein is associated with cytoplasmic filaments in Caenorhabditis elegans. J Cell Sci. 115(Pt 14), 2881-91.

111. Jedrusik M.A., Schulze E. (2007). Linker histone HIS-24 (H1.1) cytoplasmic retention promotes germ line development and influences histone H3 methylation in Caenorhabditis elegans. Mol Cell Biol. 27(6), 2229-39.

112. Garvin C., Holdeman R., Strome S. (1998). The phenotype of mes-2, mes-3, mes-4 and mes-6, maternal-effect genes required for survival of the germline in Caenorhabditis elegans, is sensitive to chromosome dosage. Genetics 148(1), 167-85

113. Wirth M., Paap F., Fischle W., Wenzel D., Agafonov D.E., Samatov T.R., Wisniewski J.R., Jedrusik-Bode M. (2009). HIS-24 linker histone and SIR-2.1 deacetylase induce H3K27me3 in the Caenorhabditis elegans germ line. Mol Cell Biol. 29(13), 3700-9.

114. Wirth M., Jedrusik-Bode M.A. (2009). Interplay between histone deacetylase SIR-2, linker histone H1 and histone methyltransferases in heterochromatin formation. Epigenetics 4(6), 353-6.

115. Studencka M., Konzer A., Moneron G., Wenzel D., Opitz L., Salinas-Riester G., Bedet C., Krüger M., Hell S.W., Wisniewski J.R., Schmidt H., Palladino F., Schulze E., Jedrusik-Bode M. (2012). Novel roles of Caenorhabditis elegans heterochromatin protein HP1 and linker histone in the regulation of innate immune gene expression. Mol Cell Biol. 32(2), 251-65.

116. Schott S., Coustham V., Simonet T., Bedet C., Palladino F. (2006). Unique and redundant functions of C. elegans HP1 proteins in post-embryonic development. Dev Biol. 298(1), 176-87.

117. Higo S., Asano Y., Kato H., Yamazaki S., Nakano A., Tsukamoto O., Seguchi O., Asai M., Asakura M., Asanuma H., Sanada S., Minamino T., Komuro I., Kitakaze M., Takashima S. (2010). Isoform-specific intermolecular disulfide bond formation of heterochromatin protein 1 (HP1). J Biol Chem. 285(41), 31337-47.

118. Eissenberg J.C. (2001). Molecular biology of the chromo domain: an ancient chromatin module comes of age. Gene 275(1), 19-29.

119. Eissenberg J.C., Elgin S.C. (2000). The HP1 protein family: getting a grip on chromatin. Curr Opin Genet Dev. 10(2), 204-10.

120. Lomberk G., Wallrath L., Urrutia R. (2006). The Heterochromatin Protein 1 family. Genome Biol. 7(7), 228.

121. Couteau F., Guerry F., Muller F., Palladino F. (2002). A heterochromatin protein 1 homologue in Caenorhabditis elegans acts in germline and vulval development. EMBO Rep. 3, 235-41.

122. Wang D., Kennedy S., Conte D. Jr, Kim J.K., Gabel H.W., Kamath R.S., Mello C.C., Ruvkun G. (2005). Somatic misexpression of germline P granules and enhanced RNA interference in retinoblastoma pathway mutants. Nature 436(7050), 593-7.

123. Brenner S. (1974). The genetics of Caenorhabditis elegans. Genetics 77, 71-94.

124. Teng Y., Girard L., Ferreira H.B., Sternberg P.W., Emmons S.W. (2004). Dissection of cis-regulatory elements in the C. elegans Hox gene egl-5 promoter. Dev Biol. Dec 15, 276:476-92.

125. Zhang T., Sun Y., Tian E., Deng H., Zhang Y., Luo X., Cai Q., Wang H., Chai J., Zhang H. (2006). RNA-binding proteins SOP-2 and SOR-1 form a novel PcG-like complex in *C. elegans*. Development 133, 1023-33.

126. Zhang H., Azevedo R.B., Lints R., Doyle C., Teng Y., Haber D., Emmons S.W. (2003).Global regulation of Hox gene expression in *C. elegans* by a SAM domain protein. Dev Cell 4, 903-15.

127. Lithgow G.J., White T.M., Melov S., Johnson T.E. (1995). Thermotolerance and extended life-span conferred by single-gene mutations and induced by thermal stress. Proc Natl Acad Sci U S A 92(16), 7540-4.

128. Solomon A., Bandhakavi S., Jabbar S., Shah R., Beitel G.J., Morimoto R.I. (2004). Caenorhabditis elegans OSR-1 regulates behavioral and physiological responses to hyperosmotic environments. Genetics 167, 161-70.

129. Cheeseman I.M., Niessen S., Anderson S., Hyndman F., Yates J.R. 3rd, Oegema K., Desai A. (2004) A conserved protein network controls assembly of the outer kinetochore and its ability to sustain tension. Genes Dev. 18(18), 2255-68.

130. Bannister A.J., Zegerman P., Partridge J.F., Miska E.A., Thomas J.O., Allshire R.C., Kouzarides T. (2001). Selective recognition of methylated lysine 9 on histone H3 by the HP1 chromo domain. Nature 410, 120-124.

131. Ross J.M., Zarkower D. (2003). Polycomb group regulation of Hox gene expression in *C. elegans*. Dev Cell 4, 891-901

132. Greenstein D., Hird S., Plasterk R.H., Andachi Y., Kohara Y., Wang B., Finney M., Ruvkun G. (1994). Targeted mutations in the Caenorhabditis elegans POU homeo box gene ceh-18 cause defects in oocyte cell cycle arrest, gonad migration, and epidermal differentiation. Genes Dev. 8(16), 1935-48.

133. Schott S., Ramos F., Coustham V., Palladino F. (2009). HPL-2/HP1 prevents inappropriate vulval induction in Caenorhabditis elegans by acting in both HYP7 and vulval precursor cells. Genetics 181, 797-801.

134. Emmons S.W. (2005). Male development *WormBook*, ed. The *C. elegans* Research Community, WormBook, doi/10.1895/wormbook.1.33.1, http://www.wormbook.org.

135. Ferreira H.B., Zhang Y., Zhao C., Emmons S.W. (1999). Patterning of *Caenorhabditis elegans* posterior structures by the Abdominal-B homolog, *egl-5*. Dev. Biol. 207, 215–228.

136. Kelly W.G., Xu S., Montgomery M.K., Fire A. (1997). Distinct requirements for somatic and germline expression of a generally expressed Caernorhabditis elegans gene. Genetics 146(1), 227-38.

137. Yang Y., Sun Y., Luo X., Zhang Y., Chen Y., Tian E., Lints R., Zhang H. (2007). Polycomb-like genes are necessary for specification of dopaminergic and serotonergic neurons in Caenorhabditis elegans. Proc Natl Acad Sci U S A 104, 852-7.

138. Schwartz Y.B., Pirrotta V. (2007). Polycomb silencing mechanisms and the management of genomic programmes. Nat Rev Genet. 8, 9-22.

139. Margueron R., Reinberg D. (2011). The Polycomb complex PRC2 and its mark in life. Nature 469(7330), 343-9.

140. Cao R., Wang L., Wang H., Xia L., Erdjument-Bromage H., Tempst P., Jones R.S., Zhang Y. (2002). Role of histone H3 lysine 27 methylation in Polycomb-group silencing. Science 298, 1039–1043.

141. Cao R., Zhang Y. (2004). The functions of E(Z)/EZH2-mediated methylation of lysine 27 in histone H3. Curr Opin Genet Dev 14, 155–164.

142. Korf I., Fan Y., Strome S. (1998). The Polycomb group in *Caenorhabditis elegans* and maternal control of germline development. Development 125, 2469–2478

143. Paulsen J.E., Capowski E.E., Strome S. (1995). Phenotypic and molecular analysis of *mes-3*, a maternal-effect gene required for proliferation and viability of the germ line in *C. elegans*. Genetics 141, 1383-1398

144. O'Rourke D., Baban, D., Demidova, M., Mott, R., Hodgkin, J. (2006). Genomic clusters, putative pathogen recognition molecules, and antimicrobial genes are induced by infection of *C. elegans* 812 with *M. nematophilum*. Genome Res. 16, 1005-16.

145. Pujol N., Zugasti O., Wong D., Couillault C., Kurz C.L., Schulenburg H., Ewbank J.J. (2008). Antifungal innate immunity in *C. elegans* is enhanced byevolutionary diversification of antimicrobial peptides. PLoS Pathog 18, e1000105.

146. Pujol N., Cypowyj S., Ziegler K., Millet A., Goncharov A., Jin Y., Chisholm A.D., Ewbank J.J. (2008). Distinct innate immune responses to infection and wounding in the *C. elegans* epidermis. Curr Biol 18, 481-9.

147. Evans E.A., Kawli T., Tan M.W. (2008). Pseudomonas aeruginosa suppresses host immunity by activating the DAF-2 insulin-like signaling pathway in Caenorhabditis elegans. PLoS Pathog. 4(10), e1000175.

148. Shapira M., Hamlin B.J., Rong J., Chen K., Ronen M., Tan M.W. (2006). A conserved role for a GATA transcription factor in regulating epithelial innate immune responses. Proc Natl Acad Sci USA 103, 14086-91.

149. Schulenburg H., Hoeppner M.P., Weiner J. 3rd, Bornberg-Bauer E. (2008). Specificity of the innate immune system and diversity of C-type lectin domain (CTLD) proteins in the nematode Caenorhabditis elegans. Immunobiology 213(3-4), 237-50.

150. Honda Y., Honda S. (1999). The daf-2 gene network for longevity regulates oxidative stress resistance and Mn-superoxide dismutase gene expression in Caenorhabditis elegans. FASEB J. 13(11), 1385-93.

151. Minniti A.N., Cataldo R., Trigo C., Vasquez L., Mujica P., Leighton F., Inestrosa N.C., Aldunate R. (2009). Methionine sulfoxide reductase A expression is regulated by the DAF-16/FOXO pathway in Caenorhabditis elegans. Aging Cell. 8(6), 690-705.

152. Song H.O., Lee W., An K., Lee H.S., Cho J.H., Park Z.Y., Ahnn J. (2009). C. elegans STI-1, the homolog of Sti1/Hop, is involved in aging and stress response. J Mol Biol. 390(4), 604-17.

153. Nicholas H.R., Hodgkin J. (2004). Responses to infection and possible recognition strategies in the innate immune system of Caenorhabditis elegans. Mol Immunol. 41(5), 479-93.

154. Lant B., Storey K.B. (2010). An Overview of Stress Response and Hypometabolic Strategies in *Caenorhabditis elegans*: Conserved and Contrasting Signals with the Mammalian System. Int J Biol Sci. 6(1), 9-50.

155. Shen X., Gorovsky M.A. (1996). Linker histone H1 regulates specific gene expression but not global transcription in vivo. Cell 86(3), 475-83.

156. Karrer K.M., Peiffer S.L., DiTomas M.E. (1993). Two distinct gene subfamilies within the family of cysteine protease genes. Proc Natl Acad Sci U S A 90(7), 3063-7.

157. Bouvet P., Dimitrov S., Wolffe A.P. (1994). Specific regulation of Xenopus chromosomal 5S rRNA gene transcription in vivo by histone H1. Genes Dev. 8(10), 1147-59.

158. Sera T., Wolffe A.P. (1998). Role of histone H1 as an architectural determinant of chromatin structure and as a specific repressor of transcription on Xenopus oocyte 5S rRNA genes. Mol Cell Biol. 18(7), 3668-80.

159. Ni J.Q., Liu L.P., Hess D., Rietdorf J., Sun F.L. (2006). Drosophila ribosomal proteins are associated with linker histone H1 and suppress gene transcription. Genes Dev. 20(14), 1959-73.

160. Kuzmichev A., Jenuwein T., Tempst P., Reinberg D. (2004). Different EZH2-containing complexes target methylation of histone H1 or nucleosomal histone H3. Mol Cell. 14(2), 183-93.

161. Jacobs S.A., Khorasanizadeh S. (2002). Structure of HP1 chromodomain bound to a lysine 9-methylated histone H3 tail. Science 295(5562), 2080-3.

162. Eissenberg J.C., Hartnett T. (1993). A heat shock-activated cDNA rescues the recessive lethality of mutations in the heterochromatin-associated protein HP1 of Drosophila melanogaster. Mol. Gen. Genet 240, 333–338

163. Laybourn P.J., Kadonaga J.T. (1991). Role of nucleosomal cores and histone H1 in regulation of transcription by RNA polymerase II. Science 254, 238–245.

164. Verschure P.J., van der Kraan I., de Leeuw W., van der Vlag J., Carpenter A.E., Belmont A.S., van Driel R. (2005). In vivo HP1 targeting causes large-scale chromatin condensation and enhanced histone lysine methylation. Mol Cell Biol. 25, 4552-64.

165. Sancho M., Diani E., Beato M., Jordan A. (2008). Depletion of human histone H1 variants uncovers specific roles in gene expression and cell growth. PLoS Genetics 4(10), e1000227

166. Koop R., Di Croce L., Beato M. (2003). Histone H1 enhances synergestic activation of the MMTV promoter in chromatin. EMBO Journal 22, 588-599.

167. Aboobaker A.A, Blaxter M.L. (2003). Hox gene loss during dynamic evolution of the nematode cluster. Curr. Biol., 13, 37–40.

168. Aboobaker A, Blaxter M. (2003). Hox gene evolution in nematodes: novelty conserved. Curr Opin Genet Dev. 13(6), 593-8.

169. Brunschwig K., Wittmann C., Schnabel R., Burglin T.R., Tobler H., Muller F. (1999). Anterior organization of the *Caenorhabditis elegans* embryo by the labial-like *Hox* gene *ceh-13.* Development 126, 1537–1546.

170. Van Auken K., Weaver D.C., Edgar L.G., Wood W.B. (2000). *Caenorhabditis elegans* embryonic axial patterning requires two recently discovered posterior-group *Hox* genes. Proc. Natl. Acad. Sci. USA 97, 4499–4503.

171. Clark S.G., Chisholm A.D., Horvitz H.R. (1993).Control of cell fates in the central body region of *C. elegans* by the homeobox gene *lin-39.* Cell 74, 43–55.

172. Maloof J.N., Kenyon C. (1998). The *Hox* gene *lin-39* is required during *C. elegans* vulval induction to select the outcome of Ras signaling. Development 125, 181–190.

173. Wang B.B., Muller-Immergluck M.M., Austin J., Robinson N.T., Chisholm A., Kenyon C. (1993). A homeotic gene cluster patterns the anteroposterior body axis of *C. elegans.* Cell 74, 29–42.

174. Chisholm A. (1991). Control of cell fate in the tail region of *C. elegans* by the gene *egl-5*. Development 111, 921–932.

175. Kenyon C. (1986). A gene involved in the development of the posterior body region of *C. elegans*. Cell 46, 477–487.

176. Salser S.J., Loer C.M., Kenyon C. (1993). Multiple HOM-C gene interactions specify cell fates in the nematode central nervous system. Genes Dev. 7, 1714–1724.

177. Salser S.J., Kenyon C. (1996). A *C. elegans Hox* gene switches on, off, on and off again to regulate proliferation, differentiation and morphogenesis. Development 122, 1651–1661.

178. Fong Y., Bender L., Wang W., Strome S. (2002). Regulation of the different chromatin states of autosomes and X chromosomes in the germ line of C. elegans. Science 296(5576), 2235-8.

179. Capowski E.E., Martin P., Garvin C., Strome S. (1991). Identification of grandchildless loci whose products are required for normal germ-line development in the nematode Caenorhabditis elegans. Genetics 129(4), 1061-72.

180. Martin C., Cao R., Zhang Y. (2006). Substrate preferences of the EZH2 histone methyltransferase complex. J Biol Chem. 281, 8365-70

181. Levine S. S., King I. F., Kingston R. E. (2004). Division of labor in polycomb group repression. Trends Biochem. Sci. 29,478 -485.

182. Simon J.A., Kingston R.E. (2009). Mechanisms of polycomb gene silencing: knowns and unknowns. Nat Rev Mol Cell Biol. 10(10), 697-708.

183. Sun Y.Y., Zhang H. (2004). A unified mode of epigenetic gene silencing. RNA Biol. 1, 132-134.

184. Silva J., Mak W., Zvetkova I., Appanah R., Nesterova T.B., Webster Z., Peters A.H., Jenuwein T., Otte A.P., Brockdorff N. (2003). Establishment of histone h3 methylation on the inactive X chromosome requires transient recruitment of Eed-Enx1 polycomb group complexes. Dev. Cell 4, 481-495.

185. Plath K., Fang J., Mlynarczyk-Evans S.K., Cao R., Worringer K.A., Wang H., de la Cruz C.C., Otte A.P., Panning B., Zhang Y. (2003). Role of histone H3 lysine 27 methylation in X inactivation. Science 300, 131-135.

186. Plath K., Talbot D., Hamer K.M., Otte A.P., Yang T.P., Jaenisch R., Panning B. (2004). Developmentally regulated alterations in Polycomb repressive complex 1 proteins on the inactive X chromosome. *J.* Cell Biol. 167, 1025-1035.

187. Dialynas G.K., Terjung S., Brown J.P., Aucott R.L., Baron-Luhr B., Singh P.B., Georgatos S.D. (2007). Plasticity of HP1 proteins in mammalian cells. JSC 120, 3415- 3424.

188. Li Y., Kirschmann D.A., Wallrath L.L. (2002). Does heterochromatin protein 1 always follow code? Proc. Natl. Acad. Sci. USA 99, 16462-16469.

189. Singh P.B., Georgatos S.D. (2002). HP1: facts, open questions, and speculation. J Struct Biol 140, 10–16.

190. Flueck C., Bartfai R., Volz J., Niederwieser I., Salcedo-Amaya A.M., Alako B.T., Ehlgen F., Ralph S.A., Cowman A.F., Bozdech Z., Stunnenberg H.G., Voss T.S. (2009). Plasmodium falciparum

heterochromatin protein 1 marks genomic loci linked to phenotypic variation of exported virulence factors. PLoS Pathog 5(9), e1000569.

191. Nielsen P.R., Nietlispach D., Mott H.R., Callaghan J., Bannister A., Kouzarides T., Murzin A.G., Murzina N.V., Laue E.D. (2002). Structure of the HP1 chromodomain bound to histone H3 methylated at lysine 9. Nature 416, 103–107.

192. Kaustov L., Ouyang H., Amaya M., Lemak A., Nady N., Duan S., Wasney G.A., Li Z., Vedadi M., Schapira M., Min J., Arrowsmith C.H. (2011). Recognition and specificity determinants of the human cbx chromodomains. J Biol Chem. 286(1)**,** 521-9.

193. Rose F.R., Bailey K., Keyte J.W., Chan W.C., Greenwood D., Mahida Y.R. (1998). Potential role of epithelial cell-derived histone H1 proteins in innate antimicrobial defense in the human gastrointestinal tract. Infect Immun. 66(7), 3255-63.

Curriculum vitae

PERSONAL INFORMATION

Name: Maja Studencka

Date of birth: 27.09.1984

Place of birth: Żywiec, Poland

Nationality: Poland

EDUCATION

2009-2012 PhD., Epigenetics and Developmental biology, Max Planck Institute for Biochemistry, Göttingen, Germany

Thesis: *The influence of post-translational modifications on biology of the linker histone HIS-24 in Caenorhabditis elegans*

Advisor: Dr. Monika Jedrusik-Bode

2003-2009 M.Sc. Biological Sciences, Jagiellonian University, Poland

M.Sc. thesis advisor: Prof. dr hab. Józefa Styrna

1999-2003 Nikolaus Kopernikus High School, Żywiec

SCHOLARSCHIPS

2008 One year scientific training in the Institute of Human Genetics, Göttingen, Germany; participation in a project „ The analysis of *Pxt1* gene function in mouse”

RESEARCH EXPERIENCE

2010-2012 Research on mechanisms of aging. (Germany).
Study of the influence of mammalian SIRT6 and *C. elegans* SIR-2.4 proteins on the cellular stress response.

2008 Research on fertility of mice males (Germany).
Study of the *Pxt1* gene functions in the spermatogenesis process of mouse. Analysis of the *Ccdc33* gene functions in the mouse development.

2006-2008 Research on fertility of mice males (Poland). Extensive sampling of sperm from different strains of mice. Analyses of the genetic background influence on the sperm quality in males with deletion of Y chromosome.

TEACHING EXPERIENCE

2011 Supervision of *exchange* student- Radosław Wesołowski, Max Planck Institute for Biochemistry, Germany. Epigenetics in *C. elegans* group.

2011 Supervision of Bachelor student- Jan Kampf, Max Planck Institute for Biochemistry, Germany. Epigenetics in *C. elegans* group.

2011 PhD Student Instructor, Georg-August- University, Göttingen, Germany.

Cell and Developmental Biology-basic course (Laboratory and Discussion Section).

CONFERENCES AND SYMPOSIA

2011 International Symposium „Chromatin Changes in differentiation and Malignancies“, Giessen, Germany

2010 International symposium- Horizons in Molecular Biology, Göttingen, Germany

2010 EMBL Conference Series: “*C.elegans* development and gene expression”, Heidelberg, Germany